Late Pleistocene deglaciation histories in the central Mérida Andes (Venezuela)

Isandra Fortuna Angel Ceballos

UNIVERSITÉ GRENOBLE ALPES

THÈSE

Pour obtenir le grade de

DOCTEUR DE L'UNIVERSITÉ GRENOBLE ALPES

Spécialité : **Terre Solide**

Arrêté ministériel : 7 août 2006

Présentée par

Isandra Fortuna ANGEL CEBALLOS

Thèse dirigée par **Julien Carcaillet**, **Laurence Audin** et **Franck Audemard**

préparée au sein du **Laboratoire ISTerre**
dans **l'École Doctorale Terre, Univers Environnement**

Late Pleistocene deglaciation histories in the central Mérida Andes (Venezuela)

Histoires de deglaciation pendant le Pléistocène Supérieur dans les Andes centrales de Mérida (Venezuela)

Thèse soutenue publiquement le **12 février 2016**,
devant le jury composé de :

M. Franck AUDEMARD
Chercheur au FUNVISIS Caracas, Venezuela, Co-directeur
M. Christian BECK
Professeur à l'Université de Savoie Mt Blanc Chambéry, Examinateur et **Président du jury**
M. Maximiliano BEZADA
Professeur à l'UPEL Caracas, Venezuela, Rapporteur
M. Julien CARCAILLET
IR CNRS à ISTerre Grenoble, Co-directeur
M. Eduardo CARRILLO
Chercheur à Robertson CGG Llandudno, Royaume-Uni Examinateur
M. Etienne COSSART
Professeur à l'Université Jean Moulin Lyon, Rapporteur

UNIVERSIDAD CENTRAL DE VENEZUELA
FACULTAD DE CIENCIAS
POSTGRADO EN GEOQUÍMICA

Late Pleistocene deglaciation histories in the central Mérida Andes (Venezuela)

Historias de desglaciación durante el Pleistoceno Tardío en los Andes centrales de Mérida (Venezuela)

Tesis Doctoral presentada ante la ilustre Universidad Central de Venezuela por Licenciada Isandra Fortuna Angel Ceballos, para optar al título de Doctor en Ciencias mención Geoquímica.

Tutores: Franck Audemard, Julien Carcaillet y Laurence Audin.

Caracas – Venezuela
Febrero, 2016

UNIVERSIDAD CENTRAL DE VENEZUELA
FACULTAD DE CIENCIAS
COMISIÓN DE ESTUDIOS DE POSTGRADO

Comisión de Estudios de Postgrado

VEREDICTO

Quienes suscriben, miembros del jurado designado por el Consejo de la Facultad de Ciencias de la Universidad Central de Venezuela, y el Consejo de Estudios de Postgrado de la Universidad Central de Venezuela, para examinar la **TESIS DOCTORAL,** presentada por la **Lic. ISANDRA FORTUNA ANGEL CEBALLOS**, titular de la cédula de identidad Nº **13.885.994**, bajo el título "**HISTORIAS DE DEGLACIACIÓN DURANTE EL PLEISTOCENO TARDÍO EN LOS ANDES CENTRALES DE MÉRIDA (VENEZUELA)"**, a fin de cumplir con el requisito legal para optar al grado académico de Doctora en Ciencias Mención: Geoquímica, dejan constancia de lo siguiente:

1.- Leído como fue dicho trabajo por cada uno de los miembros del jurado, se fijó el día viernes 12 de febrero de 2016, a las 9:00 a.m. hora venezolana, para que la Lic. Isandra Fortuna Angel Ceballos, lo defendiera en forma pública, lo que ésta hizo en el salón de seminarios "Sala de Conferencias piso 1", del Instituto ISTerre (Maison de Geosciences), mediante un resumen oral de su contenido, luego de lo cual respondió satisfactoriamente a las preguntas que le fueron formuladas por el jurado, todo ello conforme con lo dispuesto en el Reglamento de Estudios de Postgrado.

2.- Finalizada la defensa del trabajo, el jurado decidió aprobarlo, por considerar, sin hacerse solidario con las ideas expuestas por la autora, que se ajusta a lo dispuesto y exigido en el Reglamento de Estudios de Postgrado.

REPÚBLICA BOLIVARIANA DE VENEZUELA
FACULTAD DE CIENCIAS
FACULTAD DE INGENIERÍA
POSTGRADO EN GEOQUÍMICA
UNIVERSIDAD CENTRAL - CARACAS

En fe de lo cual se levanta la presente ACTA, a los doce días del mes de febrero de 2016, conforme a lo dispuesto en el Reglamento de Estudios de Postgrado, actuó como coordinador del jurado, el tutor Dr. Christian Beck.

Dr. Franck Audemard / C.I. 5.082.111
Facultad de Ingeniería, U.C.V
Jurado designado por el Consejo
de la Facultad

Dr. Julien Carcaillet Past..11CC51859
Universidad de Grenoble, Francia
Jurado designado por el Consejo
de la Facultad

Dr. Laurence Audin Past. 08CC78077
Universidad de Grenoble- Institute de
Recherche pour le Développment IRD,
Francia
Jurado designado por el Consejo
de Estudios de Postgrado

Dr. Christian Beck Past. 14DT37415
Universidad de Savoie, Francia
Jurado designado por el Consejo
de Estudios de Postgrado

Dr. Maximiliano Bezada Pa 079999656
Universidad Pedagógica Experimental
De Caracas
Jurado designado por el Consejo
de Estudios de Postgrado

Dr. Etienne Cossart Past. 07CP21175
Universidad Lyon III – Jean Moulin
Jurado designado por el Consejo
de Estudios de Postgrado

Dr. Eduardo Carrillo C.I. 11.306.440
Robertson- CGG. Llandudno Reino Unido
Jurado designado por el Consejo
de la Facultad

REPÚBLICA BOLIVARIANA DE VENEZUELA
FACULTAD DE CIENCIAS
FACULTAD DE INGENIERÍA
POSTGRADO EN GEOQUÍMICA
UNIVERSIDAD CENTRAL - CARACAS

/bs.- 12-02-2016

ACKNWOWLEDGMENTS

Many institutions and people contributed to develop this dissertation in different ways. I try to thank in a chronological sense: Eduardo Carrillo who introduces me in the tropical glaciers topic, Julien Carcaillet and Oswaldo Guzmán who introduces me in the cosmonuclide ^{10}Be technique, Etienne Jaillard and Riccardo Vassallo to provide us information for financial support and Laurence Audin to help us with the administration. Thanks Franck Audemard by scientific discussions and humor which help to really enjoy field trips. Eduardo Barreto for his valuable help in the field. Oswaldo Guzmán, Alessa Geigher, Rubén Basantes, Riccardo Vassallo, Santiago Yépez, Enzo Caraballo and Walter Reategui for scientific discussions or technical helps. Thanks Francis Coeur for rock crushing. Really thanks to Melaine Le Roy and Thomas Condom by help in the paleo ELA calculations. Again big thanks Julien Carcaillet and Laurence Audin by their patience correcting this dissertation. Julien again because he was every time available for logistical helps. Thanks to the jury members for accepting reviewing and improving my work. Thanks all people who help me with humor, patience and logistical support in the ISTerre, in general in Grenoble or in the UCV (I cannot remember all the names).

Thanks to the next institutions by financial support: ECOS-NORD Program, INSU-CNRS-IRD (France), CIGIR-FONACIT (Venezuela), FUNVISIS (Project Geodinámica Integral de los Andes de Mérida-GIAME-FONACIT 2012002202, Venezuela). Université de Grenoble and INQUA economical support in different congress and workshops.

CONTENT

ABSTRACT

The central Mérida Andes (Venezuela) landscape is characterized by the presence of well-preserved glacial landforms located between 2400 and 4978 m a.s.l. Geomorphological studies of these glacial landforms significantly contribute to the Venezuelan Andes glaciations reconstructions. However, Last Glaciation (locally called Mérida Glaciation) was poorly reconstructed because of limited chronological data. This dissertation attempts to contribute to the Last Glaciation reconstruction and paleoclimate knowledge since the late Pleistocene. In accordance to this, the methodology involved geomorphological analysis and geochronological study. Glacial landforms were dated based on the Terrestrial Cosmogenic Nuclide dating (^{10}Be). This method is suitable for dating quartz-rich materials and for the period of interest. To deduce paleoclimate conditions, an analysis based on paleo ELA was developed.

In the central Mérida Andes different Late Pleistocene glacier dynamics were identified. In the Mucubají and the Mucuchache valleys, successive stages of glacier stop-advance were identified during an overall glacier withdrawal. In the Gavidia and Mifafí valleys, glacier withdrawal was rapid with the highest retreat rates (between 4-7 km/ky). Morphometric features as glaciers bottom valley slopes, accumulation zone topography (glaciers cirques with steep walls), areas and orientation controlled different glaciers dynamics.

Glacier advances were evidenced between 2500-4200 m. MIS 3 glaciers advances has been recognized in the Sierra Nevada. These were related to the highest runoff in the north of South America produced by the Intertropical Convergence Zone (ITCZ) and the local warm and wet climate conditions (locally named El Pedregal Interstadial). LGM glacier advances were recorded in Sierra Nevada in the Mucubají and Las Tapias between 3100-3600 m. MIS 2 Glaciers advances mainly occurred during the Oldest Dryas- El Caballo Stadial at around 17 ka. These glaciers advances correlate to the cold temperatures in the North Hemisphere and the coldest temperatures recorded in tropical ice cores.

Keywords

Terrestrial cosmogenic nuclides dating, TCN, cosmogenic dating, glacial landforms, Andes Mérida, Venezuela. Pleistocene, Last Glaciation, LGM, paleo ELA, tropic paleoclimate

Introduction

Le changement climatique impacte la société de manières différentes. Celles-ci sont particulièrement sensibles dans les zones soumises aux risques naturels, les zones sensibles en termes de ressources hydriques et les zones où la densité de population est critique. Le climat à la surface terrestre est contrôlé par la radiation solaire.

La ceinture intertropicale reçoit la majorité des radiations solaires terrestres et diffuse la chaleur vers les hémisphères Nord et Sud grâce aux circulations océaniques et atmosphériques. La responsabilité des Tropiques a été suggérée dans la propagation des glaciations, en particulier par la modulation de l´humidité atmosphérique qui influence la diminution de la radiation infrarouge (Uriarte, 2003). Aussi les changements climatiques durant la Dernière Glaciation ont été associés à la réorganisation de l´atmosphère dans les tropiques et aux modifications de la Circulation Océanique Méridionale de l´Atlantique (AMOC, en anglais), et enfin au paléoclimat global (Chiang, 2009). Par conséquent, il est important de comprendre le fonctionnement passé et présent du climat dans la ceinture intertropicale. Les avancées dans cette connaissance permettront d'améliorer et de rendre plus réaliste les modèles climatiques, en vue de projections plus précises du climat et d'une diminution de l´impact négative des changements climatiques sur la société (e. g. McGregor and Nieuwolt, 1998, Chiang, 2009).

Les glaciers tropicaux sont reconnus par leur extrême sensibilité face aux changements climatiques et par leur importance comme ressource hydrique pour les populations des altiplanos Péruvien et Bolivien (e.g. Hastenrath, 1994; Kaser and Osmaston, 2002). Les glaciers tropicaux sont extrêmement intéressants dans l'étude du paléoclimat (Jomelli et al., 2009). Ces études paleoclimatiques se basent sur l'analyse de carottes de glace (e.g. Thompson et al., 1996; Thompson et al., 1998; Ramírez et al., 2003) ou de morphologies glaciaires pour la reconstruction des paléo-glaciers (e.g. Stansell et al., 2007; Jomelli et al., 2009).

Les conditions paléo-climatiques à partir des paléo- glaciers peuvent être établies selon la chronologie et des reconstructions de l´extension des glaciers. Les Andes Péruviennes, Boliviennes et Equatoriennes constituent la zone tropicale la plus étudiée

(e.g. Porter, 2001; Mark, B.G., 2008; Jomelli et al., 2009). Cependant, les glaciations dans les Andes Vénézuéliennes (aussi connu comme Andes de Mérida, MA en anglais) restent partialement connues (Porter, 2001; Lachniet and Vazquez-Selem, 2005). Par conséquent, la reconstruction des glaciations dans les Andes de Mérida constitue une contribution significative pour progresser dans la connaissance du paléoclimat aux tropiques.

Les Andes de Mérida sont caractérisées par la présence de morphologies glaciaires bien préservées entre 2400-4978 m. Actuellement, la plupart des observations morphologiques ont été compilées par Schubert (e.g. 1972; 1974; 1980; 1980a; 1992 and 1998). Les principales reliques glaciaires ont été observées sous la forme de deux complexes morainiques situés entre 2600-2800 m et 2900-3500 m. Ils ont été attribués aux Glaciations Mérida Inferieur et Supérieur (Schubert, 1970, 1974). Ces compilations souffrent d'un manque évident de données chronologiques. Les données chronologiques étant réparties sur l'ensemble du massif, il est difficile d'établir une reconstruction détaillée des glaciations (e.g. Coronato and Rabassa, 2007; Carcaillet et al., 2013). Les études géochronologiques basées principalement à partir d'analyses du radiocarbone (e.g. Schubert, 1970; Salgado-Laboriau and Schubert, 1977; Schubert and Rinaldi, 1987; Rull 1998; Mahaney et al., 2001; Dirszowsky et al., 2005; Stansell et al., 2005; Mahaney et al., 2007; Carrillo et al., 2008), de la thermoluminescence (Schubert and Vaz, 1987; Bezada, 1989), de la luminescence stimulée optiquement (Mahaney et al., 2000) et plus récent, la mesure des nucléides cosmogéniques *in-situ* (TCN) (Wesnousky et al., 2012; Guzmán, 2013).

L'étude de ces morphologies glaciaires contribue à une meilleure compréhension et reconstruction de la Dernière Glaciation dans les Andes Vénézuéliennes. La reconstruction de la Dernière Glaciation (connue dans la région comme Glaciation Mérida) était limitée par la disponibilité de chronologie glaciaire. Cette thèse a pour objet de proposer des reconstructions de l'activité glaciaire depuis la Dernière Glaciation et ainsi contribuer à la connaissance du paléoclimat dans une zone cruciale comme les Andes tropicales de Mérida.

La nécessité d'acquérir de nouvelles données est un impondérable pour reconstruire les avancés ou les reculs glaciaires. La géochronologie par TCN est une option appropriée

car les roches sont riches en Quartz et donnent, dans la majorité des cas, des âges sans ambiguïtés avec les processus dynamique étudiés (mouvements dynamiques des glaciers du Pléistocène supérieur).

Le but de cette thèse est de contribuer à: 1) reconstruire les dynamiques des glaciers depuis le Pléistocène Supérieur, 2) identifier les fluctuations glaciaires et établir les causes de l'évolution des couvertures glaciaires. 3) établir des comparaisons entre différents enregistrements paleoclimatiques locaux, régionaux et globaux.

A partir de l'acquisition de nouvelles données, nous avons tenté de répondre aux questions scientifiques suivantes:

- Quelles sont les dynamiques de déglaciation dans les Andes centrales de Mérida pendant le Pléistocène?
- Combien et auxquelles altitudes les principaux stades glaciaires ont été identifiés?
- Quelles informations apportent ces reconstructions pour la compréhension du paléoclimat?

Pour répondre toutes ces questions, nous avons daté une sélection de morphologies glaciaires avec la technique des nucléides cosmogéniques produits *in-situ* (^{10}Be). Les conditions paleoclimatiques ont été établies sur la base de calculs de paléo-lignes d´Equilibre (ELA).

L´organisation du manuscrit est divisée en trois Parties (Partie I, Partie I et Partie III), à savoir:

Partie I: Introduction générale et méthodes. Cette section apporte une description globale des glaciations et du paléo-climat, ainsi qu'un cadre générale de la géologie de la zone d'étude.

Partie II: "Résultats"

Cette section détaille les différents paramètres nécessaires à l'obtention des données chronologiques. Cette section présente aussi la morphologie glaciaire étudiée et les résultats du paléo LEG (Ligne d´Equilibre Glaciaire, ELA sigles en anglais).

Une partie de cette section est présentée sous la forme de 2 articles :
Carcaillet, J., **Angel, I**., Carrillo, E., Audemard, F.A. and Beck C. 2013. Timing of the last deglaciation in the Sierra Nevada of the Mérida Andes, Venezuela. *Quaternary Research*, Vol. 80(3): 482-494.

Angel, I., Audemard, F., Carcaillet, J., Carrillo, E., Beck, C., Audin, L. Deglaciation chronology in the Gavidia valley, Mérida Andes, Venezuela, inferred from cosmogenic ^{10}Be dating. En revision. Journal of South American Earth Sciences.

Partie III: Discussions.
Nous avons défini quelques corrélations avec le paléoclimat local, régional et global. En plus, nous avons discuté les différents facteurs climatiques et geomorphiques qui contrôlent les différentes histoires de deglaciation.

Une partie de ces travaux doctoraux ont été présentés lors des congrès nationaux et internationaux suivants:

- **Angel, I.**, Carcaillet, J., Carrillo, E., Audemard, F. and Beck, C. Glacial chronology in the Mérida Andes, Venezuela, deduced from cosmogenic ^{10}Be radionuclide dating. 8th IAG, International Conference on Geomorphology, Paris, France 2013.

- **Angel, I.**, Carcaillet, J., Carrillo, E., Audemard, F. and Beck, C. Glacial chronology deduced from cosmogenic ^{10}Be radionuclide dating in La Culata, Gavidia and Mucubají valley, Venezuelan Andes. Nordic Workshop on Cosmogenic Nuclide Dating, Aarhus, Denmark, 2014.

- **Angel, I.,** Audemard, F., Carrillo, E., Carcaillet, J. and Beck, C.. El isótopo cosmogénico ^{10}Be en la cronología de morfología glaciar en los valles de Gavidia y La Culata, Andes Venezolanos. 1er Congreso Venezolano de Geoquímica, Caracas, Venezuela, 2014.

- **Angel, I.**, Carcaillet, J., Audemard, F., Carrillo, E., Condom, T., Audin, L. and Beck, C. Asynchronous deglaciation histories in the central Venezuelan Andes. XIX INQUA Congress, Nagoya, Japan, 2015.

- **Angel, I**., Carrillo, E., Carcaillet, J., Audemard, F.A. & Beck C. 2013. Geocronología con el isótopo cosmogénico ^{10}Be, aplicación para el estudio de la dinámica glaciar cuaternaria en la región central de los Andes de Mérida. GEOS. Vol-44: 73-82.

Caractéristiques géologiques, paléoglaciologiques, climatiques et paleoclimatiques des Andes de Mérida.

Cadre géologique

Les Andes de Mérida constituent une Cordillère située dans le sud-ouest du Venezuela et orientée sur près de 400 km selon un axe SW-NE. Le point culminant est le Pico Bolívar (4978 m a.s.l.). Les Andes de Mérida sont constituées par un système cristallin de gneiss Précambrien, de schistes et roches plutoniques datant du Paléozoique au Mésozoique. La zone interne métamorphique est entourée par roches calcaires et clastiques du Jurassique et Crétacée, ainsi que par des sédiments Quaternaires (Hackley et al., 2006). L´orogenèse est liée à l´interaction géodynamique des plaques du Panamá, Caraïbe et Amérique du Sud (Taboada et al., 2000; Audemard and Audemard, 2002; Bermudez, 2009; Monod et al., 2010).

La tectonique des Andes de Mérida est principalement accommodée par la faille décrochant de Boconó, orientée NE-SW sur ~500 km de longueur (Audemard and Audemard, 2002). Les déplacements dextres sont mis en évidence par les déformations de cordons morainiques et dépôts alluviaux, ainsi que la déviation des réseaux hydrographiques. Les déplacements cumulés sont estimés entre 60 m et 1000 m en fonction des zones (Audemard and Audemard, 2002) avec des taux de déplacements Quaternaire entre 3 and 14 mm/a (Audemard, 2003).

Glaciations dans les Andes de Mérida

Les études de glaciations ont commencé à la fin du XIX^{ème} siècle (e.g. Sievers, 1885). Jahn (1925 et 1931) réalise les premières estimations des couvertures glacières existantes à l´époque. Schubert (e.g. 1972; 1974; 1975; 1980; 1992 et 1998) a développé plusieurs études glaciologiques dans la région. Les évidences

géomorphologiques liées aux glaciations ont été observées aux Andes de Mérida au-dessus de ~2500 m. Les moraines sont les principales morphologies observées entre ~2500 m et ~3500 m. Au-dessus le paysage est dominé par une géomorphologie d´érosion glacière (e.g. vallées en auge, roches moutonnées, cryoclastie) (Schubert and Vivas, 1993).

Les principales études approfondies ont concernés les morphologies associées à la Dernière Glaciation (e.g. Kalm and Mahaney, 2011). Cette période est connue dans la région comme la "Glaciation Mérida" et est traditionnellement identifiée à partir de deux cordons morainiques situés entre 2600 et 3500 m (Schubert, 1974). Le cordon situé entre 2900-3500 m est caractérisé par un till frais et chronologiquement lié aux avancées glaciaires pendant les MIS 1, MIS 2 (Glaciation Mérida Supérieure) (Schubert, 1974). Le cordon situé entre 2600 et 2800 m, est caractérisé par un till plus météorisée, généralement couvert d'une végétation plus dense et chronologiquement liée aux avancées glaciares pendant les MIS 4 et MIS 5 (Glaciation Mérida Inferieure) (Schubert, 1974).

Paléoclimat

Les études paléoclimatiques sont basées à partir d'analyses de sédiments lacustres, fluviatiles, glaciaires (e.g. Schubert, 1974; Schubert and Valastro, 1980; Salgado Labouriau, 1984; Bradley et al., 1985; Salgado-Labouriau, 1989; Weingarten , 1990; Yuretich, 1991; Salgado-Labouriau et al., 1992; Rull, 1995; Mahaney et al., 2000; Dirszowsky, 2005; Rull et al., 2005; Stansell et al., 2005; Mahaney et al., 2007; Carrillo et al., 2008; Rull et al., 2010; Stansell et al., 2010). D'autre part, des reconstructions paléoclimatiques ont été basées à partir du calcul de paléo-ELA (Stansell et al., 2007).

Le paléoclimat avant la Glaciation Mérida Inferieure n´est pas bien connu. Entre la Glaciation Mérida Inferieure et Supérieure, il a été identifié l'interstade "El Pedregal" (Dirszowsky et al., 2005; Rull, 2005). À partir d'analyses sédimentologiques et géochronologiques de 8 m de sédiments lacustres de la section PED5 (Mesa del Caballo). Le Dernier Maximum Glaciaire a été établi par l´étude palynologique de la section PED5 entre 22.75 and 19.96 Cal ka BP (Schubert et Rinaldi, 1987). Les

températures étaient ~ 9º inférieures à celles constatées d'aujourd´hui (Stansell et al., 2007).

Une période froide (El Caballo Stadial, 16.5±0.3 ka BP) a été identifiée sur la base d'études palynologiques de sédiments de la zone de Mesa del Caballo . (Rull, 1998). La température était alors 7ºC inférieure à celle d'aujourd´hui (Rull, 1998). Une autre période froide a été identifiée à 12.65 ka BP basée sur l´étude paléocologique d´une terrasse alluviale de la vallée de Mucubají (Salgado-Labouriau et Schubert, 1977). Cette période a été caractérisée par des températures 2.9ºC inférieures aux températures actuelles. Rull et al. (2005, 2010) ont associé cette période au Younger Dryas. Des conditions froides ont aussi été déterminées dans la Laguna Los Anteojos à 3900 m (Sierra Nevada) entre 12.86 ka et 11.65 ka (Stansell et al., 2010; Rull et al., 2010). Les calculs de paléo-ELA montrent un abaissement de la Paléo-ELA de 360 à 480 m par rapport aux valeurs actuelles (Stansell et al., 2010) associées à des températures inférieures de 2.2 à 3.8 ºC (Stansell et al., 2010; Rull et al., 2010). Le Younger Dryas a aussi été identifié dans les sédiments du lac de Mucubají par un accroissement de la susceptibilité magnétique entre 11.6 et 12.8 ka BP (Carrillo et al., 2008). Ces même sédiments indiquent un retour à des conditions plus tempérées au début de l'Holocène (Carrillo et al., 2008). Les analyses palynologiqes indiquent que la végétation établie durant l´Holocène est similaire à celle observée actuellement (Salgado-Labouriau et al., 1988, 1992; Rull, 1999). Quelques courts épisodes froids ont été identifiés entre 6.0 et 5.3 ^{14}C ka BP (La Culata cold/dry phase; Salgado-Labouriau and Schubert, 1976).

Conditions climatiques actuels

Le climat de la ceinture intertropicale est principalement contrôlé par la Zone de Convergence Intertropical (ITCZ). Cette zone est très dépendante des variations saisonnières du cycle solaire (Benn et al., 2005). Alors que les variations saisonnières de températures dans les Andes de Mérida ne sont pas très significatives, les variations journalières peuvent atteindre 20 ºC (Schubert and Clapperton, 1990). Ces variations de températures sont associées à l´insolation, la radiation solaire et la nébulosité (Monasterios and Reyes, 1980).

L´humidité provient de l´évaporation de l´Atlantique tropical et l´évapotranspiration du bassin de l'Orénoque, cette humidité est transportée vers les Andes par les alizés (Pulwarty et al., 1998). Le climat actuel est aussi influencé par les températures de surface de l´Océan Pacifique Equatorial (Polissar et al., 2013). Les précipitations sont saisonnières avec un maximum pendant l´été boréal et un minimum pendant l´hiver (Pulwarty et al., 1998). Cependant, Poveda et al. (2006) ont établi aussi un maximum de précipitations pendant l´automne d´Hémisphère Nord. Les modèles de précipitation sont aussi contrôlés par les caractéristiques orographiques, ainsi que les circulations atmosphériques locales (Pulwarty et al., 1998; Poveda et al., 2006).

Méthodologie

Pour établir les chronologies glaciaires et reconstruire la dynamique des paleo-glaciers, il est nécessaire d'impliquer des études géomorphologiques et géochronologiques. Les reconstructions paléoclimatiques dans ce manuscrit sont obtenues à partir d´une analyse de paléo lignes d´equlibrium glaciaire (LEG) et la comparaison avec les enregistrements proxy paléoclimatiques. Les datations de morphologies glaciares ont été réalisées par la mesure des nucléides cosmogéniques produits *in-situ* (béryllium-10, ^{10}Be).

Géochronologie par la mesure des nucléides cosmogéniques produits *in-situ* (TCN, Terrestrial Cosmogenic Nuclides)

Cette méthode est particulièrement adaptée car la lithologie des sites est riche en quartz (minérale cible pour l'extraction) et parce que l'intervalle optimum de la méthode (<100 ka) est particulièrement adaptée à la question scientifique.

Le ^{10}Be est formée par l´action des rayonnements cosmiques avec les atomes de silice et d'oxygène des premiers mètres de la lithosphère (Dunai, 2010). Le taux de production adapté à la datation dans la ceinture intertropicale a fait l'objet de nombreuses améliorations ces dernières années. Les valeurs considérées aujourd'hui varient entre 3.63±0.17 at.g^{-1}.yr^{-1} (Blard et al., 2013) et 3.97±0.09 at.g^{-1}.yr^{-1} (Kelly et al., 2013). Au début de ce travail doctoral, ces taux de production n'étaient pas encore publiés et les premières données ont été calculées avec le taux de production global de Balco et al. (2008) (4.39 ± 0.37 at.g^{-1}.yr^{-1}). Finalement tous les âges ont été recalculés avec un taux de production similaire (Kelly et al., 2013). Ce taux a été utilisé parce que

est cohérent avec les taux de production disponibles pour les Andes tropicales et sa calibration était disponible sur le code de calcul en ligne « CRONUS online calculator » (Balco et al., 2008).

Les mesures de concentration du ^{10}Be ont été réalisées par spectrométrie de masse avec un accelerateur de particules. Les échantillons ont été préalablement broyés, tamisés et séparés des minéraux magnétiques. Une fois le quartz est isolé des autres minéraux (par attaques acides successives) et dissout, le béryllium a été extrait par passage dans des résines échangeuses d'ions.

Géomorphologie et reconstruction des paléoglaciers

Les investigations géomorphologiques ont été réalisées à partir de photographies aériennes, d'observation de terrain et de modèles de terrain. Ceux-ci ont permis de sélectionner les sites d'étude et d'identifier les zones à forte densité de morphologies glaciaires. D'autre part, ces observations ont permis de faire les polygones des paleoglaciers pour les déterminations des paléo ELA.

Les reconstructions des paléoglaciers nécessitent la reconstruction des surfaces et des épaisseurs. Pour les surfaces, les délimitations des bassins versants ont été faites à l'aide de River Tools et ArcGis. Les reconstructions des épaisseurs de glace ont été basées sur les travaux de Benn et Hulton (2010), ce modèle proposé se base sur le comportement plastique de la glace en réponse à une l'application d'une force de contrainte. Les forces nécessaires pour engager une déformation sont proportionnelles à la densité de la glace, à la gravité et l´épaisseur. Pour la détermination des épaisseurs de glace, on considère que la force qui exerce les glaciers actuels est entre 50 et 150 kPa. Puisque la densité de la glace et la gravité sont connues, il est alors possible de déterminer l´ épaisseur de glace.

Les contours sont dessinés en fonction du comportement des glaciers actuels, concave dans la zone d´accumulation et convexe dans la zone d´ablation chaque 100-200 m.

Méthodes pour la reconstruction des Paléo Ligne d´Équilibre (LEG)

La reconstruction des paléo-ELA a été réalisée pour les vallées de Mucubají, Mucuchache et Mifafí. La paléo-ELA a aussi été calculé ponctuellement pour les moraines de Los Zerpa, La Victoria, El Caballo et La Canoa. L´objectif a été de faire inférences des conditions paleoclimatiques tout au long de Sierra Nevada et Sierra del Norte-Cordillera de Trujillo.

Les calculs de paléo LEG ont été réalisés à partir d'"Accumulation Area-Ratio" (AAR) et de "Area-Altitude Balance Ratio" (AABR). L´AAR assume qu'à l´état stationnaire, la zone d´accumulation du glacier occupe une proportion fixe de la surface du glacier. Pour les glaciers de hautes et moyennes latitudes, ce rapport est normalement autour 0.55-0.65 (Porter, 1975). Cette valeur est accompagnée d'une incertitude importante pour les glaciers tropicaux, mais considérant l'hypothèse d'une ablation plus importante et d'une accumulation plus basse dans les zones tropicales, les rapports sont considérés plus hauts que les rapports pour glaciers de moyenne et haute latitudes, avec des valeurs de 0.8 (Kaser and Osmaston, 2002).

La méthode AABR considère les gradients de bilan de masse et l´hypsométrie du glacier. Cette méthode est basée sur le fait que les gradients d´accumulation (b_c) et d'ablation (b_a) (BR= b_a/b_c) sont linéaires et connus. Comme la méthode AAR, les valeurs d'AABR ne sont pas bien déterminées dans la zone tropicale, jusqu'à présent les valeurs de bilan de masse (BR) sont > 3 (Kaser and Osmaston, 2002).

Les calculs des paléo-ELA ont été faits à l'aide d'un code disponible sous ArcGis (Pellitero et al., 2015).

En considérant l´incertitude associée aux calculs en fonction des différents paramètres, les valeurs utilisées dans le cadre de ce projet sont entre 0.73-0.82 (AAR) et 5 et 10 (AABR).

Résultats et discussions

Pour quoi la morphologie glaciaire a été étudiée?

L'histoire de deglaciation des Andes centrales de Mérida est encore à explorer parce qu'il existe de grandes carences en données chronologiques. Plusieurs vallées ont été étudiées dans le cadre de ce projet: la vallée de Mifafí (6 échantillons) dans la Sierra del Norte et, dans la Sierra Nevada les vallées de Mucubají (14 échantillons), Mucuchache (7 échantillons) et Gavidia (24 échantillons). Le choix de ces vallées permet d'avoir une vision globale des dynamiques glaciaires. La Sierra Nevada est la zone la plus étudiée car il s'agit du massif où sont encore présents les derniers glaciers vénézuéliens (moins de 0.017 km^2, Braun et Bezada, 2013).

Pour contribuer à la reconstruction de la Glaciation Mérida, une partie de l'échantillonnage a concerné la Sierra Nevada, Sierra del Norte (moraines El Desecho, 3 échantillons et La Culata, 12 échantillons) et Cordillera de Trujillo (Moraines de Pueblo Llano, 6 échantillons- Moraine La Canoa, 2 échantillons). Dans Sierra de Santo Domingo, il a été étudié les moraines de Los Zerpa (3 échantillons) et de Las Tapias (3 échantillons). Dans la partie Sud-Ouest, les moraines El Caballo (3 échantillons), Mucubají et Mucuchache ont été échantillonnées.

Les morphologies glaciaires échantillonnées sont principalement des blocs morainiques et des surfaces polies par le glacier (roches moutonnées). Les échantillons ont été collectés suffisamment haut pour minimiser les potentiels recouvrements par des dépôts superficiels.

Histoires de deglaciation

Les âges d'abandon des morphologies glaciaires varient entre 9.5±1.1 et 83.7±3.4 ka. Plus précisément dans les âges déduits sont dans la Sierra Nevada entre 9.5±1.1 et 37.0±1.6 ka, la Sierra del Norte entre 16.0±0.6 et 19.2±2.1 ka et la Cordillera de Trujillo entre 17.6±1.6 et 83.7±3.4 ka.

Plusieurs dynamiques glaciaires ont été identifiées dans les Andes centrales de Mérida. Dans les vallées de Mucubají et Mucuchache, la dynamique est caractérisée par plusieurs épisodes d'avancé-arrêt des langues glaciaires durant le recul général du glacier. Dans les vallées de Gavidia et Mifafí, la disparition des glaciers semble avoir été très rapide avec des vitesses de recul longitudinal extrêmement importantes (entre 4-7 km/ky). Divers caractéristiques morphométriques, tel que la pente du fond de la vallée, la topographie de la zone d´accumulation (cirques glaciaires avec les versants très abruptes), des surfaces d´accumulation et son orientation, ont aussi contrôlé les différents dynamiques glaciaires.

Les variations de comportement dynamiques des paléo-glaciers semblent effectives au moins depuis le MIS 3. Dans les vallées de Mucubají et Mucuchache, la présence de nombreux cordons morainiques frontaux suggère que les paléo-glaciers ont reculé graduellement. Dans la vallée de Mucubají, des évidences d'activité glaciaire ont été datées entre le Dernière Maximum Glaciaire (LGM) et l´Holocène au moins jusqu'à 6 ka. Dans la vallée de Mucuchache, le retrait du glacier semble plus précoce avec des âges d'abandon situés entre MIS 3 et le LGM-OtD (Oldest Dryas). Dans la vallée de Gavidia, le glacier est reculé rapidement entre 21 et 16.5 ka. La partie supérieure de la vallée de Mucuchache n´a pas donné chronologiques disponibles. L´histoire de la deglaciation a donc été établie jusqu'à 18 ka. Le glacier de la vallée de Gavidia a reculé rapidement avec une disparition extrêmement rapide entre 16.5 ka et 16 ka. Une accélération a aussi été observée dans la vallée de Mifafí, où les vitesses de recul des glaciers ont significativement augmenté entre 17-18 ka (4-7 km/ky). Dans les vallées de Gavidia et Mifafí, la disparition complète des paleoglaciers a eu lieu pendant une période de 0.5-1 ka. Ces vallées présentent des caractéristiques morphométriques similaires comme la topographie du cirque glaciaire et l'orientation NE-SO de la zone d´accumulation. Cette configuration entraine une augmentation de radiation solaire dans les zones d´accumulation en comparaison avec les vallées de Mucubají et Mucuchache (orientation NO-SE). Une comparaison des courbes hypsométriques des paleoglaciers de Mucubají, Mucuchache et Mifafí entre 17-18 ka indique que les vallées de la Sierra Nevada (Mucubají, Mucuchache) ont des valeurs entre 60-70%, alors que pour Mifafí cette valeur était de 20%. Les plus basses surfaces de la zone d´accumulation ont contrôlé aussi le recul rapide du paléo glacier.

D’autres caractéristiques mophométriques comme la pente du fond de la vallée et l´orientation, semblent aussi contrôler les dynamiques glaciaires.

Les moraines observées entre 2500-4200 m permettent de pointer des avancées glaciaires. Les avancées glaciaires observées pendant le MIS 3 (dans la Sierra Nevada) sont liées à l’accroissement des précipitations dans le nord de l´Amérique de Sud en lien avec l´activité de la Zone de Convergence Intertropicale. Ces avancées sont aussi liées aux conditions plus chaudes et humides dans l´Hémisphère Nord, qui dans les Andes vénézuéliennes correspondent à l´Interstade "El Pedregal". De nombreuses évidences d’avancées glaciaires pendant le Dernier Maximum Glaciaire ont été enregistrées dans la Sierra Nevada á Mucubají et Las Tapias entre 3100-3600 m. Elles ont été reliées aux températures froides observées dans l´Hémisphère Nord, ainsi que dans les carottes des glaciaires tropicaux.

Reconstruction des glaciations aux Andes centrales de Mérida

Jusqu’à présent, les avancées glaciaires correspondant Younger Dryas ont été reconnues dans la Sierra Nevada à des altitudes supérieures à 3860 m (3862 m et 4000 m dans la vallée de Mucubají et le Massif d’Humboldt respectivement). Les avancées glaciaires correspondant à l´OldestDryas-LGM ont été identifiées dans la vallée de Mucubají entre 3570 m et 3620 m, alors que ces avancées semblent être plus basses dans la Sierra de Santo Domingo (3100 m), la Sierra del Norte (3100 m et 3500 m) et dans la Cordillera de Trujillo (2400 et 2800 m). Les avancées glaciares pendant le MIS 3 sont observées en Sierra Nevada à la vallée de Mucuchachce et El Caballo entre 3400-3600 m. en Cordillera de Trujillo à 2800 m. Les glaciations plus anciennes que MIS 5 ne sont pas suffisamment documentées. Les seules évidences correspondent avec la section LAG à Mesa del Caballo (3500 m).

A l’échelle régionale, la relation entre les avancées glaciaires et l’altitude n´est pas évidente. Les évidences d’avancées glaciaires datées MIS 4, MIS, 3 et MIS 2 sont quelques fois localisées à des altitudes très similaires. La Glaciation Mérida a été décrite sur la base de deux complexes morainiques situés entre 2600-3500 m (Schubert, 1974). La Glaciation Mérida a été subdivisée (Mérida Supérieure et Inferieure), basée sur les âges radiocarbonique de ces deux complexes morainiques (entre 24-13 cal kyr BP ;

Schubert, 1974). La Glaciation Mérida a été aussi corrélée avec des moraines observées dans les Andes Colombiennes à 2600-2800 m (Glaciation Mérida Inférieure) et à 2900-3500 m (Glaciation Mérida Supérieure). La définition de la Glaciation Mérida a été une première bonne approximation pour comprendre la glaciation aux Andes vénézuéliennes. Toutefois, les âges de deglaciation récemment obtenues par Guzmán (2013) ou dans ce projet indiquent qu'un travail est encore nécessaire pour clairement comprendre les modalités d'extension de la glaciation Mérida. Les âges d´exposition des moraines de Pueblo Llano semblent indiquer que les glaciers sont arrivés à des altitudes plus basses (jusqu'à 2300 m) que celles décrites jusqu'à présent (2600 m, Schubert (1974)).

Les avancées glaciaires pendant le MIS 3 (observées à Mucuchache, El Caballo et Pueblo Llano) donnent de nouvelles informations sur la chronologie de la Glaciation Mérida. Si on considère la définition originale établie par Schubert (1974), Mucuchache (3400 m) et El Caballo (3600 m) seraient liés à la Glaciation Mérida Supérieure alors que les moraines de Pueblo Llano (2500 m) seraient liées à la Glaciation Mérida Inférieure. La nouvelle chronologie glaciaire acquise dans le cadre de ce projet indique que l'abandon de ces moraines a eu lieu durant l'Interstade El Pedregal identifié aux Andes de Mérida entre 25-60 ka (Dirszowsky et al., 2005; Rull, 2005).

La plupart des avancées maximales des glaciers ont été identifiées à des âges plus jeunes que le LGM *sensu stricto,* particulièrement pendant la période LGM-OtD (17-19 ka). Des avancées maximales des glaciers observées dans les Andes de Mérida sont similaires aux autres décrites dans les Andes Tropicales. Dans les Andes Equatoriennes, Péruviennes et Boliviennes, les avancées maximales des glaciers ont eu lieu principalement pendant le MIS 3. Une autre similarité est les peu d'évidences géomorphologiques associées au Younger Dryas.

Paléo Ligne d´Equilibre Glaciaire (ELA en anglais)

Les valeurs de paléo-ELA pour chaque méthode (AAR, AABR) de chaque paleoglacier ne montrent pas de différences significatives et permettent de déterminer une paleo ELA pondérée. En général, les valeurs sont 3475±27 m pour la moraine de La Canoa et 4397±33 m pour la vallée de Mifafí.

Dans la Sierra Nevada, les valeurs de paléo-ELA sont assez similaires. A 30 ka la paleo-ELA était à 3765±37 m (Mucuchache) et 3839±20 m (El Caballo) et, entre 20-22 ka à 3882±27 m (Mucuchache) et 3808±39 m (Mucubají). Des différences plus significatives existent entre les paléo-ELA calculées dans les Sierras Nevada et Santo Domingo (e.g.à 18 ka Mucuchache ELA=3965±30 m et La Victoria ELA=3669±24 m).

Contribution paléoglaciologique à l'enregistrement paléoclimatique des Andes centrales de Mérida

Les conditions paléoclimatiques comme la température et la précipitation peuvent être déterminées à partir des analyses des paléo ELA (e.g. Lachniet Vazquez-Selem, 2005; Stansell et al., 2007; Smith et al., 2011). Toutefois, il est important de rappeler que dans la région intertropicale, les rapports utilisés pour calculer les Paléo-ELA (AAR et AABR) demandent à être encore précisés (e.g Rea et al., 2009). Les interprétations paléoclimatiques sont donc accompagnées d'incertitudes significatives et non quantifiables.

Les valeurs des paléo-ELA déterminées dans ce travail sont du même ordre de grandeur que celles publiées par ailleurs (e.g. Lachniet et Vazquez-Selem, 2005; Stansell et al., 2007). Les changements de températures, précipitation, radiation solaire ou la combinaison de ces facteurs sont les responsables principaux de la variabilité des glaciers tropicaux (Kaser et Osmaston, 2002).

La valeur la plus basse des paléo ELA (3765±37 m) a été calculée pour la vallée de Mucuchache pendant le MIS 3. Cette valeur est liée aux conditions climatiques plus chaudes par rapport au LGM (réchauffement relatif de 5º C; Dirszowsky et al., 2005; Rull, 2005) et plus humides par rapport au LGM ou post-LGM. Par conséquent, les avancées glaciaires à la vallée Mucuchache et El Caballo semblent être contrôlées par la variation de la paléo-précipitation.

Les différences les plus significatives des paléo-ELA sont observées pour les périodes Post-LGM (<18 ka). Les variations des paléo-ELA observées entre la Sierra Nevada et Santo Domingo ont été attribuées aux variations significatives de régimes des

précipitations entre ces sierras, de chaque côté du col de Mucubají (Lachniet et Vazquez-Selem, 2005). Stansell et al. (2007) suggèrent que ces différences dans les valeurs des paléo-ELA ont été produites par les différences de paléo-températures.

Les valeurs de paléo-ELA de la Sierra del Norte présentent des différences plus importantes par rapport aux paléo-ELA de la Sierra Nevada et de la Cordillera de Trujillo. Ces différences indiquent que les régimes de précipitation sont différents dans les vallées entre 16 et 19 ka. La vallée de Mifafí (Sierra del Norte) a été le secteur le plus sec. Les secteurs les plus humides sont la Sierra de Santo Domingo et la Cordillera de Trujillo. Ce modèle de paléo-précipitation est similaire aux conditions climatiques actuelles observées dans les Andes centrales de Mérida.

Conclusions et Perspectives

Cette thèse contribue à détailler la Dernière Glaciation dans les Andes de Mérida. Les chronologies ont été obtenues par datation ^{10}Be de morphologies glaciaires. Les 100 échantillons ont permis d'apporter des données inédites, lesquelles constituent un complément des données publiées. Les résultats et ses interprétations paléoglaciologiques permettent aussi de progresser dans la connaissance paléoclimatique des Andes centrales de Mérida.

Histoires de déglaciation, origines et variabilités

La déglaciation pendant le Pléistocène Supérieur montre des dynamiques variées. Dans la vallée de Mucubají, le retrait glaciaire s'est établi en deux étapes. La période LGM / Late Glacial (~15 ka) montre un retrait de ~25 m/ka. Entre 15 ka et 11 ka le retrait du glacier a été significativement plus rapide (~310 m/ka).

Dans la vallée Mucuchache, l'extension maximale a été datée vers 36 ka. Le retrait glaciaire a été documenté entre le MIS 3 (~36 ka) et MIS 2 (~18 ka) avec une vitesse de recul ~0.25 km/ka. L´absence de moraines (à l'exception de placage morainiques latéraux d'extension limitée) pour les vallées de Mifafí et de Gavidia indiquent que la dynamique n´a pas été caractérisée par des longues périodes d'arrêt-avancée pendant le recul général des paléo glaciers. Dans la vallée de Gavidia, la deglaciation s'est établie en deux différents périodes. Pour la première (21 ka ~16.5 ka), le recul était de ~0.26

km/ka. Durant la deuxième période entre ~16.5 ka- ~ 16 ka, le glacier a reculé de façon extrêmement rapide (~4.7 km/ka). Dans la vallée de Mifafí (Sierra del Norte), les données suggèrent la disparition du paléo glacier la plus rapide observée (~7 km/ka).

L'origine de différences de comportement des glaciers pourrait être expliquée par les différentes orientations des zones d´accumulation et de pentes du fond des vallées.

Reconstruction de la Dernière Glaciation (Glaciation Mérida)

Les avancées glaciaires du MIS1 jusque MIS 4 ont été reconnues entre 2500-4200 m. Le MIS 4 a été identifié dans la vallée de Pueblo Llano (2500 m). Le MIS 3 a été localisé pour la première fois dans la Sierra Nevada entre 3400-3600 m (Mucuchache et El Caballo). Le MIS 2 est localisé entre 2460-3620 m. L´impact du LGM *sensu stricto* dans les Andes centrales de Mérida est observé dans les vallées de Mucubají (3600 m) et Las Tapias (3100 m). Une période très importante d'avancées glaciaires a été observée pendant l´OtD-Estadío El Caballo autour 17 ka (La Culata entre 3100-3400 m; Sierra de Santo Domingo ~ 3100 m et La Canoa ~2800 m). Les avancées glaciaires pendant le MIS 1 sont très peu documentées. Juste quelques évidences ont été observées dans la Sierra Nevada (Vallée de Mucubají à 3800 m) correspondant au Younger Dryas.

Contribution paléoglaciologique à l'enregistrement paléoclimatique des Andes centrales de Mérida

Pendant le LGM, des conditions climatiques similaires ont été déduites dans les vallées de Mucubají et Mucuchache (Sierra Nevada). Cette déduction est basée sur le calcul de valeurs similaires de paléo-ELA (3882±27 m et 3808±39 m, respectivement). Ces conditions climatiques ont été plus différentes pendant le post-LGM. Les patrons de précipitation entre les 16-19 ka (LGM-OtD-El Caballo) semblent être similaires aux conditions actuelles. Les secteurs les plus humides sont localisés dans la Sierra de Santo Domingo-Cordillera de Trujillo et les plus secs dans la vallée de Mifafí.

Les avancées glaciaires décrites durant le MIS 3 et MIS 4 ont été associées à une forte activité de la Zone de Convergente Intertropicale. Les avancées glaciaires observées durant le MIS 2 ont été associées aux températures basses dans l´Hémisphère Nord et les Andes tropicales.

Perspectives

Plus de questions scientifiques sont créés après cette thèse. Beaucoup de vallées glaciaires présentent des morphologies héritées de l'activité glaciaire, qui nécessitent de poursuivre les campagnes de datation. Cette situation ouvre une possibilité de faire plus des missions sur le terrain pour améliorer la chronologie glaciaire dans les différentes vallées des Andes vénézuéliennes. Il serait plus intéressante d´étudier la dynamique glaciaire avant le LGM et pendant le YD.

Concernant le topique de paléoclimat tropical, les résultats de cette thèse pourraient contribuer pour la quantification des conditions paléoclimatiques avec les valeurs de paléo ELA et la modélisation des glaciers (e.g. Plummer et Phillips, 2003). Il serait aussi très productif d'intégrer les valeurs des isotopes stables obtenues pendant le développement de cette thèse avec une collaboration avec le CSIC (Espagne).

La chronologie glaciaire obtenue avec ce travail de recherche peut être utilisée aussi pour faire des études de la Néotectonique aux Andes centrales de Mérida. Aussi cela a permis de faire des études de recherche pour déterminer les volumes d´eau libérée pendant la deglaciation, étudier les balances hydrologiques et de transport des sédiments.

Introducción

El cambio climático impacta en la sociedad de diferentes maneras; por ejemplo: en la temática de riesgos naturales, en la disponibilidad de recursos hídricos y en la disponibilidad de territorios en las zonas costeras. El clima terrestre está controlado por la radiación solar. La zona intertropical recibe la mayor cantidad de radiación solar y el calor es distribuido hacia los Hemisferios Sur y Norte gracias a la circulación oceánica y atmosférica.

Estudios han señalado la posible importancia de la zona intertropical para propagar las glaciaciones entre los Hemisferios, esto es debido a las posibles variaciones de la humedad atmosférica en esta región que genera la disminución de la radiación (Uriarte, 2003). Los cambios climáticos durante la Última Glaciación también han sido asociados a la reorganización de la atmósfera en la región tropical y las modificaciones de la Circulación Meridional del Atlántico (AMOC, siglas en onglés) (Chiang, 2009). Es por esto, que es importante estudiar el clima en la zona intertropical, para comprender el funcionamiento pasado, presente y futuro del clima a nivel global. Avances científicos en esta temática permitirán generar modelos climáticos más realistas y, esto conllevará, a realizar predicciones climáticas que permitan mitigar el impacto del cambio climático en la sociedad (e. g. McGregor and Nieuwolt, 1998, Chiang, 2009).

Los glaciares tropicales son reconocidos por su extrema sensibilidad ante los cambios climáticos y por su importancia como recurso hídrico en los altiplanos de Perú y Bolivia (e.g. Hastenrath, 1994; Kaser and Osmaston, 2002). Los glaciares tropicales son un recurso importante para estudiar el paleoclima (Jomelli et al., 2009). Estos estudios paleoclimáticos pueden ser desarrollados utilizando núcleos de hielo (e.g. Thompson et al., 1996; Thompson et al., 1998; Ramírez et al., 2003) o morfología glaciar para realizar la reconstrucción de paleoglaciares (e.g. Stansell et al., 2007; Jomelli et al., 2009).

Condiciones paleoclimáticas pueden ser inferidas a partir de la cronología de la morfología glaciar y la reconstrucción de los paleoglaciares. Los Andes Peruanos, Bolivianos y Ecuatorianos han sido los más estudiados dentro de la región tropical (e.g. Porter, 2001; Mark, B.G., 2008; Jomelli et al., 2009). Al contrario de los Andes

tropicales centrales, Los Andes Venezolanos (conocidos también como Andes de Mérida, MA siglas en inglés) han sido menos estudiados (Porter, 2001; Lachniet and Vazquez-Selem, 2005). Por lo tanto, la reconstrucción de las glaciaciones en los Andes de Mérida contribuye significativamente con el progreso en el conocimiento del paleoclima en la región tropical.

Los Andes de Mérida están caracterizados por la presencia de morfología glaciar preservada entre 2400-4978 m. Actualmente, la mayoría de las descripciones geomorfológicas fueron realizadas por Schubert (e.g. 1972; 1974; 1980; 1980a; 1992 y 1998). Las principales evidencias de la influencia de los glaciares en los Andes de Mérida están representadas por dos complejos morrénicos localizados entre 2600-2800 m y 2900-3500 m. Estos complejos morrénicos fueron atribuidos a las Glaciaciones de Mérida Temprana y Tardía (Schubert, 1970, 1974). En Los Andes de Mérida existe la carencia de cronología glaciar y esto limita la reconstrucción detallada de las glaciaciones en esta región (e.g. Coronato and Rabassa, 2007; Carcaillet et al., 2013). Los estudios geocronológicos están basados principalmente en análisis de radiocarbono (e.g. Schubert, 1970; Salgado-Laboriau and Schubert, 1977; Schubert and Rinaldi, 1987; Rull 1998; Mahaney et al., 2001; Dirszowsky et al., 2005; Stansell et al., 2005; Mahaney et al., 2007; Carrillo et al., 2008), termoluminiscencia (Schubert and Vaz, 1987; Bezada, 1989), luminiscencia estimulada ópticamente (Mahaney et al., 2000) y más recientemente, en los isótopos cosmogénicos producidos *in-situ* (TCN, siglas en inglés) (Wesnousky et al., 2012; Guzmán, 2013).

El estudio de la morfología glaciar en esta región, contribuye significativamente con el entendimiento y reconstrucción de la Última Glaciación (conocida en la región como Glaciación Mérida). Esta tesis tiene como objetivo general reconstruir la dinámica glaciar e historias de desglaciación durante la Última Glaciación y contribuir con el conocimiento del paleoclima en los Andes de Mérida. Para lograr estos objetivos es necesario utilizar un método paleoglaciológico que involucra un análisis geocronológico. La geocronologóa por TCN es una opción apropiada en este caso porque la litología en la región es rica en cuarzo y edades de desglaciación pueden ser obtenidas más exactamente durante incluso todo el Pleistoceno.

Esta tesis tiene como objetivos específicos los siguientes: 1) reconstruir la dinámica de los glaciares desde el Pleistoceno Superior, 2) Identificar las diferencias y posibles causas de las mismas y, 3) realizar correlaciones con los registros paleoclimáticos locales, regionales y globales.

Esta tesis pretende responder las siguientes preguntas científicas:

- ¿Cómo fue la dinámica glaciar en los Andes centrales de Mérida durante el Pleistoceno?
- ¿Qué posibles factores controlarían la dinámica glaciar e historias de desglaciación en la región durante la Última Glaciación?
- ¿Cuántos avances glaciares pueden ser identificados y cómo es su distribución altitudinal?
- ¿Qué inferencias paleoclimáticas pueden ser obtenidas a través del análisis paleoglaciológico?

Para responder a todas estas preguntas, en esta tesis se realizó un estudio geocronológico utilizando el isótopo cosmogénico producido *in-situ* ^{10}Be. Las condiciones paleoclimáticas han sido inferidas a través del análisis de las paleo Líneas de Equilibrio Glaciar (ELA, siglas en inglés).

El manuscrito está dividido en tres partes (Parte I, Parte I y Parte III):

Parte I: Introducción general y métodos. En esta sección se realiza una descripción general de las glaciaciones, el clima tropical y un marco general de la geología de la zona de estudio.

Parte II: "Resultados"

Esta sección detalla los diferentes parámetros necesarios para la obtención de los datos geocronológicos. También presenta la morfología glaciar, su cronología y los resultados de paleo ELA.

Una parte de esta sección está presentada en dos artículos:
Carcaillet, J., **Angel, I**., Carrillo, E., Audemard, F.A. and Beck C. 2013. Timing of the last deglaciation in the Sierra Nevada of the Mérida Andes, Venezuela. *Quaternary*

Research, Vol. 80(3): 482-494.

Angel, I., Audemard, F., Carcaillet, J., Carrillo, E., Beck, C., Audin, L. Deglaciation chronology in the Gavidia valley, Mérida Andes, Venezuela, inferred from cosmogenic ^{10}Be dating. En revisión. Journal of South American Earth Sciences.

Una parte de los resultados de esta tesis doctoral fueron presentados en diversos congresos:

- **Angel, I.**, Carcaillet, J., Carrillo, E., Audemard, F. and Beck, C. Glacial chronology in the Mérida Andes, Venezuela, deduced from cosmogenic ^{10}Be radionuclide dating. 8th IAG, International Conference on Geomorphology, Paris, France 2013.

- **Angel, I.**, Carcaillet, J., Carrillo, E., Audemard, F. and Beck, C. Glacial chronology deduced from cosmogenic ^{10}Be radionuclide dating in La Culata, Gavidia and Mucubají valley, Venezuelan Andes. Nordic Workshop on Cosmogenic Nuclide Dating, Aarhus, Denmark, 2014.

- **Angel, I.,** Audemard, F., Carrillo, E., Carcaillet, J. and Beck, C. El isótopo cosmogénico ^{10}Be en la cronología de morfología glaciar en los valles de Gavidia y La Culata, Andes Venezolanos. 1er Congreso Venezolano de Geoquímica, Caracas, Venezuela, 2014.

- **Angel, I.**, Carcaillet, J., Audemard, F., Carrillo, E., Condom, T., Audin, L. and Beck, C. Asynchronous deglaciation histories in the central Venezuelan Andes. XIX INQUA Congress, Nagoya, Japan, 2015.

- **Angel, I**., Carrillo, E., Carcaillet, J., Audemard, F.A. & Beck C. 2013. Geocronología con el isótopo cosmogénico ^{10}Be, aplicación para el estudio de la dinámica glaciar cuaternaria en la región central de los Andes de Mérida. GEOS. Vol-44: 73-82.

Parte III: Discusiones.

Fueron realizadas correlaciones con el paleoclima local, regional y local. Además, fueron discutidos diferentes factores climáticos y geomórficos que controlan las diferentes historias de desglaciación.

Marco geológico, paleoglaciológico, climático y paleoclimático en los Andes de Mérida.

Marco geológico

Los Andes de Mérida es una cordillera ubicada en el suroeste de Venezuela, la misma está orientada SW-NE y tiene una extensión de cerca de 400 km de largo. El punto más alto es conocido como Pico Bolívar (4978 m a.s.l.). Los Andes de Mérida están constituidos por un sistema cristalino del Precámbrico, esquistos y rocas plutónicas del Paleozóico-Mesozóico. La parte interna está constituida por rocas metamórficas, calcáreas y clásticas del Jurásico-Cretácico y también por sedimentos Cuaternarios (Hackley et al., 2006). La orogénesis está relacionada a la interacción geodinámica de las placas de Panamá, Caribe y América del Sur (Taboada et al., 2000; Audemard and Audemard, 2002; Bermudez, 2009; Monod et al., 2010).

La principal estructura que deforma a los Andes de Mérida es la falla de Boconó, es una falla transcurrente dextral orientada NE-SW con ~500 km de largo (Audemard and Audemard, 2002). La actividad de esta falla se evidencia por la deformación de cordones morrénicos y depósitos aluviales desplazados así como la desviación de ríos. Los desplazamientos acumulados de esta falla han sido estimados entre 60 m et 1000 m (Audemard and Audemard, 2002) con una tasa de deslazamiento durante el Cuaternario entre 3 y 14 mm/a (Audemard, 2003).

Última Glaciación en los Andes de Mérida

Estudios relacionados con la reconstrucción de las glaciaciones comenzaron a finales del siglo XIX (e.g. Sievers, 1885). Jahn (1925, 1931) realizó las primeras estimaciones de la cobertura glaciar existente en la época. Schubert (e.g. 1972; 1974; 1975; 1980; 1992 and 1998) desarrolló diversos estudios de geología glaciar en la región. Las evidencias geomorfológicas que soportan la actividad glaciar has sido observadas tradicionalmente en los Andes de Mérida por encima de los ~2600 m. Dichas evidencias están conformadas principalmente de dos cordones morrénicos entre ~2600 m y ~3500

m. El paisaje por encima de los 3500 m está caracterizado por morfologías de erosión glaciar como por ejemplo valles en u y rocas aborregadas (Schubert and Vivas, 1993).

En los Andes de Mérida la Última Glaciación es la glaciación mejor documentada (e.g. Kalm and Mahaney, 2011). Este período es conocido en la región como la « Glaciación Mérida » vinculado a los dos complejos morrénicos entre 2600 et 3500 m menciondos anteriormente (Schubert, 1974). El cordón situado entre 2900-3500 m está caracterizado por un till fresco correspondiente a avances glaciares ocurridos durante los estadíos isotópicos marinos (MIS en inglés) 1 y 2 (Glaciación Mérida Tardía) (Schubert, 1974). El cordón morrénico entre 2600-2800 m, está caracterizado por un till más meteorizado, cubierto generalmente por una vegetación densa y el cual, corresponde a avances glaciares ocurridos durante los MIS 4 y MIS 5 (Glaciación Mérida temprana) (Schubert, 1974).

Paleoclima

Los estudios paleoclimáticos están basados en análisis realizados en sedimento lacustre, fluvial y glaciar (e.g. Schubert, 1974; Schubert and Valastro, 1980; Salgado Labouriau, 1984; Bradley et al., 1985; Salgado-Labouriau, 1989; Weingarten , 1990; Yuretich, 1991; Salgado-Labouriau et al., 1992; Rull, 1995; Mahaney et al., 2000; Dirszowsky, 2005; Rull et al., 2005; Stansell et al., 2005; Mahaney et al., 2007; Carrillo et al., 2008; Rull et al., 2010; Stansell et al., 2010). Adicionalmente, hay inferencias paleoclimáticas basadas en estudios de paleo ELA (e.g. Stansell et al., 2007).

El paleoclima antes del período correspondiente a la Glaciación Mérida Tardía no es bien conocido. Entre la Glaciación Mérida Tardía y Temprana fue identificado el Interestadío “El Pedregal” (Dirszowsky et al., 2005; Rull, 2005). El mismo, ha sido establecido después del estudio sedimentológico y geocronológico de 8 m de sedimentos lacustres de la sección PED5 (en Mesa del Caballo). El último período glacial (LGM siglas en inglés) fue establecido en la región en base al estudio palinológico de la sección PED5 entre 22.75 y 19.96 Cal ka BP (Schubert and Rinaldi, 1987). Las temperaturas eran ~ 8º más bajas que las temperaturas actuales (Stansell et al., 2007).

Un período frío hace 16.5±0.3 ka BP fue establecido en Mesa del Caballo en base a análisis palinológicos, el mismo fue denominado como el Estadío El Caballo (Rull, 1998). La temperatura era 7ºC más baja que el valor actual (Rull, 1998). Otro período frío fue identificado a 12.65 ka BP en base a estudios palinológicos de terrazas aluviales del valle de Mucubají (Salgado-Labouriau and Schubert, 1977). Este período estuvo caracterizado por temperaturas 2.9ºC más bajas que las temperaturas actuales. Rull et al. (2005, 2010) relacionó este período frío con el Younger Dryas. Condiciones frías fueron igualmente determinadas en la Laguna Los Anteojos a 3900 m (Sierra Nevada) entre 12.86 ka y 11.65 ka (Stansell et al., 2010; Rull et al., 2010). Los cálculos de paleo ELA muestran un descenso de la paleo ELA entre 360-480 m por debajo de los valores actuales (Stansell et al., 2010), este descenso de la paleo ELA estuvo relacionando a un disminución de temperaturas 2.2-3.8 ºC (Stansell et al., 2010; Rull et al., 2010). El Younger Dryas fue identificado también en los sedimentos de la Laguna de Mucubají en base al aumento de los valores de susceptibilidad magnética entre 11.6 y 12.8 ka BP (Carrillo et al., 2008). En estos mismos sedimentos, fue inferido el regreso a condiciones más cálidas durante el inicio del Holoceno (Carrillo et al., 2008). Los análisis palinológicos indican que la vegetación que se estableció durante el Holoceno es similar a la observada actualmente (Salgado-Labouriau et al., 1988, 1992; Rull, 1999). También fue identificado un período corto y frío entre 6.0 y 5.3 ^{14}C ka BP conocido como La Culata (Salgado-Labouriau y Schubert, 1976).

Condiciones climáticas actuales

El clima de la zona intertropical está controlado principalmente por la Zona de Convergencia Intertropical (ITCZ). Esta zona es muy dependiente de las variaciones estacionarias del ciclo solar (Benn et al., 2005). Las mayores variaciones de la temperatura en los Andes de Mérida ocurren diariamente, más que estacionalmente como en las zonas templadas, las variaciones diarias pueden ser de hasta 20 ºC (Schubert and Clapperton, 1990). Estas variaciones de temperaturas están asociadas a cambios de insolación, radiación solar y nubosidad (Monasterios and Reyes, 1980).

La humedad proviene de la evaporación del Atlántico tropical y la evapotranspiración de la cuenca del Orinoco, la humedad es transportada hacia los Andes por los vientos alisios (Pulwarty et al., 1998). El clima actual también está controlado por variaciones

de temperatura en la superficie del Océano Pacífico (Polissar et al., 2013). Las precipitaciones son estacionarias con un máximo durante el verano boreal y un mínimo durante el invierno (Pulwarty et al., 1998). También Poveda et al. (2006) determinó la existencia de un período de lluvias durante el otoño en el Hemisferio Norte. Las precipitaciones en esta región, también están controladas por características orográficas y circulaciones atmosféricas locales (Pulwarty et al., 1998; Poveda et al., 2006).

Metodología

Para establecer cronologías glaciares y reconstruir la dinámica de los paleoglaciares, es necesario realizar análisis geomorfológicos y geocronológicos. Las reconstrucciones paleoclimáticas en este manuscrito son obtenidas a partir de un análisis de las paleo ELA y de comparaciones con registros proxy paleoclimáticos. El método geocronológico utilizado fue el del isótopo cosmogénico producido *in-situ* (berilio-10, ^{10}Be).

Geocronología utilizando el isótopo cosmogénico ^{10}Be producido *in-situ* (TCN, en inglés)

El empleo de este método en esta tesis se debe a que la litología en la región de estudio es rica en cuarzo (mineral objetivo para realizar la extracción del ^{10}Be), mineral en el cual está bien establecida la tasa de producción del isótopo cosmogénico y, porque este método geocronológico funciona bien para estudiar el tiempo geológico de interés en este trabajo (durante el Pleistoceno Tardío hace <100 ka).

El ^{10}Be es formado por la acción de los rayos cósmicos sobre los átomos de silicio y oxígeno en los primeros metros de la litósfera (Dunai, 2010). La tasa de producción del ^{10} Be en la zona intertropical no estaba bien establecida, razón por la cual, la misma ha sufrido diversas actualizaciones en los últimos años. Los valores reportados en la zona intertropical varían entre 3.63±0.17 at.g^{-1}.yr^{-1} (Blard et al., 2013) y 3.97±0.09 at.g^{-1}.yr^{-1} (Kelly et al., 2013). Al principio de este trabajo doctoral, las tasas de producción en la región no estaban publicadas y las primeras edades de exposición fueron calculadas con la tasa de producción global de Balco et al. (2008) (4.39 ± 0.37 at.g^{-1}.yr^{-1}). Al final, todas las edades fueron recalculadas utilizando una tasa de producción similar de Kelly et al. (2013). Esta tasa de producción fue utilizada en el presente trabajo porque es

coherente con las tasas de producción disponibles para los andes tropicales y, su calibración estaba disponible en la página para realizar los cálculos de edades en la página web « CRONUS online calculator » de Balco et al (2008).

Las medidas de concentración del ^{10}Be fueron realizadas por espectrometría de masas utilizando un acelerador de partículas. Las muestras fueron molidas, pulverizadas, tamizadas y separados los minerales magnéticos. Una vez que el cuarzo es aislado de los otros minerales (gracias a varios ataques ácidos sucesivos) y disuelto, el berilio es extraído pasando la muestra por resinas de intercambio de iones.

Análisis geomorfológico y reconstrucción de los paleoglaciares

El análisis geomorfológico fue realizado partir de fotografías aéreas, modelos digitales de terreno y el trabajo de campo. Mediante este análisis fueron identificados los sitios con una densidad alta de morfología glaciar y a través de esta información fueron seleccionados los sitios de estudio. Adicionalmente, el análisis geomorfológico permitió realizar la reconstrucción de los paleoglaciares para realizar la determinación de las paleo ELA.

La reconstrucción de los paleoglaciares necesita la reconstrucción de las superficies y espesores. Para realizar la delimitación de la superficie del paleoglaciar fueron utilizados los programas River Tools y ArcGis. Las reconstrucciones de los espesores de hielo se realizaron en base al trabajo de Benn y Hulton (2010), este modelo contempla el comportamiento plástico del glaciar ante la aplicación de una fuerza. La fuerza necesaria para generar la deformación del glaciar es proporcional a la densidad del hielo, la gravedad y el espesor. Para realizar la determinación de los espesores de hielo, se considera la fuerza actual necesaria para que los glaciares actuales puedan desplazarse, la misma varía entre 50 y 150 kPa. Ya que la densidad del hielo y la gravedad son valores conocidos, es entonces posible determinar los valores de espesores del paleoglaciar.

Las curvas de nivel de la superficie del paleoglaciar son dibujadas en función a la morfología de la superficie de los glaciares actuales; es decir, cóncavo en la zona de

acumulación y convexo en la zona de ablación. Las curvas de nivel fueron dibujadas cada 100-200 m.

Métodos para la reconstrucción de las Paleo Líneas de Equilibrio Glaciar (ELA)

La reconstrucción de las paleo ELA fueron realizadas para los valles de Mucubají, La Mucuchache y Mifafí. También fueron realizadas determinaciones de paleo ELA para las morrenas de Los Zerpa, La Victoria, El Caballo y La Canoa. El objetivo de este estudio fue de hacer inferencias paleoclimáticas en Sierra Nevada y Sierra del Norte-Cordillera de Trujillo.

Los cálculos de paleo ELA fueron realizados a partir de los métodos "Accumulation Area-Ratio" (AAR) y de "Area-Altitude Balance Ratio" (AABR). El método de AAR considera que durante el estado estacionario del glaciar, la zona de acumulación ocupa una proporción fija de la superficie del glaciar. Para los glaciares de latitudes altas y medias, la relación de estas áreas está entre 0.55-0.65 (Porter, 1975). En la región intertropical, esta relación de áreas no está del todo establecida, por lo que, los valores reportados para esta zona involucran un grado de incertidumbre alto. Sin embargo, considerando la hipótesis de que en la región intertropical la zona de ablación es más grande que la zona de acumulación, las relaciones de áreas en esta región son consideradas más altas que las reportadas en las zonas de latitudes altas e intermedias, los valores utilizados generalmente están cerca de 0.8 (Kaser y Osmaston, 2002).

El método AABR considera los gradientes del balance de masas y la hipsometría del glaciar. Este método se basa en el hecho de que los gradientes de acumulación (b_c) y ablación (b_a) ($BR= b_a/b_c$) son lineares y conocidos. Como en el caso del método AAR, los valores para el método AABR tampoco están bien determinados en la zona intertropical; en la actualidad, los valores del balance de masas (BR) son > 3 (Kaser y Osmaston, 2002) e incluso algunos han reportados valores de hasta 25 (Rea et al., 2009). Los valores de AAR utilizados para realizar los cálculos fueron 0.73-0.82 y para el método AABR fueron 5 y 10.

Los cálculos de paleo ELA fueron realizados con una herramienta informática que permite incorporarlo en ArcGis de Pellitero et al. (2015).

Resultados y discusiones

¿Por qué se estudió la morfología glaciar seleccionada?

El detalle de la historia de desglaciación en Los Andes de Mérida está limitado por la falta de cronología glaciar. Diferentes valles fueron estudiados en esta tesis: valle de Mifafí (6 muestras) en Sierra del Norte, en Sierra Nevada fueron estudiados los valles de Mucubají (14 muestras), Mucuchache (7 muestras) y Gavidia (24 muestras). Estos valles fueron escogidos porque mantienen una buena preservación de la morfología glaciar y permiten tener una visión global de las dinámicas glaciares en los Andes centrales de Mérida. La Sierra Nevada es la más estudiada porque en esta zona existen todavía relictos de los últimos glaciares (menos de 0.017 km^2, Braun y Bezada, 2013).

Para contribuir con la reconstrucción de la Glaciación Mérida, fueron recolectadas muestras de diferentes avances glaciares (representados por morrenas). Fueron recolectadas muestras en Sierra del Norte (morrenas El Desecho, 3 muestras y en La Culata, 12 muestras) y en Cordillera de Trujillo (morrenas de Pueblo Llano, 6 muestras y morrena de La Canoa, 2 muestras). En la Sierra Nevada fueron recolectadas muestras en la Sierra de Santo Domingo (morrenas de Los Zerpa, 3 muestras y Las Tapias, 3 muestras). En la parte Suroeste se estudiaron las morrenas de El Caballo (3 muestras), Mucubají y Mucuchache.

Las muestras fueron recolectadas en bloques morrénicos, superficies pulidas en paredes del valle y rocas aborregadas del fondo del valle. Los sitios estaban lo suficientemente altos para minimizar errores en las edades de exposición debido a su posible recubrimiento por sedimentos.

Historias de desglaciación

Las edades de exposición o abandono de las morfologías glaciares estudiadas varían entre 9.5±1.1 y 83.7±3.4 ka. De una forma más precisa, las edades obtenidas en Sierra

Nevada varían entre 9.5±1.1 y 37.0±1.6 ka, en Sierra del Norte varían entre 16.0±0.6 y 19.2±2.1 ka y en Cordillera de Trujillo varían entre 17.6±1.6 y 83.7±3.4 ka.

Diferentes historias de desglaciación fueron determinadas en los Andes centrales de Mérida al menos desde el MIS 3. En los valles de Mucubají y Mucuchache, la dinámica estuvo caracterizada por varios episodios de avance-estabilización de los frentes de los glaciares durante el retroceso general de los mismos. En los valles de Gavidia y Mifafí, la desaparición de los glaciares fue más rápida, con velocidades de retroceso longitudinal muy altos (entre 4-7 km/ka).

En el valle de Mucubají, las evidencias estudiadas hasta la fecha de la actividad glaciar datan desde el LGM hasta el Holoceno a 6 ka. En el valle de la Mucuchache las edades de exposición indican que las morfologías estudiadas fueron abandonadas entre el MIS 3 hasta el período entre el LGM-OtD hace unos 18 ka (Oldest Dryas). La zona alta de este valle no ha sido estudiada por lo que en esta tesis la historia de desglaciación en este valle se interpreta hasta hace 18 ka. En el valle de Gavidia, el glaciar retrocedió en dos períodos, uno entre 21-16.5 ka y otro entre 16.5-16.0 ka. La velocidad de retroceso en horizontal durante el período entre 16.5 ka y 16 ka fue más rápido (4 km/ka). Mientras que en el valle de Mifafí la velocidad de retroceso del glaciar en horizontal fue extremadamente alta a edades entre 17-18 ka (7 km/ka). En los valles de Gavidia y Mifafí la desaparición completa de los paleoglaciares tomó entre 0.5-1.0 ka. Estos valles presentan características morfométricas similares como la topografía del circo glaciar y la orientación NE-SO de la zona de acumulación. Esta configuración hace que las zonas de acumulación de estos glaciares hayan recibido más radiación solar que las zonas de acumulación de los valles de Mucubají y la Mucuchache cuya orientación es de NO-SE. La comparación de las diferentes curvas hipsométricas de los paleoglaciares de Mucubají, Mucuchache y Mifafí entre 17-18 ka indica que en la Sierra Nevada (Mucubají, Mucuchache) el área de las zonas de acumulación varía entre 60-70% mientras que para Mifafí este valor era de 20 %. El área de las zonas de acumulación también controla el retroceso rápido de los paleoglaciares. Características morfométricas como pendiente del fondo del valle, la topografía de la zona de acumulación (circos glaciares con paredes de alta inclinación), extensión de las zonas de acumulación (hipsometría) y su orientación, también controlaron las diferentes historias de desglaciación.

Contribución a la reconstrucción de la Última Glaciación en los Andes centrales de Mérida

Información sobre la glaciación previa a la Última Glaciación (antes del MIS 5) es muy escasa, sólo algunas evidencias han sido encontradas en la sección LAG de Mesa del Caballo (3500 m). Los avances glaciares durante el MIS 4 y MIS 3 son observados en la Cordillera de Trujillo (valle de Pueblo Llano a 2500 m) y en Sierra Nevada (valle de Mucuchache y El Caballo a 3600 m y 3400 m, respectivamente). Los avances ocurridos durante el LGM sólo fueron evidenciados en Sierras Nevada-Santo Domingo en Mucubají a 3500 m y Las Tapias a 3100 m. Otro grupo importante de avances glaciares ocurrieron durante el período entre el LGM-OtD, en el valle de Mucubají entre 3570 m et 3620 m. En Sierra de Santo Domingo los glaciares durante este período llegaron a los 3100 m, mientras que en la Sierra del Norte llegaron a altitudes entre 3100 m y 3500 m, por último, en la Cordillera de Trujillo fue registrado el avance glaciar a 2800 m (morrena La Canoa). Con respecto al Younger Dryas, hasta la fecha, pocas evidencias se han obtenido acerca de avances glaciares ocurridos durante este período frío, sólo han sido reconocidos en Sierra Nevada a altitudes superiores a 3800 m (3862 m y 4000 m en los valles de Mucubají y el Macizo Humboldt respectivamente).

A escala regional, la relación entre avances glaciares y sus respectivas altitudes no es evidente. Los avances glaciares fechados durante el MIS 4, MIS, 3 y MIS 2 en diversas ocasiones son encontrados a elevaciones similares. La Glaciación Mérida fue establecida en base al estudio geomorfológico, geocronológico y sedimentológico de dos cordones morrénicos localizados entre 2600-3500 m (Schubert, 1974). La definición original de la Glaciación Mérida fue una primera buena aproximación para comprender la Última Glaciación en los Andes de Mérida, sin embargo, edades de desglaciación obtenidas recientemente por Guzmán (2013) o las obtenidas en Sierra Nevada y Cordillera de Trujillo en esta tesis, indican que todavía es necesario continuar con el desarrollo de estudios científicos que permitan comprender mejor la Última Glaciación en esta región.

Los avances glaciares durante el MIS 3 (observados en Mucuchache, El Caballo y Pueblo Llano) suministraron información nueva en la cronología de la Glaciación Mérida. Si es considerado el modelo original establecido por Schubert (1974),

Mucuchache (3400 m) y El Caballo (3600 m) estarían relacionados con la Glaciación Mérida Tardía mientras que las morrenas de Pueblo Llano a 2500 m podrían estar relacionada a la Glaciación Mérida Temprana. Los resultados de edades de exposición obtenidos en esta tesis indican finalmente que el abandono de estas morrenas ocurrieron durante el Interestadío El Pedregal, el cual, fue identificado en los Andes de Mérida entre 25-60 ka (Dirszowsky et al., 2005; Rull, 2005).

La mayoría de los avances de glaciares máximos fueron identificados a edades más jóvenes que el LGM *sensu stricto* particularmente durante el período entre el LGM-OtD (17-19 ka). Algunos avances máximos estuvieron relacionados también con el MIS 4 y MIS 3.

Paleo Línea de Equilibrio Glaciar (ELA)

Los valores de paleo ELA obtenidos por cada método (AAR, AABR) para cada paleoglaciar, no muestran diferencias significativas y esto por lo tanto permite determinar un valor de paleo ELA promedio. En general, los valores se encuentran entre 3475±27 m en La Canoa y 4397±33 m en Mifafí.

En Sierra Nevada a 30 ka la paleo ELA estaba a 3765±37 m (Mucuchache) y 3839±20 m (El Caballo). Entre 20-22 ka se encontraba a 3882±27 m (Mucuchache) y 3808±39 m (Mucubají). Las diferencias más significativas que existen entre las paleo ELA ocurren entre Sierras Nevada y Santo Domingo a ~ 18 ka (e.g. at 18 ka Mucuchache ELA=3965±30 m y La Victoria ELA=3669±24 m).

Contribución paleoglaciológica al registro paleoclimático en los Andes centrales de Mérida

Las condiciones paleoclimáticas como la temperatura y la precipitación pueden ser determinadas a partir del análisis de las paleo ELA (e.g. Lachniet Vazquez-Selem, 2005; Stansell et al., 2007; Smith et al., 2011). Sin embargo, es importante recordar que en la zona intertropical, las relaciones utilizadas para hacer los cálculos de este parámetro (AAR et AABR) no están bien establecidos (e.g Rea et al., 2009). Es

importante tener en cuenta que en esta región, las interpretaciones paleoclimáticas están acompañadas de una incertidumbre no cuantificable.

Los valores de paleo ELA obtenidos en esta tesis están en el mismo orden que los valores reportados por otros trabajos como Lachniet y Vazquez-Selem (2005) y Stansell et al. (2007). Los cambios de temperaturas, precipitación, radiación solar o la combinación de estos factores, son los responsables de la variabilidad en los glaciares tropicales (Kaser and Osmaston, 2002).

El valor de paleo ELA más bajo (3765±37 m) fue calculado para el valle de Mucuchache durante el MIS 3. Este valor correlaciona con condiciones climáticas más cálidas en los Andes de Mérida en comparación con el LGM (calentamiento relativo de 5 ºC en comparación la temperatura actual; Dirszowsky et al., 2005; Rull, 2005), también correlaciona con condiciones más cálidas en el Hemisferio Norte según el registro de isótopos de oxígeno y condiciones más húmedas en comparación con el LGM o post-LGM en el norte de Suramérica. Por lo tanto, los avances glaciares de los valles de Mucuchache y El Caballo parecen haber sido controlados por variaciones en la paleoprecipitación.

Las diferencias más significativas de los valores de paleo ELA se tienen para períodos post-LGM (<18 ka). Las variaciones de las paleo ELA entre Sierra Nevada y Santo Domingo fueron atribuidas a variaciones en la paleo precipitaciones entre las sierras (Lachniet y Vazquez-Selem, 2005), sin embargo, Stansell et al. (2007) sugirió que las mismas fueron producto de variaciones de las paleo temperaturas.

Las mayores variaciones de paleo ELA se observan al comparar los valores entre Sierra del Norte y Sierra Nevada-Cordillera de Trujillo, se pudo observar un gradiente significativo N-S y NE-SO. Esto indica que las precipitaciones en estas zonas fueron contrastantes entre los diferentes valles por lo menos durante el período entre 16-19 ka. El valle de Mifafí en Sierra del Norte fue la zona más seca (4397±33 m) mientras que los sectores más húmedos fueron Sierra de Santo Domingo (e.g. 3665±89 m) y Cordillera de Trujillo (3475±27 m). Esta distribución de paleo precipitaciones es semejante a la distribución que registra actualmente esta variable climática en los Andes centrales de Mérida.

Conclusiones y Perspectivas

Esta tesis contribuye con el conocimiento de la Última Glaciación en los Andes de Mérida. Las cronologías de exposición de las morfologías glaciares fueron obtenidas utilizando el método de isótopo cosmogénico producido *in situ* ^{10}Be. Las 100 muestras presentadas en esta tesis aportan información valiosa que en conjunto con las cronologías ya publicadas, permiten tener un conocimiento más detallado de la Última Glaciación en la región. Dichos resultados y sus interpretaciones también contribuye con el conocimiento del paleoclima tropical.

Historias de desglaciación y sus orígenes

Diferentes historias de desglaciación fueron establecidas en esta región durante el Pleistoceno Tardío. El derretimiento de los glaciares de una forma muy rápida entre 0.5-1.0 ka ocurrió en los valles de Mifafí y Gavidia post-LGM, específicamente hace 18-16 ka. En los valles de Mucuchache y Mucubají las dinámicas fueron diferentes; en dichos valles se reportan las presencias de grandes morrenas que representan períodos de avance-estabilización de los glaciares durante su retroceso generalizado, en estos valles la desaparición de los glaciares fue de una forma más gradual.

Las diferentes historias de desglaciación podrían ser explicadas por las diferentes características morfométricas que presentan los diferentes valles. Dichas características son: diferentes pendientes del fondo de los valles, diferentes orientaciones y área de las zonas de acumulación.

Reconstrucción de la Última Glaciación (Glaciación Mérida)

Los avances glaciares reconocidos en la tesis están ligados a los períodos comprendidos entre el MIS 4 y MIS 1. No se observó una correlación entre elevación y avances glaciares. Fueron identificados por primera vez los avances relacionados al MIS 3 y hasta la fecha, pocos avances han estado relacionados al período Younger Dryas, sólo en Mucubají a elevaciones mayores a los 3800 m.

Contribución paleoglaciológica al registro paleoclimático de Los Andes centrales de Mérida

Durante el LGM fueron inferidas condiciones climáticas similares entre los valles de Mucubají y Mucuchache (Sierra Nevada). Esta deducción se obtiene a partir de la comparación de los valores de paleo ELA, los cuales resultaron ser más similares que para el período post LGM (3882±27 m y 3808±39 m, respectivamente). El patrón de precipitaciones entre los 16-19 ka (LGM-OtD-El Caballo) parece ser similar al que se aprecia actualmente en la región, siendo los sectores más húmedos los correspondientes a la Sierra de Santo Domingo-Cordillera de Trujillo y el más seco correspondía al valle de Mifafí.

Los avances glaciares relacionados al MIS 4 y MIS 3 estuvieron relacionados a una fuerte actividad de la Zona de Convergencia Intertropical que generaban más precipitaciones en el Norte de América del Sur y temperaturas más cálidas (comparadas con las presentes durante el LGM) en los Andes centrales de Mérida (período conocido como el Interstadío El Pedregal). Los avances glaciares durante el MIS 2 estuvieron principalmente asociados a las bajas temperaturas en el Hemisferio Norte y las más bajas temperaturas registradas en los Andes tropicales.

Perspectivas

En los Andes de Mérida aún quedan varias morfologías glaciares aún sin determinar su edad de exposición. Este hecho ofrece la oportunidad de realizar más trabajos de cronología glaciar en otros valles glaciares de la región. Especial interés debe realizarse en estudiar historias de desglaciación antes del LGM y durante el YD.

Con respecto al tópico del paleoclima tropical, los resultados de esta tesis pueden contribuir con la cuantificación de las condiciones paleoclimáticas utilizando los valores de paleo ELA y la modelización de los paleo glaciares (e.g. Plummer and Phillips, 2003). También sería muy provechoso integrar los valores de isótopos estables obtenidos durante el desarrollo de esta tesis y una colaboración con el CSIC (España).

La cronología glaciar obtenida en esta tesis también puede ser utilizada para hacer estudios de Neotectónica en los Andes centrales de Mérida. También podrían ser

realizados estudios para determinar volúmenes de agua liberados durante la desglaciación, estudiar balances hídricos y de transporte de sedimentos.

Changes in the present-day climatic conditions impact society in different aspects. World climate in an overall scale is controlled by atmospheric, oceanic and terrestrial interactions supported by solar radiation. Tropical areas receive most of the solar radiation and heat is distributed to the North and South Hemisphere by atmospheric and oceanic circulation (e.g. Chiang, 2009). Last Glaciation climate changes have been related to reorganizations in the atmosphere circulation from the tropics, impacting Atlantic Meridional Overturning Circulation (AMOC) (Chiang, 2009). Therefore, a better characterization of the present and past tropical climate is key to understand the present and past global climates. Results should allow constraining climate models and improves future climate projections and society impacts of the climate changes.

Tropical glaciers are known to be extremely sensitive to global climate change and also an important water resource, especially for populations of the Peruvian and the Bolivian altiplanos (e.g. Hastenrath, 1985; Kaser and Osmaston, 2002). Glacier landforms from tropical former glaciers offer an attractive proxy for the study of past tropical glaciations and palaeoclimate conditions (Jomelli et al., 2009). Previous studies have been carried out using ice cores (e.g. Thompson et al., 1995; Thompson et al., 1998; Ramírez et al., 2003) and using former or paleo glacier landforms (e.g. Stansell et al., 2007; Jomelli et al., 2009).

For better determining paleoclimate conditions using former glaciers is necessary to well understand glaciations extensions and timing. In the tropics, glaciations reconstructions in the tropical Andes are the most documented (e.g. Porter, 2001; Jomelli et al., 2009). Among them, the Venezuelan Andes, called the Mérida Andes (MA), is one of the tropical areas most affected by glaciations. However, glaciations reconstructions are less detailed (Porter, 2001; Lachniet and Vazquez-Selem, 2005; Coronato and Rabassa, 2007).

In the MA a detailed bibliographic compilation about glacial landforms observations were made by Schubert (e.g. 1972; 1974; 1980; 1992 and 1998). Conversely to glacial landforms descriptions, glaciations timing is poorly constrained. Geochronological data is not regionally uniform and enough to allow a more detailed reconstruction (e.g. Porter, 2001; Coronato and Rabassa, 2007). Geochronological studies were based on

radiocarbon chronology (Schubert, 1970; Salgado-Laboriau and Schubert, 1977; Schubert and Rinaldi, 1987; Rull, 1998; Mahaney et al., 2001; Dirszowsky et al., 2005; Stansell et al., 2005; Mahaney et al., 2007 and Carrillo et al., 2008), thermoluminescence (TL) (Schubert and Vaz, 1987 and Bezada, 1989), optically stimulated luminescence (OSL) (Mahaney et al., 2000) and more recently, Terrestrial Cosmogenic Nuclide (TCN) dating (Wesnousky et al., 2012; Guzmán, 2013; Carcaillet et al., 2013).

This dissertation mainly contributes in three aspects. Firstly, in reconstruct deglaciation histories and glaciers advances in the central MA during the late Pleistocene. Secondly, studying Quaternary glaciers variabilities and deducing its causes. Third, deducing paleoclimate conditions and compare to local, regional and global paleoclimate proxy records.

This dissertation attempts to represents a contribution to our understanding of tropical Andean glaciations and tropical paleoclimate variability answering the next questions:

- How were the deglaciation histories in the central MA during the late Pleistocene? Is there any geographical trend?
- How many distinct glaciers episodes could be identified in the central MA? Is there any correlation between glaciers advances and elevations? How was the extent of the Last Glacial Maximum (LGM) period in the MA?
- What are possible causes of late Pleistocene glaciers variabilities in the central MA?
- What can be our contribution to the Mérida Andes paleoclimate knowledge?

In order to answer these questions in this dissertation, a paleoglaciological study was developed. Geomorphological analysis focus in glacial landforms was carried out to select the study area and samples locations whereas the Terrestrial Cosmogenic Nuclides (TCN) using the ^{10}Be nuclide dating was selected as geochronological method.

This dissertation was divided in three parts (Part I, Part I and Part III).

Part I: General introduction and methods. This section provides fundamental aspects about tropical glaciations and tropic climate and an overview of the geological and

geomorphic context of the Mérida Andes. A detailed section on the methods and materials is presented. Part I is constituted by sections I, II, III and IV.

Part II: "Results"

This section provides details on input parameters used to compute ages from TCN measurement as well as raw data and geomorphological setting of sampled valleys. ELA (Equilibrium Line Altitude) results are presented. Part II is constituted by section V.

Section V includes two scientific papers:

Carcaillet, J., **Angel, I**., Carrillo, E., Audemard, F.A. and Beck C. 2013. Timing of the last deglaciation in the Sierra Nevada of the Mérida Andes, Venezuela. *Quaternary Research*, Vol. 80(3): 482-494.

Angel, I., Audemard, F., Carcaillet, J., Carrillo, E., Beck, C., Audin, L. "under review". Deglaciation chronology in the Gavidia valley, Mérida Andes, Venezuela, inferred from cosmogenic ^{10}Be dating. Journal of South American Earth Sciences. SUBMITTED

Part III: Discussions. This section discusses the results in an overall frame. Namely, the geomorphic and climate factors controlling the former glacier evolution are discussed. Global, regional and local climate correlations are examined. Part III is constituted by sections VI and VII (Conclusions and perspectives).

Other articles and abstracts related to the PhD project:

- **Angel, I.**, Carcaillet, J., Carrillo, E., Audemard, F. and Beck, C. 8th IAG, International Conference on Geomorphology, Paris, France 2013. Glacial chronology in the Mérida Andes, Venezuela, deduced from cosmogenic ^{10}Be radionuclide dating.

- **Angel, I.**, Carcaillet, J., Carrillo, E., Audemard, F. and Beck, C. Nordic Workshop on Cosmogenic Nuclide Dating, Aarhus, Denmark, 2014. Glacial chronology deduced from cosmogenic ^{10}Be radionuclide dating in La Culata, Gavidia and Mucubají valley, Venezuelan Andes.

- **Angel, I.,** Audemard, F., Carrillo, E., Carcaillet, J. and Beck, C. 1er Congreso Venezolano de Geoquímica, Caracas, Venezuela, 2014.El isótopo cosmogénico ^{10}Be en la cronología de morfología glaciar en los valles de Gavidia y La Culata, Andes Venezolanos.

- **Angel, I.**, Carcaillet, J., Audemard, F., Carrillo, E., Condom, T., Audin, L. and Beck, C. XIX INQUA Congress, Nagoya, Japan, 2015. Asynchronous deglaciation histories in the central Venezuelan Andes.

- **Angel, I**., Carrillo, E., Carcaillet, J., Audemard, F.A. & Beck C. 2013. Geocronología con el isótopo cosmogénico ^{10}Be, aplicación para el estudio de la dinámica glaciar cuaternaria en la región central de los Andes de Mérida. GEOS. Vol-44: 73-82. In **Appendix**.

The **Sections I** and **II** provide fundamentals aspects and a tropical Andes glaciation state of arts. These sections attempt to continuing reflect the importance of developing studies on tropic paleoclimate and the Mérida Andes glaciations. Since the results correspond to the Last Glacial cycle, concepts about glaciations and climate events during this period are presented in **Section I**. A background about climate of the tropics, tropical glaciers behaviors and a tropical Andean glaciations state of arts is presented. Concepts about tropical glaciers mass balances and paleo equilibrium lines altitudes (ELA) are also presented. The **Section II** focuses on approaches for reconstructing and dating Quaternary glaciations, emphasizing its different applications and limitations.

I-1.0 Quaternary Glaciations background

I-1.1 Generalities and causes

The Quaternary Period is related to considerable climate instabilities and subdivided into *glacial* and *interglacial* periods. Glacial periods are cold phases of major expansion of glaciers and ice sheets. Interglacial are warmer and generally wetter periods (Nesje and Olaf Dahl, 2000).

Northern Hemisphere ice sheets (Laurentide and Finno-Scandinavian) formation was originally related to variations observed in astronomical parameters. Specifically, with changes in the Pliocene Earth inclination axis (Uriarte, 2003). Low values involve high orbit eccentricity, and maximum distance between Earth and Sun during summer solstice in the Northern Hemisphere. Therefore, summers were colder and climate conditions allowed glaciations onset. Another important condition to glaciation initiation involves more snow precipitations during winter time. For that purpose, warmer oceans were necessarily involved, in order to provide high humidity toward the Northern Hemisphere (Uriarte, 2003).

One explanation involves a North-Atlantic relative warm, because of the Mexican Gulf strong current circulation (Uriarte, 2003). It provides abundant snow precipitations in the Northern Hemisphere. Another cause was proposed by Haug et al. (2005), based on alkenone unsaturation ratios and diatom oxygen isotope ratios studied in a sediment

core of the western subarctic Pacific Ocean. Results indicate that 2.7 million years ago late summer sea surface temperatures increased in this ocean region. At the same time, winter sea surface temperatures cooled. Winter icebergs became more abundant and global climate evolved into glacial conditions. Summer warming extended into the autumn in the Pacific Ocean, and this fact, provided water moisture in the northern North America. Precipitation produced snow, thus allowing the initiation of Northern Hemisphere glaciation.

The recurrence period of Earth glacial cycles between 1.5 and 0.6 Myr were every ~41 kyr. After 0.6 Myr, glaciations cycle were mainly each ~100 kyr, traducing the obliquity cycles of the Earth (Rutheford and D´Hondt, 2000). The first glaciation frequency of 41 kyr were explained by astronomical variations (e.g. Rutheford and D´Hondt, 2000; Uriarte, 2003). Until present, the mechanisms behind large amplitude glaciations oscillations (100 kyr) remain poorly understood. Significant discussions oppose two main theories, the astronomical one and the geochemical theory (Paillard, 2015).

Glaciations each 100 kyr seems to be related to low atmospheric carbon dioxide content during glaciations periods, based on studies from Antarctica ice cores (Paillard, 2015). The atmospheric CO_2 partial pressure increases significantly, by about 50 ppm, several millenia before any important change in a continental ice volume. Therefore, an active role of greenhouse gases seems to be related to the ice age initiation.

I-1.2 Glacials and interglacials classifications and limitations

Different parts of the world assigned different glacial and interglacial names based on stratigraphic correlations on terrestrial glacial deposits in Europe and North America (Table I-1). One classification was assigned for European Alps, other one for northwestern Europe and other for Central North America. These classifications are still used, but are too general and misleading (Nesje and Olaf Dahl, 2000).

Glacial and interglacial periods are more recently proposed based on oxygen isotope records, deduced from fossils and microfossils analyze in marine sediments cores (Nesje and Olaf Dahl, 2000). The marine isotope signal is mainly controlled by the global volume of terrestrial ice. Isotopic signal fluctuations can be considered as a record of glacial and interglacial fluctuations. A system of *marine isotope stages (MIS)*

was developed and used to note glacial chronologies in this dissertation (Figure I-1). Isotope stages have a given number, even numbers reflecting stadial cold stages, while odd numbers denote interstadial warm phases. The deep sea oxygen record is global and therefore geographically consistent (Shackleton and Opdyke, 1973; Nesje and Olaf Dahl, 2000).

Table I-1. Main glacial and interglacial periods of Western Europe and North America following the classical system (From Nesje and Olaf Dahl, 2000). From younger to older interglacial in italics, glacials in ***bold.***

European Alps	Norwest Europe		Britain	North America
Würm	**Weichsel**		**Devensian**	**Wisconsinan**
R/W	*Eem*		*Ipswichian*	*Sangamon*
		Warthe		
Riss	**Saale**		**Wolstonian**	**Illinoian**
		Drenthe		
M/R	*Holstein*		*Hoxnian*	*Yarmouth*
Mindel	**Elster**		**Angilan**	**Kansan**
G/M	*Cromerian*		*Cromerian*	*Aftonian*
Gunz				**Nebraskan**

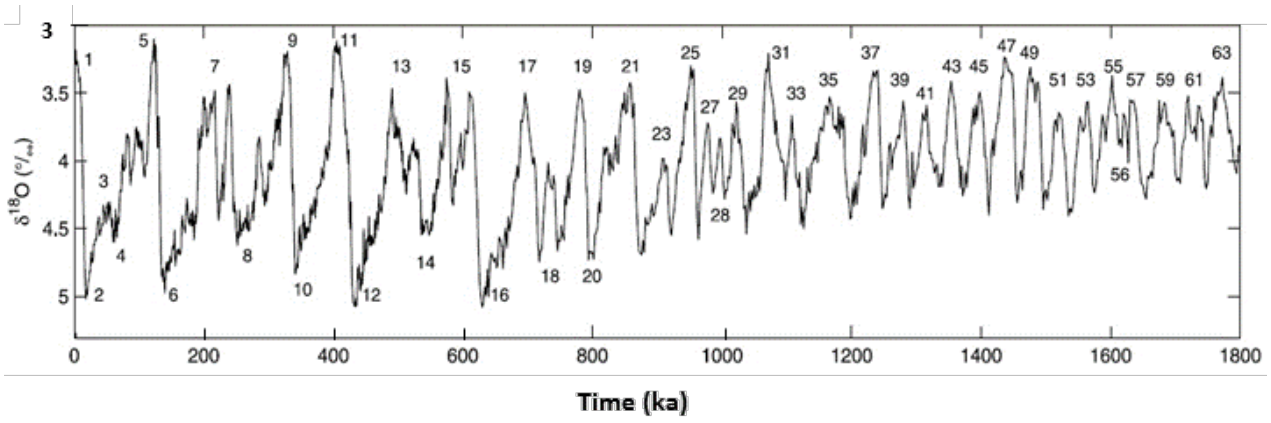

Figure I-1. Marine Isotopes Stages (MIS) for the last 1.8 Ma. Even numbers reflect stadial glacial/cold stages, while odd numbers denote interstadial interglacial/warm phases. This graphic is based on the LR04 $\delta^{18}O$ stack (constructed by the graphic correlation of 57 globally distributed benthic $\delta^{18}O$ records) (Modified from Lisiecki and Raymo, 2005).

I-1.3 Last Glaciation and climate events involved

All the results presented in this dissertation are related to the Last Glaciation and different climates events presented in this subsection I-1.3.

I-1.3.1 Last Glaciation

Last Glaciation began around 115 ka ago (Uriarte, 2003). Artic marine sediments indicate a thermohaline circulation reduction and an ice sheets extension (Uriarte, 2003). Based on Milankovicth cycle, Last Glaciation should begin first in the Northern Hemisphere (Uriarte, 2003). However, paleoclimate reservoirs in the Southern Hemisphere indicate that it began almost at the same time. In the Southern Hemisphere, climate conditions became colder (Uriarte, 2003). Glaciers advances happened in the Patagonia and ice sheet extension in Antarctica (Uriarte, 2003). Explanations about the glaciation variation from the Northern to the Southern Hemispheres are still not understood and must be clarified to better understand future climate changes.

A possible factor, which controls Last Glaciation evolution between hemispheres is related to the Tropics climate. Specifically, water moisture in the troposphere could be related (Uriarte, 2003). During cold climate conditions, subtropical areas became drier and water moisture decreased from 0.1% to 0.01% leading to a decrease of infrared emission of 26 W/m^2 (Pierrehumbert, 1998). Last Glaciation propagation in the planet could be explained by humidity changes in the Tropics, due to this infrared emission reduction (Uriarte, 2003). Also Last Glaciation climate changes could be explained by reorganizations in the atmosphere from the Tropics which impacted Atlantic Meridional Overturning Circulation (AMOC). Thus, the Tropics could play a key-role on the climate changes initiated by the North Atlantic (Chiang, 2009). Therefore, studies to contribute to better understand paleoclimate conditions in the tropics and its role on globalizing glaciations are necessary.

An overall Last Glaciation division is made on the basis of significant sea level changes during the last 115 ka. Three sub-divisions are proposed: 115-80 kyr, 80-30 kyr and 30-19 kyr before present (Figure I-2). Marine Isotopes Stages related to the Last Glaciation go from MIS 5 to MIS 2. Based on the LR04 $\delta^{18}O$ stack variations (Lisiecki and Raymo, 2005), coldest climate temperatures are related to MIS 2 whereas warmest climate conditions are related to MIS 5 (Figure I-2).

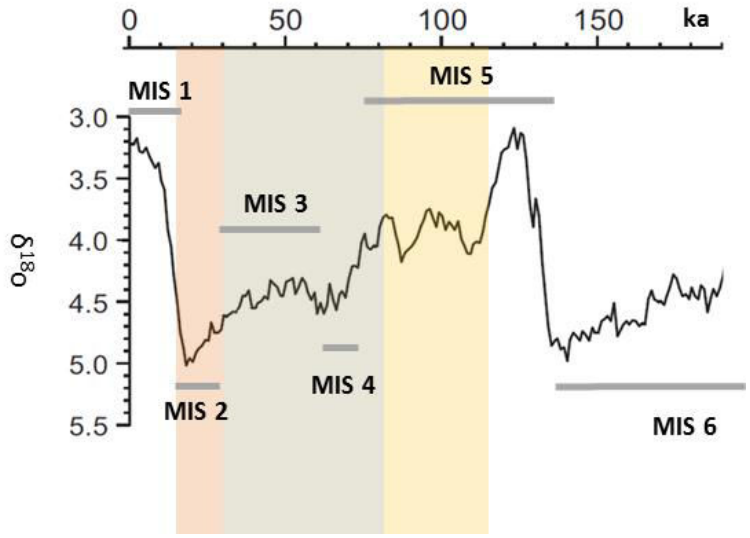

Figure I-2. Marine Isotopes Stages (MIS) last 190 ka. Last Glaciation is related to MIS 1 until MIS 5. Horizontal bars indicate the length of each stage. Rectangles red, gray and orange indicate the overall Last Glaciation subdivision based on sea level changes. This graphic is based on the LR04 $\delta^{18}O$ stack (constructed by the graphic correlation of 57 globally distributed benthic $\delta^{18}O$ records) (Modified from Lisiecki and Raymo, 2005).

I-1.3.2 Dansgaard-Oeschger (D-O) and Heinrich events

The last glacial cycle was characterized by several of abrupt/millennial-scale climate variations, based on high-resolution ice-core and marine sediment records (e.g. Heinrich, 1988; Dansgaard et al., 1993; Bond et al., 1999; Alley et al., 2003). The Greenland ice core records indicate evidences of large and rapid (few decades) shifts in air temperature (up to 15 ºC) during the last 110 ka (Stuiver and Grootes, 2000; NGRIP members, 2004; Huber et al., 2006). Twenty-five rapid changes between stadial (cold) and interstadial (warm) conditions were identified with an average spacing of ~1.5 ka. These are named Dansgaard-Oeschger (D-O) events (NGRIP members, 2004). Sediment cores from the North Atlantic show that D-O events are associated with changes in Atlantic Meridional Overturning Circulation (AMOC) (Boyle, 2000). Each cycle of fast temperatures drops lead to a Heinrich Event. It involves a massive iceberg discharge during which, ice-rafted debris (IRD) in the North Atlantic (between 40 and 55ºN) was widespread (Naafs et al., 2013).

I-1.3.3 Last Glacial Maximum

The term 'Last Glacial Maximum' (LGM) refers to the maximum extension of worldwide ice volume during the Last Glacial cycle (Hughes and Gibbard, 2014). The LGM was originally described by CLIMAP Project Members (1976, 1981) as the interval 23-14 ^{14}C-ka BP with a mid-point at 18 ^{14}C ka BP (Shackleton et al., 1977). It was identified by two independent proxies: in the marine isotope record and changes in global sea level (Mix et al., 2001).

The $\delta^{18}O$ signal in the marine record is known to be shifted to the global maximum ice volume (Mix et al., 2001; Thompson and Goldstein, 2006). Consequently, the global sea-level minimum is likely to be closer to the accurate global Last Glacial Maximum (Hughes and Gibbard, 2014). Based on evidences of global sea-level changes from sediments of the northern Australia continental margin, Yokoyama et al. (2000) concluded that the global land-based ice volume was at its maximum from at least 22-19 cal. ka BP. As noted earlier, the age of 21 cal. ka BP is now widely used as a time marker of the global LGM (Mix et al., 2001; MARGO Project Members, 2009). However, Shakun and Carlson, (2010) suggested a global average age of 22.2 ± 4.0 ka best defines the LGM, based on 56 terrestrial records.

I-1.3.4 Late Glacial (LG)

Late Glacial is a period related to the sequence Oldest Dryas (OtD), Bølling, Older Dryas, Allerød, and Younger Dryas (YD). These episodes were originally defined as periods of biostratigraphic change reflected in terrestrial records in Denmark (Iversen, 1954). These episodes are widely used in other geological contexts, and in areas for which they were never initially intended. In this dissertation Blunier et al. (1998) classification was used. Authors propose: the Oldest Dryas stadial (17,50 to14,60 Cal kyr BP), the Bølling warming interstadial (14,60 to 14,10 Cal kyr BP), the Older Dryas cold stadial (14,10 to 13,90 Cal kyr BP), the Allerød warming interstadial (13,90 to 12,85 Cal kyr BP) and the Younger Dryas stadial (12,85 to 11,65 Cal kyr BP).

I-2.0 Tropical Andes, climate and glaciers behaviors

This section presents an overview of tropical climate and tropical glaciers behaviors. Differences in glaciers dynamics between tropical and temperate areas are detailed.

I-2.1 Climate of the tropical Andes, overview

The tropical zone can be divided into two sub-zones with different climate characteristics (Figure I-3). Troll (1941) distinguished the inner tropical climate with homogeneous annual precipitation. Outer tropics are characterized by a dry season from May to September, when subtropical conditions prevail. Meanwhile, a wet season happens from October to March, when tropical conditions prevail.

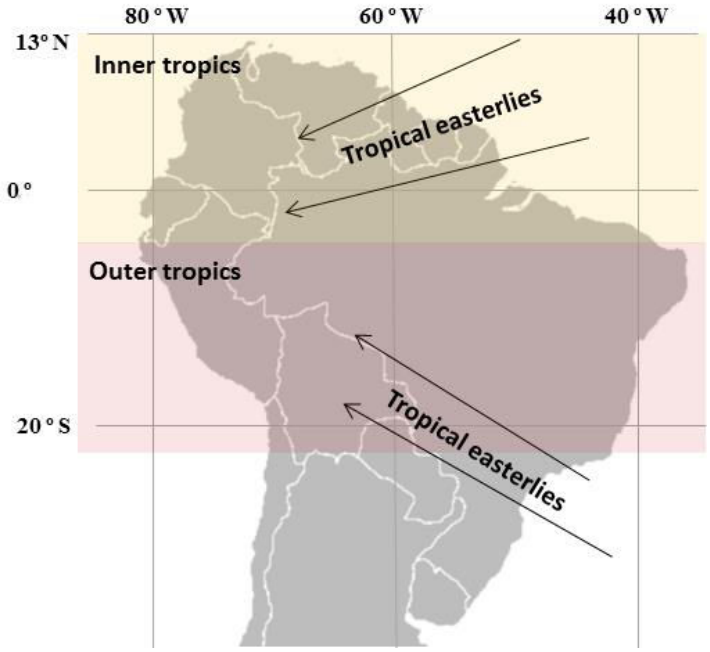

Figure I-3. Andes inner and outer tropics locations based on Rabatel et al. (2013). Venezuela, Colombia and Ecuador belong to the inner tropics (orange rectangle) whereas Perú and Bolivia belong to the outer tropics (red rectangle). This tropical area is affected by different tropical easterlies directions close to the Equator (Modified from Rodbell et al., 2009).

In the tropical area the climate is characterized by homogeneous annual temperature, with a slight seasonality of air temperature in the outer tropics. This temperature variation is 1° to 2 ºC during the austral wet summer (October-March) higher than the austral dry winter (May-September) (Rabatel et al., 2013).

In the tropical zone, annual incident solar radiation is also fairly constant. The seasonality of the solar irradiance in the outer tropics is attenuated by pronounced cloud cover seasonality (maximum during austral summer) (Rabatel et al., 2013). In the inner tropics, moisture remains almost unchanged throughout the year. Meanwhile, the outer

tropics are characterized by pronounced seasonality of specific moisture, cloud cover and precipitation (Rabatel et al., 2013).

In the Tropics the annual precipitation is controlled by the seasonal migration of the Inter Tropical Convergence Zone (ITCZ). The ITCZ could be defined as the area in the vicinity of the equator of trade wind convergence, ascending air, low atmospheric pressure, deep convective clouds and heavy precipitation (Henderson-Sellers and Robinson, 1986). The ITCZ migrates seasonally in the tropical Atlantic. It reaches maximum northern latitude at 10º N in August and maximum southern latitude at 1º S in March (mean latitudes at longitude 30º W) (Nobre and Shukla, 1996).

Precipitation in the tropical Andes is derived from the tropical Atlantic Ocean via the tropical easterlies winds (Poveda et al., 2006). Humidity is transported to the high Andes via convective circulations over the eastern tropical Andes. The gigantic Amazon basin and the rain-forest mainly influence the precipitations in the central tropical Andes during May-September (Figure I-4). The trajectory of the easterlies and the seasonality of precipitation are governed by the annual displacement of the ITCZ. The outer tropics of the Southern hemisphere (e.g., La Paz, Bolivia; 16ºS) thus experience a single marked wet season during the peak summer months. Whereas the humid inner tropics (e.g., Quito, Ecuador; 0.5º S) experiences two wet seasons. One wet season during the spring, with the southward passage of the belt of convective activity (ITCZ). Another one, during the fall with its northward returns (Rodbell et al., 2009). In addition to the marked seasonality of precipitation, strong trans-andean precipitation gradients exist (Rodbell et al., 2009). The wettest parts of the tropical Andes are in the eastern foothills, where mean annual precipitation can exceed 4000 mm (Hoffman, 1975). In contrast, the western Andes experience much lower mean annual precipitation, commonly <1000 mm (e.g., 650 mm for Huaráz, Peru).

Inner tropical glaciers receive precipitation all year round and are most sensitive to changes in temperature (Kaser, 2001). Meanwhile, outer tropical glaciers have an annual mass-balance sensitive to variations in both precipitation and temperature (Kaser and Georges, 1997).

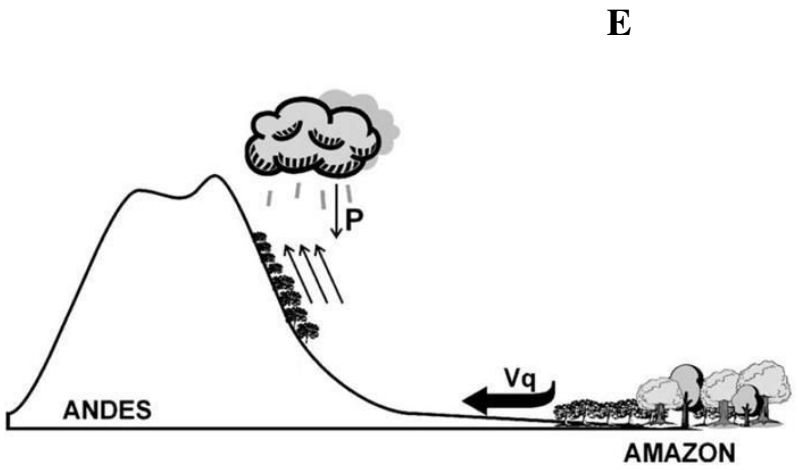

Figure I-4. Schema to show the Amazon basin and rain-forest influence in the central tropical Andes precipitations (P) during the May-September. Moisture from the Amazon is transported by the trade winds (Vq) (Modified from Poveda et al., 2006).

The tropical area receives most of the Earths sun radiation. Heat is distributed to the North and South Hemisphere by atmospheric and oceanic circulation. Therefore, tropical area plays an important role in the current and past global climate. It seems to be related to glaciations propagations in both hemispheres: 1) due to moisture troposphere variations and 2) because of atmospheric reorganizations impacting the AMOC. Therefore, understanding present and past tropical climate variability is key to model the global climate evolution. Special interest is dedicated to develop paleoclimates studies in tropical South America because current models that simulate past and future climates have significant deficiencies (e.g. Li et al., 2006; Yin et al., 2014). Proxy paleoclimate studies are scarce, when a comparison to the mid- and high-latitudes of both hemispheres is attempted (Jomelli et al., 2009). Tropical paleoclimate studies have been developed from different geological materials: lake sediments, marine sediments, ice-cores and paleoglaciers or former glacier landforms.

I-2.2 Tropical Andean glaciers

By the end of the last century, total surface of tropical glaciers represented about 2500 km^2. It represents around 0.15% of the global glacier area and about 4% of the mountain glaciers area (Kaser and Osmaston, 2002). Tropical glaciers are distributed over 3 highest East African mountains (Rwenzori, Kilimanjaro and Mt Kenya), the Indonesian Puncanck Jack in Irian Jaya and South American Andes between Bolivia and Venezuela (23.53ºN-23.53ºS) (Figure I-5). 99% of tropical glacier surface is located in the Andes

and especially in Peru and Bolivia (Kaser and Osmaston, 2002). Tropical Andes glaciers are an important water resource for populations of the Peruvian and Bolivian altiplanos. Glaciers provide water for agricultural and domestic consumption as well as power generation (Vergara et al., 2007).

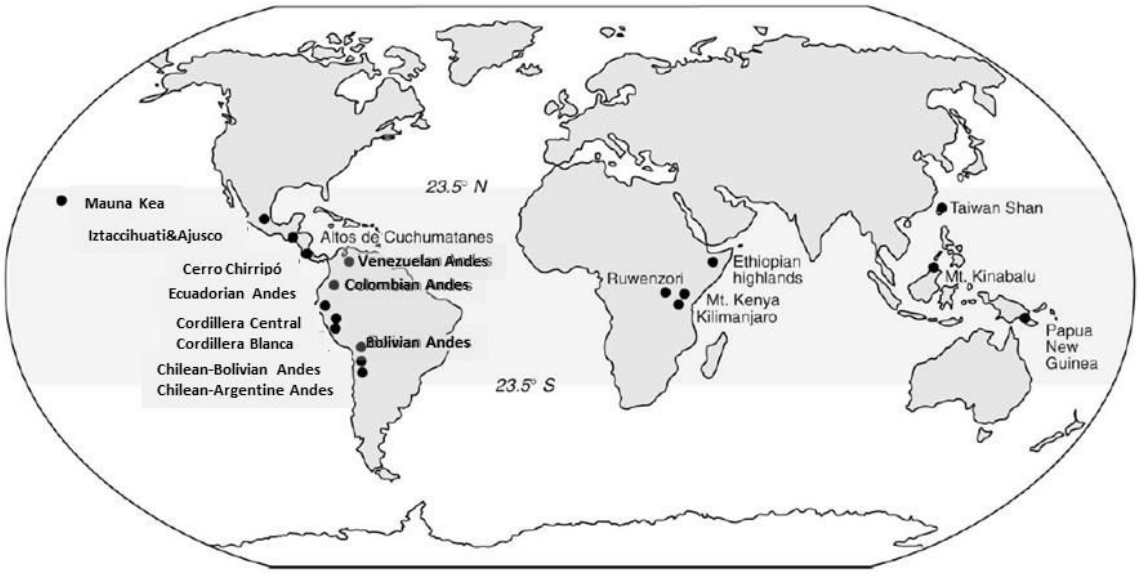

Figure I-5. Tropical glaciers distribution. (Porter, 2001).

Tropical glaciers are known to be extremely sensitive to climate change (e.g. Kaser and Osmaston, 2002). Therefore, tropical glaciers offer an attractive proxy for the study of paleoclimate conditions (Jomelli et al., 2009). Glacier response induced by a climate change mainly depends on: a) climate (related in the mass balance) and b) the local topography (mainly the glacier surface hypsometry) (Oerlemans, 2001). Different relations between these factors provide glaciers variabilities even inside the same area (Oerlemans, 2001). Paleoclimate interpretations need to consider this local variability (Winkler et al., 2010).

In the tropics the mid-day sun is overhead at least once a year and never less than 43º above the horizon. Tropical glaciers receive high solar radiation throughout the year (Benn et al., 2005). Consequently, annual variations in mean daily temperatures are smaller than diurnal temperature ranges (Kaser and Osmaston, 2002).

The thermal homogeneity of the tropics is in sharp contrast to the mid- and high-latitudes, where annual temperature fluctuations are larger than diurnal variations (Benn et al., 2005). The constancy of mean daily temperatures in the tropics means that the 0ºC atmospheric isotherm is fairly stable around a constant altitude. Meanwhile ice ablation occurs on the lower parts of glaciers all year round (Benn et al., 2005). Tropical glaciers are differentiated from temperate glaciers because they are affected by annual migrations of the ITCZ.

I-2.2.1 Mass balance

A glacier mass balance profile allows the estimation of the inputs (accumulation) and outputs (ablation) of a glacial ice system. Glacier mass balance inputs include precipitation in different forms (snow, hail, frost and rainfall) and lateral inputs (avalanches) (Bennet and Glasser, 2009). Mass balance outputs could be produced by four ways: ice melt, serac fall, iceberg calving and sublimation. Glacial meltwater is derived from direct melting of ice on the surface, or within the glacier. On the surface, melting highly depends of the solar radiation. At the base of the glacier, heat leading to melting is supplied by ground friction of the ice flow. Also geothermal heat of the Earth contributes to the glacier melting (Bennet and Glasser, 2009). When there is an imbalance between accumulation and ablation, the glacier extension changes. Climate conditions which allow more ablation than accumulation provide negative mass balances and glaciers retreats. Whereas climate conditions which allow more accumulation than ablation provide positive mass balances and cause a glacier advance (Bennet and Glasser, 2009).

Tropical and temperate glaciers behavior also differs because of different mass balance profiles (Benn et al., 2005). More significant difference is related to glacier ablation which happens through the year in the tropical glaciers (Figure I-6 B, C). Accumulation gradient is lower and timing is different compare to temperate glaciers (Benn et al., 2005). Accumulation in temperate Andean glaciers happens during austral winter (Figure I-6 A) whereas in outer tropics it happens during austral summer. The inner tropics are mainly controlled by the ITCZ displacement providing a bimodal accumulation regime (Figure I-6 C).

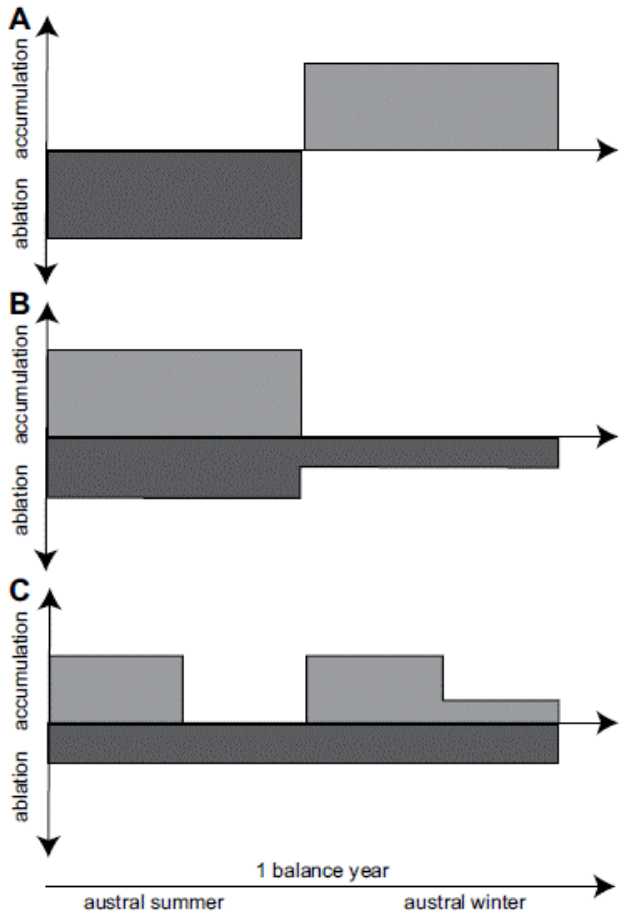

Figure I-6. Idealized mass balance characteristics of the Andes temperate glaciers (A), outer tropical glaciers (B), and wet inner tropical glaciers (C). Tropical glaciers have ablation all year round and accumulation depends of its location in the inner and outer tropics. It is controlled by the ITCZ (From Rodbell et al., 2009).

I-2.2.2 Equilibrium Line Altitudes (ELA)

The ELA refer to the altitude where bn= 0 where bn is the net mass balance at the end of the (summer) ablation season (Figure I-7) (Paterson, 1994). This definition does not apply in tropical regions, because there is a year-round ablation and there is a distinct dry season (Benn et al., 2005). The annual mass balance cycles of tropical and sub-tropical glaciers are thus highly variable (Kaser and Osmaston, 2002).

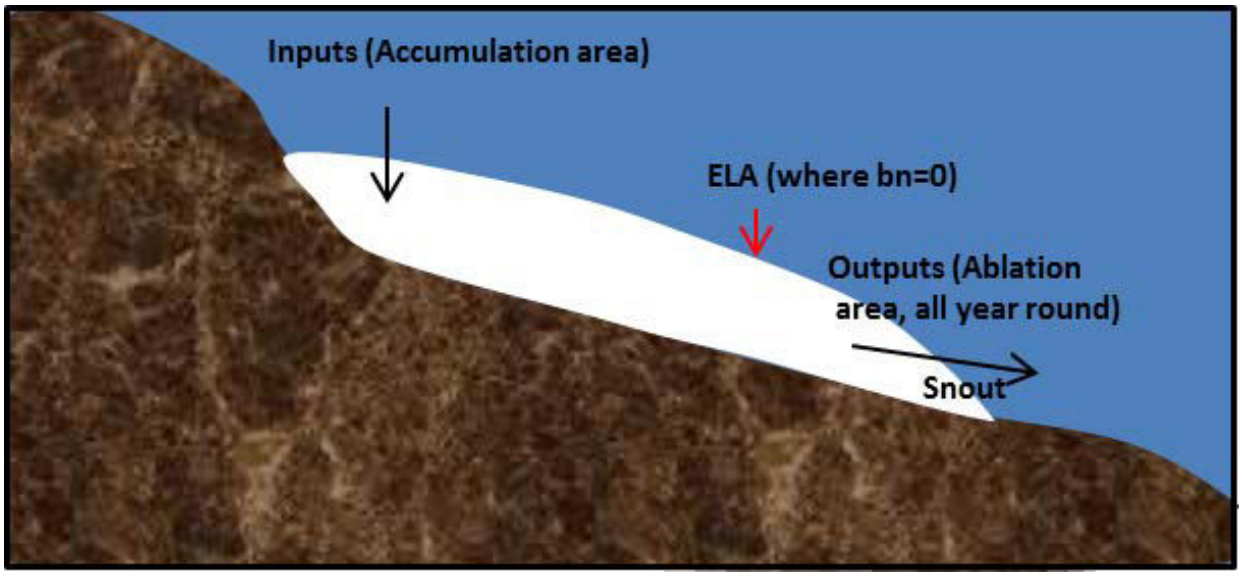

Figure I-7. Mountain glacier representations with different parameters which allow characterizing glaciers dynamics. Accumulation area, Ablation area, ELA: equilibrium line altitude and Snout. In tropical glaciers ELA is located closer to the Snout, in comparison to temperate glaciers because of more ablation gradient.

Kaser (2001) modeled the vertical mass balance profiles of glaciers in the humid inner tropics, the subtropics, and the mid-latitudes. This author evaluated the sensitivity of the equilibrium line altitude (ELA) to variations in precipitation, temperature, and net short wave radiation. In the inner tropics, ELA response is far more sensitive to changes in temperature than those in the dry subtropics (Kaser, 2001). In contrast, a small increase in precipitation would dramatically increase these glaciers net mass balance (Robdell et al., 2009). Sensitivity studies revealed that these subtropics glaciers are especially sensitive to changes in atmospheric moisture (Kaser, 2001; Robdell et al., 2009). Atmospheric moisture also affects the ratio between sublimation and melting on the ice surface. Therefore, ELA variations in outer tropical glaciers tend to be more sensitive to precipitation changes.

Paleoclimate studies involving former glaciers are based on the ELA steady-state. It represents a glacier in equilibrium with climate, under a geometry configuration limited by moraines (a depositional glacial landform better described in Section II) (e.g. Benn et al., 2005; Stansell et al., 2007). However, special care is necessary with this approach because nonclimatic factors could controls moraines landscape distribution (Barr and

Lovell, 2014). For example uplift, subsidence or accumulation area topography (see detail in **section II.1.1.1.2**-Topographic control).

I-3.0 Tropical Andean Glaciations

This section presents an overall overview of tropical Andean glaciations based on reviews from Coronato and Rabassa (2007) and Smith et al. (2008). This state is focused on Peruvian, Ecuadorian and Bolivian Andes glaciations because are the most studied. More detailed information about the Venezuelan Andes glaciations are in **section III-2.0**-Glaciation reconstruction. In this compilation, only published ages or morphostratigraphy (see details in Paleoglaciology and Geochronological methods) deductions based on published ages were considered. Ages used were determined using radiocarbon dating or terrestrial cosmogenic nuclide (TCN) using ^{10}Be nuclide dating.

In this overall review studied locations are:

- Ecuador, Rucu Pichincha in the Western Cordillera at 0º12 S-78º35 W (Figure I-8, site 1); Papallacta valley in the Eastern Cordillera at 0º20 S-78º12 W (Figure I-8, site 2); Chimborazo-Carihuairazo volcanoes in the Western Cordillera at 1º30 S-78º50 W (Figure I-8, site 3); and Cajas National Park in the Southern Ecuadorian Andes at 2º40, 3º00 S-79º00, 79º25 W (Figure I-8, site 4).

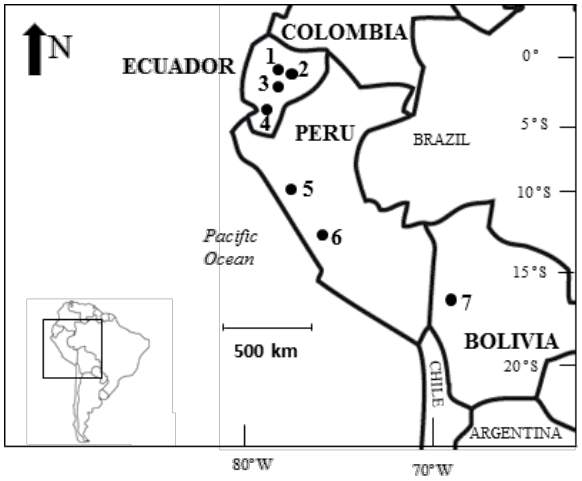

Figure I-8. Location of different areas involved in the compilation of the Tropical Andes Glaciations. Numbers are the location of the different areas. 1: Rucu Pichincha. 2: Papallacta valley. 3: Chimborazo-Carihuairazo. 4: Cajas National Park. 5: Cordillera Blanca valleys. 6: Junín Plain. 7: Milluni and Zongo valley, Cordillera Real (Modified from Smith et al., 2008).

- Perú: Cordillera Blanca valleys in the central Peru at 9º30 S-77º15 W (Figure I-8, site 5); and Junín Plain valleys at 11º S, 76º W (Figure I-8, site 6).

- In Bolivia in the Milluni and Zongo valleys at 16º 16 S-68º 08 W (Figure I-8, site 7).

I-3.1 Previous MIS 5 and MIS 5 glaciers advances (Smith et al., 2008)

Glaciers advances before and during the early MIS 5 in Peru were evidenced in Cordillera Blanca, based on exposure ages (TCN dating) of moraines located between 3627-3890 m (Smith et al., 2008). Exposure ages range between 76±2 and 439±13 ka (Cojup moraines, Figure I-9). Also a previous MIS 5 glacier advance was evidenced in the Junín plain valleys (Smith et al., 2005 a, b). Moraines boulders ages range from 51±1 ka to 1606±12 ka (TCN ages). Glaciers advances were proposed around 175–225 and 340–440 ka (moraine complex (GD) located between 4168-4464 m (Figure I-9), where exposure ages are mainly distributed.

In Papallacta valley (Ecuador), previous MIS 5 glaciers advances could be related to moraines complexes located at elevations < 3400 m. A lava flow partially fills the valley and overlay the moraines. It was dated (using the fission track method) older than 150-180 ka (Heine, 1995 in Smith et al., 2008) (M1, M2, Figure I-9). At ~2750 m in the Chimborazo and Carihuairazo Massif, an old till deposits with different weathering degrees was related to a previous MIS 5 glacier advance. However, chronological data is lacking. These till deposits were correlated up to the Cajas National Park (2800 m), similar periods of glacier advance were assumed. Previous MIS 5 glacier advance was also evidenced in Rucu Pichincha valley based on very weathered moraines complexes between 3500-3600 m (Heine and Heine, 1996). However, chronological data is lacking (M1, M2 and M3, Figure I-9).

Glacier advances during MIS 5 in the Mérida Andes are related to basal till in the Pedregal section from Mesa del Caballo (3500 m). They are also related to glaciofluvial gravel and till from La Canoa section RF3 (2800 m) (Kalm and Mahaney, 2011).

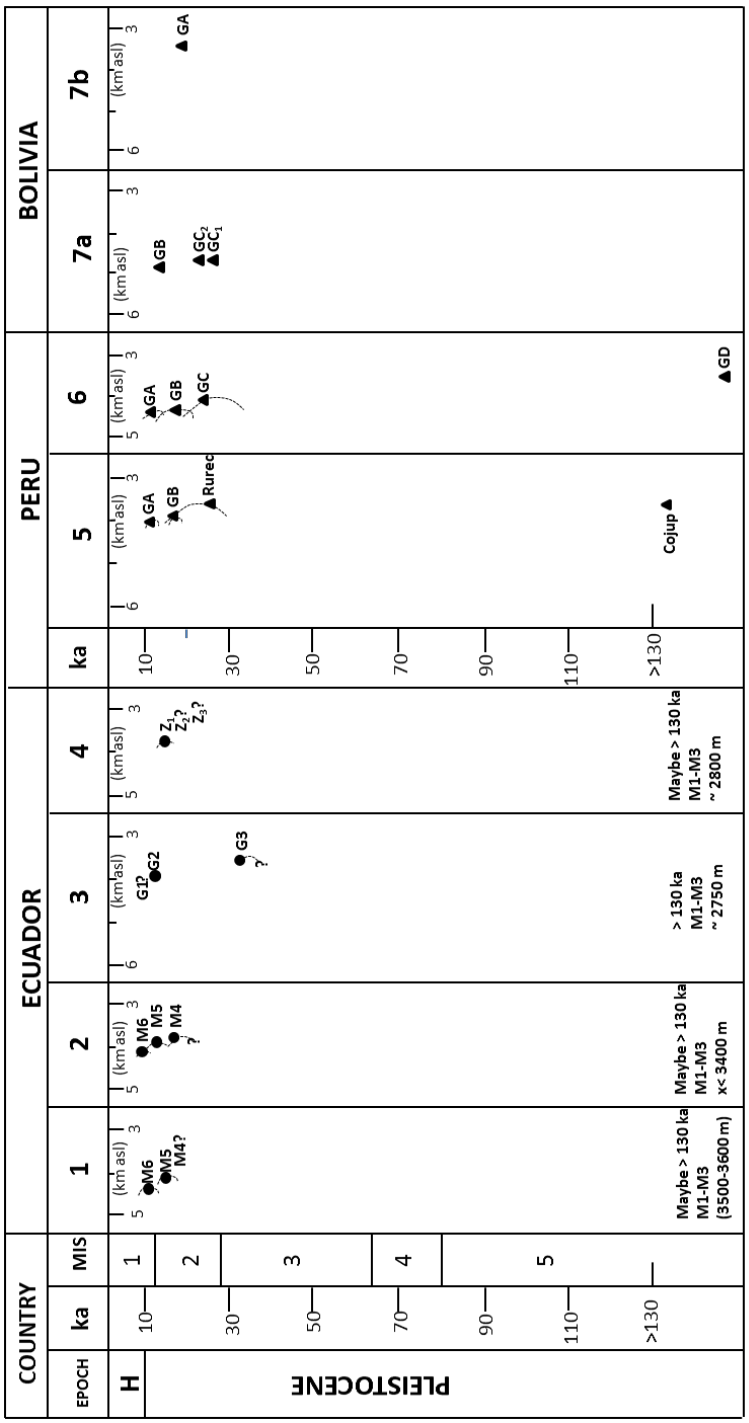

Figure I-9. Schematic representation of the tropical Andes glaciers advances. Location based on moraines elevation (km asl) and ages (Radiocarbon (dots) and TCN (triangles) dates). The symbol ***?*** *indicates a moraine complex only with a morphostratigraphy age or limit maximum age not known.* ***H:*** *Holocene. Time (ka). Marine Isotope Stages (MIS). Locations 1: Rucu Pichincha. 2: Papallacta valley. 3: Chimborazo-Carihuairazo. 4: Cajas National Park. 5: Cordillera Blanca valleys. 6: Junín Plain. 7a: Milluni and 7b: Zongo valley, Cordillera Real (Modified from Smith et al., 2008).*

I-3.2 MIS 3, MIS 2 and MIS 1 glaciers advances (Coronato and Rabassa, 2007; Smith et al., 2008)

In Bolivia, MIS 3, MIS 2 and MIS 1 glacier advances were reported in Cordillera Real. Two moraine complexes are related to MIS 3 glacier advances. Moraines located at high elevations date between 28-35 kyr BP based on a radiocarbon age obtained from a peat layer in till (Coronato and Rabassa, 2007), whereas moraines at low elevations were related to an older glacier advance not identified because of lack of dating. In the Milluni valley, Cordillera Real, two moraine complexes were dated. Old moraines (GC at ~ 4595 m) yielded, ages (TCN) ranging from 14.5±0.4 to 31.8±1.1 ka (Smith et al., 2005a) (Figure I-9). Some of these moraines were related to the Local LGM (LLGM) as suggested by the ages of two moraine levels (GC_1 25-30 ka and GC_2 22-26 ka, between 4595-4640 m) (Smith et al., 2005a). Young moraines at higher elevations (GB at ~ 4640 m) date from 8.2±0.6 to 16.2±0.5 ka (TCN). These moraines were related to a Late Glacial (LG) advance (Smith et al., 2005a). In Bolivia in the Zongo valley, at least one MIS 2 glacier advance was identified based on exposure age of 17.8±0.9 ka and related to a moraine complex at ~ 3400 m (Smith et al., 2005a).

In Peru in the Junín plain, based on exposure ages (TCN), three moraine complexes were related to glacier advances during MIS 3, MIS 2 and MIS 1 (Figure I-9) (Smith et al., 2005 a, b). The lowest complexes (GC terminal moraines) located between 4159-4388 m are dated from 17.3±0.6 ka to 31.3±1.4. Ages are mainly distributed between 21-31 ka and 21-24 ka. These moraines were related to the LLGM. Exposure ages from moraines located a middle elevations (GB, located between 4252-4391 m), range from 13.6±0.6 ka to 21.3 ± 0.6 ka, with age concentration between 15-19 ka. These moraines located at middle elevations were related to a LG re-advance (Smith et al., 2005a, b). A younger advance was evidenced based on the higher moraine complex (GA, located between 4392-4412 m), with age concentration between 12-14 ka. In the Cordillera Blanca valleys, a glacier advance MIS 3-MIS 2 is represented by Rurec moraines located between 3700-4000 m. These moraines ages range from 16.7±1.7 to 29.3±1.2 ka (TCN dating; Farber et al., 2005; GC, Figure I-9). MIS 2 and MIS 1 glaciers advances were identified in Laguna Baja moraines (GB) between 3800-4000 m. Moraines exposure ages range from 14.2±0.7 ka to 16.1±0.9 ka (Farber et al., 2005). The

Manachaque moraines (GA, at 4045 m) were related to LG and Holocene re-advance (TCN dating between 10.4±0.4 and 12.7±0.4 ka) (Figure I-9).

In Ecuador in the Chimborazo/Carihuairazo Massif, a MIS 3 complex moraine at 3770 m, indicates a maximum limiting age of 33.3±0.3 ^{14}C ka BP, based on peat layers underlying full glacial till (G3, Figure I-9) (Clapperton and McEwan, 1985). Two moraines complexes (3900-4050 m and 4300-4400 m) were related at least to MIS 1 glacier advance (G2 and G1, Figure I-9), based on radiocarbon ages of 10.7±0.1 and 11.4±0.1 ^{14}C ka BP (G2 moraines between ca. 12.7 and 13.4 Cal. ka BP, respectively) (Clapperton and McEwan, 1985). Samples were collected on the upper and lower peat layers within laminated fine-grained sediments underlying till. Peat layers were located in a drained glacial lake basin up valley of G2 moraines. G1 by morphostratigraphy has to be younger than G2. No ages are presented. In the Rucu Pichincha MIS 2 and MIS 1 glaciers advances are related to M4 (at ~ 3700 m), M5 (between 4100-4200 m) and M6 moraines (between 4200-4400 m; Figure I-9). Peat from a palaeolake/bog enclosed by M5 moraines gave minimum-limiting radiocarbon dates. M5 moraines ages are 11.2±0.1 ^{14}C ka BP (ca. 13.0 Cal. ka BP) and 13.0±0.1 ^{14}C ka BP (ca. 15.5 Cal. ka BP). Heine (1995) proposed that the M4 moraines were deposited during the global LGM. Bracketed age for M6 moraines is between 11.2±0.1 ^{14}C ka BP (age of underlying peat, ca. 13.0 Cal. ka BP) and 8.2–9.0 ka (age of overlying HL-4 tephra from Rosi, 1989). Heine and Heine (1996) indicated not advance during the YD of glaciers at Rucu Pichincha.

In Ecuador in the Cajas National Park, MIS 2 and MIS 1 glaciers advances are related to a moraine complex located between 3700-3080 m (GZ, Figure I-9), based on radiocarbon ages in lacustrine sediments (Hansen et al., 2003). Three moraines are involved in this group, Z_1 (3760 m), Z_2 (3360 m) and Z_3 (3080 m). Between Z_1 and Z_2 is located Laguna Chorreras at 3700 m and up valley Z_1 is located Laguna Pallcacocha at ~ 4060 m. Hansen et al. (2003) reported a radiocarbon age of 13.2±0.1 ^{14}C ka BP from the organic material collected at the base of a core from Laguna Chorreras. Sedimentation beginning was estimated at ca. 17.0 Cal. ka BP. The oldest radiocarbon age in the Pallcacocha lacustrine sediments core was 11.8±0.1 ^{14}C ka BP, and the base of the core was estimated to date at ca. 14.5 Cal. ka BP (Hansen et al., 2003). Therefore,

Z_1 ages are between 14.5 Cal. ka BP – 17.0 Cal. ka BP and Z_2 and Z_3 older than 17.0 Cal. ka BP.

In the Papallacta valley, MIS 2 and MIS 1 glaciers advances are related to M4 or Sucus moraines (~3850 m), M5 or Portrerillos moraines (~3900 m) and M6 (~4055 m) (Figure I-9). Heine (1995) and Heine and Heine (1996) interpreted the M4 moraines as the landform associated with the maximum extent of MIS 2 glaciation (i.e., LGM moraines). M5 moraines were interpreted as older than ca. 12.3±1.3 ^{14}C ka BP but younger than the LGM, meanwhile M6 moraines were related to LG advances (bracketed by radiocarbon ages of ca. 10.5±0.8 ^{14}C ka BP below and ca. 7.9±0.9 ^{14}C ka BP above). Clapperton et al. (1997) disagreed with Heine interpretation of M4, and established Sucus or M4 advance and Potrerillos or M6 advance. Clapperton et al. (1997) reported seven minimum-limiting radiocarbon ages on plant material and peaty organic matter in sediments. This material was located overlying till between two Sucus lateral moraines. Based on the radiocarbon dating, the Sucus advance occurred before ca. 13.1 ^{14}C ka BP (average age (n=7) ca. 15.6 Cal. ka BP). The Potrerillos moraines are bracketed between 10.9 ^{14}C ka BP (average age (n=11) ca. 12.8 Cal. ka BP), and 10.035 ^{14}C ka BP (average age (n=5) ca. 11.3 Cal. ka BP). Clapperton et al. (1997) interpreted the Potrerillos advance as contemporaneous with the YD climate reversal.

Considering the Andean glaciations overview herein presented, the following remarks can be raised. Previous MIS 5 glaciations are poorly constrained and there is no evidence of MIS 4 glaciers advances. Better constrained are MIS 2 and MIS 1 glaciations, maybe related to the better preservation of the glacial landforms. Tropical Andean glaciers seem to have reached its maximum extensions before the global LGM. Finally, the Younger Dryas (YD) advance seems not to be extensively evidenced in this area.

This **Section II** presents methods for the study of glaciations. The main objective is to show limitations of the different methods and their impact in the glaciations interpretations.

II-1.0 Methods for glaciations reconstruction studies

II-1.1 Paleoglaciology

Paleoglaciology allows reconstructing former glaciers and ice sheets. These reconstructions are related to paleo temperatures and paleo precipitations, so paleoclimate conditions can be studied. Paleoglaciology is based on the glacial inversion method (Figure II-1). This method is the conceptual process used to determine glaciers and ice sheet evolution through time using the landforms originated from glaciers or ice sheets activity (Bennet and Glasser, 2009). Once we understand how landforms are modeled by current glaciers, then, we can use their spatial and temporal distributions to reconstruct the vertical and horizontal former glacier extent (Bennet and Glasser, 2009). Using geochronological methods applied on former glaciers landforms, a timing of glacier evolution, advance and retreat, can be reconstructed. The direct relation to climatic variations is obtained using paleo ELA reconstructions and evaluating different proxy records.

II-1.1.1 Moraines, an important glacial feature in paleoglaciology studies

A moraine is a geomorphic marker constituted by till (non-stratified and unsorted semi-angular clasts directly deposited by glaciers). It is originated from glacial erosion of the bedrock. Moraines are developed in almost all glacial environments; the most commonly are end moraines and other ice-marginal moraines (Schomacker, 2011). Ice-marginal moraines are formed at the glaciers margins (involving lateral and frontal moraines). Ground moraines or till plains are formed in subglacial environments, and hummocky moraines are formed in dead-ice environments (Schomacker, 2011). End moraines or terminal moraines indicate the former glaciers maximum extent. It is an important glacial feature studied in this dissertation (Figure II-2). In alpine landscapes, lateral moraines additionally aid in deciphering past ice thickness (Figure II-2), whereas frontal moraines denote glaciers advances (Figure II-2). The distribution of ground

moraine or till plains indicate deposition by warm-based glaciers and are thus an important key to understanding past glacier dynamics (Schomacker, 2011).

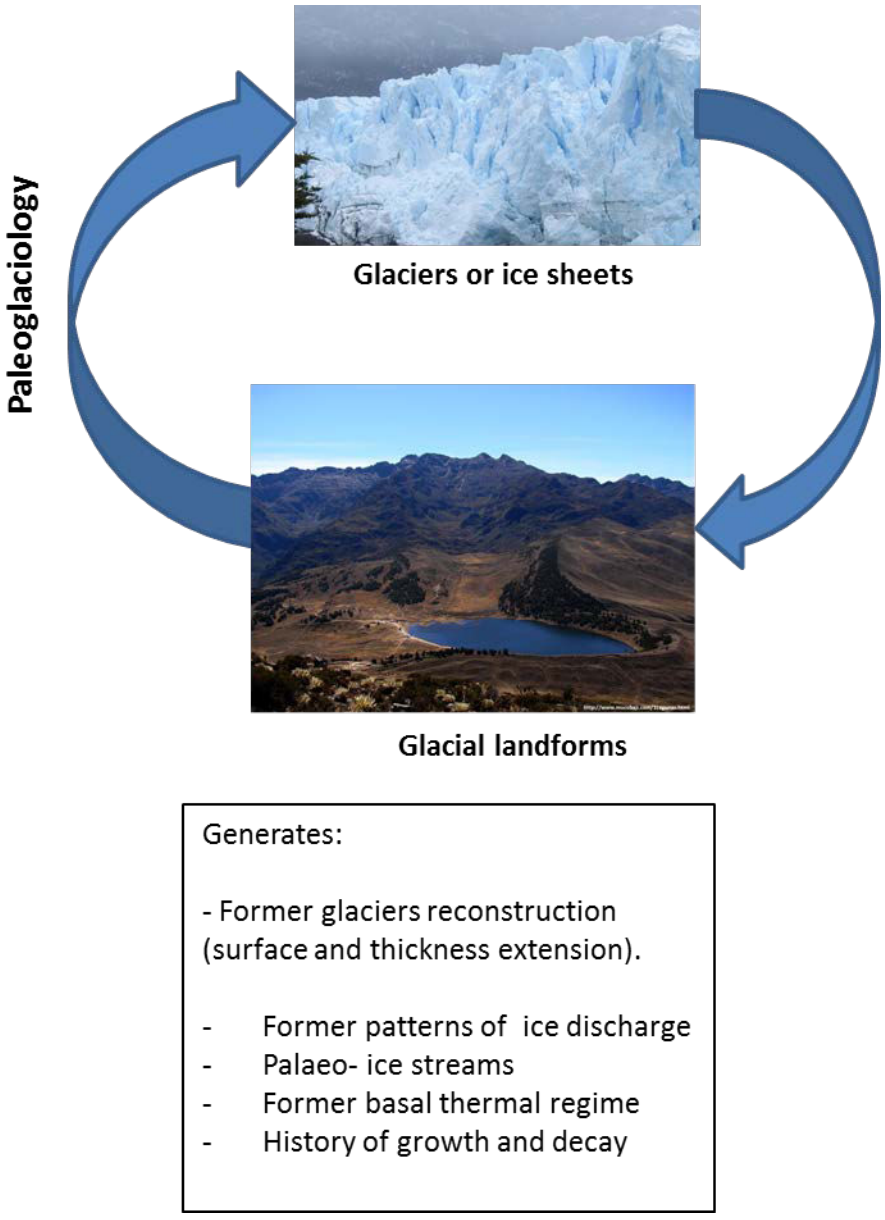

Figure II-1. Glacial inversion method. It is a method used for paleoglaciology studies. From analysis and mapping of glacial landforms, former glacier surfaces and thicknesses are reconstructed. Geochronology allows knowing glaciation timing. Paleoclimate conditions are inferred from ELA values analysis.

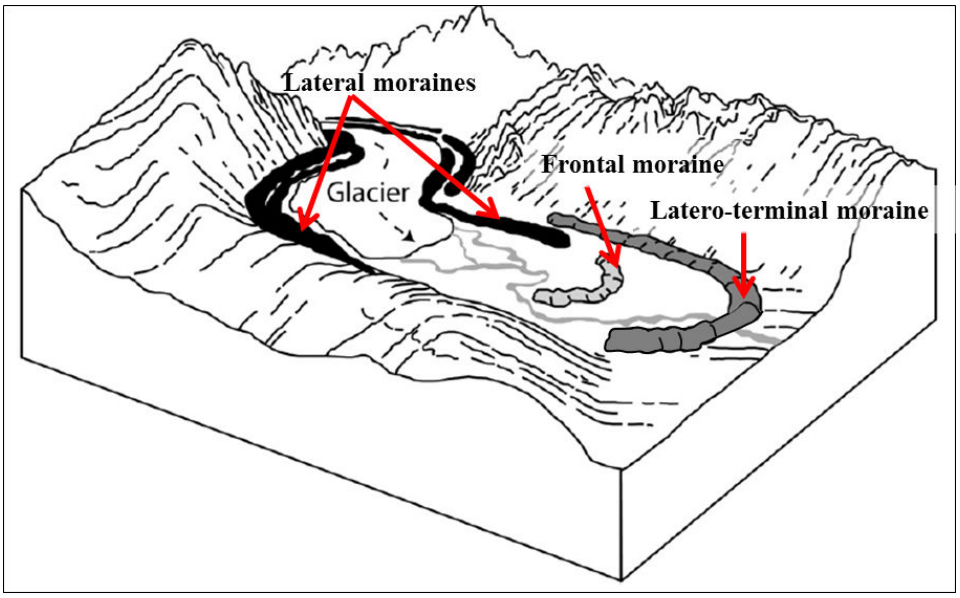

Figure II-2. Lateral, frontal and latero-terminal moraines. Ice-marginal moraines used to delimit former glacier extensions. Latero-terminal or only terminal moraines denote the maximum former glacier extension (Modified from Barr and Lovell, 2014).

Moraines could be formed by accumulation of supra-, en-, and subglacial debris, abandoned at the glacier margins (Eyles, 1983; Benn, 1992). In front of the glacier tongue proglacial debris are pushed (bulldozed) during the glacier advance. Subglacial sediments are squeezed beneath glacier margins. Finally, bedrock and unconsolidated sediments are thrust into imbricated ridges during the glacier advance (Barr and Lovell, 2014). Individual moraines are often produced through a combination of these processes. The internal structure and composition of marginal moraines are largely determined by their mode of formation and is therefore highly variable on different sites.

In the ice-marginal moraines, debris must accumulate at glacier margins. These debris are typically transported englacially or supraglacially. Factors as glacier velocity, the volume of debris within/upon a glacier, and the duration of ice margin stability (i.e., still-stand duration) control the volume of material available for moraines formation (Andrews, 1972; Kirkbride and Winkler, 2012).

Chronological information about glacier advances can be deduced from morphostratigraphic analyses of the moraines distribution in the landscape. This

geomorphic approach considers that spatial relations of different landforms allow deducing the relative moraines ages (Hughes et al., 2005). In a glacier valley, terminal moraines in the lowest part of the valley were deposited before the upper moraines, since the destructive character of bulldozer effect of advancing ice tongues. When a moraine overlay another one, the unaltered moraine is considered as the youngest. This approach allows establishing that along the same lateral moraine ridge extension it is isochrone.

During glaciations reconstructions, it is important to know that moraines are a partial record of the glaciation history. Moraines indicate glacier advances. However, all glacier advances occurred in a valley could be poorly represented by the moraines distribution in the landscape. Different processes contribute to remove material from pre-existent moraines: a) a more extended and younger glacier advance, b) proglacial erosion, c) denudation and, d) gravitational processes (landslides). The combination of these processes removes previous moraine materials and erases part of the glaciation records (Kirkbride and Brazier, 1998). Because of this fact, an integration with proglacial sediments studies, as for example from a proglacial lake or terraces, complements glaciations reconstructions studies.

II-1.1.1.1 Moraines to reconstruct paleoclimate and limitations

Moraines indicate glacier advances and involve a glacier period in equilibrium with climate (i. e. when mass balance is equal 0) and then, a period with positives mass balances. Benn and Evans, (2010); Lukas et al, (2012) proposed that the moraine size can be related to: a) glacier equilibrium duration with climate, b) glacier front speed (which controls the deposition rate) and c) capacity of the glacier to erode rock material (glacier size vs lithology).

Paleoclimate reconstructions are commonly based on former glaciers using lateral and frontal moraines analyses. This approach relies on the assumption that the distribution of moraines in the modern landscape is an accurate reflection of former ice margin positions during climatically controlled periods of glacier margin stability (Barr and Lovell, 2014). However, the validity of this assumption is debated because a number of additional, no climatic factors are known to influence the moraine distribution. For example topography, could be an important factor (Barr and Lovell, 2014).

II.1.1.1.2 Topographic control on the moraines distribution in the landscape

Topography controls the location and timing of moraines formation, glacier extension and dynamics, as well as the margin stability (Barr and Lovell, 2014). Glaciers are developed in the topography above the regional climatic-ELA (i.e., in the accumulation zone upon which snow and ice can accumulate and persist interannually) (Kessler et al., 2006; Kaplan et al., 2009). Mountains topography can vary significantly, from flat plateaus to high relief peaks which directly regulate the size and shape of glaciers (Manley, 1955; Ives et al., 1975; Sugden and John, 1976; Golledge, 2007). Mountains topography thereby determines morphology and the moraines distribution. For example, plateaus located above the ELA provide large areas for snow and ice accumulation, whereas the steepest slopes have little capacity to produce snow accumulation. Thus, flat topography allows more extensive glaciers and moraines development, whereas non plateau topography will restrict glaciation to smaller and not abundant ice masses and moraines (Sugden and John, 1976) (Figure II-3). Despite same climatic conditions prevail in both cases.

Moreover steep slopes in the accumulation areas will influence the debris provision for moraine formation. Steep slope walls are more instable and debris collapses are higher, so available material is higher for the moraine formation (Figure II-3) (Kessler et al., 2006; Kaplan et al., 2009).

II-1.2 Geochronological methods used to study Quaternary glaciations

Quaternary glaciations studies are based on geomorphological glacial analysis and dating. Also are based on pro-glacial sediments sequence (lacustrine or continental) descriptions and timing. Glacial landforms commonly dated are moraines, polished surfaces and roches moutonnées (erosional glacier landforms).

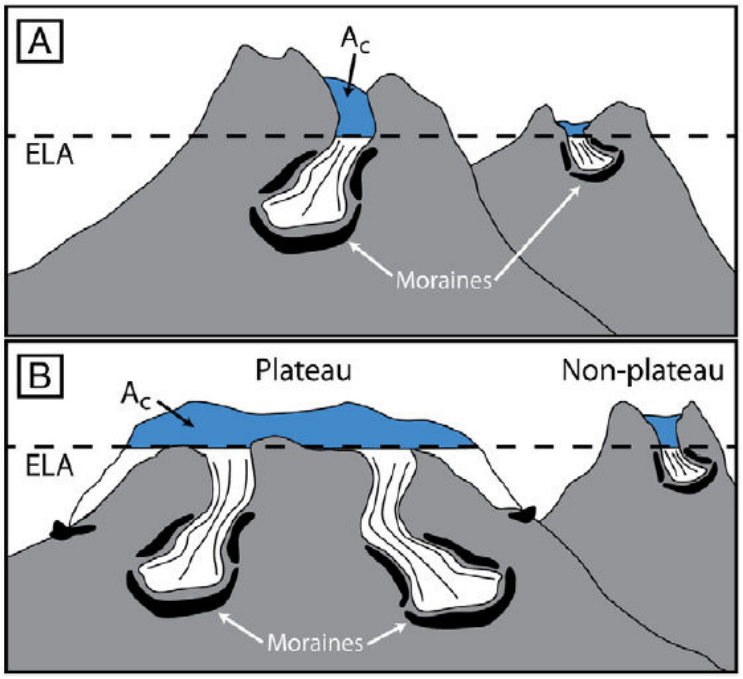

Fig. II-3. Illustration of how, under uniform climatic conditions (reflected by a uniform ELA), (A) mountain height and (B) plateau and nonplateau topography can lead to variations in glacier dimensions and thereby control moraine location. Blue zones represent glacier accumulation areas (Ac) (From Barr and Lovell, 2014).

Various dating techniques are commonly used (lichenometry, dendrochronology, radiocarbon dating and Terrestrial Cosmogenic Nuclide (TCN) dating) (Figure II-4). The selection of geochronological techniques depends of the available material to date and the time window of interest.

Lichenometry is a surface-exposure dating method that uses lichen-growth rates to infer the age of recent glacial landforms (Briner, 2011). The method is particularly useful in regions above and beyond the tree-line and especially in Arctic-Alpine environments because erosion of glacial landforms is low (Armstrong, 2004). However, in high elevation areas of the tropical Andes, this method has been successfully used (e.g. Rabatel et al., 2005; Jomelli et al., 2009). This is because the external conditions are equivalent to those of artic areas (low erosion). This method is restricted to date only Neoglacial deposits (within the last 500 years) and require knowing the lichen ecology (i.e. thallus growth rate) in the studied area (Armstrong, 2004). Dendrochronology technique dates current or sub fossils logs. Moraines can be dated until 11 ka (Briner, 2011). Dendrochronology was

mainly used in boreal and temperate regions because the annual growth of the trees rings is completely understood. However, during the last decade this technique has been also used in the tropical regions (e.g. Wils, et al., 2010). Lichenometry and dendrochronology are dating techniques suitable for Holocene glacier dynamics.

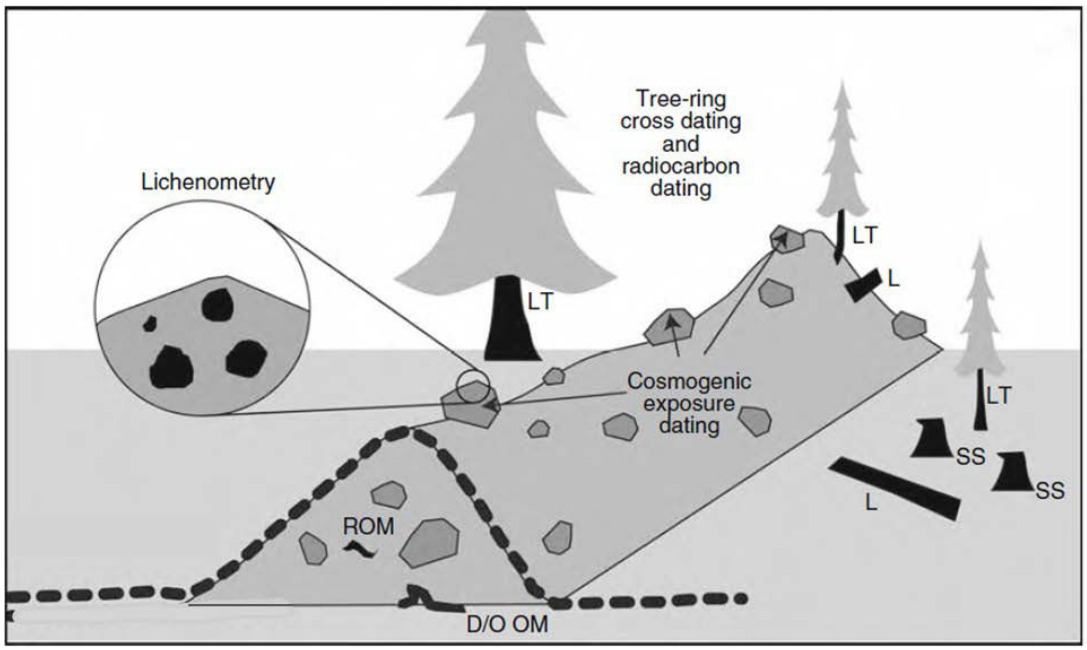

Figure II-4. Common methods used to date glacial landforms. Targets for radiocarbon and dendrochronology dating are labeled: LT living tree, L log, SS sheared stump, ROM reworked organic material, D/O OM deformed/overridden organic material. Targets for cosmogenic exposure dating (boulders preferably located on the moraine crest) (Modified from Briner, 2011).

Radiocarbon dating involves ^{14}C determination in dead organisms. Assuming that the organism death and landform deposition was contemporaneous, age of the deposit could be estimated (Libby, 1955; Taylor and Lloyd, 1992). Deposit ages can be estimated for the last 45.00 kyr (Siame et al., 2000). Studies have applied radiocarbon dating to sediments below, within, and above moraines to provide maximum (below and within) and minimum (above) age constraints (Brinier, 2011). The radiocarbon dating provides only bracketing ages (i.e. an age interval) of the glaciers advances (Balco, 2011). In high elevation area, organic remains are scarce leading to low preservation of available materials to be dated (Balco, 2011).

Radiocarbon dating is used to date sedimentary material as lake sediments or peatbog samples, directly related to glacial landforms (i.e. proglacial lake sediments developed upstream moraines ridges which provide minimum-limiting ages for down valley moraines) (Robdell et al., 2009). Furthermore, organic matter in outwash material (sand and gravel) down valley from moraines allow the calculation of maximum-limiting ages (e.g., Gonzalez et al., 1965; Mercer and Palacios, 1977; Helmens, 1988). This requires the assumption of evident relationship between dated outwash materials and the nearby moraine ridge. When this assumption is not clear, radiocarbon ages from organic matter in these stratigraphic settings are ambiguous (Robdell et al., 2009).

Terrestrial Cosmogenic Nuclide (TCN) dating (the methodological aspect will be discuss in detail in Chapter IV- Methods and Materials) is based on the quantification of isotopes produced by the interaction of cosmic rays with Earth chemical targets (Gosse and Phillips, 2001; Dunai, 2010). Geological surfaces exposure time to the cosmic rays are determined using the TCN dating. Glacial landforms exposure times can be interpreted as a chronological markers for the former glacier activity reconstruction. It is easily related to the deglaciation age of a glacial landform and overcomes the absence of organic material trapped necessary for radiocarbon dating.

This thesis is based on TCN dating because this method coupled to geomorphological investigations provides more accurate ages for glaciations reconstructions. Specifically ^{10}Be *in-situ* nuclide dating was used because of the regional lithology (granites and gneisses). These rocks have high quartz content; ^{10}Be is the most suitable nuclide (see more in Chapter IV- Methods and Materials). Uncertainties in the ^{10}Be *in-situ* nuclide dating are lower than 15% (Dunai, 2010). Contrary to radiocarbon dating, the TCN dating allows dating exposure ages of glacial landforms from the Late, Middle and Early Pleistocene (e.g. Smith et al., 2005b; Heyman, 2014).

III-1.0 General geological settings

The Mérida Andes (MA), also known as the Venezuelan Andes, is a ~400 km long SW-NE belt, located in the Southwest of Venezuela. The highest peak is the Pico Bolivar (4978 m a.s.l.). The MA has a crystalline core of Precambrian gneiss, schist and Paleozoic to Mesozoic plutonic rocks (Hackley et al., 2006). These metamorphic and igneous rocks are overlain by Jurassic and Cretaceous clastics and calcareous rocks, and flanked by Eocene to Pliocene molasse rocks and Quaternary sediments (Hackley et al., 2006) (Figure III-1).

The orogenesis is strongly connected to the geodynamic interaction of the Panamá Arc, Caribbean and South American plates and other minor continental blocks (Taboada et al., 2000; Audemard and Audemard, 2002; Bermudez, 2009; Monod et al., 2010). Interactions of these plates leads to the oblique convergence between the Maracaibo Triangular Block (MTB) and South America Plate, and is responsible for the present MA build-up (Kellogg and Bonini, 1982; Colletta et al., 1997; Audemard and Audemard, 2002; Audemard, 2003; Bermudez, 2009; Monod et al., 2010) (Figure III-2).

MA uplift is evidenced by: 1) the axial valleys display well-preserved Quaternary staircase terrace systems with more than 500 m of vertical drop between the oldest terrace and present river beds (Audemard, 2003). 2) Rivers cutting across the structural grain of the chain show very distinct transverse “wine cup” profiles (Audemard, 2003). 3) Synorogenic mollasic deposits along both flanks of the chain, deposited in flexural basins, whose thicknesses reach 8 and 3 km on the northwest and southeast of the MA, respectively (Audemard, 2003). Uplift of the MA may be attributed solely to tectonics or, more specifically, thrust faulting and folding along the margins of the range (e.g., Audemard and Audemard, 2002). Uplift rates in the MA have been estimated based on: 1) the depths of formation of the igneous and metamorphic rocks in the highest summits of the chain with an average uplift rate during the last 3-5 Ma of 2–5 mm/a (Audemard 2003). 2) Boulders in a faulted alluvial fan along the Northwestern foothills where uplift rate during the late Pleistocene ranged between 0.7-1.7 mm/a (Wesnousky et al., 2012).

3) Incision rate of the Santo Domingo river in fluvial terraces from the Southeastern flank with an uplift during the last 70 ka of 1.1 mm/a (Guzmán et al., 2013).

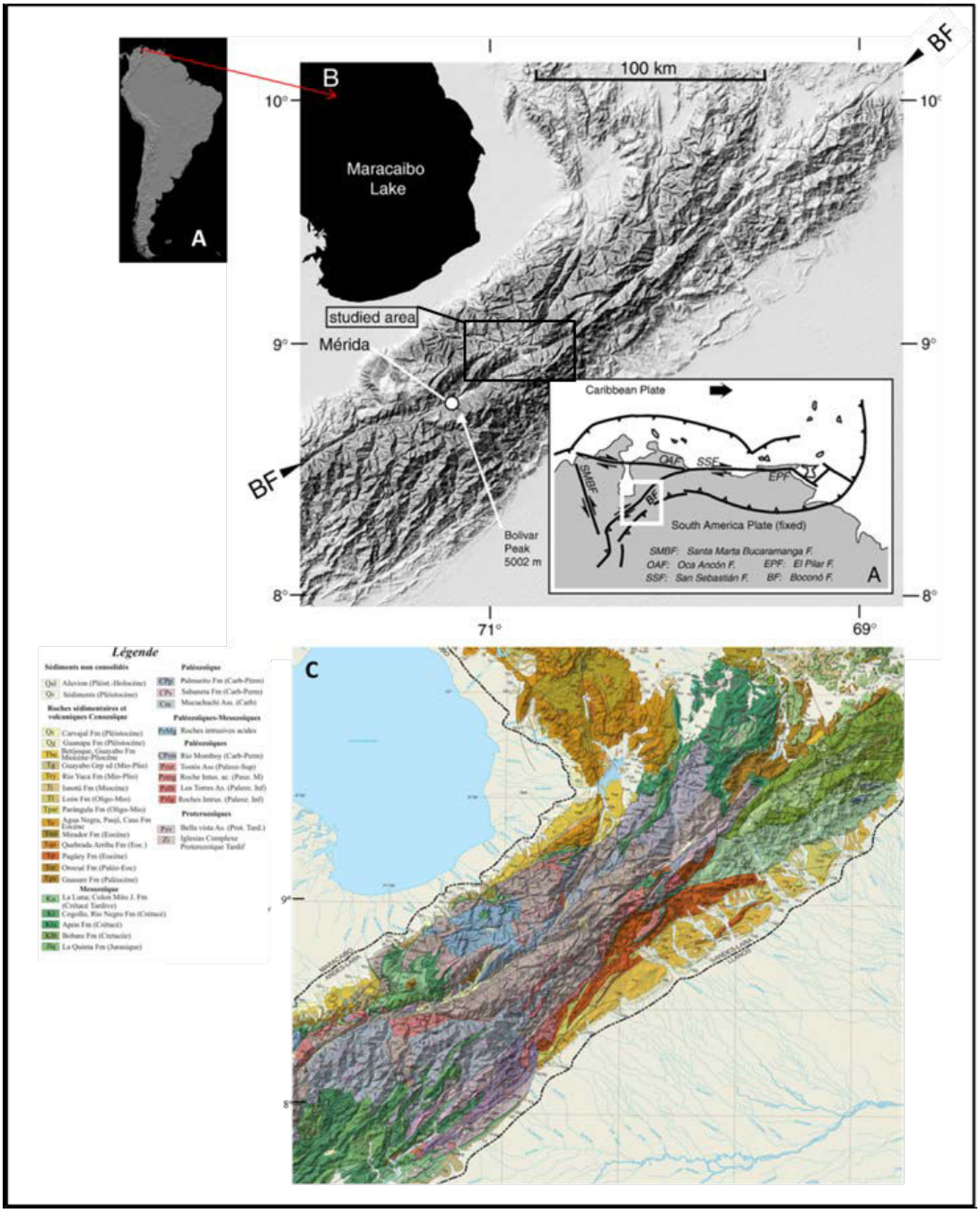

Figure III-1. Mérida Andes location (study area indicated by the black rectangle). A) Digital Elevation Model (DEM) from South America (Modified from: photojournal.jpl.nasa.gov/catalog/PIA03389) B) DEM from Mérida Andes with the main faults in Venezuela (Modified from Carrillo et al., 2008). C) Modified Geological map from the study area from Hackley et al. (2006)(Modified from Carrillo, 2006)

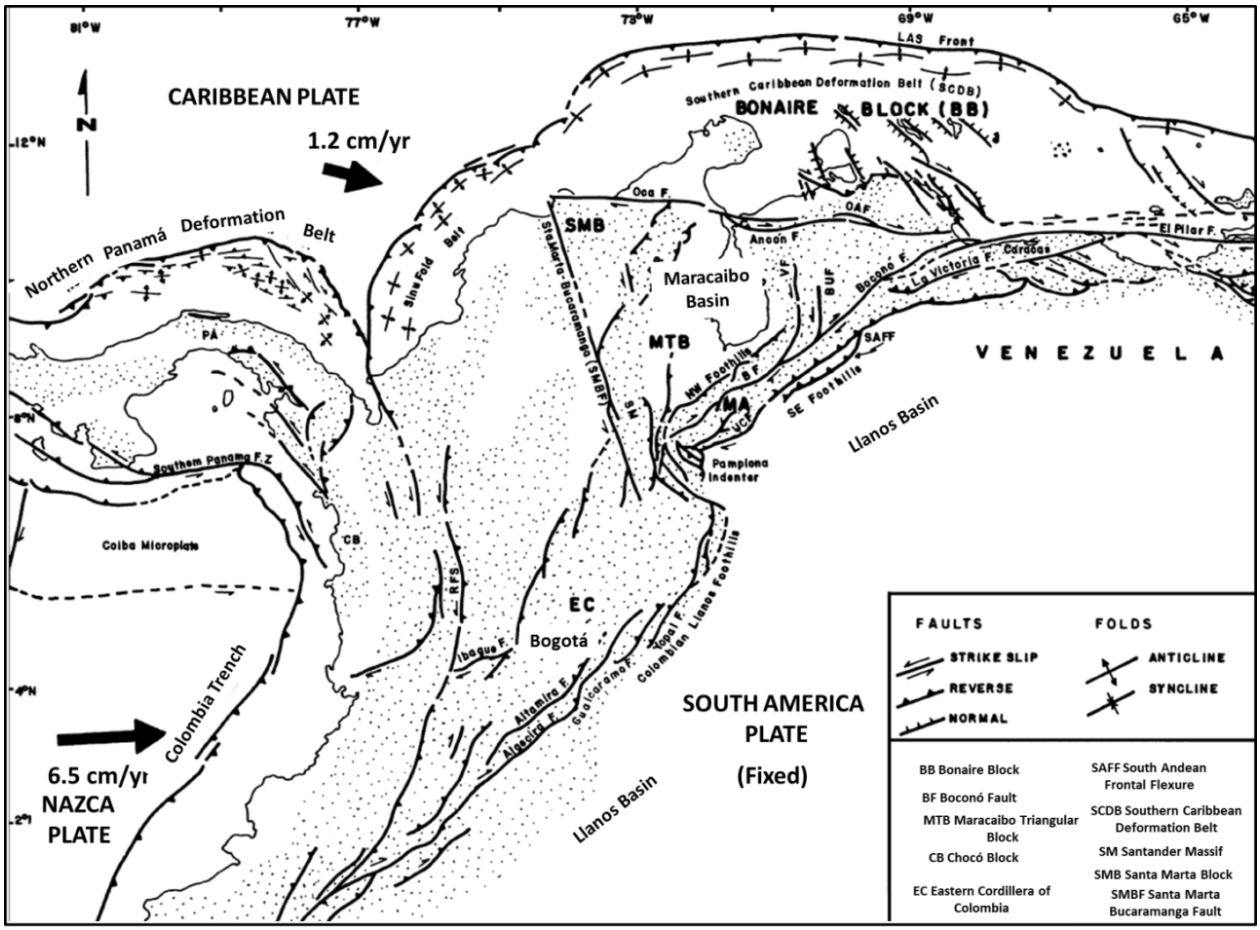

Figure III-2. Geodynamic settings in the North of South America where is the MA located. (Modified from Audemard and Audemard, 2002). (BB) Bonaire Block; (BF) Boconó Fault; (BUF) Burbusay Fault;(CB) Chocó Block; (EC) Esatern Cordillera of Colombia; (LAS) Lesser Antilles Subduction; (MTB) Maracaibo Triangular Block; (OAF) Oca-Ancón Fault; (PA) Panama Arc; (POF) Piedemonte Oriental Fault; (PR) Perijá Range; (SAFF) South Andean Frontal Flexure; (SCDS) Southern Caribbean Deformation Belt; (SM) Santander Massif; (SMB) Santa Marta Block; (SMBF) Santa Marta-Bucaramanga Fault; (UCF) Uribante-Caparo Fault; (VF) Valera Fault.

Tectonic evolution models of the MA could be divided in symmetric and asymmetric (e.g. Kellogg and Bonini, 1982; Colletta et al., 1997; Audemard and Audemard, 2002, Monod et al., 2010). In the first group, the MA is conceived as a symmetric chain with a major axial strike slip fault in the center (Boconó fault), and with bounding reverse faults on both sides of the mountain. The MA is interpreted as a positive flower structure and originates along Boconó fault by pure transpression (e.g. Rod et al., 1958; Shagam, 1972; Stéphan, 1982).

The asymmetric models are revealed by the gravimetric survey of Hospers and Van Wijnen (1959). This asymmetry is explained by two types of subduction models. The first type proposes a doubly-vergent orogen, which is produced by the incipient continental subduction of the MTB toward the Southeast (e.g. Kellogg and Bonini, 1982; De Toni and Kellogg, 1993; Colletta et al., 1997) (Figure III-3A). The other type applies an "orogenic float" model to the whole of the Caribbean-South American plates boundary zone. In this case, a major mid-crustal detachment underlying the MA, Maracaibo basin, Perijá and Santa Marta ranges is proposed, with either north-west- or south-east-directed subduction of the underlying lower crust, and varying importance of strike-slip faults (e.g. Audemard, 1991; Jácome et al., 1995; Yoris and Ostos, 1997; Audemard and Audemard, 2002; Cediel et al., 2003; Monod et al., 2010) (Figure III-3B).

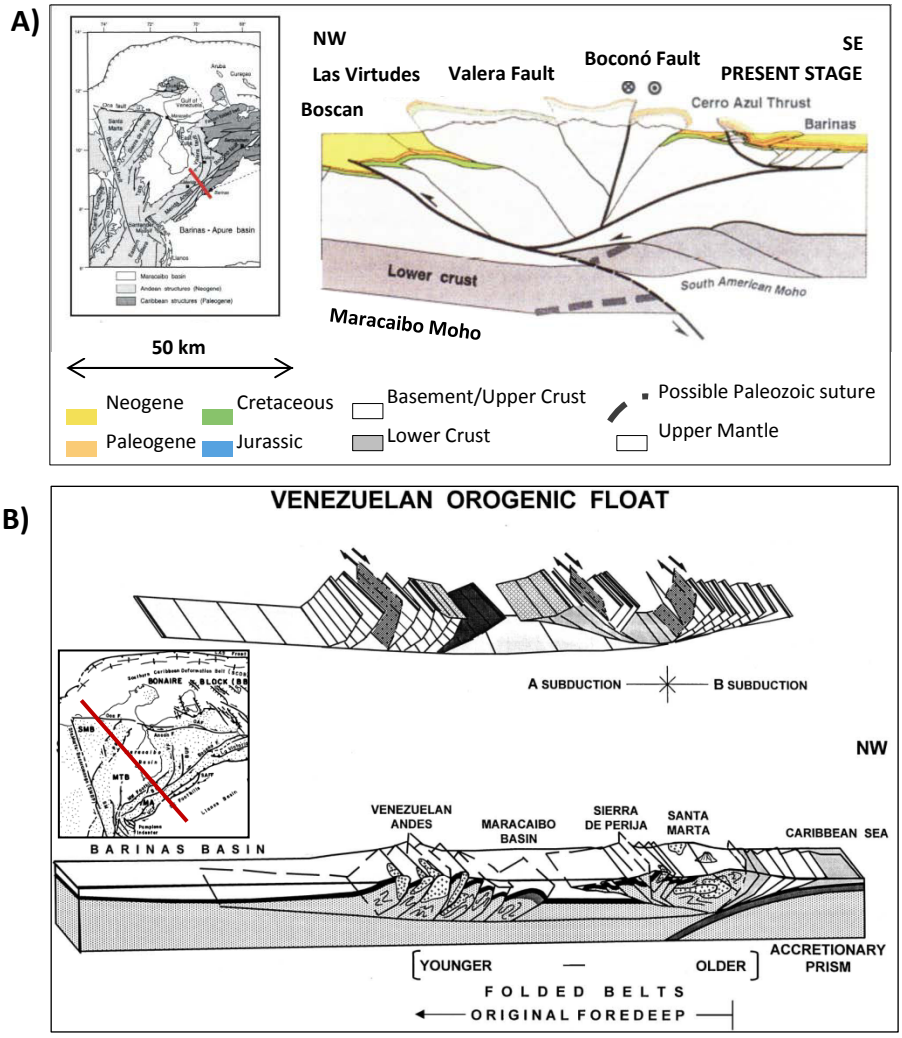

Figure III-3. Crustal models of MA. A) Modified Intracontinental collision model from Colletta et al. (1997). B) Modified crustal model from Audemard and Audemard (2002).

In the MA have been identified at least seven tectonic blocks with contrasting exhumation and cooling histories (Bermúdez et al., 2010). The Sierra Nevada, Sierra La Culata and El Carmen blocks, located in the central part of the MA, cooled rapidly but with diachronism during the late Miocene-Pliocene. Major surface uplift and exhumation occurred in the Sierra Nevada block since before 8 Ma. A second phase of uplift and exhumation affected the El Carmen and Sierra La Culata blocks during the late Miocene-Pliocene. The highest topography and steepest relief of the belt coincides with these blocks (Bermúdez et al., 2010). 70 peaks higher than 4300 m a.s.l have been identified in the central part of the MA, 54 peaks in the Sierra del Norte, 14 in the Sierra Nevada de Mérida and 2 in the Sierra de Santo Domingo (Silva, 2001).

Present-day deformation in the Mérida Andes is mainly accommodated by the Boconó Fault. It is a NE–SW trending right-lateral strike–slip (RLSS) fault that extends for about 500 km (Audemard and Audemard, 2002). It extends between the Táchira depression, at the border between Colombia and Venezuela, and the town of Morón located on the Caribbean coast (Audemard and Audemard, 2002). In Morón, the Boconó fault exhibits a 45° clockwise bend, thus prolonging into the east–west striking San Sebastián–El Pilar fault system (Audemard and Audemard, 2002) (Figure III-2).

Right-lateral offsets of Quaternary features by the Boconó Fault (BF) such as moraines, drainages, alluvial deposits and shutter ridges, range from 60 to 1000 m depending on their age (Audemard and Audemard, 2002). During Quaternary, slip rates values for the BF are between 3 and 14 mm/a (Audemard, 2003). In the central MA, at the Apartaderos Pull-apart basin, the BF slip rates for the south and north strands range, between 5–9 mm/a based on the Mucubají valley, Los Zerpa and La Victoria moraines studies (Schubert, 1980a; Soulas, 1985; Soulas et al., 1986; Audemard et al., 1999; 2008; Wesnousky et al., 2012) and between 2.3–3.0 mm/a based on El Desecho moraine study (Audemard et al., 1999), respectively. In this region, the Boconó Fault cuts Precambrian basement and Late Quaternary glacial sediments of the two last major glaciations. Deposits of the last Pleistocene glaciation, known here as the Mérida Glaciation (MIS1, MIS 2; Schubert, 1974; Schubert and Vivas, 1993) are particularly abundant along the central section of the Boconó Fault.

III-2.0 Glaciations reconstructions in the central Mérida Andes

Glaciers studies in the Mérida Andes started late XIXth century (e.g. Sievers, 1885). Jahn (1925 and 1931) made the first planimetric measurements of the existent glaciers. A large and detailed bibliographic compilation about glaciological observations in Venezuela was made by Schubert (e.g. 1972; 1974; 1975; 1980; 1992 and 1998). Typical features of high mountains affected by glaciations have been observed in the MA above ~2500 m (Figure III-4). These features are mainly composed of depositional glacial materials as till and moraines. Landscape is dominated by erosional glacial landforms at elevations higher than 3500 m (e.g. cirques, glacial step, glacier valley, horn, roche moutonnée; Schubert and Vivas, 1993). In this section are presented some geomorphological descriptions extracted from previous studies. Specific glacial morphologies in each studied valley are presented in **Results section V**.

Royo and Gómez (1959), Schubert (1970, 1972, 1974) and Schubert and Valastro (1974) described glacial morphologies in Páramo de La Culata, Páramo de Piedras Blancas and Sierra de Santo Domingo (Figure III-6 numbers 1, 2, 5 and 6). These authors determined that the landscape in the central MA is mainly characterized by two moraine complexes between 2600-2800 m and 2900-3500 m. Best preserved moraines complexes are located in the region between Mucuchíes town (MU) (by the Chama river) and Santo Domingo town (DO) (by the Santo Domingo river) (Figure III-6). This preservation has been attributed to the flatter topography in this region compare to the others and small periglacial erosion during the Holocene (Schubert, 1984).

The upper moraine level (between 2900-3500 m) is characterized by fresh and preserved till, in the form of high ridges with an internal fabric which reflects the down valley glacier movement (Schubert, 1974). The lowest moraine complex covered by abundant vegetation (between 2600-2800 m) is characterized by extremely weathered till, deeply eroded, which still shows striated and faceted pebbles (Schubert, 1974).

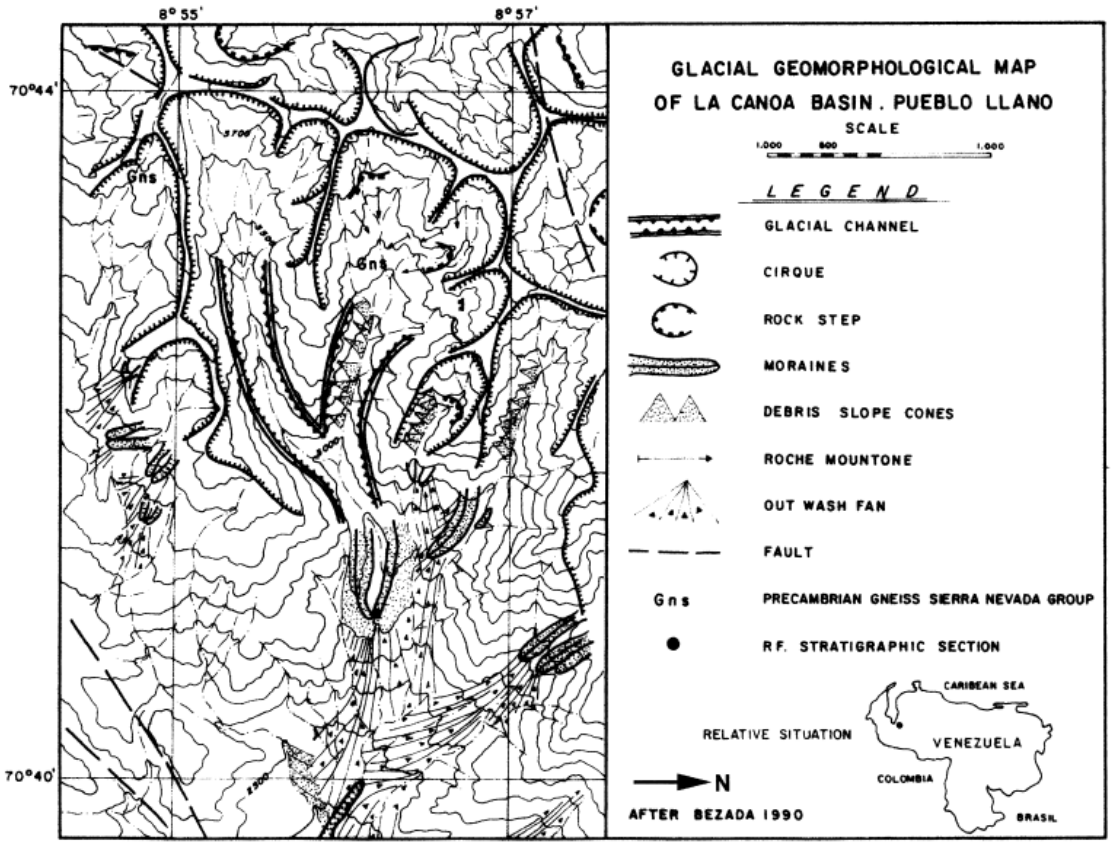

Figure III-4. Example of geomorphological features in the central MA. Geomorpgological map for La Canoa at Pueblo Llano (From Bezada, 1990).

Glaciations in the central MA have been mainly established based on the geomorphological and limited chronological data. Morphostratigraphy and till sediments descriptions in Páramo de la Culata (in Sierra del Norte), Sierra de Santo Domingo, Sierra Nevada and La Canoa in Pueblo Llano valley were used. Schubert (1974) recognized two moraines complexes. Author proposes the name of Mérida Glaciation. Mérida Glaciation was divided in the Early (moraines between 2600-2800 m) and Late Mérida Glaciation (moraines between 2900-3500 m) (Schubert, 1970, 1974).

MIS 1 and MIS 2 glaciers advances are related to Late Mérida Glaciation (Late Wisconsin) which is better constrained and range between 25-13 ky (based on radiocarbon dating; Schubert 1974; Schubert and Valastro, 1974; Schubert and Clapperton, 1990).

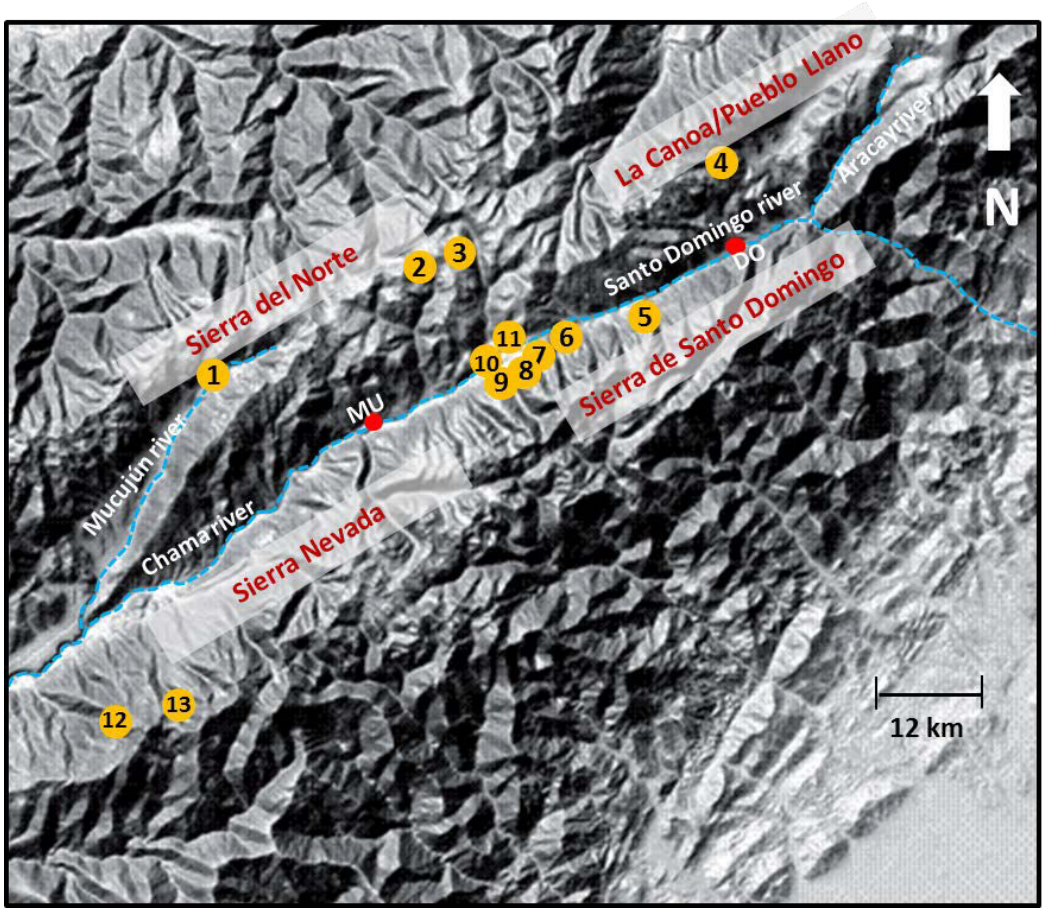

Figure III-6. Location of glaciations and paleoclimate studies developed in the central Mérida Andes. 1: Páramo de La Culata/ La Culata moraine, 2: Páramo de Piedras Blancas, 3: Laguna Verde Alta/Páramo de Piedras Blancas, 4: La Canoa moraine / RF3 section, 5: Los Zerpa moraine, 6: La Victoria moraine, 7: Mucubají valley, 8: El Caballo moraine, 9: Mucuchache valley, 10: PED5 section, 11:LAG 4 and LAG 5 sections, 12: Laguna Los Anteojos, Humboldt Massif, 13: Lago Verde, Humboldt Massif (DEM from FAQ, 2004).

A Younger Dryas (YD) glacier advance was recorded close to Lago Verde in the Humboldt Massif at 10.52±2.00 ^{14}C BP (12.40 ka cal BP, Figure III-6 number 13), based on analyses of peat in moraine and outwash deposits at 4000 m (Mahaney et al., 2008). In the Mucubají valley (Figure III-6 number 7), peat samples covered by glaciofluvial materials (till and outwash) were collected 150 m up-valley from a small push moraine (site MUM7B, 3800 m; Mahaney et al., 2008). Peat samples were dated at 13.29 ± 0.22, 13.64 ± 0.15 and 13.66 ± 0.44 cal ka BP. These deposits have been connected to the moraine which has been associated to the YD glacier advance (Mahaney et al., 2008).

MIS 2 glaciers advances are evidenced during a local last glacial maximum (LLGM) established in Los Zerpa (~3100 m) and La Victoria (~3250 m) terminal moraines in Sierra Nevada (Figure III-6 numbers 5, 6; Wesnousky et al., 2012). Terminal moraines were dated at 16.7±1.4 ka and 15.2±0.9 ka respectively. These ages are based on weighted averages exposure ages using ^{10}Be nuclide dating. MIS 2 glacier advances are evidenced in Sierra del Norte in La Culata moraine (Figure III-6 number 1) at 14.1±1.0 ka and 15.2±0.9 ka (3400-3500 m), based on average exposure age using ^{10}Be nuclide dating (Wesnousky et al., 2012).

Lowest moraines level between 2600-2800 m was stablished as glaciers advances during the Early Mérida Glaciation, during MIS 4 and MIS 5 (Schubert, 1974). This stage is poorly constrained. Only few chronological data are available and ages range between ~60 and ~90 ka (Mahaney et al., 2000; Mahaney et al., 2001; Dirszowsky et al., 2005; Mahaney et al., 2010a). Kalm and Mahaney (2011) indicate evidences of Early Mérida Glaciation at PED5 section in Mesa del Caballo at ~3500 m (Figure III-6 number 10), As well in the RF3 section in La Canoa valley at Pueblo Llano at ~2800 m (Figure III-6 number 4). Finally, evidences have been reported in Los Zerpa terminal moraine at Los Frailes. However, chronological data is not presented for Los Zerpa and Wesnousky et al. (2012) based on ^{10}Be nuclide dating determine this moraine age at 16.7±1.4 ka. The chronostratigraphy of the mid to upper PED5 section placed a minimum age on the glaciolacustrine sequence at ~60 ka (Mahaney et al., 2010a). In the RF3 section of La Canoa moraine (Pueblo Llano, Figure III-6 number 4) is recorded the oldest evidence of the Early Mérida Glaciation, based on the lowest glaciotectonized diamict dated at 81 ka using optically-stimulated luminescence (OSL; Mahaney et al., 2000).

Possible evidences of the previous MIS 5 glaciers advances have been indicated in the Chama, Mucujún (2600 m), Aracay and Santo Domingo river valleys (Figure III-6), in the form of isolated outcrops of a diamicton (Schubert, 1984). Also in Mesa del Caballo, Mahaney et al. (2010b) studied LAG 4 and LAG 5 sections close to El Caballo moraine at ~3500 m (Figure III-6 numbers 8 and 11). Authors found evidences of two glaciers advances, based on differences in the weathered state of light and heavy minerals between till layers in LAG 5 (equivalent to the entire LAG 4 section). A sharp

relation was identified between these two glaciers advances which indicate a hiatus of unknown length in time. The weathered state of sands with clay mineral composition, in the paleosols of LAG 4 and LAG 5 suggests an age further back in Pleistocene time. Authors proposed the ice source was probably initially located at 2-4 km to the south of Mesa del Caballo. This assumption is based on the Boconó fault movement. The ice source was located at the south of the Mucuchache valley (Figure III-6 number 9).

III-3.0 Paleoclimate settings

Quaternary climate studies in the MA are based on analysis of lacustrine, fluvial, glacial deposits and paleosols (e.g. Schubert 1974; Schubert and Valastro, 1980; Salgado Labouriau, 1984; Bradley et al., 1985; Salgado-Labouriau, 1989; Weingarten, 1990; Yuretich, 1991; Salgado-Labouriau et al., 1992; Rull, 1995; Mahaney et al., 2000; Dirszowsky, 2005; Rull et al., 2005; Stansell et al., 2005; Mahaney et al., 2007; Carrillo, 2006; Carrillo et al., 2008; Rull et al., 2010; Stansell et al., 2010). Also paleoclimate deductions have been obtained based on paleo ELA reconstruction (Stansell et al., 2007).

Paleoclimate information before Early Mérida Glaciation is not extensively detailed. Few evidences of glacial deposition prior to Mérida Glaciation (Wisconsinan, Weichselian) have been observed. The "El Pedregal interstadial" has been described between the Early and the Late Mérida Glaciation (Figure III-7) (Dirszowsky et al., 2005; Rull, 2005). These studies were based on sedimentology and geochronology analysis of 8 m of predominantly lacustrine material from the PED5 section. Warmer and wetter climate conditions have also been described from analyses of alluvial terraces: 1) 2nd alluvial terrace in the valley of Rio Motatán at Tuñame with peaty layers dated (^{14}C on wood) between 50.6 and 33.7 ^{14}C ka BP) (Schubert and Valastro, 1980; Schubert and Vivas, 1993). 2) The RF3 section in La Canoa valley at Pueblo Llano, with dating of sandy silt between 31-26 ka (OSL ages) overlain by glacially deformed sand which allow extending the interstadial conditions to the immediate onset of the Late Mérida Stadial at ca. 25 ka (Schubert and Clapperton, 1990).

Last Glacial Maximum (LGM) was established based on palynological analysis between 22.75 and 19.96 cal ka BP of PED5 section (Figure III-7) (Schubert and Rinaldi, 1987). Temperatures were at least 8.8±2°C cooler than today in the MA

(Stansell et al., 2007). This study was based on a paleo ELA variations considering precipitation variation (ΔP) between -500 and 500 mm/yr.

El Caballo Stadial is a cold period dated at 16.5±0.3 ka BP which was identified from pollen inventory in fluvioglacial sediments from Mesa del Caballo section (PED5 section). Temperatures were probably around 7°C lower than today (Rull, 1998; Figure III-7).

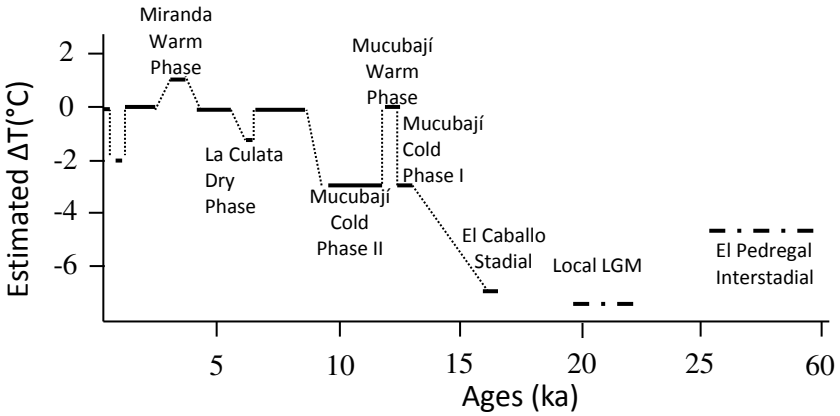

Figure III-7. Paleoclimate phases determined in the MA (Based on Salgado-Laboriau and Schubert, 1976, Salgado-Laboriau et al., 1977, Schubert and Rinaldi, 1987, Salgado-Laboriau, et al., 1988, Rull, 1998, Dirszowsky et al., 2005)(Modified graphic from Carcaillet et al., 2013).

Based on paleoecological analysis of the Late Quaternary terrace from Mucubají valley (Figure III-7), Salgado-Labouriau and Schubert (1977) defined the Mucubají Cold phase at 12.65 ka BP. This phase had an average temperature 2.9°C lower than current temperatures. Rull et al. (2005, 2010) relate the Younger Dryas (YD) glacier readvance to the cold period of the Mucubají phase. Abruptly colder and drier climate conditions in Sierra Nevada occurred between 12.85 ka and 11.75 ka (Stansell et al., 2010). This assumption is based on geochemical and clastic sediment analyses from Laguna Los Anteojos at 3900 m. These authors established that the maximum glacier extension occurred at 12.65 ka. ELA values were ~360 to 480 m lower than today and temperature declined between 2.2-2.9 ºC colder than today. Rull et al, (2010) using a high palynological analysis from Laguna Los Anteojos, also determined cold climate conditions between 12.86 ka and 11.65 ka. Temperatures were 2.5-3.8 ºC colder than today. Carrillo et al. (2008) determined cold climate conditions during the YD (~11.6

ka- ~12.8 ka BP) based on magnetic susceptibility in core sediment from Mucubají Lake. Abrupt warming at the onset of the Holocene (~11.6 ka BP) was also recognized.

Finally, pollen records have shown that vegetation and climate was similar than today during most of the Holocene (Salgado-Labouriau et al., 1988, 1992; Rull, 1999). Some short cold events occurred at 6.0–5.3 ^{14}C ka BP (La Culata cold/dry phase; Salgado-Labouriau and Schubert, 1976), also between the eleventh to seventh centuries (Rull et al., 1987). The coldest period was recognized between the 13th to 17th centuries; Piedras Blancas phase IV (Rull et al., 1987). Whereas relatively warm conditions occurred between 9.4–6.3 and 3.6–2.5 ka BP (Miranda warm phases; Salgado-Labouriau et al., 1988; Schubert and Vivas, 1993).

III-4.0 Present-day climate in the Venezuelan Andes

The climate of the northern tropics is mainly controlled by the Intertropical Convergence Zone (ITCZ), which is highly dependent on the seasonal cycle of solar declination (Benn et al., 2005). Average temperature in the Mérida Andes varies little seasonally, but diurnal temperature fluctuations may be as much as 20°C (Schubert and Clapperton, 1990). These temperature variations are determined by insolation, solar radiation and cloudiness factors (Monasterios and Reyes, 1980).

Moisture is predominantly derived from evaporation over the tropical Atlantic and evapotranspiration from the Orinoco River Basin, which is advected toward the Andes by easterly trade winds (Pulwarty et al., 1998). Modern climate data from the MA also demonstrate the pervasive influence of equatorial Pacific SSTs (Polissar et al., 2013). Precipitation is highly seasonal, with a maximum during the boreal summer and minimum during winter (Pulwarty et al., 1998). However, more recently, Poveda et al. (2006) established maximum precipitations during fall and spring seasons (North Hemisphere). Patterns are also affected by orographic controls and local mountain circulation systems (Pulwarty et al., 1998; Poveda et al., 2006).

Climate in the MA is also locally influenced by the Maracaibo, Los Llanos and Lara-Falcón basins (Figure III-8) (Monasterios and Reyes, 1980). The NE areas are influenced by the Lara-Falcón basin, which is characterized by a bimodal rainfall

pattern with the lowest precipitations (e.g. Cende 653 mm). Los Llanos basin mainly influences the southern MA hillsides, where rainfall pattern is unimodal and high (e.g. Mesitas 840 mm). Northernmost of the MA is characterized by a bimodal rainfall pattern originated from the Maracaibo Lake basin and with values higher than 1000 mm (e.g. La Culata; Figure III-8; Monasterio and Reyes, 1980).

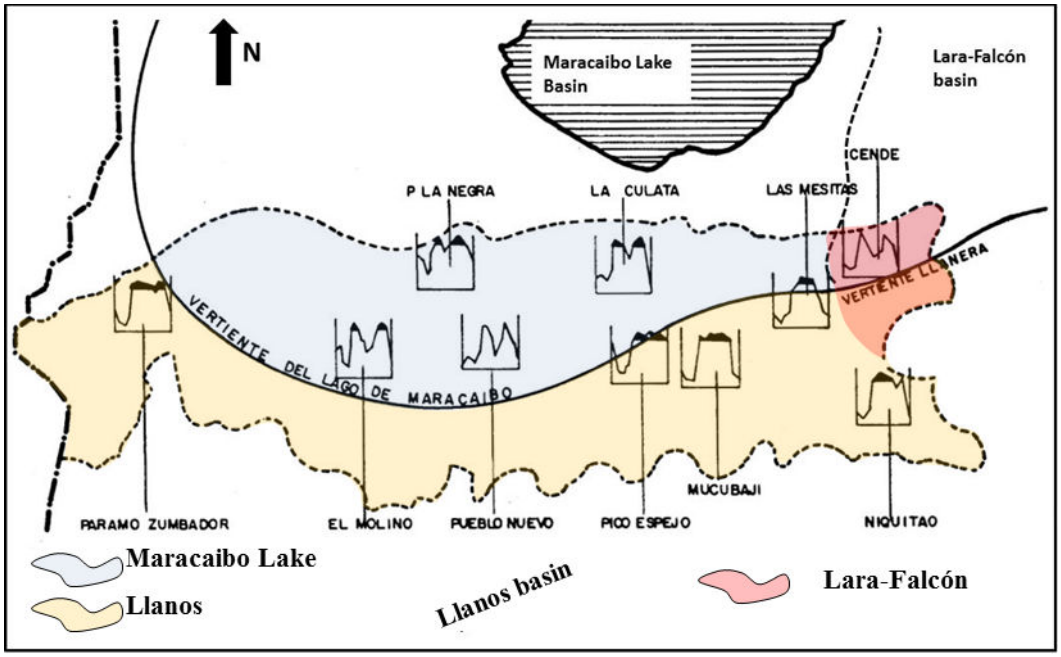

Figure III-8. Schematic rainfall patterns distributions in the MA. Valleys close to the Maracaibo lake basin have bimodal rainfall pattern whereas valleys toward Los Llanos basin have unimodal patterns. Valleys close to the Lara-Falcón basin have bimodal pattern and the lowest rainfall values (Modified from Monasterios and Reyes, 1980).

In order to study the deglaciation histories to reconstruct glaciations and establish paleoclimate deductions, paleoglaciological researches imply the use of glacial geomorphology and geochronology studies. The paleoclimate deductions made in this dissertation are based on the paleoglaciological approach of paleo ELA and paleoclimate proxy records correlations. The geomorphological analysis was initially used to select which glacial landforms study. The Terrestrial Cosmogenics Nuclides (TCN) using the ^{10}Be cosmonuclide dating was used as a geochronology method to determine deglaciation ages of the glacial landforms. The geomorphological analysis was also used to determine paleo ELA values.

Section IV begins with fundamental aspects of the geochronology based on TCN ^{10}Be cosmonuclide dating (**IV-1**). Then, reasons on the selection of the study area and samples locations selected are exposed in an overall perspective (**IV-2**) (more details about why each valley or moraines were selected are present in **section Results V**). Methodology used for samples preparation, analysis and exposure ages calculations are present in **IV-3, IV-4** and **IV-5**. Former glaciers surface and thicknesses reconstructions methodology are presented in section **IV-6**. Finally, paleo ELA reconstruction methods are presented in section **IV-7**.

IV-1.0 Geochronology method based on Terrestrial Cosmogenics Nuclides (TCN)- ^{10}Be nuclide dating

Lithology in the area is mainly felsic composition, rich in quartz. Thus, the TCN- ^{10}Be cosmonuclide dating was used to study deglaciation ages of the glacial landforms. To better understand the geochronological method some fundamentals aspects are presented.

IV-1.1 Interaction between cosmic rays and matter

Cosmic rays are high-energy, charged particles that enter the Earth environment (atmosphere, hydrosphere and lithosphere). The majority of cosmic-ray particles are protons (~83%), but they also include α-particles (~13%), electrons (~3%), and heavy nuclei (~1%) (Dunai, 2010).

Cosmic rays produce nuclear reactions with atmospheric targets and produce secondary particles (Figure IV-1). Because some charged particles interact with the matter in the atmosphere, cosmic rays composition changes from the top of the atmosphere to the Earth´s surface. At the top of the Earth's atmosphere the cosmic rays are largely composed of protons (87%), α-particles (12%) and heavier nuclei (~1%) (Dunai, 2010). At the sea level, the cosmic rays composition is mainly neutrons (98%) (Dunai, 2010). This new composition of the cosmic rays interacts with the lithosphere, specifically with target atoms (e.g. Si, O, Mg, Fe, Al, Cl, K) within minerals (e.g. quartz and olivine) (Bierman, 1994; Gosse and Phillips, 2001). Cosmogenic nuclides (TCN) also called *in situ* cosmogenic nuclides (e.g. ^{3}He, ^{21}Ne, ^{22}Ne, ^{36}Cl, ^{26}Al, ^{10}Be) are produced (Bierman, 1994; Gosse and Phillips, 2001).

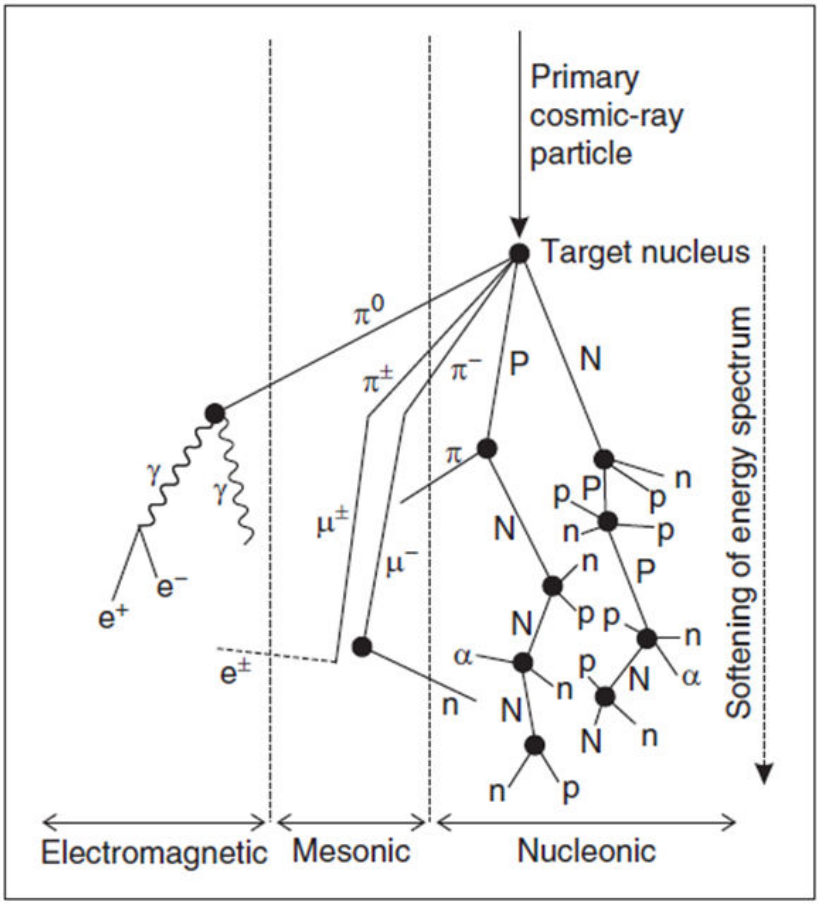

Figure IV-1 Cosmic rays and Earth matter interaction in the atmosphere. It is showed the cascade reaction as result of particles interaction. Abbreviations used: n neutron, p proton (capital letters for particles carrying the nuclear cascade), α alpha particle, $e^{\pm}$ electron or positron, γ gamma-ray photon, π pion, μ muon (Dunai, 2010).

IV-1.2 Terrestrial Cosmogenics Nuclides (TCN)-^{10}Be nuclide dating

Since the beginning of the eighties, TCN dating was a useful tool to quantify surface geological processes. Nowadays technical improvements and developments allow to measure low concentration ($^{10}Be/^{9}Be \approx 10^{-16}$) with low analytical uncertainties (< 5%).

In this study the beryllium-10 (^{10}Be) nuclide dating was used because production principles of ^{10}Be in Quartz are the more documented and the collected lithologies are mainly granites and gneiss. This isotope has a lifetime of 1.36+/- 0.07 Ma and it is obtained by spallation reactions mainly on silicon and oxygen atoms in the minerals structures (Dunai, 2010). As cosmic rays energy strongly decreases with the depth of penetrated material, depth production decrease by an exponential law (Gosse and Phillips, 2001). By convention, the reference production rate is proposed for a Sea-Level and High Latitude (SLHL) location. This SLHL production must be scaled to the sample site in order to take in to account local parameters.

IV-1.3 SLHL TCN production rate scaling (local parameters controlling the ^{10}Be production rate)

IV-1.3.1 Magnetic field and latitudinal dependence

Because incoming cosmic rays is modulated by the Earth magnetic field (Carcaillet, 2003), the ^{10}Be production rate, and consequently ^{10}Be concentration, is controlled by the intensity of the magnetic field. This latitudinal modulation being significant for low latitude (<50°), it is particularly critical for TCN dating in tropical areas.

IV-1.3.2 Altitudinal dependence

The only fraction of the cosmic rays with enough energy allows the production of TCN. Because this fraction decreases with the atmosphere depth, the TCN production varies with elevation with maximum production in elevation and minimum at sea-level.

IV-1.3.3 Topographic dependence

Sampling in area surrounded by relief requires considering the proportion of cosmic rays flux shielded by topography. This is reached by calculation of the part of the semi-hemispherical sky shielded using clinometers at the sampling site (Figure IV-2) (Siame, 2000; Gosse and Phillips, 2001; Dunai, 2010).

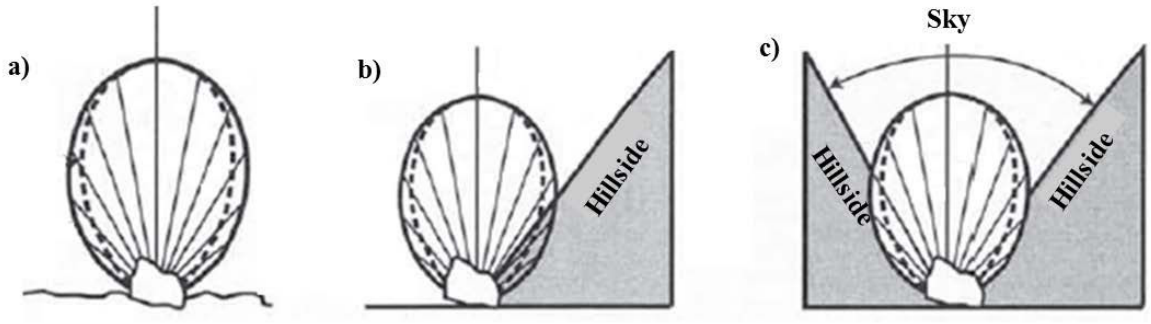

Figure IV-2. [10] Be production depending of the topography around the place of the sample collection (Modified from Siame et al., 2000). a) Sample location receives more cosmic rays from all directions. b) It is an intermediate case where cosmic rays do not impact from all directions because of hillside which shield the boulder. c) It is the case with the highest shielding factor.

IV-1.3.4 Depth production

In rocks, ^{10}Be is mainly generated by neutrons and muons collisions. ^{10}Be concentration varies with the sampling depth (which follow an exponential law, Figure IV-3), the exposure duration and the surface erosion (Gosse y Phillips, 2001).

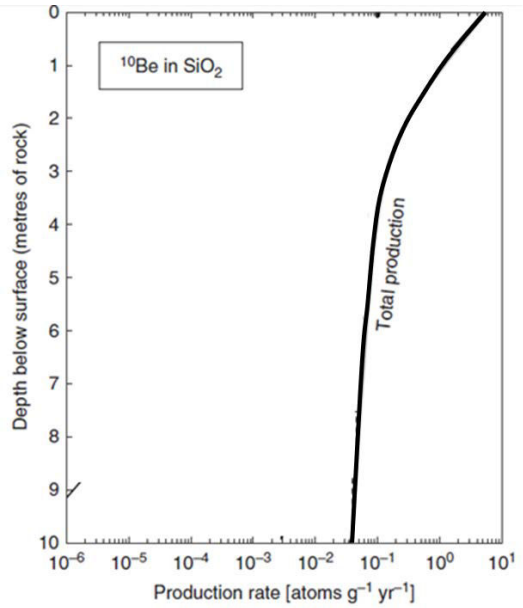

Figure IV-3. The ^{10}Be production in quartz as a function of depth below surface at Sea Level and High Latitude (SLHL; Modified from Dunai, 2010).

Considering erosion rate and cosmic radiation through the time, ^{10}Be concentration in rocks can be modeled as follow:

$$C(x,\varepsilon,t) = C_{inh}.e^{-\lambda t} + \frac{Po.Pn}{\frac{\varepsilon}{\Lambda_n}+\lambda}.e^{-\frac{x}{\Lambda_n}}\left[1-e^{-1\left(\frac{\varepsilon}{\Lambda_n}+\lambda\right)}\right] + \frac{Po.P\mu s}{\frac{\varepsilon}{\Lambda_{\mu s}}+\lambda}.e^{-\frac{x}{\Lambda_{\mu s}}}\left[1-e^{-1\left(\frac{\varepsilon}{\Lambda_{\mu s}}+\lambda\right)}\right] + \frac{Po.P\mu f}{\frac{\varepsilon}{\Lambda_{\mu f}}+\lambda}.e^{-\frac{x}{\Lambda_{\mu f}}}\left[1-e^{-1\left(\frac{\varepsilon}{\Lambda_{\mu f}}+\lambda\right)}\right]$$

Equation IV-1

C(x, ε, t) is the ^{10}Be concentration at a depth **x** (below the surface in cm) with an erosion rate **ε** (cm/yr) and an exposure time **t**. P_o is the ^{10}Be production rate in atoms/grams/year (at/g/a). C_{inh} is the ^{10}Be concentration in atoms/grams (at/g) inherited from previous exposures (if is effective). *Pn*, *Pμs*, *Pμf* (in atoms g^{-1} yr^{-1}) are the relative contributions of neutrons, slow muons and fast muons (*Pn=97.85%*, *Pμs=0.65%*, *Pμf=1.65%;* Braucher et al., 2003). SLHL reference production rate is done for surface. Because of the exponential law production drop, sample thickness (cm) must be taken in account for calculation.

IV-1.3.5 Temporal evolution of TCN concentration

During continuous exposure, ^{10}Be concentration increases with time until it reaches a steady state when production and losses due to erosion and radioactive decay are equal. This state is reached earlier when the erosion rate of the surface is high (Figure IV-4). Accurate exposure time calculation is thus possible when the concentration has not reached this steady state.

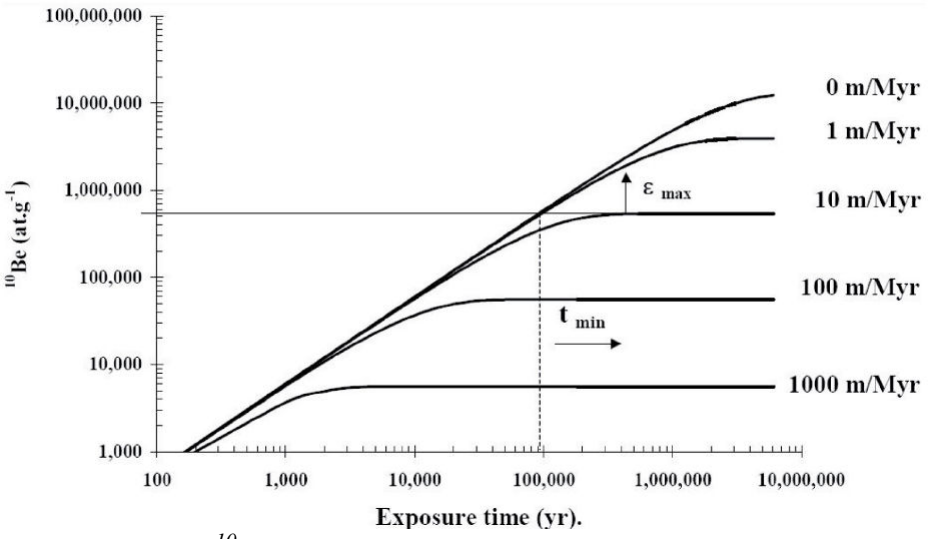

Figure IV4. Theoretical ^{10}Be concentrations evolutions with exposure time for different erosion rates (Brown et al., 1991). A ^{10}Be concentration could be interpreted as an age (exposure time) or as an erosion rate (m/Myr). Based on the geological and geomorphological context could be assumed if erosion is equal to or different from 0

m/Myr. Considering ε=0, a ^{10}Be concentration of 550.000 at.g^{-1}represent 90 ka as exposure age. Considering erosion significant >0 the maximum erosion is 10 m/Myr (Modified from Le Roy, 2012).

When erosion is not high is thus possible determine accurate exposure ages. The geological and geomorphological context allows inferring erosion hypotheses where samples were collected. If erosion is assumed 0 cm/yr, ^{10}Be is determined using:

$$C_{(0,t)} = \frac{P_0}{\lambda}(1 - e^{-\lambda t_{\min}})$$

Equation IV-2

The minimum age (t_{min}) is found using:

$$-t_{\min} = \frac{1}{\lambda} \cdot Ln(1 - \frac{\lambda \cdot C(0,t)}{P_0})$$

Equation IV-3

IV-1.4 ^{10}Be nuclide dating implications on glaciation reconstruction studies

Glacial erosion generates landforms that are exposed to cosmic rays after glaciers retreat. ^{10}Be geochronology is suitable to date exposure time of these abandoned glacial landforms. This could be referred also as deglaciation ages which can be interpreted to identify climate changes which control former glacier dynamics. Erosion could happen after glacial landforms deglaciation and could remove some of the cosmogenic nuclides. It is important to evaluate this process. Observation of evidences of glacier activity (i.e. striation, polished surfaces) and/or consideration of published data of rock erosion, allow to precise the computed age. Because the sampled surface can undergo unquantifiable erosion, exposure ages are assumed as minimum estimates (Nishiizumi et al., 1989; Briner and Swanson, 1998; Siame et al., 2000; Gosse and Phillips, 2001; Dunai, 2010; Balco, 2011).

IV-2.0 Study area location and samples collection

Glacial landforms selection was based on aerial photographs from Cartografía Nacional mission of 1952. Previous glaciations studies developed by Schubert (e.g. 1972; 1974; 1980; 1992 and 1998) and paleoclimate studies in the Venezuelan Andes (e.g. Salgado-Laboriau and Schubert, 1977; Schubert and Rinaldi, 1987; Rull 1998; Mahaney et al.,

2001; Dirszowsky et al., 2005; Stansell et al., 2005; Mahaney et al., 2007) were also used. Finally, glacial landforms selection was based on geological maps and present-day climate conditions distributions. We focused the study on the central Mérida Andes because numerous glaciers landforms are well preserved (see more in **Section III-2.0**). Moreover, this area shows contrasted climate settings (**Section III-3.0**). Valleys from Sierra del Norte (Maracaibo Lake influence), Sierra Nevada and Cordillera de Trujillo (more Los Llanos basin influence) were selected (Figure IV-5).

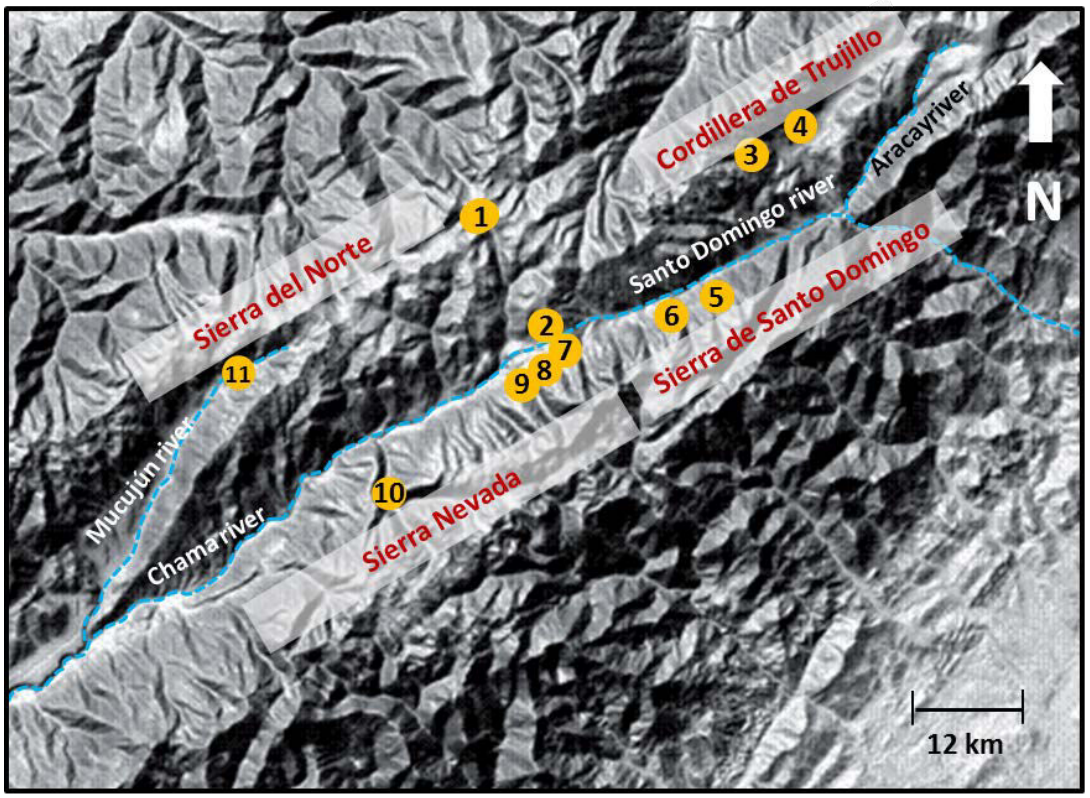

Figure IV-5. Location of Glacial landforms studied. 1: Mifafí valley 2: El Desecho moraine, 3: La Canoa moraines, 4: Pueblo Llano moraines, 5: Las Tapias moraines, 6: Los Zerpa moraines, 7: Mucubají valley, 8: El Caballo moraine, 9: Mucuchache valley, 10: Gavidia valley, 11: La Culata moraine (DEM from FAQ, 2004).

Sample locations were selected based on geomorphological interpretations of aerial photographs and field observations. Samples were collected on:

- Striated /polished rocks and roches moutonnées. Samples were carefully collected on landforms where minimum potential coverage by superficial deposits and erosion existed.

- Moraines boulders. Boulders (mainly > 0.4 m^2) well-anchored in the moraine to avoid any post-deposition movements were selected.

Because ^{10}Be production decrease in depth, samples collection have to be restricted to the first centimeters of the rocks. Samples thicknesses were lower than 5 cm and in general samples weighed ~ 1kg of rock. Because of ^{10}Be production is latitudinal, altitudinal and topographical shielding dependent, to each sample GPS location, geological description, topographic shielding and elevation were noticed. A total of 100 samples were collected, prepared and analyzed in the frame of this project (details about glacial landforms sampled and samples collected to each valley are presented in the **Results section V**).

IV-3.0 Samples preparation

Chemical targets were prepared at the cosmogenic laboratory at ISTerre, France. The methodology followed adapted procedures from Brown et al. (1991) and Merchel and Herpers (1999). Samples preparation methodology could be divided in 2 steps: quartz separation from bulk material and Chemical ^{10}Be extraction in the BeO form, to be discussed next.

IV-3.1 Quartz separation from bulk material

Samples were crushed and sieved. The 200-500 μm fractions were separated from magnetic minerals using Frantz magnetic separator (when considerable quantities were present in the sample, determined from visual inspection). Samples (~80-120 g) are placed in a previous weighed Nalgen bottles. The first chemical attacks were performed using hydrochloric acid (HCl 36%) to remove any carbonate minerals. In a second time, samples were mixed with successive HCl (36%)-H_2SiF_6 (35%) solution to remove minerals except quartz. HCl-H_2SiF_6 mixture (from 50%-50% until 10%-90%, respectively) was changed every ~ 2 days until the sample was pure quartz (until ~ 2 months).

IV-3.2 Chemical *^{10}Be extraction in the BeO form*

Once purified, samples were decontaminated from the atmospheric ^{10}Be adsorbed on quartz by three sequential dissolutions (10% quartz dissolved each one, using ratio 1g of quartz:4 ml HF) with fluorhydric acid (HF 40%) (Brown et al., 1991). Samples were dried, quartz mass was weighed and a ^{9}Be solution (1000 mg/l, Scharlau batch

14569501, ~300 μg/sample) was added. Spike addition fixe the $^{10}Be/^{9}Be$ ratio for AMS measurement and reduces perturbations due to leakage during chemical handling. Total dissolution was made with HF (1g of quartz:4 ml HF). Analytical blanks were prepared (each 10-15 samples) using ~50 ml HF and ~500 μg ^{9}Be spike.

For safety reasons, the solution is transferred to a Teflon beaker in order to substitute to HCl mixture. This substitution includes successive acid attack to remove organic compound (using $HClO_4$), destroy fluorures (using HNO_3) and finally, substitute in HCL.

Successive sample precipitations were made to extract ^{10}Be using NH_4OH. This decisive step is important because it allows to remove boron from sample because it precipitates at pH >8 while ^{10}Be precipitates at pH ~7.

The separation of beryllium from other chemical elements was made with ion exchange resins. The first anion exchange resin (DOWEX 1×8, 100-200 mesh) separates (using 10.2 M HCl) potentially metals highly concentrated in quartz (iron, titanium, manganese). The second cation exchange (DOWEX 50W×8, 100-200 mesh, with 1 M HCl) was used to separate Be from aluminum and its isobar boron. Finally, the solution is evaporated until ~ 3 ml and precipitated with NH_4OH in order to remove the residual boron. The final step is to precipitate beryllium oxy-hydroxide ($Be(OH)_2$) by evaporation (~200°C) in porcelain capsule. The Beryllium oxide (BeO) is produced by heating at 900°C. BeO is mixed with niobium (Nb) and placed in a copper cathode to prepare the sample to AMS analyze.

IV-4.0 ^{10}Be concentration determination using Accelerator Mass Spectrometry (AMS)

The samples were mixed with Niobium in order to improve the conductivity of the electric current and introduce it in a sample holder (cathode). Analyses were made in the French AMS facility "ASTERisque" (Aix en Provence). Because of ^{10}B is 10^8 times more abundant than ^{10}Be and have a similar q/m ratio. The ^{10}Be determination is not possible to realize using a standard Mass Spectrometry (MS) because of the ^{10}B interference. To minimize this isobar interference, samples were analyzed with the AMS facility which allows the separation of both isobars (B and ^{10}Be).

To obtain the ^{10}Be concentration is necessary first to measure ^{10}Be/^{9}Be samples ratios and then, compare to a ^{10}Be/^{9}Be standard ratio (NIST Standard Reference 4325 with a ratio of 2.79 10^{-11}). The ^{10}Be concentration is determined because the ^{9}Be concentration is known in each sample (the ^{9}Be concentration is hold by spike addition).

The samples analyses began with the BeO ionization using the Cesium electrons. The charged molecules are introduced into the 90° injection magnet where the first separation is made. Then, BeO^- is introduced inside the accelerator tank with 5 MV. Molecules are broken and Be^{+2} are injected in the analyze magnet where the radius curvature is adjusted to allow the $^{10}Be^{+2}$ and $^{9}Be^{+2}$ flux to go on to the detector. An ultimate separation of the remaining B^{3+} is realized by crossing the flux into a carbon foil. This is based on the Bethe-Bloch law where elements are separated not only with their charge but also with their atomic numbers (higher is the atomic number, i.e. 5 for ^{10}B and 4 for ^{10}Be, higher will be the energy loss, lower will be the capacity to cross the carbon foil). ^{10}Be and ^{9}Be atoms are successively measured in the detector (Figure IV-6).

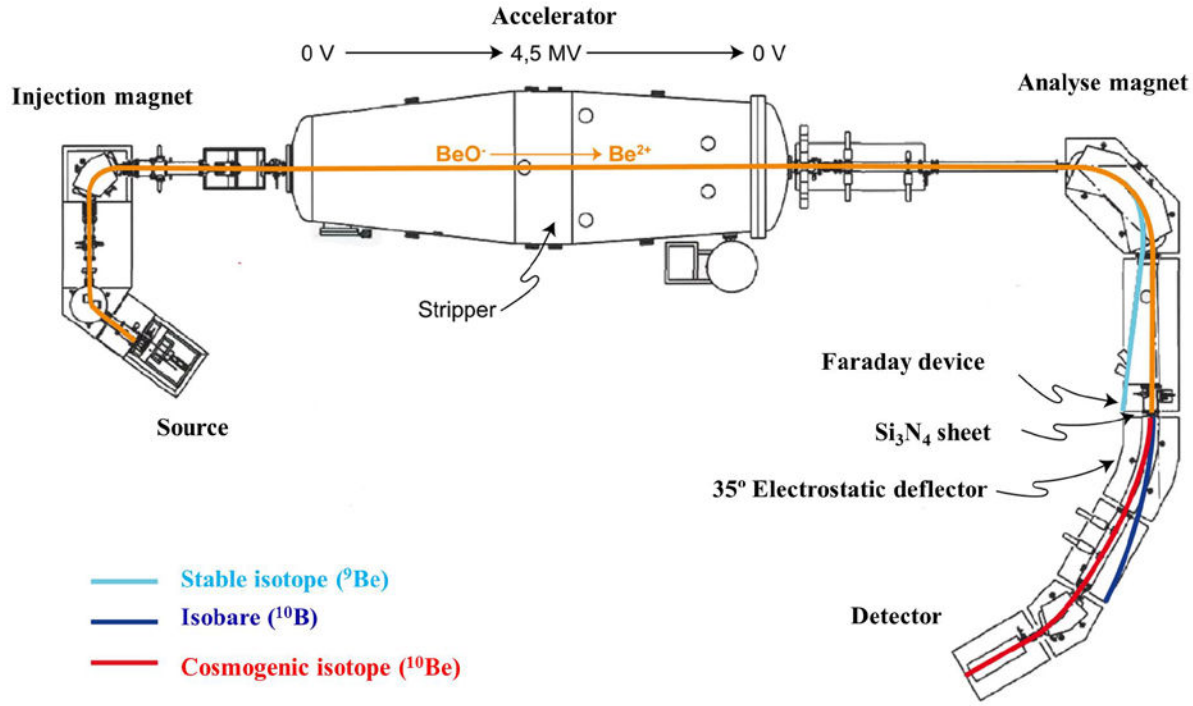

Figure IV-6. Accelerator Mass Spectrometry machine in the ASTERisque laboratory. It shows the different isotopes trajectories until the detector (Modified from Le Roy, 2012)

The analytical incertitude ($\sigma R_{10/9}$) is calculated using the counts number of "^{10}Be event" in the analyzer detector (n). The analytical incertitude is determinate by multiple standard ratios measures ($\sigma R_{10/9NIST}$) and using the next errors propagation equation:

$$\sigma R_{10/9} = \sqrt{\left(\frac{\sqrt{n}}{n}\right)^2 + \left(\sigma R_{(10/9)}{}^{NIST}\right)^2}$$

Equation IV-4

IV-4.1 ^{10}Be concentration calculation

The isotopic ratio ($R_{10/9}$) has to be transformed in beryllium atoms per quartz grams ($N10$) to obtain the time exposition ages. In the samples there are three main Be sources: a) from the sample rock ($n_{10}{}^{S}$ *and* $n_9{}^{S}$), b) the ^{9}Be spike ($n_{10}{}^{C}$ *and* $n_9{}^{C}$) and c) possible sample pollution during preparation ($n_{10}{}^{P}$and $n9^{P}$) (coming from acids or in general used chemical reactive). The isotopic ratio could be represented by:

$$R_{(10/9)} = \frac{n_{10}{}^{S} + n_{10}{}^{C} + n_{10}{}^{P}}{n_9{}^{S} + n_9{}^{C} + n_9{}^{P}}$$

Equation IV-5

Because of natural ^{10}Be abundance in the environment is very low and ^{9}Be is fixed by the addition of spike (~300 µg), ($n9^{S}$ +$n9^{P}$) is assumed to be negligible. The possible addition of ^{10}Be present in the spike and acids is related to the chemical blank ($n_{10}{}^{B}$). Equation III-5 could be written as:

$$R_{(10/9)} = \frac{n_{10}{}^{S} + n_{10}{}^{B}}{n_9{}^{C}}$$

Equation IV-6

The number of atoms of ^{9}Be spike added in the sample is calculated using:

$$n_9{}^{C} = \frac{M_C N_A}{A_{Be}}$$

Equation IV-7

Where Mc is the spike mass added to each sample, N_A is the Avogadro´s number (6.022 10^{23} at.mol^{-1}) and A_{Be} is the molar mass of beryllium (9.012 g. mol^{-1}).

^{10}Be concentration in the sample (N_{10}) is obtained from:

$$N_{10} = \frac{n_{10}{}^{s}}{M_q}$$

Equation IV-8

Where $n_{10}{}^{s}$ is the ^{10}Be atoms number in the sample and M_q is the quartz mass.

Then, substituting equations IV-7 and IV-8 in equation IV-5 is possible to determine ^{10}Be concentration as a function of isotopic ratio ($R_{10/9}$), the quartz mass sample (M_q) and the ^{9}Be spike mass (Mc).

$$N_{10} = \frac{1}{M_q}\left(\frac{R_{10/9} M_C N_A}{A_{Be}} - n_{10}{}^{B}\right)$$

Equation IV-9

And $n_{10}{}^{B}$ is the ^{10}Be from the blank. For each chemical sample set, 2 blanks were prepared and their weighted average was subtracted from the beryllium ratios of sample, where $n_{10}{}^{B}$ could be determined by:

$$n_{10}{}^{B} = \frac{R_{10/9}{}^{B} M_C{}^{B} N_A}{A_{Be}}$$

Equation IV-10

Finally, combining equations IV-9 and IV-10 is possible to determine the ^{10}Be concentration for each sample:

$$N_{10} = \frac{(R_{10/9} M_C - R_{10/9}{}^{B} M_C{}^{B}) N_A}{M_q A_{Be}}$$

Equation IV-11 or

$$N_{10} = \frac{(R_{10/9}{}^{S} - R_{10/9}{}^{B}) N_9^{C}}{M_q}$$

Equation IV-12

IV-5.0 ^{10}Be production rates, erosion value, scaling scheme and exposure ages calculation

SLHL production rates have been determined by three methods (Gosse and Phillips, 2001): (i) geological calibration based on accurate dated surfaces (using another geochronology method, as ^{14}C or U-Th system). (ii) determined by laboratory measurements by two ways: 1) using slabs of known composition which have been exposed in a nuclear accelerator beam line particles with energy similar to the secondary radiation flux on the Earth. 2) Using target materials which are exposed to actual cosmic radiation at high altitudes for periods of years (iii) by numerical simulation of the nuclear interactions and other physical processes that produce cosmogenic nuclides. Although all three have been useful, spallogenic production rates used in most cosmogenic nuclides applications have been derived from geological calibration (Gosse and Phillips, 2001). Production rates are scaled to sea level at high latitudes (SLHL). For tropical latitudes where the magnetic field modulation is maximum, there was significant uncertainties about the scaled ^{10}Be production rates as is suggested in Carcaillet et al. (2013) (**Results Section V-2.1.1**) and Angel et al., "under review" (**Results Section V-2.1.2**).

Some recent production rates have been determined at high altitudes in the tropical Andes. Kelly et al. (2013) estimated a (SLHL) *in situ* ^{10}Be production rate in Quelccaya Ice Cap (13.95°S, 70.89°W, 4857 m), in the tropical Peruvian Andes, which range between 3.97±0.09 to 3.78±0.09 at.g^{-1}.yr^{-1} for 4.5 m/Myr and 0 m/Myr erosion respectively. Blard et al. (2013) computed a (SLHL) production rate of 3.63±0.17 at.g^{-1}.yr^{-1} from the Bolivian Uturuncu volcano (22° S, 67° W, 3800-4900 m). Martin et al. (2015) computed a SLHL production rate of 3.76 ± 0.15 at.g^{-1}.yr^{-1}from the Challapata fan-delta in Bolivia (19°S, 3800 m). However, at the beginning of this project, these production rates were unavailable. In this project was initially used the global SLHL ^{10}Be production rate published by Balco et al. (2008) (4.39 ± 0.37 atoms g^{-1} yr^{-1}) (used in the Mucubají article Chapter V). Then, a production rate was determined in the

Andes by Kaplan et al. (2011) (3.81±0.13 at.g^{-1}.yr^{-1}) and it was used in the Gavidia article (Results Section V). Finally, a "tropical" SLHL production rate from Kelly et al. (2013) allowed to precise the ages. All the TCN exposure ages from this project (Carcaillet et al., 2013; Angel et al., "under review") and from previous published studies (Wesnousky et al., 2012; Guzmán, 2013) were recalculated (**Section Results V**). The Kelly's production rate was selected because it was available in the CRONUS online calculator and the value is consistent with the one published by Martin et al. (2015).

Low long-term erosion rates of the rock surfaces in the tropical Andes have been reported between 0.3–0.5 m.Myr^{-1} (Smith et al., 2005b) and 4.5 m.Myr^{-1} (Kelly et al., 2013). Smith et al. (2005b) studied moraines boulders from the Junín Plain in the central Peru at elevations between 4200-4400 m. Kelly et al. (2013) studied moraines boulders from the Quelccaya Ice Cap, Peruvian Andes at around 4800 m. Simulation considering exposure age of GA-1301FE give 16.39 ka and 17.39 ka with erosion 0 cm/yr and 4.5 cm/yr, respectively. Ages differences are around 6%. For this reason and because most of the sampled surface indicate the presence of the striations and polished surfaces, erosion rate of 0 m.Myr^{-1} was assumed for calculations. Moreover calculations are based on the assumption of no ^{10}Be inheritance. No snow coverage correction was considered because the snow falls are low and MA climate conditions prevent long periods of snow cover.

Balco et al. (2008) CRONUS online calculator is used for calculations. The selected scaling scheme is the time dependent model from Lal (1991), modified by Stone (2000). It was selected because it considers the geomagnetic field variation (Balco et al., 2008). This is important in the present study because the magnetic modulation has a particularly critical effect in the vicinity of the magnetic Equator where the samples were collected.

IV-6.0 Geomorphological analysis and former glaciers reconstructions

To develop a geomorphological interpretation of the glacial landforms, aerial photographs and a digital elevation model (DEM) with a 30 m resolution (FAQ, 2004) were used. Moreover, Google Earth images and software ArcGIS 10.0 were also used.

Former glacier outline reconstruction was based on field observations and aerial photographs and DEM geomorphological interpretations. Catchment delimitation was performed using River Tools. Then more exactly former glacier delimitations were made based on exposure ages and geomorphological interpretation (i.e. glacier front from a glacial landform with exposure age until glacier cirque considering glacier thicknesses). Thicknesses were calculated using the excel spreadsheet from Benn and Hulton (2010). This excel spreadsheet assumes a perfectly plastic ice rheology (i.e. ice return to the original position after stress is eliminated). It is based on the assumption that the ice deforms in response to the driving stress (τ^D) (stress produced by the glacier weight effects). The ice moves when the driving stress is equal to the yield stress (τ^Y; the stress after which glacier has not a plastic rheology; Equation IV-13; Benn and Hulton, 2010).

$$\tau_Y = \tau_D = \rho g H \frac{\partial h}{\partial x}$$ Equation IV-13

Where ρ is the ice density (~900 kg/m^3), g is the gravitational acceleration (9.81 m/s^2), H is the glacier thickness, h is the ice surface elevation and x is the horizontal coordinate (with the glacier front as 0 m), with the x-axis parallel to the glacier flow. This model is particularly adapted to reconstruction of former glaciers with low slopes such icecap but it has been used for reconstruction of valley former glaciers (e.g. Zebre and Stepisnik, 2014). This model was used in this dissertation because more systematic thicknesses are obtained, especially when target elevations (elevations of glacier landforms which could indicate glacier thickness) are not extensively available in the field.

Variable inputs in the model are: the longitudinal profiles (horizontal x and vertical y) of the valley bottom, shape factors (consider the valley shape restrictions in the glacier movement) which were obtained for each transverse topographical profile using Profiler v.2 spreadsheet from Benn and Hulton (2010). Target elevations and basal shear stress were also variables to use as inputs. Moraine thickness could be used as a target elevation but this value was not available to all former glaciers. Therefore, reconstructions based on a sensitivity analysis considering a range of basal shear stress for modern glaciers (50, 100 and 150 kPa; Paterson, 1981) was made. The basal shear stress is the normal stress (perpendicular) at the glacier base.

The ice surface elevation to each point along the longitudinal profile in the flow line was the most important result of the model. For each longitudinal profile, three ice surfaces were obtained (for three different basal shear stresses of 50, 100 and 150 kPa). The former glaciers were reconstructed using contour intervals each 100 m in a geographical information system (ArcGIS; Figure IV-7). La Victoria, Mifafí and La Canoa/Pueblo Llano former glacier was reconstructed using 200 m contours intervals. Ice surface contours have been drawn based on current world glaciers. Contours display a distinct pattern, becoming increasingly concave below and convex above the ELA, while remaining almost straight at the approximate mean altitude of the glacier (Porter, 1975; Carr and Coleman, 2007; Carr et al., 2010).

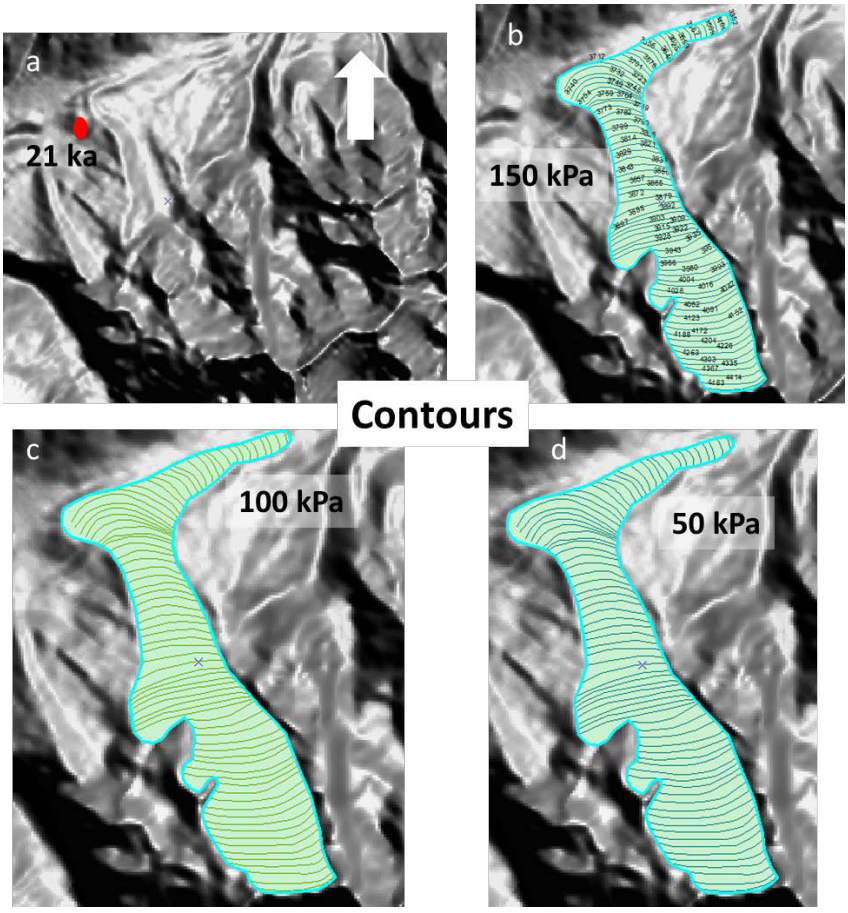

Figure IV-7. Former glacier located in the Mucubají valley at 21 ka and contours drawn. a) The red point shows the sample location and age of the frontal moraine used to draw the former glacier polygon. b), c), d) Former glaciers polygons and contours to each basal shear stress (50, 100 and 150 kPa).

For each valley at a specific age (the exposure age obtained for a glacial landform) (Figure IV-7), three ice surfaces were obtained (for 50, 100 and 150 kPa). Then, to each ice surface a DEM was reconstructed using ArcGIS 10.0 and was used as an input for paleo ELA calculations using Pellitero et al. (2015).

IV-7.0 Paleo ELA reconstruction

The Mucubají, Mucuchache and Mifafí valleys; Los Zerpa, La Victoria, El Caballo and La Canoa moraines were selected to determine paleo ELA values. The objective was to deduce paleoclimate conditions along the Sierra Nevada and Sierra del Norte-Cordillera de Trujillo. Paleoclimate deductions were made considering paleo ELA variations trends and paleoclimate proxy records.

Multiple methods have been mentioned in the bibliography to reconstruct former glaciers ELA in the tropics (e.g. Porter, 2001; Kaser and Osmaston, 2002; Benn et al., 2005). All methods involve a hypothetical steady-state where no advance and retreat happened at the time of the ELA calculation. Methods commonly used are: (1) Accumulation Area Ratios (AAR); (2) Area–Altitude Balance Ratios (AABR); (3) Maximum Elevation of Lateral Moraines (MELM); (4) Terminus to Head Altitude Ratios (THAR); and (5) gross morphological indices such as glaciation threshold and cirque floor altitudes (Stansell et al., 2007). In the frame of this project the Accumulation Area Ratios (AAR) and Area–Altitude Balance Ratios (AABR) were the used methods. It is because these methods are based on assumed forms of the glacier mass–balance gradient, more compatible with the concept of the steady-state ELA.

IV-7.1 Accumulation-area ratio (AAR)

This method assumes that, under steady-state conditions, the accumulation area of the glacier (**Sc** in Figure IV-8) occupies a fixed proportion of the glacier area (**Sc+Sa** in Figure IV-8). Steady-state AARs (**Sc/Sc+Sa**) for mid- and high-latitude glaciers lie in the range 0.5–0.8 (Meier and Post, 1962; Hawkins, 1985), with typical values around 0.55–0.65 (Porter, 1975). Because of glaciers in the humid tropics have steeper ablation gradients and less steep accumulation gradients than the mid-and high-latitude glaciers, they tend to have higher steady-state AARs (~0.8; Kaser and Osmaston, 2002). Former steady-state AARs may substantially differed from modern values in the same region. It

is due to changes in the climatic regime, debris cover or glacier hypsometry, so precautions are required to select the most suitable ratio.

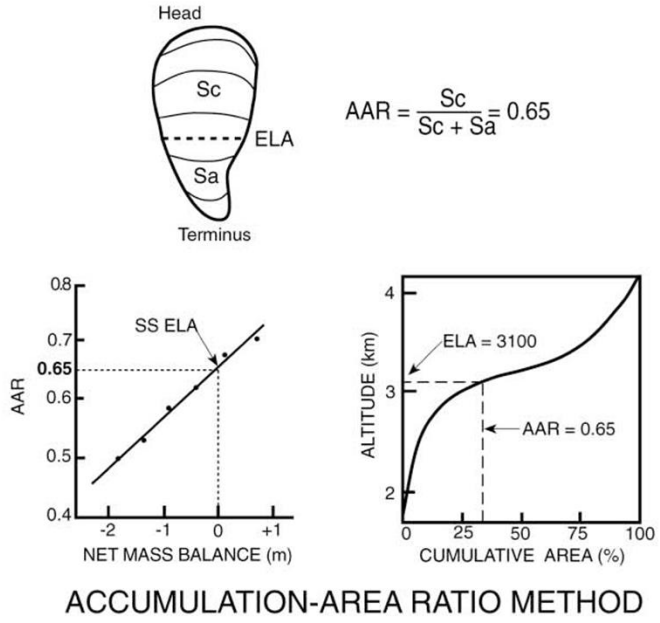

Figure IV-8. Method for paleo ELA reconstructions "accumulation-area ratio" (AAR). Accumulation area (S_c), ablation area (S_a), glacier steady state (SS) (Modified from Porter, 2001).

IV-7.2 Area–Altitude Balance Ratios (AABR)

The AABR method considers mass balance gradients and reconstructed glacier hypsometry. This method is based on the assumption of the ablation (b_a) and accumulation (b_c) gradients are linear and its ratio (BR= b_a/b_c) is known. For glacier free of debris cover, BR is typically 1.8–2.0 in the mid-latitudes and > 3 in the tropics (Kaser and Osmaston, 2002).

AAR and BR ratios at high or mid-latitudes are better constrained than in the tropics because uncertainties are higher (e.g. Rea et al., 2009). Mass balance data of the current glacier relict located in the Mérida Andes is absent. Without references of balance ratios in this region, paleo ELA calculations were made using sensitivity analysis (i.e. different ratios used in general in the tropical glaciers were evaluated). Selected AAR ratios were 0.73 and 0.82. BR ratios of 5 and 10 were used. These values were selected based on observed ranges for tropical glaciers from Kaser and Osmaston (2002). These

ratios were also used because are recommended by Stansell et al. (2007) who reconstructed paleo ELA in the MA during the Last Glacial Maximum (LGM).

A GIS tool running in ArcGIS was used to estimate AAR and AABR ELA values (Pellitero et al., 2015). For each valley three paleo glacier surfaces (corresponding to 50, 100 and 150 kPa shear stresses) were obtained for a specific ages (the age obtained from the ^{10}Be cosmonuclide dating). Data helped to build a DEM in order to reconstruct former glacier surface and then it was used for paleo ELA calculations. Thus, three paleo ELA values were also obtained to each valley at a specific age.

IV-7.3 Paleo ELA corrections

It is important to consider the sea level changes and uplift effect on the paleo ELA. During 22-17 Cal kyr BP, sea-level was between 115-125 m lower than today (Fairbanks, 1989; Hanebuth et al., 2000; Yokoyama et al., 2000). The eustatic fall of sea-level leads to raise the overall elevation of the topography. Paleo ELA should thus be corrected from this change (Porter, 2001). However, the transfer of the water budget from the oceans to land displaced enough atmospheric mass to compensate the lower sea level. Recent study recommended not correcting paleo ELA from this effect (Osmaston, 2006). In the following, no sea level change corrections were considered.

However, uplift corrections of paleo ELA must be considered (Osmaston, 2006) because during after uplift a single point in the topography is higher comparing to its initial elevation and involves different climate conditions. In the central MA uplift rates are estimated at ~1 mm/a (Audemard, 2003; Wesnousky et al., 2012; Guzmán et al., 2013). Elevation increase for post MIS 3 periods is ~30 m. Because this value is in the range of paleo ELA uncertainties, this correction was not considered.

The central Mérida Andes was selected because glacial landforms are the best preserved in the Venezuelan Andes. Integration of data obtained in this dissertation and those from the bibliography, significantly contributes with the deglaciation history in the northern Andes. Results are presented in three subsections:

V-1.0 Generalities about studied glacial landforms and detail of TCN dating (^{10}Be concentrations, ^{10}Be production rates and exposure ages). V-1.0 explains why glacier landforms were chosen. Moreover, a specific aspect dealt with concerns the input parameters used to calculate TCN ages (^{10}Be production rates, blank values).

V-2.0 Detailed glacial geomorphological features and deglaciation chronologies. V-2.0 is dedicated to the description of the glacial geomorphology in all the locations studied. Previous studies in the different valleys, samples location and exposure ages are also presented.

V-3.0 Paleo ELA values. Previous related studies developed in the central MA are briefly described in relation with data computed in this present study.

V-1.0 Generalities about studied glacial landforms, ^{10}Be concentrations, ^{10}Be production rates and exposure ages

V-1.1 Why glacial landforms studied?

The deglaciation histories in the central MA are poorly constrained because of the lack of detailed deglaciation valley studies. To resolve this lack, several valleys were sampled: Mifafí (6 samples), Mucubají (14 samples), Mucuchache (7 samples) and Gavidia (24 samples) (Figure V-1). These valleys were studied to understand the causes of former glaciers dynamics variabilities supposed between the northern Sierra Nevada and the southern Sierra del Norte hillsides. Sierra Nevada is the most studied area because current glaciers remains are still present (less than 0.017 km^2, Braun and Bezada 2013). More valleys of this area were studied to bring high resolution of the Sierra Nevada deglaciation history.

The area where valleys were studied (between Mifafí, Mucubají, Mucuchache and Gavidia, Figure V-1) is dry as suggested by the arid plant cover. The annual precipitation in the Mifafí valley can be estimated from the one of the Pico Águila

station (860 mm) (Figure V-1, Table V-1). In the Mucubají valley the annual precipitation is 968 mm (Mucubají station). San Rafael de Mucuchíes meteorological station close to the Gavidia and Mucuchache valleys indicate an annual precipitation of 630 mm (Figure V-1). Sierra de Santo Domingo is wetter than Sierra Nevada with annual precipitation higher than 1000 mm (Santo Domingo station, 1359 mm and Pueblo Llano station, 1251 mm). In this area, different morphological features as valley bottom slopes and accumulation zone aspects are present. For example, the Mucubají valley presents abrupt slopes changes (~5-7º and more than 20º) and accumulation zone oriented NW-SE. Whereas the Gavidia valley has nearly low and homogeneous slopes (between 5-7º) and accumulation zone oriented NE-SW.

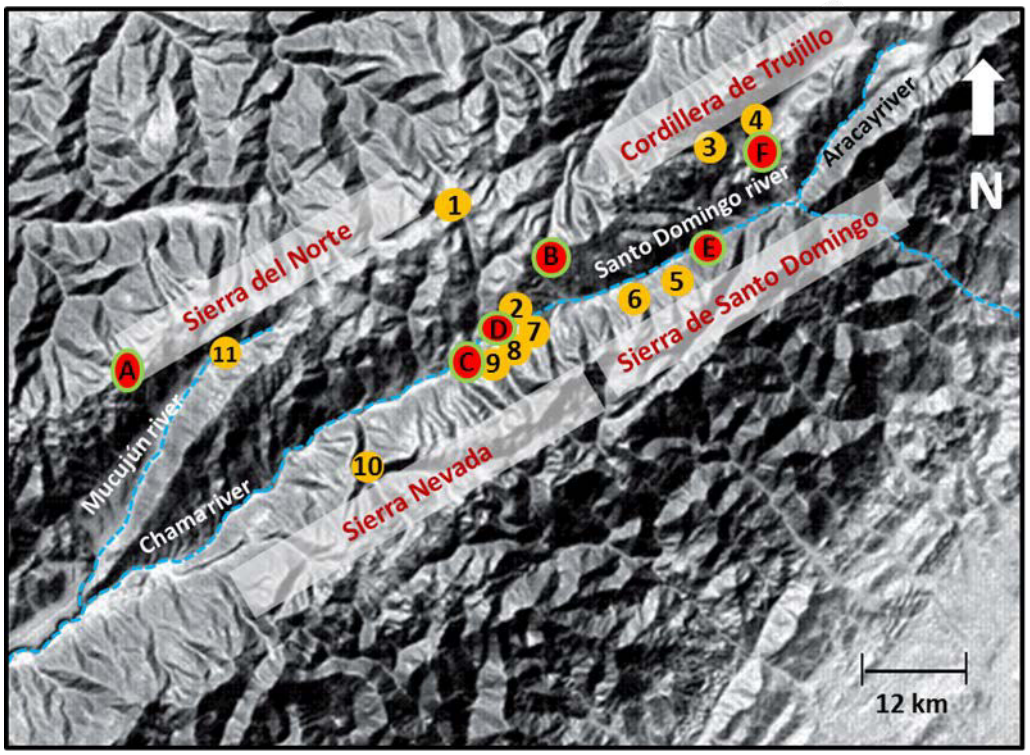

Figure V-1. Location of tudied glacial landforms and meteorological stations in the central MA. Glacial landforms in numbers 1-11. Meteorological stations in letters A-F. 1: Mifafí valley 2: El Desecho moraine, 3: La Canoa moraines, 4: Pueblo Llano moraines, 5: Las Tapias moraines, 6: Los Zerpa moraines, 7: Mucubají valley, 8: El Caballo moraine, 9: Mucuchache valley, 10: Gavidia valley, 11: La Culata moraine. A: Páramo La Culata. B: Pico Espejo. C: San Rafael de Mucuchíes. D: Mucubají valley. E: Santo Domingo. F: Pueblo Llano.

Table V-1. *Mean annual temperature and precipitation from meteorological stations in the central MA (Monasterio and Reyes 1980 and Instituto Nacional de Meteorología e Hidrología de Venezuela INAMEH http://www.inameh.gob.ve). In parenthesis, letter identifying meteorological station letter in Figure V-1.*

Station	Latitude	Longitude	Elevation (m)	Mean temperature	Annual rainfall (mm)
Paramo de La Culata (A)	8.73	-71.10	3027	10	1170
Pico El Águila (B)	8.85	-70.82	4118	2.8	798
San Rafael de Mucuchies (C)	8.76	-70.87	3156	10.6	630
Mucubaji (D)	8.80	-70.82	3550	5.4	968
Santo Domingo (E)	8.85	-70.68	2155	16.1	1359
Pueblo Llano* (F)	8.92	-70.66	2369	16.3	1261

To improve the Mérida Glaciation reconstruction glacier advances in the Sierra del Norte, Sierra Nevada and Cordillera de Trujillo (Pueblo Llano-La Canoa moraines) were studied. In Sierra del Norte, terminal moraines from El Desecho (3 samples) and La Culata (3 moraines, 12 samples) were dated. The Mifafí former glacier was delimited studying a lateral moraine located between Mifafí valley and El Desecho moraine (MIF moraine, 3 samples, Figure V-1). In Sierra de Santo Domingo, Los Zerpa (3 samples) and Las Tapias terminal moraines (3 samples) were studied. In the Sierra Nevada, El Caballo (3 samples), Mucubají and Mucuchache moraines were studied. In the Trujillo Cordillera the terminal moraine from La Canoa (2 samples) and frontal moraines from the Pueblo Llano valley (2 moraines, 6 samples) were dated. These moraines are located at the lowest elevations between 2500-2850 m

Sampled glacial landforms were moraine boulders and roches moutonnées (Figure V-2). Sampled materials were at sufficient height above the surface, in order to minimize the potential coverage by superficial deposits. Sampled boulders are well-anchored to avoid any post-depositional movements (Figure V-2).

V-1.2 ^{10}Be concentrations

Beryllium 10 concentrations were deduced from AMS analyses and calibrated against NIST Standard Reference Material 4325. This Standard Reference Material use a certified $^{10}Be/^{9}Be$ ratio of $2.79 \pm 0.03.10^{-11}$ and a ^{10}Be half-life of $1.387 \pm 0.012.10^{6}$ yr (Korschinek et al., 2009; Chmeleff et al., 2010). Samples preparation and analyses were carried out in four campaigns. Four $^{10}Be/^{9}Be$ blanks values were used to correct samples ratios. These values range from $1.96\pm0.61.10^{-15}$ to $2.97\pm0.74.10^{-15}$ (Table V-2). The

^{10}Be concentrations range from (225.00 ± 8.31 to 1426.90 ± 45.71).10^5 atoms per gram of quartz (at.g^{-1}) (Table V-2).

Figure V-2. Examples of landforms sampled. A) Moraine boulder in La Culata moraine. B) Moraine boulder in La Mucuchache moraine. Postglacial valley with u-shape is also observed. C) Roche moutonnée in the Gavidia valley.

V-1.3 ^{10}Be production rates used and influences in the exposure ages

Different ^{10}Be production rates (i.e. production rate by neutron spallation appropriate for sea-level, high-latitude sites SLHL) were used. Initially, a global averaged ^{10}Be production rate reference of 4.39 ± 0.37 atoms g^{-1} yr^{-1} (Sea-Level High-Latitude SLHL)

Table V-2. ^{10}Be concentrations results of the central Mérida Andes. (a) The shielding factors were calculated following the method of Dunne et al. (1999). (b) Samples were prepared and analyzed in four campaigns, blank values are indicated.

Samples	Sample Thickness	Shielding factor[(a)]	Original scaled production rates		^{10}Be/^{9}Be Blank x 10^{-15}[(b)]	^{10} Be concentraction	
			Spallations	Muons		Value	Uncertainty
	cm		atoms/g/yr			10^3 atoms/gQtz/yr	
Do 02-09	3	0.933	28.18	0.624		578.59	60.14
Do 03-09	5	0.956	28.06	0.614		544.90	31.10
Do 05-09	3	0.962	27.74	0.609		483.46	40.89
Do 06-09	4	0.480	13.59	0.602		279.95	12.68
Do 07-09	4	0.992	28.16	0.603		533.66	45.35
Do 08-09	4	0.971	26.68	0.592		479.88	21.06
PL-0109	4	0.986	15.48	0.442		299.18	24.35
PL-0209	4	0.983	15.31	0.440		284.77	24.12
LZ09-01	3	0.980	20.35	0.471		301.42	27.95
LZ09-02	3	0.981	20.22	0.469		270.19	19.41
Mu09-01	4	0.986	26.16	0.535		477.12	16.54
Mu09-02	3	0.999	26.32	0.533	2.30±0.85	522.40	41.55
Mu09-03	3	0.999	26.08	0.531		440.60	28.60
Mu09-04	4	0.996	26.25	0.533		372.93	11.46
Mu09-05	4	0.995	26.33	0.535		375.45	27.10
Mu09-06	2	0.995	26.86	0.541		463.22	34.48
Mu09-07	3	0.907	25.20	0.549		374.12	16.53
Mu09-08	3	0.951	26.82	0.553		408.50	16.71
Mu09-10	4	0.941	30.94	0.601		306.04	9.55
Mu09-11	3	0.819	29.03	0.627		334.55	10.27
Mu09-12	3	0.941	31.55	0.608		324.42	26.38
Mu09-13	3	0.897	28.58	0.591		301.52	9.74
Mu09-14	3	0.945	28.44	0.573		305.27	24.76
Mu09-15	3	0.968	28.32	0.564		390.44	34.08
GA-1201	3	0.488	8.88	0.480		225.00	8.31
GA-1203	1	0.942	19.10	0.510		294.39	22.92
GA-1205	1.5	0.927	19.24	0.515		334.48	43.33
GA-1206	2	0.920	19.66	0.523		375.30	19.66
GA-1207	2	0.989	21.93	0.533		410.76	18.19
GA-1208 L	6	0.543	12.15	0.535	2.97±0.74	306.78	16.78
GA-1209	1.5	0.934	21.05	0.539		364.73	19.10
GA-1211	3	0.973	22.33	0.543		388.66	14.74
GA-1212	3.5	0.829	19.73	0.553		374.10	18.62
GA-1213	2	0.955	23.85	0.569		444.47	15.66
GA-1214 L	5	0.999	25.21	0.571		467.38	16.45

Table V-2 (cont.)

GA-1215 L	5	0.985	24.59	0.567		440.60	15.77
GA-1216 L	2.3	0.523	13.22	0.572		363.55	24.36
GA-1217 L	3.5	0.520	12.89	0.565		359.80	21.77
GA-1218 L	2.5	0.524	13.00	0.566		426.25	14.71
GA - 1301FE	2	0.958	25.08	0.583		438.48	13.71
GA - 1302FE	3	0.922	24.59	0.588		459.75	14.62
GA - 1303FE	4.5	0.922	23.88	0.579		372.93	20.96
GA - 1301	4	0.995	25.88	0.580		461.34	14.75
GA - 1302	1	0.973	26.38	0.597		469.50	16.66
GA - 1303	5	0.992	28.36	0.611		507.51	15.91
GA - 1304	5	0.984	28.88	0.619		499.87	15.51
GA - 1305	2	0.985	29.49	0.628		509.09	15.89
GA - 1306	2.5	0.982	26.06	0.587		454.03	17.19
CU - 1301	4	0.984	20.03	0.505		353.89	13.17
CU - 1302	4	0.981	20.10	0.507	2.28±0.59	371.10	12.16
CU - 1303	5	0.987	23.15	0.544	1.96±0.61	427.85	51.43
CU - 1304	1.5	0.981	24.34	0.502		407.71	13.44
CU - 1305	4	0.98	23.17	0.547		428.23	24.85
CU - 1306	4	0.978	22.76	0.542		427.30	46.55
CU - 1309	4	0.956	20.08	0.514		396.53	23.06
CU - 1310	2	0.987	21.65	0.526		522.38	57.65
CU - 1311	3	0.981	20.85	0.517		392.49	14.55
CU - 1312	3	0.958	19.68	0.508		375.14	14.39
CU - 1313	3	0.960	19.94	0.510		391.15	13.93
CU - 1315	2.5	0.988	19.90	0.502		358.78	16.28
MUCU -1401	2	0.990	23.56	0.480		667.86	32.55
MUCU-1402	2	0.985	23.32	0.510		972.23	37.19
MUCU-1403	3	0.985	23.12	0.515		1020.45	36.31
MUCUF-1401	4	0.875	19.73	0.523		380.09	15.78
MUCUF-1402	4	0.811	19.01	0.533		111.81	13.47
MUCUF-1403	3	0.857	20.48	0.535		410.21	13.37
MUCUF-1404	4	0.796	17.51	0.526		384.58	25.03
TAPIAS-1401	4	0.980	17.03	0.465		356.76	14.43
TAPIAS-1402	3	0.980	17.16	0.467		314.52	19.28
TAPIAS-1403	3	0.980	17.27	0.469	1.96±0.61	360.40	15.54
CABA-1401	3	0.994	24.74	0.562		862.78	34.57
CABA-1402	4	0.982	24.13	0.558		927.13	36.16
CABA-1403	4	0.982	24.08	0.557		738.68	25.18
MIF-1401	3	0.968	23.35	0.552		445.11	21.22
MIF-1402	4	0.968	23.35	0.552		492.01	35.94
MIF-1403	1	0.968	23.35	0.552		428.27	22.74
DESE-1401	3	0.984	21.86	0.529		409.90	20.60
DESE-1402	4	0.984	21.96	0.531		416.89	14.00
DESE-1403	4	0.996	22.02	0.528		517.28	71.88

Table V-2 (cont.)

PL-1405	4	0.973	14.44	0.429	1315.70	47.16
PL-1406	5	0.976	14.14	0.425	1070.43	35.72
PL-1407	5	0.973	14.22	0.426	1426.90	45.71
PL-1408	5	0.973	13.45	0.415	838.75	26.12
PL-1409	5	0.973	13.45	0.415	944.10	29.95
PL-1410	5	0.973	13.45	0.415	771.26	24.22

was used (Balco et al., 2008). A specific value for a low latitude area (tropical Andes) was firstly unavailable. Originally exposure ages from the Mucubají valley and Los Zerpa moraines (Carcaillet et al., 2013, **section V-2.1.1**) were computed using the global average production rate (Table V-3). A second ^{10}Be production rate used was obtained from the Lago Argentino in the Andes mountains (Kaplan et al., 2011). It is 3.81±0.13 at.g^{-1}.yr^{-1}. Original exposure ages from the Gavidia valley were calculated using Kaplan et al. (2011) (Table V-3). These values are also presented in a submitted article in **section V-2.1.2** (Angel et al., submitted). Recently, a SLHL "tropical" ^{10}Be production rate was proposed. It is 3.78±0.09 at.g^{-1}.yr^{-1} (when erosion is 0 cm/yr Kelly et al., 2013). This value was determined for the tropical Peruvian Andes and is suitable for high altitudes/low latitudes areas. This value is more convenient to compute results from the Mérida Andes. Thus, a final exposure ages updated based on Kelly et al. (2013), when erosion is 0 cm/yr, was made for all the studied glacial landforms. Mucubají valley and Los Zerpa moraines updated results are around 14 % older than the original values, whereas updated results from the Gavidia valley are ~ 3 % older than the original values (Table V-3). Exposure ages range from 5.8±0.7 to 83.7±3.4 ka (Table V-3).

The topographic shielding factors were calculated following the method of Dunne et al. (1999) (Table V-2). No snow coverage correction was considered because the snow falls are low and MA climate conditions prevent long periods of snow cover. All the ages were computed using Cronus online calculator from Balco et al. (2008). The selected scaling scheme is the time dependent model from Lal (1991) modified by Stone (2000).

Table V-3. *Exposure ages in the central Mérida Andes. Original values are referred to the Mucubají, Los Zerpa and Gavidia results which are present in a published (Carcaillet et al., 2013) and submitted article (Angel et al., submitted) (see section* ***V.1.1.3*** *for details). Modified exposure ages were computed using Kelly et al. (2013)* ^{10}*Be production rate.*

Samples	**Latitude**	**Longitude**	**Elevation**	**Site information**	**Boulder size**	**Original Ages**			**Modified Ages**		
						Value	External uncertainty	Internal uncertainty	Value	External uncertainty	Internal uncertainty
	°N	°W	m		m	ka			ka		
Do 02-09	8.760	-71.05	4198	Pegmatite dome. Glacial step.		19.185	2.052	2.109	-	-	-
Do 03-09	8.763	-71.050	4172	Pegmatite dome. Boulder.	1 x 1.7 x 1	18.224	1.127	1.095	-	-	-
Do 05-09	8.774	-71.033	4097	Pegmatite dome. Glacial step.		16.521	1.454	1.455	-	-	-
Do 06-09	8.773	-71.036	4076	Pegmatite dome. Glacial step.		18.899	0.965	0.902	-	-	-
Do 07-09	8.773	-71.039	4081	Valley axis. Glacial step.		17.841	1.578	1.592	-	-	-
Do 08-09	8.766	-71.048	4012	Valley axis. Glacial step.		17.001	0.846	0.779	-	-	-
PL-0109	8.930	- 70.691	2910	Left lateral-terminal moraine	3 x 5 x 4	18.208	1.547	1.544	-	-	-
PL-0209	8.927	- 70.690	2896	Right lateral-terminal moraine	6.5 x 5.5 x 4	17.568	1.550	1.546	-	-	-
LZ09-01	8.812	-70.788	3127	Frontal moraines crest Boulder	4.2 x 2.7 x 1	13.8	1.7	1.4	-	-	-
LZ09-02	8.812	- 70.787	3113	Frontal moraines crest Boulder	3.7 x 2 x 2.3	12.5	1.4	0.9	14.9	1.1	1.1

Samples	**Latitude**	**Longitude**	**Elevation**	**Site information**	**Boulder size**	**Original Ages**			**Modified Ages**		
						Value	External uncertainty	Internal uncertainty	Value	External uncertainty	Internal uncertainty
	°N	°W	m		m	ka		ka			
Mu09-01	8.801	-70.828	3620	Frontal moraines crest Boulder	7 x 4.5 x 4	16.8	1.5	0.6	19.9	0.8	0.7
Mu09-02	8.795	-70.834	3589	Frontal moraines crest Boulder	1.6 x 1.2 x 0.9	18.1	2.1	0.6	21.5	1.8	1.8
Mu09-03	8.795	- 70.827	3572	Frontal moraines crest Boulder	1.7 x 1.5 x 0.7	15.7	1.7	1.1	18.5	1.3	1.3
Mu09-04	8.787	- 70.823	3607	Frontal moraines crest Boulder	1.3 x 1 x 0.8	13.3	1.2	0.4	15.8	0.6	0.5
Mu09-05	8.785	- 70.823	3615	Frontal moraines crest Boulder	3.5 x 1.5 x 1.2	13.3	1.5	1.0	15.9	1.2	1.2
Mu09-06	8.785	- 70.822	3620	Frontal moraines crest Boulder	1.4 x 1.3 x 0.8	16.0	1.8	1.3	18.9	1.5	1.5
Mu09-07	8.779	- 70.820	3697	Striated bedrock valley axis		13.8	1.3	0.6	16.4	0.8	0.8
Mu09-08	8.779	-70.819	3727	Striated bedrock valley axis	~2 m high	14.2	1.3	0.6	16.8	0.8	0.7
Mu09-10	8.767	-70.813	4067	Striated bedrock valley axis	~2 m high	9.1	0.8	0.3	11.0	0.4	0.4
Mu09-11	8.763	-70.812	4213	Moraine boulder Boulder	2 x 1.5 x 1	10.6	1.0	0.3	12.9	0.5	0.4
Mu09-12	8.766	- 70.812	4091	Striated bedrock valley axis		9.5	1.1	0.8	11.5	1.0	1.0
Mu09-13	8.769	- 70.816	3982	Moraine valley axis Boulder	3 x 2 x 1.5	9.7	0.9	0.3	11.8	0.5	0.4
Mu09-14	8.772	-70.815	3862	Moraine valley axis Boulder	1.5 x 1.5 x 1.5	9.9	1.2	0.9	12.0	1.0	1.0
Mu09-15	8.776	-70.816	3804	Striated bedrock valley axis		12.9	1.6	1.2	15.4	1.4	1.4
GA-1201	8.694	70.940	3198	Polished rock		21.7	1.1	0.9	22.5	1.0	0.9

Samples	**Latitude**	**Longitude**	**Elevation**	**Site information**	**Boulder size**	**Original Ages**			**Modified Ages**		
						Value	External uncertainty	Internal uncertainty	Value	External uncertainty	Internal uncertainty
	°N	°W	m		m	ka		ka			
GA-1203	8.674	70.919	3374	Roche moutonnée		14.0	1.2	1.2	14.6	1.2	1.2
GA-1205	8.667	70.912	3428	Roche moutonnée		15.6	2.1	2.2	16.3	2.1	2.2
GA-1206	8.663	70.909	3494	Roche moutonnée		17.0	1.1	1.0	17.7	1.0	1.0
GA-1207	8.662	70.906	3568	Roche moutonnée		16.8	0.9	0.8	17.4	0.9	0.8
GA-1208 L	8.654	70.909	3635	Polished rock (side-wall valley)		21.8	1.4	1.3	22.6	1.3	1.3
GA-1209	8.653	70.908	3592	Boulder in a lateral moraine	1.5 x 1.8 x 1.2	15.6	1.0	0.9	16.2	0.9	0.9
GA-1211	8.648	70.910	3654	Roche moutonnée		15.7	0.8	0.7	16.3	0.7	0.6
GA-1212	8.646	70.911	3737	Roche moutonnée		16.9	1.0	0.9	17.6	1.0	0.9
GA-1213	8.641	70.916	3810	Roche moutonnée		16.7	0.8	0.6	17.3	0.7	0.6
GA-1214 L	8.648	70.915	3884	Polished rock (side-wall valley)		16.6	0.8	0.6	17.3	0.7	0.6
GA-1215 L	8.648	70.916	3870	Polished rock (side-wall valley)		16.1	0.8	0.6	16.7	0.7	0.6
GA-1216 L	8.647	70.915	3840	Polished rock (side-wall valley)		23.3	1.6	1.8	24.2	1.7	1.8
GA-1217 L	8.647	70.915	3820	Polished rock (side-wall valley)		23.6	1.6	1.6	24.6	1.6	1.6
GA-1218 L	8.644	70.914	3805	Polished rock (side-wall valley)		27.2	1.3	1.1	28.2	1.2	1.1
GA - 1301FE	8.646	70.926	3909	Roche moutonnée		15.7	0.7	0.5	16.4	0.6	0.5

Samples	**Latitude**	**Longitude**	**Elevation**	**Site information**	**Boulder size**	**Original Ages**			**Modified Ages**		
						Value	External uncertainty	Internal uncertainty	Value	External uncertainty	Internal uncertainty
	°N	°W	m		m	ka		ka			
GA - 1302FE	8.643	70.930	3964	Roche moutonnée		16.7	0.8	0.6	17.4	0.7	0.6
GA - 1303FE	8.641	70.930	3929	Roche moutonnée		14.1	0.9	0.9	14.7	0.9	0.9
GA - 1301	8.647	70.924	3930	Roche moutonnée		16.0	0.7	0.6	16.7	0.7	0.6
GA - 1302	8.649	70.923	3964	Roche moutonnée		16.0	0.8	0.6	16.7	0.7	0.6
GA - 1303	8.655	70.927	4150	Roche moutonnée		16.1	0.7	0.6	16.7	0.7	0.5
GA - 1304	8.626	70.933	4208	Striated rock		15.6	0.7	0.5	16.2	0.6	0.5
GA - 1305	8.625	70.933	4197	Striated rock		15.7	0.7	0.5	16.2	0.6	0.5
GA - 1306	8.631	70.924	3945	Roche moutonnée		15.8	0.8	0.7	16.3	0.3	0.6
CU - 1301	8.760	-71.052	3401	Boulder in a lat.-ter. left moraine	1 x 1 x 1	16.811	0.739	0.649	-	-	-
CU - 1302	8.763	-71.050	3414	Boulder in a lat.-ter. left moraine	1 x 2 x 3	17.491	0.704	0.597	-	-	-
CU - 1303	8.774	-71.036	3701	Boulder in a lat.-ter. left moraine	1 x 1.2 x 0.6	17.494	2.151	2.196	-	-	-
CU - 1304	8.774	-71.033	3755	Boulder in a lat.-ter. left moraine	1.2 x 1 x 2	16.009	0.646	0.546	-	-	-
CU - 1305	8.773	-71.036	3701	Boulder in a lat.-ter. left moraine	1 x 1.7 x 1	17.479	1.096	1.059	-	-	-
CU - 1306	8.773	-71.040	3668	Boulder in a lat.-ter. left moraine	2.2 x 4 x 5	17.819	1.993	2.030	-	-	-
CU - 1309	8.766	-71.048	3464	Boulder in a lat.-ter. left moraine	2.3 x 2 x 1.6	18.628	1.171	1.135	-	-	-

Samples	**Latitude**	**Longitude**	**Elevation**	**Site information**	**Boulder size**	**Original Ages**			**Modified Ages**		
						Value	External uncertainty	Internal uncertainty	Value	External uncertainty	Internal uncertainty
	°N	°W	m		m	ka		ka			
CU - 1310	8.764	-71.045	3516	Boulder in a lat.-ter. left moraine	0.6 x 0.4 x 1.2	22.356	2.535	2.638	-	-	-
CU - 1311	8.764	-71.047	3469	Boulder in a lat.-ter. left moraine	0.6 x 1.6 x 1.6	17.784	0.780	0.688	-	-	-
CU - 1312	8.752	-71.051	3403	Boulder in a lat.-ter. left moraine	1.6 x 3 x 4	18.033	0.811	0.723	-	-	-
CU - 1313	8.752	-71.051	3424	Boulder in a lat.-ter. left moraine	2 x 3 x 4	18.495	0.788	0.690	-	-	-
CU - 1315	8.753	-71.052	3365	Boulder in a lat.-ter. left moraine	3 x 5 x 7	17.142	0.876	0.808	-	-	-
MUCU -1401	8.773	70.842	3679	Block in a lateral moraine (right).	2.5 x 1.60 x 1.4	25.655	1.392	1.369	-	-	-
MUCU-1402	8.774	70.843	3669	Block in a lateral moraine (right).	2 x 0.5 x 0.80	35.483	1.599	1.591	-	-	-
MUCU-1403	8.774	70.843	3669	Block in a lateral moraine (right).	1 x 0.5 x 0.81	36.947	1.581	1.568	-	-	-
MUCUF-1401	8.760	70.836	3603	Roche moutonée. 2nd step.		18.094	0.863	0.786	-	-	-
MUCUF-1402	8.756	70.836	3683	Roche moutonnée. 4th step.		5.777	0.710	0.691	-	-	-
MUCUF-1403	8.755	70.834	3704	Roche moutonnée. 4th step.		18.754	0.752	0.642	-	-	-
MUCUF-1404	8.764	70.838	3554	Roche moutonnée. 1st step.		20.388	1.415	1.402	-	-	-
TAPIAS-1401	8.814	70.774	3097	Block in a lateral moraine (right).	0.60 x 0.30 x 0.8	19.634	0.919	0.834	-	-	-

Samples	**Latitude**	**Longitude**	**Elevation**	**Site information**	**Boulder size**	**Original Ages**			**Modified Ages**		
						Value	External uncertainty	Internal uncertainty	Value	External uncertainty	Internal uncertainty
	°N	°W	m		m	ka		ka			
TAPIAS-1402	8.814	70.774	3096	Block in a lateral moraine (right).	0.60 x 1 x 1	17.341	1.141	1.104	-	-	-
TAPIAS-1403	8.814	70.774	3096	Block in a lateral moraine (right).	0.40 x 0.30 x 0.60	19.561	0.961	0.885	-	-	-
CABA-1401	8.777	70.837	3788	Block in a lateral moraine (left)	5 x 4 x 4	30.534	1.422	1.390	-	-	-
CABA-1402	8.777	70.837	3778	Block in a lateral moraine (left)	1.5 x 1.80 x 1	33.155	1.515	1.493	-	-	-
CABA-1403	8.777	70.837	3775	Block in a lateral moraine (left)	1.2 x 0.8 x 0.8	27.436	1.137	1.038	-	-	-
MIF-1401	8.819	-70.863	3740	Boulder in a lateral moraine	3 x 3 x 2	17.946	0.954	0.896	-	-	-
MIF-1402	8.819	-70.863	3740	Boulder in a lateral moraine		19.696	1.516	1.519	-	-	-
MIF-1403	8.819	-70.863	3740	Boulder in a lateral moraine		17.322	1.007	0.960	-	-	-
DESE-1401	8.801	-70.844	3556	Block in a lateral moraine (left).		17.695	0.983	0.928	-	-	-
DESE-1402	8.800	-70.845	3548	Block in a lateral moraine (left).	1.6 x 0.4 x 0.3	17.901	0.732	0.628	-	-	-
DESE-1403	8.802	-70.843	3548	Block in a lateral moraine (left).	0.6 x 0.5 x 0.5	21.781	3.085	3.325	-	-	-
PL-1405	8.940	-70.677	2795	Moraine boulder.	2.5 x 1 x 0.40	75.476	3.278	3.318	-	-	-
PL-1406	8.939	-70.677	2782	Moraine boulder.	0.70 x 0.60 x 0.79	62.856	2.590	2545	-	-	-
PL-1407	8.939	-70.677	2782	Moraine boulder.	0.70 x 0.60 x 0.80	83.662	3.372	3282	-	-	-
PL-1408	8.947	-70.665	2684	Moraine boulder.	0.50 x 0.60 x 0.60	50.135	1.967	1.942	-	-	-
PL-1409	8.947	-70.665	2684	Moraine boulder.	0.30 x 0.40 x 0.49	58.184	2.315	2236	-	-	-
PL-1410	8.947	-70.665	2684	Moraine boulder.	0.30 x 0.40 x 0.50	45.732	1.802	1796	-	-	-

V-2.0 Detailed glacial geomorphological features and deglaciation chronologies

Valleys and results presentation is based on a geographical subdivision (Sierra Nevada: V-2.1, Sierra del Norte: V-2.2 and Cordillera de Trujillo: V-2.3). In Sierra Nevada, Mucubají and Los Zerpa results are gathered in Carcaillet et al. (2013) and in V-2.1.1, this manuscript. Results are also published in a Spanish article (Angel et al., 2013, appendix 1). Gavidia valley results are present in a submitted article (Angel et al., Journal of South American Earth Sciences, V-2.1.2). Sierra del Norte (La Culata, Desecho, Pueblo-Llano/La Canoa moraines) and Cordillera de Trujillo will be submitted in the next months.

V-2.1 Sierra Nevada

V-2.1.1 Mucubají and Los Zerpa

Well-preserved glacial landforms (moraines and roches moutonnées) along all the Mucubají valley extension are present in Figure V-3. This valley was selected to study a detailed deglaciation history in the Sierra Nevada northern hillside. It was selected because of its morphological features: accumulation zone orientation (NW-SE) and abrupt changes of the valley slopes (from ~5-7º to 20º). Los Zerpas moraines allow dating a glacier advance in the Sierra de Santo Domingo.

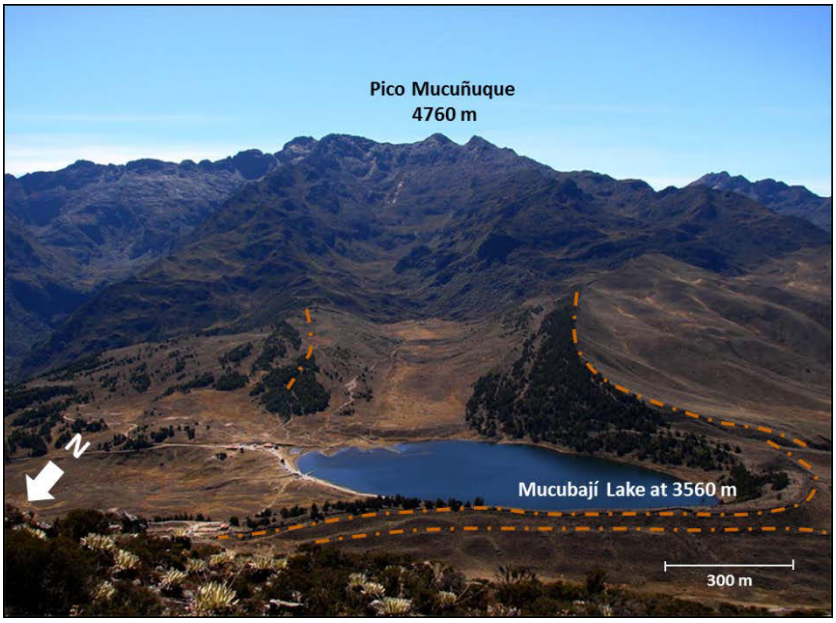

Figure V-3. Mucubají post-glacial valley (u-shape) in the Sierra Nevada. At elevations lower than 3700 m, the landscape is characterized by a well-shape moraine ridge (50 m

high) (orange lines). At elevations higher than 3700 m landforms are erosional glacial features as roches moutonnée (modified from original photo of http://www.mucubaji.com/1Lagunas.html).

Mucubají deglaciation history is the best documented in the central MA. Deglaciation chronology was based on ^{14}C (Schubert, 1970; Schubert, 1972; Salgado-Laboriau, 1977; Schubert and Rinaldi, 1987; Mahaney et al., 2005; Carrillo, 2006; Carrillo et al., 2008; Mahaney et al., 2008). Schubert (1970) and (1972) highly contribute in the reconstruction of the Mérida Glaciation. Glacier advances in Sierra Nevada, specifically in Sierra de Santo Domingo (Northside of the Mucubaji pass, 3000-3500 m, towards Santo Domingo river, Figure V-1) were dated older than 10-13 ka BP. These chronologies were obtained using radiocarbon dating of carbonaceous sediments and peat within fluvioglacial deposits. In the Mucubají valley, moraines located at ~3500 m were related to the LGM (Salgado-Labouriau et al., 1977). This is based on a minimum deglaciation age of 12.65±0.13 ^{14}C ka from a basal peat in an outwash terrace up-valley (3650 m) of the Late Mérida Stadial moraines. Schubert and Rinaldi (1987) date an outwash fan at 3400 m bounded by two Late Stadial moraines. The outwash fan has a basal age of 19.08±0.82 ^{14}C ka BP (Schubert and Rinaldi, 1987).

Studies developed in the Mucubají valley were mainly interpreted in a paleoclimate sense (e.g. Schubert and Rinaldi, 1987) and deglaciation history was not enough constrained. Some scientific questions can still be raised: A push moraine was related to the YD but is it observed a glacier advance during the OtD? How was the detailed glacier dynamic in this valley since the LGM? (YD, OtD and LGM initially described in **Sections I-1.3.4 and I-1.3.3**) How is it related to other glacier dynamics in the same Sierra Nevada or Sierra del Norte? A deglaciation chronology based on ^{10}Be exposure dating compiled with previous studies greatly contributed to answer these scientific questions.

The deglaciation chronologies proposed by Carcaillet et al. (2013) established a detailed post-LGM history. Los Zerpa moraines allow studying a glacier advance in Sierra de Santo Domingo. However, considering the recent SLHL ^{10}Be production rate (Kelly et al., 2013), updated exposure ages were derived (Table V-3). Original exposure ages from the Mucubají valley and Los Zerpa moraines increased by ~14 % and some paleoclimate interpretations changed. In the following, updated exposure ages were

considered for discussions. Values range from 11.0±0.4 ka to 21.5±1.8 ka in the Mucubají valley. Los Zerpas moraines were dated at 14.9±1.1 ka and 16.4±1.6 ka (Table V-3).

Quaternary Research 80 (2013) 482–494

Contents lists available at ScienceDirect

Quaternary Research

journal homepage: www.elsevier.com/locate/yqres

Timing of the last deglaciation in the Sierra Nevada of the Mérida Andes, Venezuela

Julien Carcaillet [a,*], Isandra Angel [b], Eduardo Carrillo [b], Franck A. Audemard [c], Christian Beck [d]

[a] ISTerre, Université de Grenoble 1, UMR CNRS 5275, F-38041 Grenoble, France
[b] Instituto de Ciencias de la Tierra, Universidad Central de Venezuela, Apdo. 3805, Caracas 1010-A, Venezuela
[c] Fundación Venezolana de Investigaciones Sismológicas, FUNVISIS, El Llanito, Caracas 1030, Venezuela
[d] ISTerre, Université de Savoie, UMR CNRS 5275, F-73376 Le Bourget-du-Lac, France

ARTICLE INFO

Article history:
Received 10 January 2013
Available online 29 September 2013

Keywords:
Terrestrial cosmogenic nuclides dating
Glacial landforms
Andes de Mérida
Venezuela
Pleistocene
Holocene

ABSTRACT

In the tropical Mérida Andes (northwestern Venezuela), glacial landforms were found at altitudes between 2600 and 5000 m, corresponding to 600 km^2 of ice cover during the maximum glacial extension. However, the lack of sufficient absolute age data prevents detailed reconstruction of the timing of the last deglaciation. On the northwestern flank of the Mucuñuque Massif, successive moraines and striated eroded basement surfaces were sampled for cosmogenic ^{10}Be investigation. Their compilation with published data allows the establishment of a detailed chronology of the post-LGM glacier history. The oldest moraines (18.1 and 16.8 ka) correspond to the Oldest Dryas. Successive moraine ridges indicate stops in the overall retreat between the LGM and the Younger Dryas. The cold and short Older Dryas stadial has been identified. Results indicate that most of the ice withdrew during the Pleistocene. The dataset supports an intensification of the vertical retreat rate from ~25 m/ka during the late Pleistocene to ~310 m/ka during the Pleistocene/Holocene. Afterwards, the glacier was confined and located in the higher altitude zones. The altitude difference of the Younger Dryas moraines in the Mucubají, La Victoria and Los Zerpa valleys indicates a strong effect of valley orientation on the altitude of moraine development.

Introduction

Deciphering the late Pleistocene glacier activity in tropical mountains greatly contributes to the understanding of global climate changes. Only a few mountain ranges have sufficient elevation and precipitation to allow glacier formation in the tropics. The Mérida Andes of Venezuela (Fig. 1A) is a key place because numerous landforms of post-LGM (last glacial maximum) glacier activity have been observed since the 19th century (Sievers, 1885). Jahn (1912, 1925) produced planimetric measurements of glaciers and published the first glacier mapping at the scale of the Mérida Andes. It was established that two moraine levels existed, located at 2600–2800 and 2900–3500 m asl (Schubert, 1970, 1974; Schubert and Valastro, 1974; Schubert and Rinaldi, 1987; Schubert and Clapperton, 1990), and associated with the last glaciations. Glacier surveys indicated that ice covered most of the relief during the LGM, which has been locally named the Mérida Glaciation (Schubert, 1974). Since this eponymous glaciation, the glaciers of the Mérida Andes retreated from ~600 km^2 to ~2.9 km^2 in 1952, and then to 0.26 km^2 in 2009 (Schubert, 1980, 1998; Schubert and Vivas, 1993; Yépez and Carrillo, 2009; Kalm and Mahaney, 2011). During the LGM, the Equilibrium Line Altitudes (ELA) were between 3920 and 3320 m asl. Nowadays, the present ELA is estimated between 4880 and 4470 m asl (Stansell et al., 2007) with a present-day retreat rate estimated at 30 m^2/yr (Carrillo and Yépez, 2008). Consequently, the ultimate glaciers are located around the main summits of the cordillera (i.e., Bolívar, Humboldt and Bonpland peaks; Schubert, 1998).

Several scattered data based on radiocarbon (Schubert, 1970; Abbott et al., 2003; Stansell et al., 2005), OSL (Mahaney et al., 2000), cosmogenic (Wesnousky et al., 2012) and palynological (Salgado-Labouriau, 1989; Salgado-Labouriau et al., 1992; Rull et al., 2005) investigations delineated the glacier evolution since the LGM. However, the data are too sparse to allow the construction of a robust and complete chronology of the glacier extension since the LGM. A critical need for dating still exists in order to better constrain both the timing of the LGM and subsequent glacier retreat. We present a compilation of 29 published ages and 16 new Terrestrial Cosmogenic Nuclide (TCN) dates attained in the same area (i.e., the north flank of the Mucuñuque massif Figs. 1A and B). The dataset allows the establishment of the pattern of the deglaciation in the central zone of the Mérida Andes. We selected this area because glacial landforms are particularly well-preserved along a vertical transect ranging between ~3100 and ~4200 m asl. This timing is important because the glacial chronologies in the intertropical belt are rare and need to be clarified. The established chronology is discussed herein with respect to local, regional and global paleoclimatic records.

* Corresponding author at: ISTerre, 1381 rue de la Piscine, 38400 Saint Martin d'Hères, France. Fax: +33 4 76 63 52 52.
E-mail address: Julien.Carcaillet@ujf-grenoble.fr (J. Carcaillet).

0033-5894/$ – see front matter © 2013 University of Washington. Published by Elsevier Inc. All rights reserved.
http://dx.doi.org/10.1016/j.yqres.2013.08.001

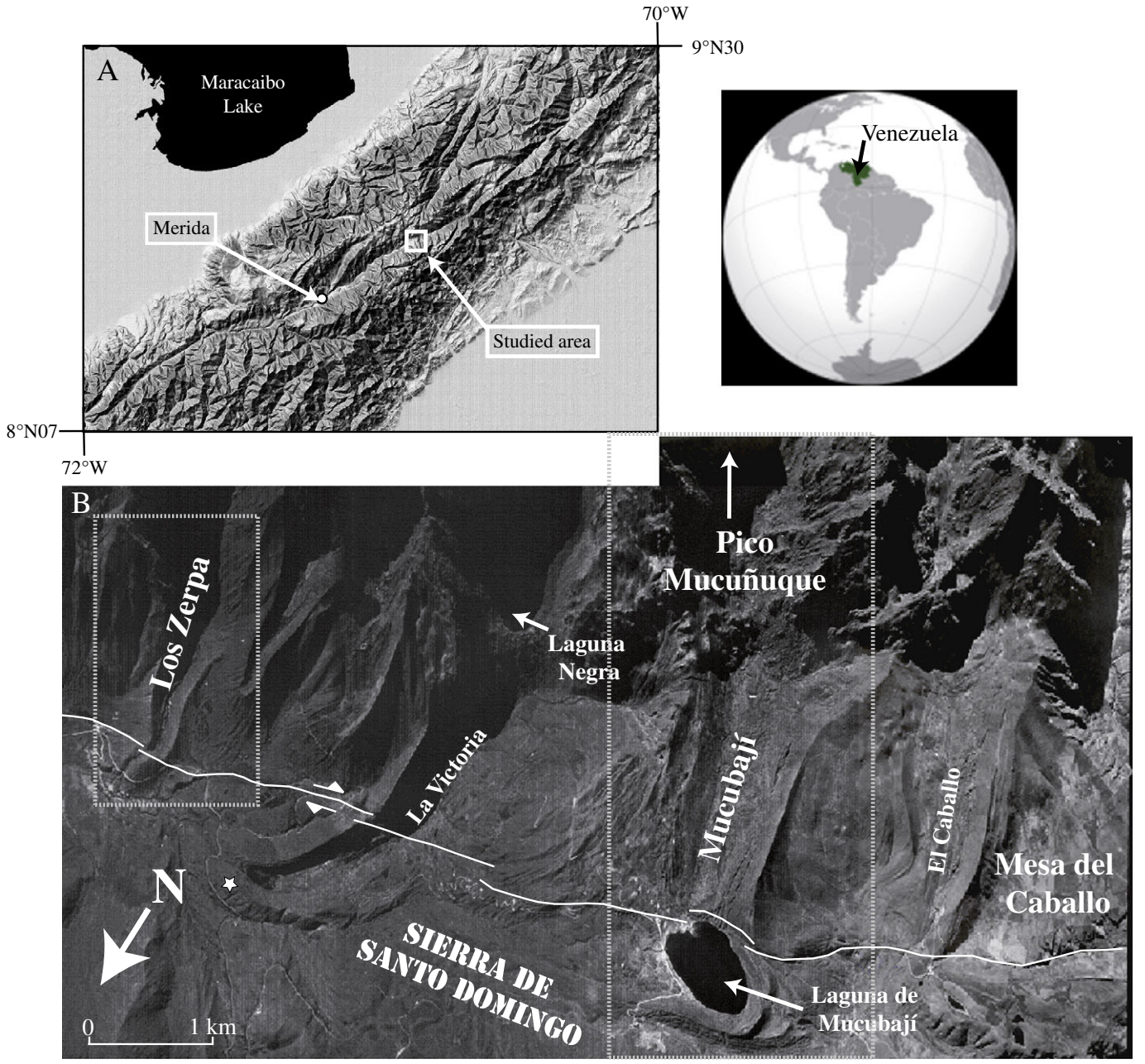

Figure 1. A) Digital shaded-relief map of the central Mérida Andes. The white box indicates the study area (map modified from Garrity et al., 2004). B) Aerial photograph of the study area. Dashed gray boxes indicate Figs. 2A and B; the white line indicates the Boconó fault and names refer to the text. White star indicates the Wesnousky et al. (2012) sampling sites on the La Victoria Moraine (see text for details).

Geological and geomorphic setting

The Mérida cordillera is located in the west of Venezuela (Fig. 1A) and appears to be a northern extension of the Northern Andes cordillera in Colombia. Trending ~N45°, the cordillera extends over 400 km and reaches a maximum elevation of ~5000 m asl. in the Sierra Nevada of Mérida (Pico Bolívar). Its formation is strongly connected to the geodynamic interaction of the Panama Arc, the Caribbean and the South American plates, which started during the Miocene (Audemard and Audemard, 2002) and is being exhumed at rates estimated between 0.2 and 0.6 km/Ma (Bermúdez et al., 2010). At present, tectonic deformation is mainly accommodated by the Boconó fault which is the most active structure of the area (total length ~500 km) and which strongly controls the topography of the axis of the Venezuelan Andes (Rod, 1956; Schubert, 1982; Audemard et al., 2008).

We focus our study on the western termination of the "Sierra de Santo Domingo" (Fig. 1B). The Santo Domingo valley, running parallel to the cordillera, is a wide valley along the Boconó fault. We sampled glacier morphologies in the Mucuñuque massif, in the U-shaped Mucubají Valley and the moraine complex of Los Zerpa. Samples consist of Precambrian to Palaeogene granites and gneiss.

The Los Zerpa moraines (Fig. 2A) are located ~4 km to the east of the Laguna de Mucubají. Their shape is particularly well-preserved with >1 km long lateral moraines and a frontal moraine (~3120 m asl) shifted by dextral strike-slip movement of the Bocoño fault (Schubert and Sifontes, 1970). The shift of ~70 m suggests an average slip rate

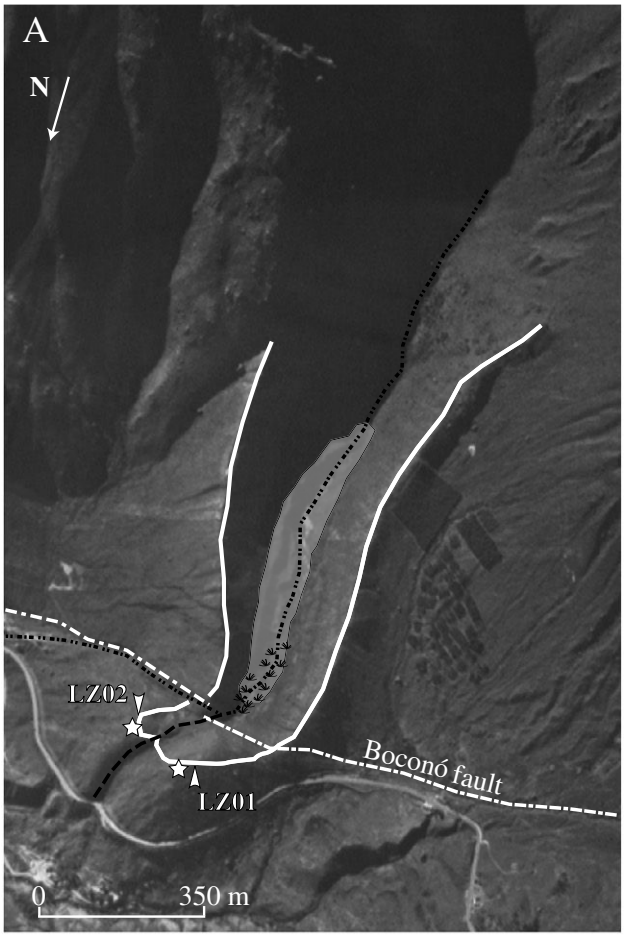

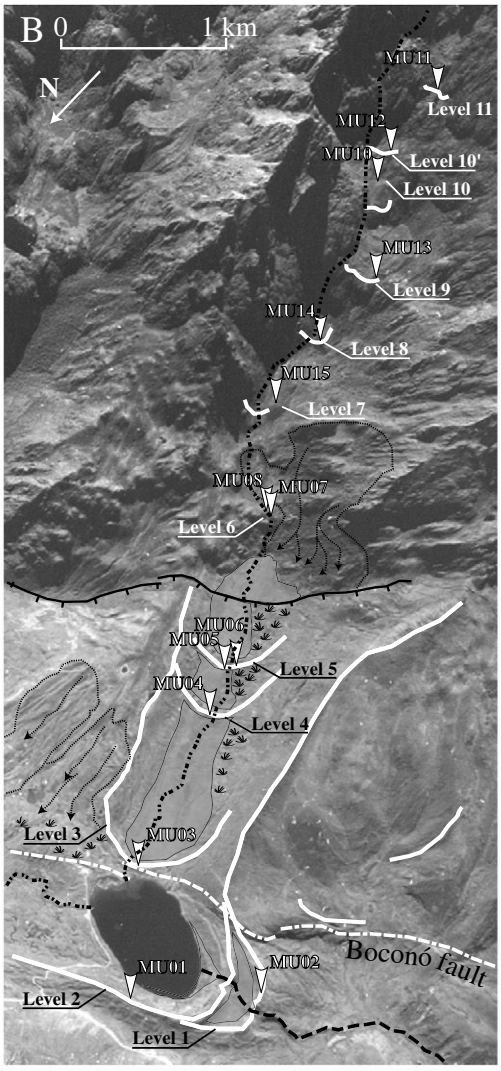

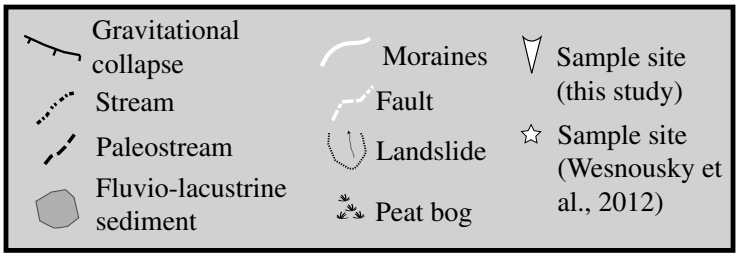

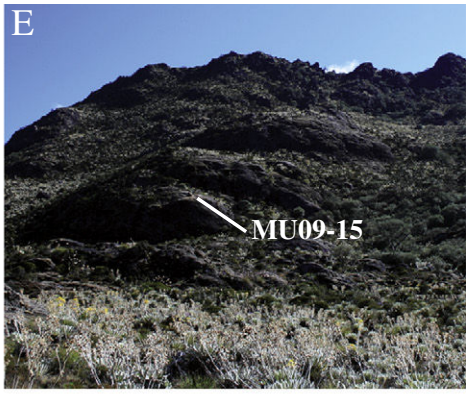

Figure 2. Enlarged aerial photographs of the two studied valleys (A — Los Zerpa and B — Mucubají). Levels refer to the text. Fault scarps, glacial and paraglacial landforms are represented (see caption for details). C, D, E) photographs of sampled boulders and striated bedrocks. White stars indicate Wesnousky et al. (2012) sampling sites on the La Victoria Moraine (see text for details).

between 0.55 (Wesnousky et al., 2012) to 1 cm/yr (Audemard, 1997; Audemard et al., 1999). Note that a paleo-outlet cut the frontal moraine but was abandoned because of the tectonic displacements. At ~1.5 km to the west, the La Victoria latero-frontal moraines have also been shifted by the Boconó fault (Fig. 1B). Lateral moraines are well developed between the Laguna Negra (3470 m asl) and the Laguna Victoria (3220 m asl). We have not sampled boulders along this moraine, but the dates published by Wesnousky et al. (2012) are presented in Table 2.

The Mucubají Valley (Fig. 2B) is a NNW–SSE oriented valley and is bordered by the Laguna de Mucubají (3540 m asl) formed by a moraine dam that was apparently created during the ultimate ice advance of the Mérida glaciations (i.e., LGM) (Dirszowsky et al., 2005; Rull, 2005; Stansell et al., 2005) and the Pico Mucuñuque (4670 m asl). The valley presents a U-shaped postglacial morphology with a complex cirque system near the headwall. The valley profile shows two distinct zones:

- A nearly flat lower sector (3550/3700 m asl) formed by paraglacial sediments (mainly till) overlain by coarser fluvio-lacustrine (clay to gravel) and Holocene peat/lacustrine deposits (Stansell et al., 2005; Carrillo et al., 2006). We identified five main recessional moraines abandoned during successive phases of glacier retreat. With an apparent height of ~50 m, the lower moraine is the biggest of the area and is skewed to the north in the Santo Domingo valley to a minimum altitude of 3400 m asl. The moraines located above are well-shaped arched ridges with apparent heights lower than 5 m. However, the one located immediately above the lake reveals that the minimum height is actually ~15 m. Indeed, the filling by superficial materials of the depressions located behind the moraines contributes to reducing the overall apparent height of the moraines. The area is faulted by the Boconó fault system (Fig. 2B). This zone has been slid over the crystal basement toward the north forming a 6 to 8 meter high scarp (Audemard et al., 2010).
- An arched upper sector (3700/4600 m asl) formed by the Iglesias group (Bellizzia et al., 1976; Gonzales de Juane et al., 1980) that is composed of Precambrian high-grade metamorphic rocks, banded gneiss, amphibolites, schist and granitic dikes (Schubert, 1970). Above 3700 m asl, the glacial landforms are mainly striated bedrocks (roches moutonnées) easily identifiable in the topography by the presence of bedrock bars cutting the valley. This area comprises a diamict (till) succession related to earlier phases of the late glacial period followed by the Younger Dryas advance (Mahaney et al., 2008). The whole forms a characteristic concave valley profile with ~20° of maximum slope.

Methods: Sampling strategy, chemical preparation and data treatment

In the Mucubají Valley, we identified 11 distinct levels with large boulders (>1 m) entrapped in moraine crest lines (Figs. 2C, D) and striated bedrock surfaces (roches moutonnées) suitable for cosmogenic investigation (Fig. 2E). We particularly focused attention on the sampling of materials that were sufficiently elevated, in order to minimize the potential coverage by superficial deposits, and well-anchored to avoid any post-deposition movements. As these rocks have high quartz content, we extracted the TCN in-situ produced beryllium-10 (^{10}Be).

Chemical targets were prepared at the cosmogenic laboratory at ISTerre following procedures adapted from Brown et al. (1991) and Merchel and Herpers (1999). Measurements were carried out at the French National AMS facility (Accelerator Mass Spectrometry) at ASTER in Aix-en-Provence. Ages were calculated using the online Cronus calculator (Balco et al., 2008). Because of the lack of production rate calibration sites in the tropical belt, the ages have been computed using a global averaged reference production rate of 4.39 ± 0.37 atoms g^{-1} yr^{-1} (Sea-Level High-Latitude SLHL). This production rate is higher (~15%) than those calculated by Putnam et al. (2010) in New Zealand (3.74 ± 0.08 atoms g^{-1} yr^{-1}) and Kaplan et al. (2011) in Patagonia (3.71 ± 0.11 atoms g^{-1} yr^{-1}). The data can be affected by the inherent uncertainty associated with a difference between the averaged and accurate local production rates. The choice falls on this production rate because the Putman et al. (2010) and the Kaplan et al. (2011) production rates are scaled for mid- and high-latitude zones, and the magnetic modulation has a particularly critical effect in the vicinity of the magnetic equator where the deflection of primary cosmic ray is at maximum (see Dunai, 2010).

For all these reasons, we used the averaged production rate using the time-dependent scaling scheme of Lal (1991) modified by Stone (2000) in order to take the geomagnetic field variation into account (Balco et al., 2008). Since the reference production rate coupled with the Lal/Stone scaling scheme is lower than the others proposed in the Cronus Calculator (see Balco et al., 2008 for details), the exposure ages calculated using this scheme yield a maximum difference ranging from 8 to 15%. Dates are thus given in ^{10}Be-ka (Table 1) in order to allow straightforward correction for future refinements in scaling schemes and production rate computation.

Results of ^{10}Be measurements

Dating of 11 meter-size moraine blocks (mainly <3650 m asl) and 5 striated bedrock surfaces (>3650 m asl) was performed to provide a chronology of the last deglaciation. Table 1 presents sample information, scaling factor, production rates, concentrations deduced from AMS measurements and exposure ages computed with the online version of Cronus calculator (Balco et al., 2008). The preservation of striations on polished surfaces and the absence of significant exfoliation on moraine boulders support the absence, or extremely low rate, of erosion of rock surfaces. Nonetheless, because this is only established from field observations, it is important to consider the TCN age interpretations as the estimated minimum. Furthermore, lateral moraines are more than 100 m above the valley floor. This indicates a minimum 100 m thickness of the ice tongue, which is sufficient to avoid TCN production in the underlying bedrock during the last climatic cycle and on abraded rock surfaces for resetting TCN inherited from previous glacial stages. We thus consider that samples are free of inherited ^{10}Be. The presented chronology can reasonably reflect the last glacial retreat history (Table 1).

Results from the Mucubají Valley range between 3.01 ± 0.10 (Mu09-13) and 5.22 ± 0.42 (Mu09-02) 10^5 atoms per gram of quartz (atoms g^{-1}). Once computed as exposure ages, results range between 18.14 ± 2.11 and 9.08 ± 0.82 ^{10}Be-ka (Table 1, Fig. 3A), which is compatible with the absence or moderate inheritance. Indeed, the results show a post-LGM distribution and an altitudinal dependence of exposure ages. In the flat lower valley (Level 1 to Level 5, Fig. 2B), sampled glacial landforms date from 18.14 ± 2.10 to 13.27 ± 1.20 ^{10}Be-ka. Because all sampled sites are recessional moraines, the deduced age distribution can be considered as successive stages of glacier stop during an overall global withdrawal from the LGM to the late Pleistocene.

However, the exposure ages of Mu09-04 (13.27 ± 1.20 ^{10}Be-ka) and Mu09-05 (13.32 ± 1.48 ^{10}Be-ka) are abnormally young with respect to the neighboring samples (Fig. 2 and Table 1). Given the associated uncertainties, their exposure ages agree with the general chronology of the glacial retreat. Upstream of Level 5, a macrofossil collected at ~50 cm from the base of the sediment was dated at 15.73 ± 0.20 cal ka BP (CAMS-104915, Table 2) which correlates with exposure ages of Level 5 moraine boulders (13.32 ± 1.48 [Mu09-05] and 15.96 ± 1.80 ^{10}Be-ka [Mu09-06]). In the following, we establish a composite Level 4/5 by combination of ages of Mu09-04, -05, -06 and CAMS-104915 because the age distribution falls into the same time interval and, according to their respective uncertainties, are impossible to distinguish.

Above 3700 m (Level 6 to Level 11, Fig. 2), the slope drastically steepens up to 20% and increases the elevation to 4670 m asl.

Table 1
TCN results of the Mucubají valley and the Los Zerpa moraines. (a) The topographic scaling factor has been calculated following the method of Dunne et al. (1999). (b) AMS analyses have been carried out at the French AMS facility ASTER. Beryllium 10 concentrations were calibrated against NIST Standard Reference Material 4325 using its certified $^{10}Be/^{9}Be$ ratio of $2.79\,10^{-11}$ and a ^{10}Be half life of $1.387 \pm 0.012\,10^{6}$ yr (Korschinek et al., 2009; Chmeleff et al., 2010). Results have been corrected from the chemical blank ($^{10}Be / {}^{9}Be_{blank} = 2.30 \pm 0.85 \times 10^{-15}$). Propagated uncertainties include counting statistics, a conservative estimate of 1% for instrumental variability, the uncertainty of the standard deviation and chemical blank. (c) Ages have been computed with the Cronus Calculator (Balco et al., 2008) using the time-dependent production rate of Lal (1991) modified by Stone (2000). (d) Internal uncertainties consider the analytical uncertainties, while the external uncertainties include 6% uncertainty in the production rate and 8% uncertainty in the ^{10}Be decay constant. In the Results section, results are presented with the external uncertainties. No correction for snow or other coverage have been taken into account, the sample thickness correction has been calculated with a 2.7 density factor.

Sample	Level	Latitude	Longitude	Elevation	Site information	Sample informations	Thickness	Shielding factor[a]	Scaled production rates		^{10}Be concentration[b]		Ages[c, d]		
									Spallation	Muons	Value	Uncertainty	Value	External uncertainty	Internal Uncertainty
		°N	°W	m asl		Apparent size (length * width * height)	cm		atoms/g/yr		$\times 10^3$ atoms/gQtz/yr		ka		
LZ09-01	-	8.8117	70.7884	3127	Frontal moraines crest	Boulder (4.2 * 2.7 * 1)	3	0.980	20.35	0.471	301.42	27.95	13.837	1.740	1.352
LZ09-02	-	8.8117	70.7874	3113	Frontal moraines crest	Boulder (3.7 * 2 * 2.3)	3	0.981	20.22	0.469	270.19	19.41	12.481	1.386	0.944
Mu09-01	2	8.8009	70.8279	3620	Left side frontal moraines crest	Boulder (7 * 4.5 * 4)	4	0.986	26.16	0.535	477.12	16.54	16.784	1.536	0.625
Mu09-02	1	8.7954	70.8343	3589	Frontal moraines crest	Boulder (1.6 * 1.2 * 0.9)	3	0.999	26.32	0.533	522.40	41.55	18.144	2.112	1.563
Mu09-03	3	8.7951	70.8270	3572	Frontal moraines crest	Boulder (1.7 * 1.5 * 0.7)	3	0.999	26.08	0.531	440.60	28.60	15.661	1.673	1.084
Mu09-04	4	8.7874	70.8233	3607	Frontal moraines crest	Boulder (1.3 * 1 * 0.8)	4	0.996	26.25	0.533	372.93	11.46	13.273	1.195	0.431
Mu09-05	5	8.7850	70.8229	3615	Frontal moraines crest	Boulder (3.5 * 1.5 * 1.2)	4	0.995	26.33	0.535	375.45	27.10	13.321	1.483	1.016
Mu09-06	5	8.7852	70.8224	3620	Frontal moraines crest	Boulder (1.4 * 1.3 * 0.8)	2	0.995	26.86	0.541	463.22	34.48	15.957	1.801	1.269
Mu09-07	6	8.7790	70.8197	3697	Striated bedrock valley axis		3	0.907	25.20	0.549	374.12	16.53	13.841	1.322	0.647
Mu09-08	6	8.7785	70.8189	3727	Striated bedrock valley axis	~2 m high	3	0.951	26.82	0.553	408.50	16.71	14.201	1.335	0.615
Mu09-10	10	8.7667	70.8129	4067	Striated bedrock valley axis	~2 m high	4	0.941	30.94	0.601	306.04	9.55	9.078	0.818	0.304
Mu09-11	11	8.7633	70.8119	4213	Moraine boulder	Boulder (2 * 1.5 * 1)	3	0.819	29.03	0.627	334.55	10.27	10.629	0.956	0.348
Mu09-12	10′	8.7659	70.8121	4091	Striated bedrock valley axis		3	0.941	31.55	0.608	324.42	26.38	9.483	1.113	0.825
Mu09-13	9	8.7689	70.8164	3982	Moraine valley axis	Boulder (3 * 2 * 1.5)	3	0.897	28.58	0.591	301.52	9.74	9.732	0.881	0.336
Mu09-14	8	8.7719	70.8152	3862	Moraine valley axis	Boulder (1.5 * 1.5 * 1.5)	3	0.945	28.44	0.573	305.27	24.76	9.925	1.164	0.858
Mu09-15	7	8.7758	70.8161	3804	Striated bedrock valley axis		3	0.968	28.32	0.564	390.44	34.08	12.864	1.566	1.188

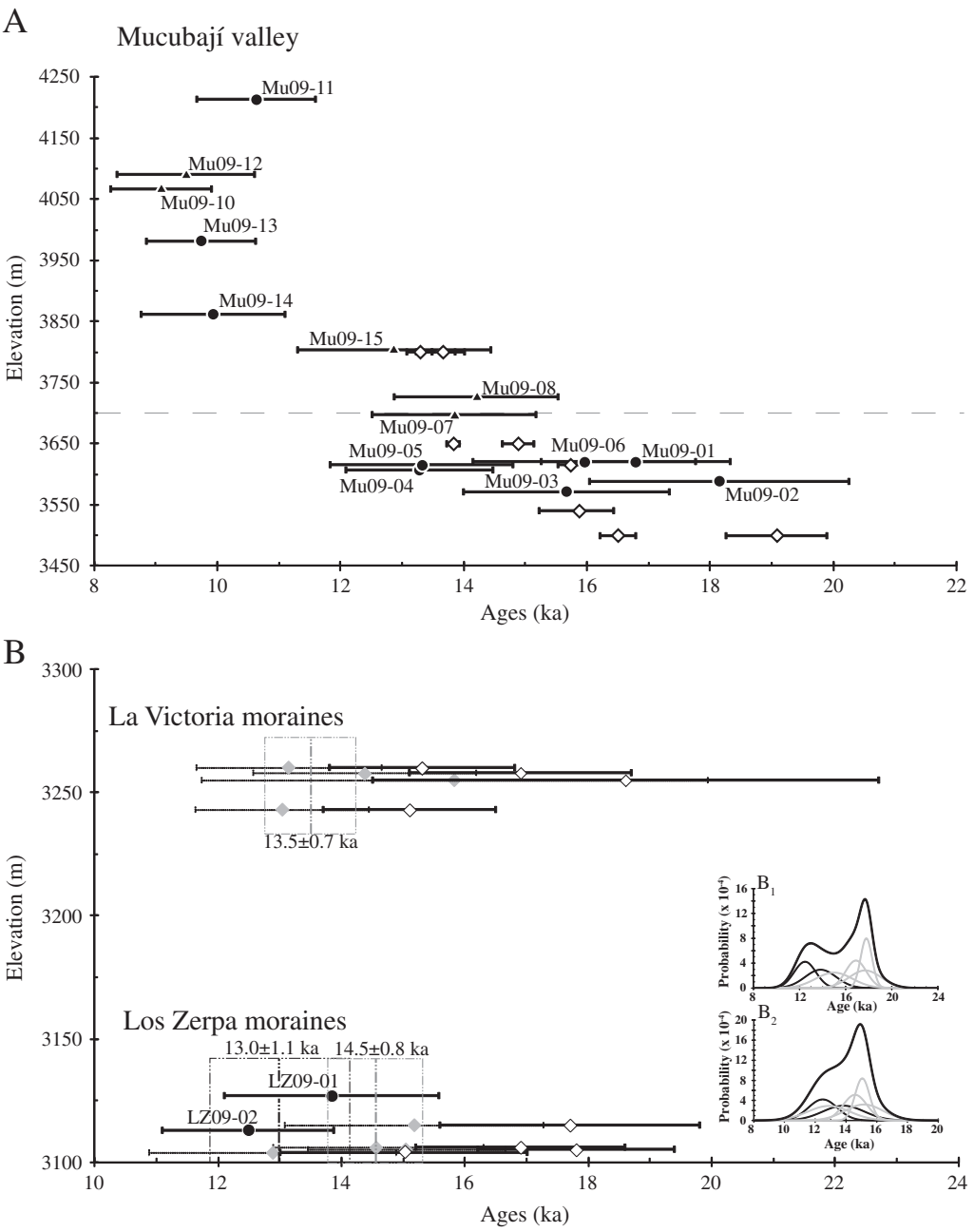

Figure 3. TCN results versus elevation in the Mucubají valley (A) and, Los Zerpa and La Victoria frontal moraines (B). Dotted horizontal line separates the flat lower sector from the steep sector in the Mucubají valley. Black dots and triangles are TCN dating of boulders moraines and striated bedrock respectively (this study), white diamonds are published data (see Table 2 for details), gray diamonds are recomputed TCN data of Wesnousky et al. (2012) with a time dependant production rate (see Results section, Tables 1 and 2 for details). Dotted box represents weighted average ages, in black the present study and in gray the recomputed TCN data (Wesnousky et al., 2012). Inserts B_1 and B_2 are individual probability distributions of exposure ages before (B_1) and after (B_2) computation of data published by Wesnousky et al. (2012). Light gray curves are data published by Wesnousky et al. (2012); dark gray curves are data of the present study. Black curves are the sum of the individual probabilities.

Surprisingly, the age distribution is comparatively narrow with respect to the lower sector and ranges between 14.20 ± 1.33 and 9.08 ± 0.82 ^{10}Be-ka. TCN ages decrease with elevation except for the highest elevation sample, which is abnormally old with respect to the others (Mu09-11, 10.63 ± 0.96 ^{10}Be-ka). The sample can be regarded as an outlier due to probably inherited ^{10}Be content produced from previous exposure before its abandonment or partial ice shielding due to low ice cover thickness. Since the area has been affected by mass wasting, the sampled boulder could have been deposited by gravitational collapse after a pre-exposure on the scarp. Because some sampled landforms are striated bedrock, no information permits the determination of glacier advances or retreats. We thus propose to combine Mu09-10 (9.08 ± 0.82 ^{10}Be-ka) and Mu09-12 (9.48 ± 1.11 ^{10}Be-ka) and consider the weighted average ages (WA 9.22 ± 0.66 ^{10}Be-ka) as the ultimate chronological marker of the glacier retreat. The established chronology agrees with a rapid retreat of the glacier tongue during the Pleistocene/Holocene transition.

Samples of the Los Zerpa moraines have been collected from meter-scale boulders located on the frontal moraine on either side of the paleo-outlet. TCN results (LZ09-01 and LZ09-02) are lower than those measured in the Mucubají valley but the concentrations are consistent (3.01 ± 0.28 and 2.70 ± 0.19 · 10^5 at·g·qtz, WA 2.80 ± 0.16 · 10^5 at·g·qtz). Once computed as exposure ages, samples LZ09-01 and LZ09-02 provide ages of 13.84 ± 1.74 and 12.48 ± 1.39

Table 2
Published chronological data of the Mesa del Caballo, Mucubají valley and La Victoria/Los Zerpa Moraines. (a) Values with * are estimated, (b) ^{14}C dates are calibrated (^{14}C cal ka BP) or uncalibrated (^{14}C ka BP), (c) TCN dating of Wesnousky et al. (2012) computed using the time-invariant production model, and (d) TCN ages that have been recalculated using the time-dependent production rate (See Discussion section for detail).

Sample	Latitude [(a)]	Longitude [(a)]	Elevation [(a)]	Sample informations	Ages[(b, c)]				Reference	Modified ages[(d)]	
					Methods	Value	Uncertainty −	Uncertainty +		Value	Uncertainty
	°N	°W	m asl		ka					ka	
Ped 5	8.78*	70.84*	3500*	~1 m from the base of the deposits — Mesa del Caballo	^{14}C ka	> 59.8	0	0	Dirszowsky et al. (2005)		
Ped 5	8.78*	70.84*	3500*	~1 m from the base of the deposits — Mesa del Caballo	^{14}C ka	>60.72	0	0	Dirszowsky et al. (2005)		
CAMS-139847	8.78*	70.84*	3500*	Peat layer — Mesa del Caballo	^{14}C ka	>50.2	0	0	Wesnousky et al. (2012)		
Ped 5-3 III	8.78*	70.84*	3500*	Peat layer — Mesa del Caballo	^{14}C ka	47.84	0.88	0.88	Mahaney et al. (2001)		
Ped 5-3 IV	8.78*	70.84*	3500*	Peat layer — Mesa del Caballo	^{14}C ka	53.14	1.16	1.16	Mahaney et al. (2001)		
Ped 5-3 VI	8.78*	70.84*	3500*	Peat layer — Mesa del Caballo	^{14}C ka	60.24	2.84	2.84	Mahaney et al. (2001)		
Ped 5-3 VII Top	8.78*	70.84*	3500*	Peat layer — Mesa del Caballo	^{14}C ka	58.35	2.79	2.79	Mahaney et al. (2001)		
Ped 5-3 VII Middle	8.78*	70.84*	3500*	Peat layer — Mesa del Caballo	^{14}C ka	>64.64	0	0	Mahaney et al. (2001)		
Ped 5-3 VII Bottom	8.78*	70.84*	3500*	Peat layer — Mesa del Caballo	^{14}C ka	>63.48	0	0	Mahaney et al. (2001)		
Ped 5-3 VII Top	8.78*	70.84*	3500*	Peat layer — Mesa del Caballo	^{14}C ka	56.94	2.26	2.26	Mahaney et al. (2001)		
PED 5	8.78*	70.84*	3500*	Peat layer — Mesa del Caballo	^{14}C (cal ka BP)	22.75–19.96	1.04–0.27	1.14–0.28	Schubert and Rinaldi (1987)		
0	8.78*	70.84*	3500*	Peat layer — Mesa del Caballo	^{14}C (cal ka BP)	19.08	0.82	0.82	Schubert and Rinaldi (1987)		
0	8.78*	70.84*	3500*	Peat layer — Mesa del Caballo	^{14}C (cal ka BP)	16.5	0.29	0.29	Schubert and Rinaldi (1987)		
MUCL0202	8.80*	7.83*	3540	Lake sediment	^{14}C (cal ka BP)	15.87	0.65	0.56	Carrillo et al. (2008)		
CAMS-104915	8.784	70.82	3615	Peat bog — Aquatic macrofossils	^{14}C (cal ka BP)	15.73	0.207	0.195	Stansell et al. (2005)		
0	8.78*	70.82*	3650	Sediment Mucubají terrasse	^{14}C (cal ka BP)	14.88	0.25	0.25	Salgado-Labouriau et al. (1977)		
0	8.78*	70.82*	3650	Sediment Mucubají terrasse	^{14}C (cal ka BP)	13.83	0.1	0.1	Salgado-Labouriau et al. (1977)		
MUM 7B	8.77*	70.81*	3800*	organic alluvium	^{14}C (cal ka BP)	13.29	0.22	0.19	Mahaney et al. (2008)		
MUM 7B	8.77*	70.81*	3800*	Peat	^{14}C (cal ka BP)	13.64	0.14	0.22	Mahaney et al. (2008)		
MUM 7B	8.77*	70.81*	3800*	Peat	^{14}C (cal ka BP)	13.66	0.44	0.36	Mahaney et al. (2008)		
CAMS-104914	8.784	70.82	3615	Peat bog	^{14}C (cal ka BP)	6.28	0.063	0.021	Stansell et al. (2005)		
VEN 19	8.8141	70.8006	3255	Gneiss boulder la Victoria Moraine	^{10}Be	18.6	4.1	4.1	Wesnousky et al. (2012)	15.8	3.4
VEN 20	8.81.42	70.8006	3258	Gneiss boulder la Victoria Moraine	^{10}Be	16.9	1.8	1.8	Wesnousky et al. (2012)	14.4	1.5
VEN 21	8.8142	70.801	3260	Gneiss boulder la Victoria Moraine	^{10}Be	15.3	1.5	1.5	Wesnousky et al. (2012)	13.1	1.2
VEN 23	8.8139	70.7993	3243	Metagranite boulder la Victoria moraine	^{10}Be	15.1	1.4	1.4	Wesnousky et al. (2012)	13.0	1.2
VEN 25	8.8121	70.7881	3115	Gneiss boulder Los Zerpa	^{10}Be	17.7	2.1	2.1	Wesnousky et al. (2012)	15.2	1.7
VEN 26	8.812	70.7873	3104	Gneiss boulder Los Zerpa	^{10}Be	15	2	2	Wesnousky et al. (2012)	12.9	1.7
VEN 27	8.8117	70.7875	3105	Gneiss boulder Los Zerpa	^{10}Be	17.8	1.6	1.6	Wesnousky et al. (2012)	15.1	1.4
VEN 28	8.8118	70.7873	3106	Gneiss boulder Los Zerpa	^{10}Be	16.9	1.7	1.7	Wesnousky et al. (2012)	14.6	1.4

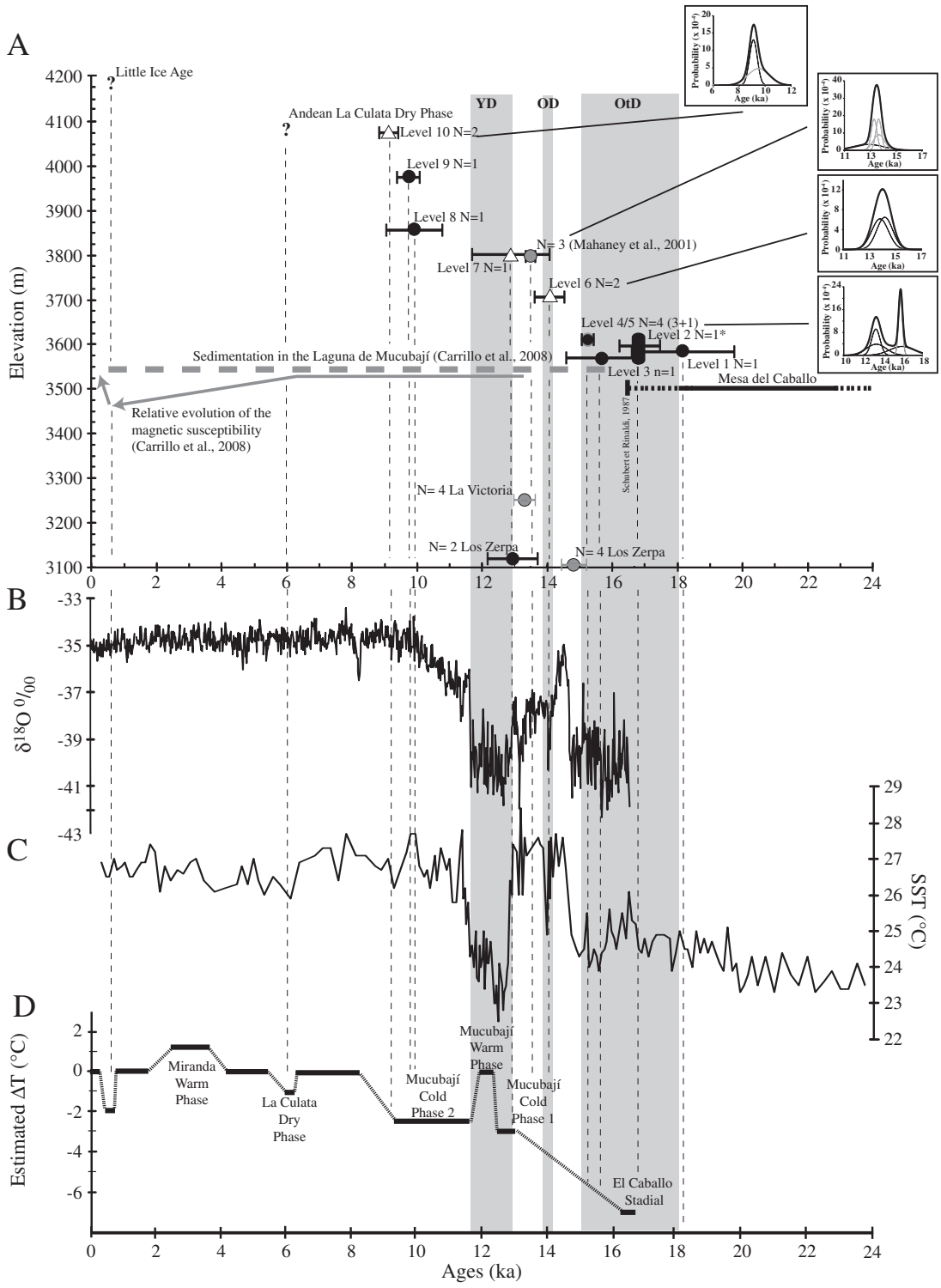

Figure 4. Correlations of altitudinal location of the glacier front since the LGM (A) and global (B), regional (C) and local (D) paleoclimatic proxy records. (A) Synthetic evolution of the ice retreat in Mucubají valley. Black dots (moraine samples) and white triangle (striated bedrock samples) are weighted average ages deduced from TCN dating (this study) except for Level 4/5 which includes published data (the weighted averages have been calculated with internal uncertainties because of the proximity of the sampling sites for each level). Gray dots are WA deduced from published data (see Table 2 for details). Question marks indicate time periods of possible glacier reactivation not confirmed in this present study. N is the number of data used for the WA calculation. The * refers to the thickness (~100 m) of the moraine Level 2. Inserts are individual exposure age probability distributions of level (light gray curves are published data, dark gray curves are data of the present study, black curves are the sum of the individual probabilities). Dashed gray line represents the time period of sedimentation of the Laguna de Mucubají (Carrillo et al., 2008). Gray bands localize characteristic cold periods based on GISP2 curves. YD: Younger Dryas, OD: Older Dryas and OtD: Oldest Dryas (B) GISP2 $\delta^{18}O$ values (‰) (Stuiver et al., 1995). (C) Sea Surface Temperature (SST) deduced from Mg/Ca sediment record of the Cariaco Basin (Lea et al., 2003). (D) Noticeable climatic episodes since the LGM in the Mérida Andes deduced from palynological investigations (after Rull, 1999).

^{10}Be-ka, respectively (Table 1, Fig. 3B). These reliable ages indicate that the boulders have the same exposure history despite the fact that the LZ09-02 and LZ09-01 boulders emerge by ~2 m and ~1 m above the surface of the moraine. This indicates a similar and consequently continuous exposure since the moraine abandonment and a moderate abrasion of the moraine ridge.

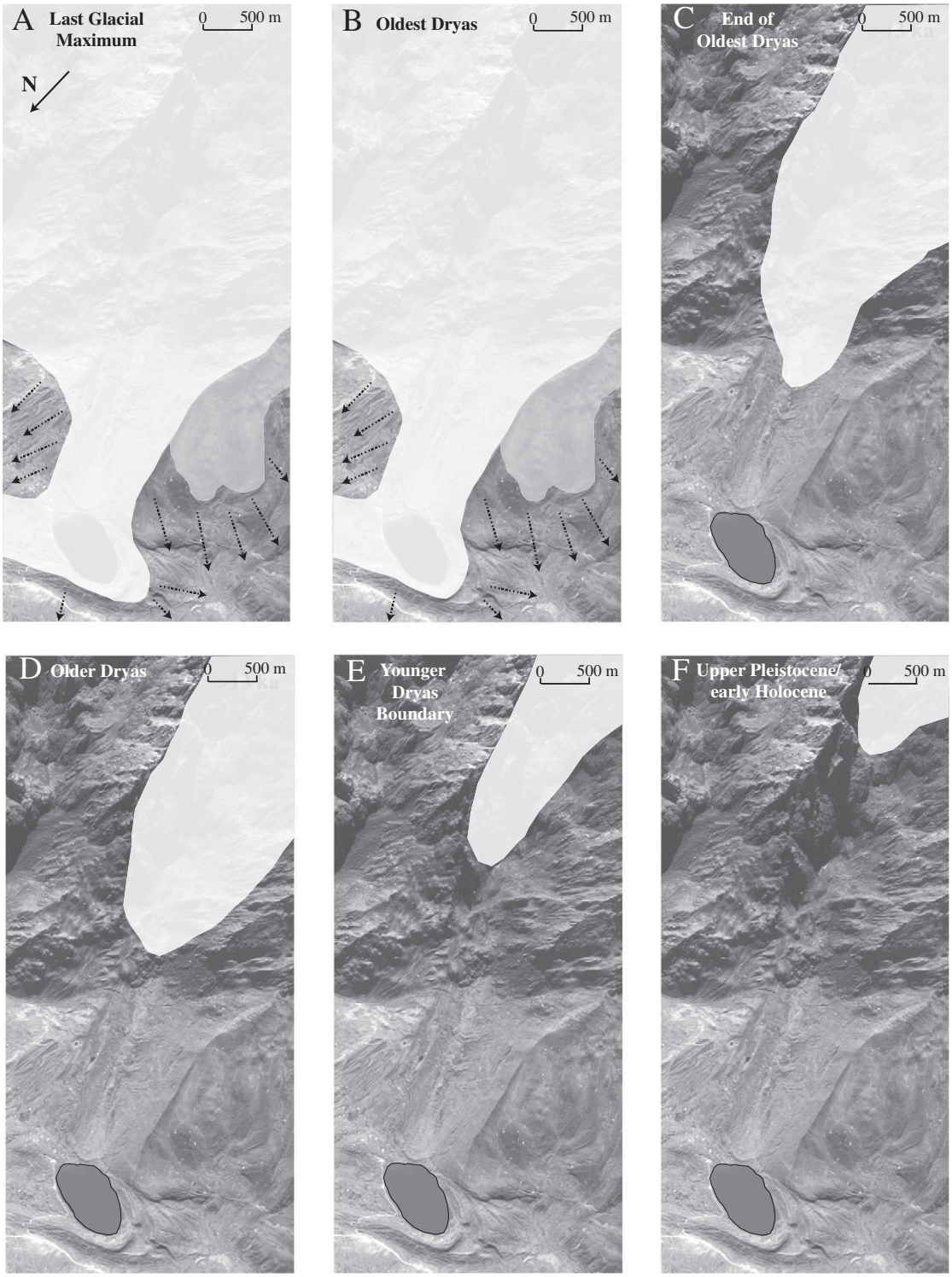

Figure 5. Timeline of the deglaciation in the Mucubají valley. The white cover indicate the glacier extent deduced from the present study, the gray cover indicate the presumed glacier location in the Mesa del Caballo deduced from field work and dating correlations, dashed arrows are the paraglacial outwash sediments.

However, dating of the Los Zerpa moraines shows significant discrepancies between the present data (13.84 ± 1.74 and 12.48 ± 1.39 ^{10}Be-ka, WA 13.0 ± 1.1 ka) and those (Table 2, WA 16.9 ± 1.3 ka for los Zerpa and 16.5 ± 1.6 ka for La Victoria) published by Wesnousky et al. (2012) (Fig. 3B1). Disparity can be justified by either a small but significant erosion or partial coverage of the sampled boulder. The boulders collected for the current study and by Wesnousky et al. (2012) were separated by less than 100 m, implying that the potential erosion would have affected all sampled boulders. During sampling, we carefully applied a sampling strategy similar to the one of Wesnousky et al. (2012), taking care to sample boulders well-anchored in the moraine and sufficiently high (>1 m) above the moraine to reduce superficial coverage. The age differences result only from the choice of the scaling scheme used in the Cronus calculator. We used the time-dependent production rate of Lal (1991) modified by Stone (2000), while Wesnousky et al. (2012) chose the time-invariant production rate, i.e. with no geomagnetic modulation of the production rate (see details in the Methods section and in Balco et al., 2008). Once computed

with the time-dependent production rate, the Wesnousky et al. (2012) results (WA 14.5 ± 0.8 ka [Los Zerpa] and 13.5 ± 0.7 [La Victoria]) agree with those of the present study (Fig. 3B). Wesnousky et al. (2012) associated the abandonment of the Los Zerpa and La Victoria recessional moraines as a small late glacial advance after the LGM. With this recomputation, the whole dataset of La Victoria and the Los Zerpa moraines are consistent (Fig. 3B). These ages are compatible with sedimentological information of the paleo-lake formed behind the Los Zerpa frontal moraines, where organic material was radiocarbon dated at ~9.5 cal ka BP (Carrillo et al., 2006).

Discussion

Compilation of TCN results (Table 1) with published data (Table 2) allows the deciphering of the Pleistocene–early Holocene glacier activity in the Mucubají area (Fig. 4). The early Mérida glaciations have been identified by dating of paraglacial materials in the Mesa del Caballo (Schubert, 1974; Dirszowsky et al., 2005; Rull, 2005). The Mesa del Caballo (Fig. 1B) is a fan complex resulting from the damming of the drainage following the shift of the Boconó fault. The sedimentary deposit is mainly composed of ~40 m of tills interbedded with lacustrine and soil horizons. Mixed proglacial sediments increase in the upper layers (see sedimentary description in Dirszowsky et al., 2005). The lowermost soil layers, located ~1 m from the base of the sedimentary column, were dated at ~60 ka (Mahaney et al., 2001; Dirszowsky et al., 2005; Wesnousky et al., 2012) but were subsequently determined to likely correspond to Dansgaard/Oeschger event 19 (67–70 ka) and called the "Pedregal interstade" (Dirszowsky et al., 2005).

The most noticeable glacial landforms are the well-preserved lateral moraines of several hundreds of meters in length and up to 150 m high. They were formed by paleo-glaciers that flowed in NW–SE to N–S directions in El Caballo and Mucubají valleys (Fig. 1B). These moraine complexes were attributed to the ultimate LGM advance (Schubert, 1974), as suggested by the associated fluvio-glacial sediments deposited on the Mesa del Caballo and dated between 22.75 to 19.66 cal ka BP (Schubert and Rinaldi, 1987; Rull, 1998). In the Mucubají valley, the distal moraine complexes are two latero-frontal moraines developed downstream of the Laguna de Mucubají (Levels 1 and 2, Fig. 2B). The two moraine ridges were dated at 18.14 ± 2.11 and 16.78 ± 1.54 ^{10}Be-ka, respectively. Furthermore, Carrillo et al. (2008) demonstrated the initiation of sedimentation at about 15.9 ka in the lake dammed by the Level 2 moraine (Fig. 2B, Table 2). This agrees with the TCN ages of Levels 1 and 2. The lowermost moraine (Level 1, 18.1 ± 2.1 ^{10}Be-ka) corresponds to the maximum glacier extent of the LGM (Fig. 5A). The upper moraine (Level 2, 16.8 ± 1.5 ^{10}Be-ka) is the largest recessional moraine preserved in the area and was developed during the so-called Oldest Dryas or locally named the "El Caballo Stadial" stage (Figs. 4D and 5B). The Level 2 moraine presumably caused the break of sedimentation in the Mesa del Caballo, which is indicated by the radiocarbon dating of organic material entrapped in the upper sedimentary layer and dated at 16.5 cal ka BP (Schubert and Rinaldi, 1987).

Furthermore, high amounts of coarse materials have been observed at the base of the lake sediment (Carrillo et al., 2008). Even if this layer has been interpreted as a seismo-turbidite, the existence of sand material is compatible with a long lasting presence of a glacier front in the vicinity of the lake and the presumable transitional calving glacier configuration feeding the sediments with outwash material trapped in the ice. Since the lake is surrounded by the Levels 2 and 3 moraines (Fig. 2B), the time lag (~1 ka) corresponds to the required time for melting the glacier on a surface equivalent to the lake. In this context, the melting rate was thus ~0.3 km^2/ka.

Whereas several authors proposed a late end of the LGM before 13 ka (Rull, 1996; Dirszowsky et al., 2005), we identified 3 recessional frontal moraines (Levels 3 to 5) and 2 striated bedrock units (Levels 6 and 7) dated from 15.6 to 12.9 ka. The landforms defined the glacier front during successive step between the Oldest Dryas and the Younger Dryas

Table 3
Mean annual temperature, precipitation and evaporation survey (Venezuelan National Meteorological Institute, http://www.inameh.gob.ve/) of meteorological stations on both sides of the Mucubají pass (i.e. Santo Domingo valley, North and Mucuchies valley, South). The periods of survey are noticed. The mean annual values have only been computed for complete years; the number of considered years are noted.

Station	Latitude [a]	Longitude [a]	Elevation [a]	Distance from the Laguna de Mucibaji	Mean temperature	Period of survey	Number of years	Mean precipitation	Period of survey	Number of years	Mean evaporation	Period of survey	Number of years	Ratio precipitation/evaporation
	°N	°W	m asl	km	°C			mm/yr			mm/yr			
Santo Domingo	8.87	70.67	2100	16	15.6	1980/1983	3	1277	1965/1995	23	1172	1979/1983	5	1.09
Los Plantios	8.82	70.78	3000	6	8.1	1971/1983	7	1017	1970/1995	22	872	1970/1983	14	1.17
Mucubají	8.80	70.82	3600	0	6.0	1970/1983	11	922	1969/1995	24	907	1970/1983	14	1.02
Mucuchies	8.77	70.9	3000	12	11.4	1951/1976	12	690	1941/1984	30	–	–	–	–
Mucuruba	8.71	71.0	2400	20	14.4	1982	1	830	1950/1983	30	1402	1963/1983	27	0.59
Tabay	8.64	71.1	1700	32	–	–	–	1566	1950/1995	29	–	–	–	–

boundary (Figs. 5B, C, D, and E). With Levels 2 to 5 being formed by frontal moraines, the glacier retreat appears to have been at least interrupted or even temporarily reversed by significant glacier readvances. The glacier activity matches the rise of temperature in the Mérida Andes from −7 to −3°C compared with the present day (Fig. 4D) and of sea-surface temperature (SST) from 24 to 27°C (Fig. 4C). Exposure ages of striated bedrocks assigned to Level 6 (Table 1) point the timing of the ice front during the sharp and cold Older Dryas period (Fig. 5D). This is also evidenced in Los Anteojos lake sediments (Mérida Andes) by high titanium and clastic contents, as well as by low biogenic silica concentration between 14.1 and 13.9 ka (Stansell et al., 2010). This temperature drop is also significant in GISP2 and SST records (Figs. 4B and C).

Peat samples covered by glaciofluvial materials (till and outwash) collected 150 m up-valley from a small push moraine (site MUM7B, 3800 m asl) have been dated at 13.29 ± 0.22, 13.64 ± 0.15 and 13.66 ± 0.44 cal ka BP (Mahaney et al., 2008 and Table 2) and indicate the maximum ages of glaciofluvial deposits. Mahaney et al. (2008) "approximately" associated them with the Younger Dryas (Mahaney et al., 2008 and Fig. 5E). These ages agree with TCN dating of a striated surfaces collected at ~3800 m asl (Level 7, 12.9 ± 1.6 ^{10}Be-ka) and are compatible with the presence of fluvio-glacial terrace deposits at ~3650 m asl dated at 14.88 ± 0.25 and 13.83 ± 0.1 cal ka BP (WA 14 ± 0.1 ka; Table 2, Salgado-Labouriau et al., 1977). The location of landforms in relation to each other and the absence of erosion/deformational features in downvalley terraces indicate the occurrence of a glacier re-advance, which appears to be the last significant advance of the Pleistocene (Salgado-Labouriau et al., 1977; Mahaney et al., 2007a,b). Ages can be related to the Younger Dryas Boundary (YDB) identified at 12.9/12.5 ka in several places of the Central/South America, such as in Mexico (Israde-Alcántara et al., 2012), Colombia (van't Veer et al., 2000), Peru (Seltzer et al., 2002), Bolivia (Sylvestre et al., 1999; Blard et al., 2011), Patagonia (Heusser, 1993; Glasser et al., 2012) and also in the Cariaco basin sediments (Fig. 4C). In Venezuela, some limnological evidence attests to the existence of a significant dry period after ~13.4 ka (Salgado-Labouriau, 1980) and glacier advances after 12.9 ka in the vicinity of high-altitude lakes of the central Mérida Andes (Rull et al., 2005; Carrillo et al., 2008; Stansell et al., 2010). The second part of the YD is interrupted by a warm and wet period revealed by pollen records (Fig. 4D) and to a lesser extend in SST record (Fig. 4C). This drastic change, attributed to change of the Atlantic Ocean circulation (Stansell et al., 2010), is compatible with older and probably maximized radiocarbon dating deduced from peat buried beneath the YD moraine and belong in the time interval of the TCN age (Mu09-15).

Once recomputed with a time-dependant production scheme (see Methods section for details and Table 2), the TCN dating of Wesnousky et al. (2012) allows the relation of the La Victoria and Los Zerpa moraines to the Younger Dryas (Figs. 3B, 5E and Table 2). Because of the proximity of the valleys to one another, the altitudinal lag of the YD moraines cannot be justified by global climate changes but rather by local conditions connected to valley orientation and climate regime. In the Mérida Andes the steep topography controls local climate (Pulwarty et al., 1998), and moisture is carried by easterly trade winds charged with humidity originating from the Caribbean Sea and tropical lowlands (Villagrán, 1993). Modern meteorological survey data (Table 3) indicate a clear climate divide between the wetter Santo Domingo valley and dryer Mucuchies valley. These opposed climate conditions and valley orientations seem to have been sufficient to result in an altitudinal lag of the YD moraines.

In the Mucubají valley, the age distribution suggests a rapid ice melting during the upper Pleistocene/early Holocene transition (Fig. 4). From Level 8 (Mu09-14, 3862 m asl) to Level 10 (Mu09-10 and Mu09-12, average 4079 m asl), the ages are remarkably consistent with a WA age of 9.72 ± 0.43 ka including Mu09-12 or, 9.49 ± 0.48 ka excluding Mu09-12 (see Result section for details). We considered 3 different levels (Levels 8, 9, and 10), which define the glacier front during upper Pleistocene/early Holocene (Figs. 4A and 5F). Levels 8 and 9, corresponding to frontal moraines, were abandoned during a sharp period of warming identified by a rise of ~1.5°C in the SST record, and Level 10 corresponds to a weak warming centered around 9 ka (Fig. 4C). The extreme age and altitude differences between the lower and higher sites (Level 8 and Level 10, respectively) indicate a rise of the vertical ice retreat with a rate of ~310 m/ka, whereas it was ~25 m/ka between the Oldest Dryas and late Pleistocene. The particularly short time interval associated with the ~250-m rise of the ice front demonstrates the strong climate forcing on the glacier balance during the beginning of the Holocene and agrees with the absence of frontal moraine relics in this area. Other information endorse this observation, such as the high magnetic susceptibility of the lakes sediments (Mucubají and Negra) since the Younger Dryas and up to 10 ka (Stansell et al., 2005; Carrillo et al., 2008) and palynological records, which emphasize climate conditions close to present day (Rull, 1996).

Even if no TCN data present a chronological constraint since the Pleistocene/Holocene transition, sediment descriptions of the Laguna de Mucubají (Carrillo et al., 2008) and peat bogs (Stansell et al., 2005) indicate a glacial activity at least up to ~6 ka (i.e., La Culata Dry Phase). This short period has been identified as cooler and dryer than the overall Holocene (Salgado-Labouriau and Schubert, 1976), with a negative hydrological budget and a decreased precipitation/evaporation ratio (Rull, 1996). This event was identified from decreases of the magnetic susceptibility, indicating a reduction of magnetic mineral inputs in the lake sediments (Carrillo et al., 2008) and the development of organic-rich sedimentation in bogs (Stansell et al., 2005). However, the origin of this magnetic career reduction and its relation with glacier activity is still subject to debate because of the absence of glacial relicts. Mahaney et al. (2007b) suggested that the sediment variation could have been the consequence of many parameters (hydrologic, climatic, geomorphic or tectonic).

The Little Ice Age (LIA) was suggested at different locations in the Venezuelan Andes by evidence of ice re-advances above 4200 m asl (Schubert, 1972; Schubert and Valastro, 1974; Schubert, 1975; Rull and Schubert, 1989) and related to a temperature drop of 3.2 ± 0.4°C and a 20% increase of precipitation (Polissar et al., 2006). In the Mucubají area, only an increase of magnetic susceptibility between 605 and 130 cal yr BP, assigned to an enhanced input of detrital material in the lake (Polissar et al., 2006), supports possible glacier erosion. However, while LIA moraines have been described in the Humboldt massif (Schubert, 1972, 1998), in the upper Mucubají area the valley opens and forms a glacial cirque mainly covered by mass-wasting deposits (Mahaney et al., 2007b). The absence of moraines does not allow confirmation of a glacier re-advance. Susceptibility variation can be linked to intensification of runoff related to an increase of precipitation (Polissar et al., 2006).

Conclusions

Sixteen new TCN and compiled published ages of glacial landforms provide the first post-LGM chronology of the ice retreat in the Venezuelan Andes. The constructed chronology agrees with the paleoclimatic records, indicating the direct control of the global climate on the evolution of South American tropical glaciers. The most extensive glacial advance has been dated at 18.1 ka, but the largest moraine ridge has been dated at 16.8 ka. In the lower zone of the Mucubají valley (<3700 m), five moraine ridges dated between 18.1 and 15.8 ka indicate successive stages of breaks in the overall glacier retreat. Above 3700 m asl, new dating of striated bedrock provides the timing of the end of deglaciation up to the Pleistocene/Holocene transition. In particular, our results provide additional information on the occurrence of the Oldest, Older and Younger Dryas and indicate the disappearance of the glacier at ~9.5 ka. Possible reactivations of confined glaciers suggested from limnological investigations at ~6 ka and during the LIA have not been confirmed by this study.

The chronological dataset allows the calculation of vertical ice retreat of 25 m/ka before the Younger Dryas, connected to the temperature evolution from −7°C (LGM) to −3°C (~13 ka). After the Younger Dryas and up ~9.5 ka, the retreat was stronger, with an approximate 310 m/ka vertical rate associated with an increase in temperature of 3°C.

The altitude difference of the Younger Dryas moraines in the Mucubají (~3800 m), La Victoria (~3250 m) and Los Zerpa (~3100 m) valleys suggests local effects on glacier evolution due to contrasted climate conditions on both side of the Mucubají pass.

Acknowledgments

Travel, fieldwork and logistics were supported by the "Ecos-Nord" Venezuela–France cooperation (N° V08U01), the University of Savoie APS/BQR Grant B2010-27 and FUNVISIS. Funding for chemical sample preparation was provided by the cosmogenic laboratory of ISTerre. Beryllium 10 analyses were performed at the French Accelerator Mass Spectrometry Facility, ASTER (INSU-CNRS). We thank Maurice Arnold and Georges Aumaître for assistance during AMS measurements, Thomas Condom and Melaine Le Roy for fruitful discussions, Francis Coeur for rock crushing, and Elizabeth Hardwick and Matthias Bernet for improvement of the writing. We warmly express thanks to the staff of the Santo Domingo Hotel for their privileged reception.

We also thank the administration of the INPARQUES National Park for issuing us a research permit.

Reference

Abbott, M.B., Wolfe, B.B., Wolfe, A.P., Seltzer, G.O., Aravena, R., Mark, B.G., Polissar, P.J., Rodbell, D.T., Rowe, H.D., Vuille, M., 2003. Holocene paleohydrology and glacial history of the central Andes using multiproxy lake sediment studies. Palaeogeography, Palaeoclimatology, Palaeoecology 194, 123–138.

Audemard, F.A., 1997. Holocene and historical earthquakes on the Boconó fault system, southern Venezuelan Andes: trench confirmation. Journal of Geodynamics 24 (1–4), 155–167.

Audemard, F.E., Audemard, F.A., 2002. Structure of the Mérida Andes, Venezuela: relations with the South America-Caribbean geodynamic interaction. Tectonophysics 345, 299–327.

Audemard, F.A., Pantosti, D., Machette, M., Costa, C., Okumura, K., Cowan, H., Diederix, H., Ferrer, C., Participants, Sawop, 1999. Trench investigation along the Mérida section of the Boconó fault (central Venezuelan Andes), Venezuela. In: Pavlides, S., Pantosti, D., Peizhen, Z. (Eds.), Earthquakes, Paleoseismology and Active Tectonics. Selected papers to 29th General Assembly of the Association of Seismology and Physics of the Earth's Interior (IASPEI), Thessaloniki, Greece, August 1997. Tectonophysics, 308, pp. 1–21.

Audemard, F.A., Ollarves, R., Bechtold, M., Díaz, G., Beck, C., Carrillo, E., Pantosti, D., Diederix, H., 2008. Trench investigation on the main strand of the Boconó fault in its central section, at Mesa del Caballo, Mérida Andes, Venezuela. Tectonophysics 459, 38–53.

Audemard, F.A., Beck, C., Carrillo, E., 2010. Deep-seated gravitational slope deformations along the active Boconó Fault in the central portion of the Mérida Andes, western Venezuela. Geomorphology 124 (3–4), 164–177.

Balco, G., Stone, J.O., Lifton, N.A., Dunai, T.J., 2008. A complete and easily accessible means of calculation surface exposure ages or erosion rates from ^{10}Be and ^{26}Al measurements. Quaternary Geochronology 3, 174–195.

Bellizzia, A., Pimentel, N., Bajo de Osuna, R., 1976. In: Ministerio de Minas e Hidrocarburos (Ed.), Mapa geológico-estructural de Venezuela. Scale 1: 500,000. Foninves, Caracas.

Bermúdez, M.A., Kohn, B., van der Beek, P., Bernet, M., O'Sullivan, P., Shagam, R., 2010. Spatial and temporal patterns of exhumation across the Venezuelan Andes: implications for Cenozoic Caribbean geodynamics. Tectonics 29. http://dx.doi.org/10.1029/2009TC002635.

Blard, P.-H., Sylvestre, F., Tripati, A.K., Claude, C., Causse, C., Coudrain, A., Condom, T., Seidel, J.-L., Vimeux, F., Moreau, C., Dumoulin, J.-P., Lavé, J., 2011. Lake highstands on the Altiplano (Tropical Andes) contemporaneous with Heinrich 1 and the Younger Dryas: new insights from ^{14}C, U–Th dating and δ^{18}O of carbonates. Quaternary Science Review 30, 3973–3989.

Brown, E.T., Edmond, J.M., Raisbeck, G.M., Yiou, F., Kurz, M.D., Brook, E.J., 1991. Examination of surface exposure ages of Antarctic moraines using in situ produced ^{10}Be and ^{26}Al. Geochimica et Cosmochimica Acta 55, 2269–2283.

Carrillo, E., Yépez, S., 2008. Evolución de glaciares en Venezuela: glaciares de los Picos Humboldt y Bonpland. Boletín Geológico 42, 97–108.

Carrillo, E., Audemard, F., Beck, C., Cousin, M., Jouanne, F., Cano, V., Castilla, R., Melo, L., Villemin, T., 2006. A Late Pleistocene–Holocene natural seismograph along the Boconó Fault (Mérida Andes, Venezuela): the moraine-dammed Los Zerpa paleolake. Bulletin de la Société Géologique de France 177, 3–17.

Carrillo, E., Beck, C., Audemard, F.A., Moreno, M., Ollarves, R., 2008. Disentangling Late Quaternary climatic and seismo-tectonic controls on Lake Mucubají sedimentation (Mérida Andes, Venezuela). Palaeogeography, Palaeoclimatology, Palaeoecology 259, 284–300.

Chmeleff, J., von Blanckenburg, F., Kossert, K., Jakob, J., 2010. Determination of the ^{10}Be half-life by multicollector ICP-MS and liquid scintillation counting. Nuclear Instruments and Methods in Physics Research B 268 (2), 192–199.

Dirszowsky, R.W., Mahaney, W.C., Hodder, K.R., Milner, M.W., Kalm, V., Bezada, M., Beukens, R.P., 2005. Lithostratigraphy of the Mérida (Wisconsinan) glaciation and Pedregal interstade, Mérida Andes, northwestern Venezuela. Journal of South American Earth Sciences 19, 525–536.

Dunai, T.J., 2010. Cosmogenic Nuclides. Principles, Concepts and Applications in the Earth Surface Sciences. Cambridge University Press (198 pages).

Dunne, J., Elmore, D., Muzikar, P., 1999. Scaling factors for the rates of production of cosmogenic nuclides for geometric shielding and attenuation at depth on sloped surfaces. Geomorphology 27 (1–2), 3–11.

Garrity, C.P., Hackley, P.C., Urbani, F., 2004. Digital shaded-relief map of Venezuela. http://pubs.usgs.gov/of/2004/1322.

Glasser, N.F., Harrison, S., Schnabel, C., Fabel, D., Jansson, K.N., 2012. Younger Dryas and early Holocene age glacier advances in Patagonia. Quaternary Science Reviews 58, 7–17.

Gonzales de Juane, C., Iturralde de Arozena, J., Picard, X., 1980. Geología de Venezuela y de sus cuencas petrolíferas. 2 vol. Foninves (1030 pp.).

Heusser, C.J., 1993. Late-glacial of southern South America. Quaternary Science Reviews 12, 345–350.

Israde-Alcántara, I., Bischoff, J.L., Domínguez-Vázquez, G., Li, H.-C., DeCarli, P.S., Bunch, T.E., Wittke, J.H., Weaver, J.C., Firestone, R.B., West, A., Kennett, J.P., Mercer, C., Xie, S., Richman, E.K., Kinzie, C.R., Wolbach, W.S., 2012. Evidence from central Mexico supporting the Younger Dryas extraterrestrial impact hypothesis. Proceeding of the National Academy of Sciences 109 (13), 738–747.

Jahn, A., 1912. La cordillera venezolana de los Andes. Revista Técnica del Ministerio de Obras Públicas 21 (2), 451–488.

Jahn, A., 1925. Observaciones glaciológicas en los Andes Venezolanos. Cultura Venezolana 64, 265–280.

Kalm, V., Mahaney, W.C., 2011. Late Quaternary glaciations in the Venezuelan (Mérida) Andes. In: Ehlers, J., Gibbard, P. (Eds.), Quaternary Glaciations-Extent and Chronology Part IV — A Closer Look. Oxford University Press, Oxford, pp. 835–841.

Kaplan, M.R., Strelin, J.A., Schaefer, J.M., Denton, G.H., Finkel, R.C., Schwartz, R., Putnam, A.E., Vandergoes, M.J., Goehring, B.M., Travis, S.G., 2011. In-situ cosmogenic ^{10}Be production rate at Lago Argentino, Patagonia: implications for late-glacial climate chronology. Earth and Planetary Science Letters 309, 21–32.

Korschinek, G., Bergmaier, A., Faestermann, T., Gerstmann, U.C., Knie, K., Rugel, G., Wallner, A., Dillmann, I., Dollinger, G., von Gostomski Lierse, Ch., Kossert, K., Maitia, M., Poutivtsev, M., Remmert, A., 2009. A new value for the half-life of ^{10}Be by heavy-ion elastic recoil detection and liquid scintillation counting. Nuclear Instruments and Methods in Physics Research B 268 (2), 187–191.

Lal, D., 1991. Cosmic ray labeling of erosion surfaces: in situ nuclide production rates and erosion models. Earth and Planetary Science Letters 104, 429–439.

Lea, D.W., Pak, D.K., Peterson, L.C., Hughen, K.A., 2003. Synchroneity of tropical and high-latitude Atlantic temperatures over the last glacial termination. Science 301, 1361–1364.

Mahaney, W.C., Milner, M.W., Voros, J., Kalm, V., Hütt, G., Bezada, M., Hancock, R.G.V., Autreiter, S., 2000. Stratotype for the Mérida Glaciation at Pueblo Llano in the Northern Venezuela Andes. Journal of South American Earth Sciences 13, 761–774.

Mahaney, W.C., Russell, S.E., Milner, M.W., Kalm, V., Bezada, M., Hancock, R.G.V., Beukens, R.P., 2001. Paleopedology of Middle Wisconsin/Weichselian paleosols in the Mérida Andes, Venezuela. Geoderma 104, 215–237.

Mahaney, W.C., Dirszowsky, R.W., Milner, M.W., Harmsen, R., Finkelstein, S., Kalm, V., Bezada, M., Hanckock, R.G.V., 2007a. Soil stratigraphy and ecological relationships of a late Glacial-Holocene fluvial terrace sequence, Sierra Nevada National Park, Northern Venezuelan Andes. Journal of South American Earth Sciences 23, 46–60.

Mahaney, W.C., Dirszowsky, R.W., Kalm, V., 2007b. Comment on "Quaternary deglacial history of the Mérida Andes, Venezuela" by N.D. Stansell, et al. Journal of Quaternary Science 22, 1–5.

Mahaney, W.C., Milner, M.W., Kalm, V., Dirszowsky, R.W., Hancock, R.G.V., Beukens, R.P., 2008. Evidence for a Younger Dryas glacial advance in the Andes of northwestern Venezuela. Geomorphology 96, 199–211.

Merchel, S., Herpers, U., 1999. An update on radiochemical separation techniques for the determination of long-lived radionuclides via accelerator mass spectrometry. Radiochimica Acta 84, 215–219.

Polissar, P.J., Abbott, M.B., Wolfe, A.P., Bezada, M., Rull, V., Bradley, R.S., 2006. Solar modulation of Little Ice Age climate in the tropical Andes. Proceedings of the National Academy of Science 103, 8937–8942.

Pulwarty, R.S., Barry, R.G., Hurst, C.M., Sellinger, K., Mogollon, L.E., 1998. Precipitation in the Venezuelan Andes in the context of regional climate. Meteorology and Atmospheric Physics 67, 217–237.

Putnam, A.E., Schaefer, J.M., Barrell, D.J.A., Vandergoes, M., Denton, G.H., Kaplan, M.R., Finkel, R.C., Schwartz, R., Goehring, B.M., Kelley, S.E., 2010. In situ cosmogenic 10Be production-rate calibration from the Southern Alps, New Zealand. Quaternary Geochronology 5, 392–409.

Rod, E., 1956. Strike-slip faults of northern Venezuela. Bulletin of the American Association of Petroleum Geologists 40, 457–476.

Rull, V., 1996. Late Pleistocene and Holocene climates of Venezuela. Quaternary International 31, 85–94.

Rull, V., 1998. Palaeoecology of pleniglacial sediments from the Venezuelan Andes. Palynological record of El Caballo stadial, sedimentation rates and glacier retreat. Review of Palaeobotany and Palynology 99, 95–114.

Rull, V., 1999. Palaeoclimatology and sea-level history in Venezuela. New data, land–sea correlations and proposals for future studies in the frame of the IGBP-PAGES Project. Interciencia 24, 92–101.

Rull, V., 2005. A Middle Wisconsin interstadial in the northern Andes. Journal of South American Earth Sciences 19, 173–179.

Rull, V., Schubert, C., 1989. The Little Ice Age in the tropical Venezuelan Andes. Acta Cienifica Venezolana 4, 71–73.

Rull, V., Abbott, M.B., Polissar, P.J., Wolfe, A.P., Bezada, M., Bradley, R.S., 2005. 15,000-yr pollen record of vegetation change in the high altitude tropical Andes at Laguna Verde Alta, Venezuela. Quaternary Research 64, 308–317.
Salgado-Labouriau, M.L., 1980. A pollen diagram of the Pleistocene–Holocene boundary of lake Valencia, Venezuela. Review of Palaeobotany and Palynology 38, 297–312.
Salgado-Labouriau, M.L., 1989. Late Quaternary climatic oscillations in the Venezuelan Andes. Biology International 18, 12–14.
Salgado-Labouriau, M.L., Schubert, C., 1976. Palynology of Holocene peat bogs from central Venezuelan Andes. Palaeogeography, Palaeoclimatology, Palaeoecology 19, 147–156.
Salgado-Labouriau, M.L., Schubert, M.L., Valastro, S.J., 1977. Paleoecologic analysis of a Late Quaternary terrace from Mucubají, Venezuelan Andes. Journal of Biogeography 4, 313–325.
Salgado-Labouriau, M.L., Bradley, R.S., Yuretich, R.F., Weingarten, B., 1992. Paleoecological analysis of the sediments of Lake Mucubají, Venezuelan Andes. Journal of Biogeography 19, 317–327.
Schubert, C., 1970. Glaciation of the Sierra de Santo Domingo, Venezuelan Andes. Quaternario 13, 225–246.
Schubert, C., 1972. Geomorphology and glacier retreat in the Pico Bolívar area, Sierra Nevada de Mérida, Venezuela. Zeitschrift für Gletscherkunde und Glazialgeologie 8, 189–202.
Schubert, C., 1974. Late Pleistocene Mérida glaciation, Venezuelan Andes. Boreas 3, 147–152.
Schubert, C., 1975. Glaciation and periglacial morphology in the northeastern Venezuelan Andes. Eiszeitalter und Gegenwart 26, 196–211.
Schubert, C., 1980. Contribución al inventario mundial de glaciares. Boletín de la Sociedad Venezolana de Ciencias Naturales 34 (137), 267–279.
Schubert, C., 1982. Neotectonics of Boconó Fault, western Venezuela. Tectonophysics 85, 205–220.
Schubert, C., 1998. Glaciers of Venezuela. In: Williams, R.S., Ferrigno, J.G. (Eds.), Satellite Image Atlas of Glaciers of the World. U.S. Geological Survey Professional Paper 1386-I, Washington D.C.
Schubert, C., Clapperton, C.M., 1990. Quaternary glaciations in the northern Andes (Venezuela, Colombia and Ecuador). Quaternary Science Reviews 9 (2–3), 123–135.
Schubert, C., Rinaldi, M., 1987. Nuevos datos sobre la cronología del estadio tardio de la Glaciacion Mérida, Andes Venezolanos. Acta Científica Venezolana 38, 135–136.
Schubert, C., Sifontes, R., 1970. Boconó fault, Venezuelan Andes: evidence of postglacial movement. Science 170, 66–69.
Schubert, C., Valastro, S., 1974. Late Pleistocene glaciation of Páramo de La Culata, north-central Venezuelan Andes. Geologische Rundschau 63, 516–538.
Schubert, C., Vivas, L., 1993. El Cuaternario de la Cordillera de Mérida; Andes Venezolanos. Universidad de Los Andes/Fundación Polar, Mérida, Venezuela (345 pp.).
Seltzer, G.O., Rodbell, D.T., Baker, P.A., Fritz, S.C., Tapia, P.M., Rowe, H.D., Dunbar, R.B., 2002. Early warming of tropical South America at the last glacial-interglacial transition. Science 296 (5573), 1685–1686.
Sievers, W., 1885. Über Schneeverhältnisse in der Cordillere Venezuelas. Jahresbericht der Geographischen Gesellschaft in München 10, 54–57.
Stansell, N.D., Abbott, M.B., Polissar, P.J., Wolfe, A.P., Bezada, M., Rull, V., 2005. Late Quaternary deglacial history of the Mérida Andes, Venezuela. Journal of Quaternary Science 20 (7–8), 801–812.
Stansell, N.D., Polissar, P.J., Abbott, M.B., 2007. Last glacial maximum equilibrium-line altitude and paleo-temperature reconstructions for the Cordillera de Mérida. Venezuelan Andes. Quaternary Research 67, 115–127.
Stansell, N.D., Abbott, M.B., Rull, V., Rodbell, D.T., Bezada, M., Montoya, E., 2010. Abrupt Younger Dryas cooling in the northern tropics recorded in lake sediments from the Venezuelan Andes. Earth and Planetary Science Letters 293, 154–163.
Stone, J.O., 2000. Air pressure and cosmogenic isotope production. Journal of Geophysical Research 105, 23753–23759.
Stuiver, M., Grootes, P.M., Braziunas, T.F., 1995. The GISP2 $\delta^{18}O$ climate record of the Past 16,500 years and the role of the sun, ocean, and volcanoes. Quaternary Research 44 (3), 341–354.
Sylvestre, F., Servant, M., Servant-Vildary, S., Causse, C., Fournier, M., Ybert, J.P., 1999. Lake-level chronology on the southern Bolivian Altiplano (18°–23°S) during late-glacial time and the early Holocene. Quaternary Research 51, 54–66.
van't Veer, R., Islebe, G.A., Hooghiemstra, H., 2000. Climatic change during the Younger Dryas chron in northern South America: a test of the evidence. Quaternary Science Reviews 19, 1821–1835.
Villagrán, M., 1993. Una Interpretación climática del registro palinológico del ultimo ciclo glacial-postglacial en sudamérica. Bulletin de l'Institut français d'études andines 22 (1), 243–258.
Wesnousky, S.G., Aranguren, R., Rengifo, M., Owen, L.A., Caffee, M.W., Krishna Murari, M., Pérez, O.J., 2012. Toward quantifying geomorphic rates of cristal displacement, landscape development, and the age of glaciation in the Venezuelan Andes. Geomorphology 141–142, 99–113.
Yépez, S., Carrillo, E., 2009. Evolución de los glaciares venezolanos, picos Humboldt y Bonpland. 3er ciclo de conferencias y segundo curso internacional de cambios ambientales globales. Caracas.

V-2.1.2 Gavidia valley

The Gavidia valley is one of the few valleys in Sierra Nevada with NE-SW oriented accumulation zone. The valley is characterized by low valley bottom slopes (~5-7º). This valley is not directly connected to the Chama river catchment (Figure V-1). How does the Gavidia glacier dynamics compare to the Mucubají glacier? Is there any influence of the geomorphological features before in the deglaciation history? When did glacier fill the entire valley? When does it disappear? These questions remained open because of absence of deglaciation chronologies in the Gavidia valley. Original exposure ages range from 14.6±1.2 ka to 28.2±1.2 ka considering the Lago Argentino production rate (Kaplan et al., 2011). Updated exposure ages, considering the recent ^{10}Be production rate (Kelly et al., 2013), were recalculated (Table V-3). Updated ages are ~3 % older than the original values. These differences do not significantly impact the interpretations.

Deglaciation chronology in the Mérida Andes after cosmogenic ^{10}Be dating, (Gavidia valley, Venezuela)

Isandra Angel[a,c], Franck Audemard[b], Julien Carcaillet[a], Eduardo Carrillo[c], Christian Beck[d], Laurence Audin[e]

[a]ISTerre, Université de Grenoble 1, UMR CNRS 5275, F-38041 Grenoble, France

[b]Fundación Venezolana de Investigaciones Sismológicas, FUNVISIS, El Llanito, Caracas 1070, Venezuela

[c]Instituto de Ciencias de la Tierra, Universidad Central de Venezuela, Apdo. 3805, Caracas 1010-A, Venezuela

[d]ISTerre, Université de Savoie, UMR CNRS 5275 F-73376 Le Bourget-du-Lac, France

[e]ISTerre, IRD, Université de Grenoble 1, F-38041. France

Corresponding author

Isandra Angel
ISTerre

1381 rue de la Piscine,
38400 Saint Martin d'Hères
France

Tel: 33 (0)4 76 63 59 30
Fax: 33 (0)4 76 63 52 52

E-mail Address: iangel_ceballos@yahoo.com

Abstract

Understanding the timing of the tropical glaciations in the Northern Andes, has important implications for deciphering the regional-scale climate change during the last glacial cycle. In the Venezuelan Andes the last glaciation (Mérida Glaciation) is poorly reconstructed because of limited chronological data. Despite well preserved glacial landforms are located between 2600 and 4978 m a.s.l. This paper presents 24 exposure ages from glacial landforms mainly sampled in the Gavidia valley. Exposure ages were obtained based on terrestrial cosmogenic ^{10}Be exposure dating. Results indicate deglaciation began between ~21 ka-16.5 ka and the full deglaciation occurred at ~ 16 ka. The glacier retreated during two distinct phases. The oldest one occurred since the LGM until middle OtD or the local climate event El Caballo Stadial. The youngest phase occurred at ages younger than ~16.5 ka.

Asynchronous deglaciation histories in the Mérida Andes post LGM were observed. This is based on comparisons with other deglaciation histories of the area. This behavior is related in this study to different local paleoclimate conditions, valley orientation, insolation and catchments steepness.

Keywords

Terrestrial cosmogenic nuclides dating, TCN, cosmogenic dating, glacial landforms, Andes Mérida, Venezuela. Pleistocene, Late Glacial, LGM

1. Introduction

Glaciers studies in the Mérida Andes mountains date from the beginning of the XIXth century (Sievers, 1885 and Goering, 1962). Jahn (1912, 1925 and 1931) made the first planimetric measures for the existent glaciers. Then, a large and detailed bibliographic compilation about glaciological observations was made by Schubert (e.g. 1972; 1974; 1980; 1980a; 1992 and 1998). From Last Glacial Maximum (LGM) and the middle of XX century, glacier covering were reduced from around 200 km^2 (Schubert y Clapperton, 1990) to 10 km^2 (Schubert, 1992). Finally, glacier surface was reduced from 0.33 km^2 during in 2008 (Carrillo and Yépez, 2008) to 0.017 km^2 in 2011 (Braun and Bezada 2013).

Deglaciation studies of tropical former glaciers allow improving future climatic projections. Deglaciation studies in the tropical Andes are mainly developed in the Peruvian, Bolivian or Ecuadorian Andes. Despite well preserved glacial landforms in the Mérida Andes are also present. In this area, deglaciation chronologies are not regionally uniform and data are too scattered to reconstruct a more detailed deglaciation history. First geochronological studies were based on radiocarbon chronology (Schubert, 1970; Salgado-Laboriau and Schubert, 1977; Schubert and Rinaldi, 1987; Rull 1998; Mahaney et al., 2001; Dirszowsky et al., 2005; Stansell et al., 2005; Mahaney et al., 2007 and Carrillo et al., 2008), Thermoluminescence (TL), (Schubert and Vaz, 1987 and Bezada, 1989), Optically Stimulated Luminescence (OSL, Mahaney et al., 2000) and more recently, Terrestrial Cosmogenic Nuclide (TCN) dating (Wesnousky et al., 2012; Angel et al., 2013; Carcaillet et al., 2013 and Guzmán et al., 2013).

We propose here a new glacial chronology based on 24 new TCN ages from the Gavidia valley. We aim to precise (i) the timing of the last deglaciation in the Gavidia valley, (ii) the comparison with other deglaciation histories in the MA maily based on ^{10}Be cosmonuclide dating and, (iii) the comparison with global, regional and local paleoclimate records.

2. Regional setting

2.1 Geologic, geomorphic and tectonic settings

The Mérida Andes (MA) cordillera is located in the west of Venezuela (Fig. 1) and appears to be the northern topographic extension of the Eastern Cordillera of Colombia. Trending ~N45°, the cordillera extends over 400 km and reaches a maximum elevation of 4978 m asl (meter above sea level) at the Pico Bolívar. Its orogenesis is strongly connected to the geodynamic interaction of the Panamá Arc, Caribbean and the South American plates. Also other minor continental blocks are connected (Taboada et al., 2000; Audemard and Audemard, 2002; Bermudez, 2009; Monod et al., 2010). The present MA mountain build up is a direct consequence of the oblique convergence between the Maracaibo Triangular Block and the South American Plate (Colletta et al., 1997; Audemard and Audemard, 2002).

Tectonic markers attesting the ongoing growth of the topography are (Audemard, 2003): a) the axial valleys that display well-preserved Quaternary staircase terrace systems. Terraces have more than 500 m of vertical offset between the oldest terrace and present river beds. b) Rivers cutting across the structural grain of the chain show very distinct transverse “wine cup” profiles. Finally, c) synorogenic mollasic deposits along both flanks of the chain deposited in flexural basins, whose thicknesses reach 8 and 3 km on the northwest and southeast of the MA, respectively. Quaternary uplift of the MA may be attributed to thrust faulting and folding along the margins of the range (e.g., Audemard and Audemard, 2002). Uplift rates in the MA were estimated based on: a) the depths of formation of the igneous and metamorphic rocks outcropping at the highest summits of the chain (Uplift rate ~2–5 mm/a) b) boulders in a faulted alluvial fan along the Northwestern foothills (Uplift rate 1.7-0.7 mm/a, Wesnousky et al., 2012) and, c) incision rate of the Santo Domingo river in fluvial terraces from the Southeastern flank (uplift rate ~1.1 mm/a, Guzmán et al., 2013).

Numerous glacial landforms were described since the 19th century, mainly moraines, glacier cirques, glacier valleys, glacier lakes and paraglacial sediment deposits (Sievers, 1885, Jahn 1912, 1925; Schubert, 1970, 1974; Schubert and Valastro, 1974; Schubert and Rinaldi, 1987; Bezada, 1989, Schubert and Clapperton, 1990). Tectonic control in the glacial landforms has been extensively studied in this region where current deformation is mainly accommodated by the Boconó fault (Audemard, 2003). This

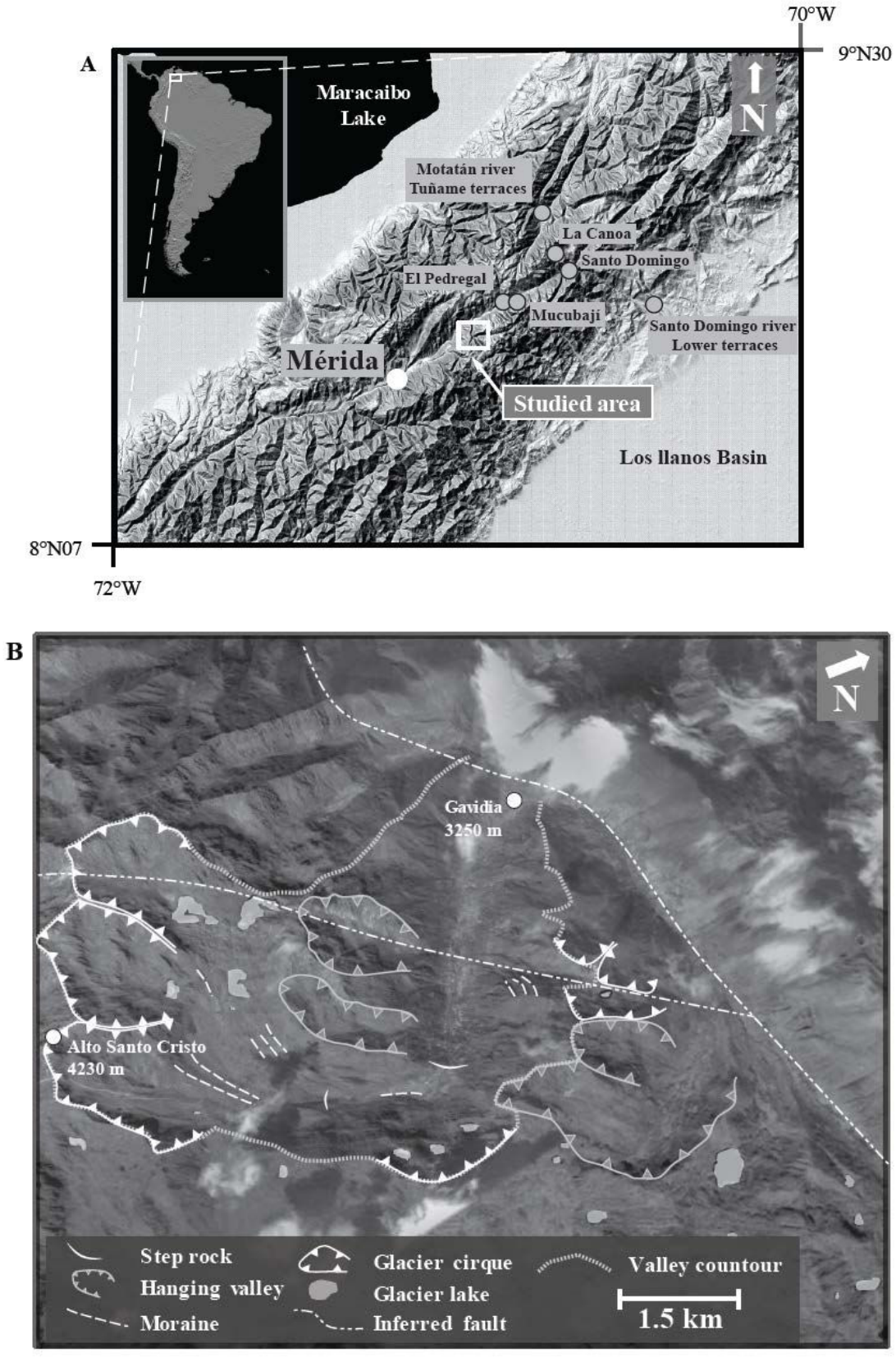

Figure 1. A) Digital shaded-relief map of the central Mérida Andes. The dots indicate location cited in the study (see text for details) B) Aerial photography (Google earth,

2014a) of the Gavidia valley with main geomorphological landforms and valley contours.

structure is a NE–SW trending, dextral fault that extends for about 500 km down the backbone of the MA (Fig. 1). It runs slightly oblique to the MA chain axis and bounds the Caribbean Coast range of northern Venezuela on its western flank. Quaternary tectonic rates range from 3 to 14 mm/a (Audemard, 2003). Between 5–9 mm/a based on the Mucubají valley, Los Zerpa and La Victoria moraines shifts (Schubert, 1980a; Soulas, 1985; Soulas et al., 1986), between 2.3–3.0 mm/a based on El Desecho moraine study (Audemard et al., 1999) and between <5.5 to 6.5 mm/a based on right-lateral offset of La Victoria and Los Zerpa moraines (Wesnousky et al., 2012).

2.1.1 Geomorphic description:

The Gavidia valley is located in the Sierra Nevada de Mérida, in the Venezuelan Andes (Fig. 1). It is a postglacial u-shaped valley with the headwall at Pico Alto Santo Cristo (4230 m). This area is deformed by two different inferred faults (Fig. 1B). The rock lithology is dominated by quartz gneiss from the Iglesias Complex (Hackley et al., 2005). Foliation and glacier striations are easily recognizable and discernable on large bedrock surfaces (Fig. 2A). The valley bottom exposes numerous striated and polished surfaces (roches moutonnées), although moraine development is not as evident as those described in other nearby glacier valleys. Dispersed polished surfaces appear along the valley side-walls (Fig. 2). Finally, the valley profile can be separated in two main areas:

- Low part (~3250-~3600 m a.s.l) has a NW-SE orientation and stretches for about 4 km length with frequent roches moutonnées (Fig. 2). The valley exhibits a < 5° dipping slope, as well as perpendicular hanging valleys (Fig. 1B). A ~40 m high step crossing the valley defines the upper limit of this part, close to sample GA-1207 (Fig. 1).

- In the high part (~3600-~4200 m a.s.l), the valley is NE-SW orientation with ~5 km length with an average slopes ranging between 3-7°. The highest part is mainly filled by gelifract deposits. In this upper area is under the influence of two glacier cirques (Fig.1B). Small moraine developments are found with ridges <10 m high. A glacier valley step of ~100 m high is evidenced close to sample GA-1212 (Fig.1B).

2.1 Paleoclimatic setting

Quaternary climate studies in the MA are based on analysis of lacustrine, fluvial, glacial deposits and paleosols (e.g. Schubert, 1974; Schubert and Valastro, 1980a; Salgado Labouriau, 1984; Bradley et al., 1985; Salgado-Labouriau, 1989; Weingarten , 1990; Yuretich, 1991; Salgado-Labouriau et al., 1992; Rull, 1995; Mahaney et al., 2000; Dirszowsky, 2005; Rull et al., 2005; Stansell et al., 2005; Mahaney et al., 2007; Carrillo et al., 2008; Rull et al., 2010; Stansell et al., 2010). Influence of glaciations in the central MA is mainly evidenced from two moraine complexes mapped between 2600-2800 m and 2900-3500 m. Moraines complexes were observed in Páramo de La Culata, Páramo de Piedras Blancas and Sierra de Santo Domingo. These two complexes were first pointed out by Royo and Gómez (1959) and later assigned to the Early and Late Mérida Glaciation respectively (Schubert, 1970 and 1974). Early Mérida Glaciation is poorly constrained, only few chronological data are available and ages range between ~60 and ~90 ka (Mahaney et al., 2000; Mahaney et al., 2001; Dirszowsky et al., 2005; Mahaney et al., 2010; Mahaney et al., 2011). Late Mérida Glaciation (Late Wisconsin) is better constrained and range between 25-13 ka (Schubert and Clapperton, 1990). Last one includes the Last Glacial Maximum (LGM) between 22.75 and 19.96 Cal ka BP (Schubert and Rinaldi, 1987).

Paleoclimate information before the Early Mérida glaciation is not extensively available. Sparse evidences of glacial deposition prior to Mérida Glaciation have been observed. Between the Early and the Late Mérida Glaciation were stablished interstadial conditions. These conditions were stablished based on sedimentological studies of 8 m record of predominantly lacustrine material from the PED5 section (Fig. 1A) (Dirszowsky et al., 2005; Rull, 2005). Warmer and wetter climate conditions were also interpreted during the same period from alluvial terraces analysis: 1) A terrace in the valley of Motatán river with peat layers dated (^{14}C on wood) between 50.6 and 33.7 ^{14}C ka BP (Schubert and Valastro, 1980; Schubert and Vivas, 1993) and, 2) Terraces from the lower part of the Santo Domingo river (Fig. 1A) with ages ranging between 65 and 22 ka (Guzmán et al., 2013). OSL ages between 31–26 ka from sandy silt overlain by glacially deformed sand, extend the record of interstadial conditions to the immediate onset of the Late Mérida Stadial (ca. 25 ka). These ages were determined on the study of RF3 section (2800 m a.s.l.) in La Canoa valley at Pueblo Llano (Fig. 1A) (Schubert and Clapperton, 1990).

Modern equilibrium line altitudes (ELA) are estimated between 4880 and 4470 m a.s.l. During the LGM, ELAs were 850 to 1420 m lower than the present. Local LGM temperatures were at least 8.8±2°C cooler than today, based on a combined energy and mass-balance equation to account for an ELA lowering (Stansell et al., 2007). In the Mucubají valley LGM is related to the frontal moraine at an exposure age of 18.14 ± 2.11 ka (weighted average, Carcaillet et al., 2013).

El Caballo Stadial, a cold period dated at 16.5±0.3 ka BP was identified based on pollen content of fluvioglacial sediments from Mesa del Caballo section. Temperatures were around 7°C lower than today (Rull, 1998). Local Last Glacial Maximum (LLGM) established for Sierra Nevada at 16.7±1.4 ka and from Sierra del Norte at 15.2±0.9 ka could be related to this period (Wesnousky et al., 2012). In Los Zerpa and La Victoria moraines, recalculated ages and addition of new samples analyses indicate weighted average age of the abandonment 14.5 ± 0.8 ka and 13.5 ± 0.7, respectively. In this scenario, Los Zerpa moraines formation was related to the Younger Dryas (Carcaillet et al., 2013).

Stansell et al. (2005) concluded that in Sierra del Norte, glaciers had significantly retreated by 15.70 ka BP. Then, several minor glacial advances and retreats between 14.85 and 13.83 ka BP also happened. However, authors do not specify how long glaciers retreat. A moraine inset into the former laterofrontal moraines of La Culata (Sierra del Norte) was interpreted as a small Late Glacial readvance at weighted average exposure age of 14.1±1.0 ka (Wesnousky et al., 2012). In Sierra Nevada, records indicate initial glacial retreat at 14.24 ka BP (Stansell et al., 2005). However, TCN dating at least indicates an early deglaciation at 18.14 ± 2.11 ka, based on weighted average exposure age of the Mucubají terminal moraine (Carcaillet et al., 2013).

Based on paleoecological analysis of the Late Quaternary terrace from Mucubají valley, Salgado-Labouriau and Schubert (1977) defined Mucubají Cold phase at 12.65 ka BP. An average temperature 2.9°C lower than current temperature was inferred during this period. Rull et al. (2005, 2010) relate this to the Younger Dryas (YD) advance, based on pollen analysis from Laguna Verde Alta between 12.60 and 11.00 ka BP. Whereas in Laguna Los Anteojos (Sierra Nevada) based on geochemical and sedimentological analyses was determined between 12.86 and 11.65 ka BP. Temperature decline between

2.5 and 3.8 ºC (Stansell et al., 2010). Results show that glaciers advanced at ~12.85 ka BP. Glaciers reached their maximum extent at ~12.65 ka BP. Then glaciers retreated until complete deglaciation of the watershed at ~11.75 ka BP.

During the YD, ELA values were 360 to 480 m lower than the present (Stansell et al., 2010). In the Humboldt Massif, till and paraglacial outwash deposits underlying peats, provide maximum limiting ages for the late Pleistocene glacier advances. Advance happened at 12.4 ka (Mahaney et al., 2008). Carrillo et al. (2008) determined from magnetic susceptibility record in the Mucubají core sediment, a cold climate condition during the YD (~11.6 ka- ~12.8 ka BP). Also abrupt warm climate conditions were determined at the onset of the Holocene (~11.6 ka BP).

Pollen records indicate that vegetation and climate have remained similar to today through most of the Holocene (Salgado-Labouriau et al., 1988, 1992; Rull, 1999). However, some minor cold events occurred at 6.0–5.3 ^{14}C ka BP (La Culata cold/dry phase; Salgado-Labouriau and Schubert, 1976). Also occurred within the XI to XIV centuries named "Piedras Blancas cold phase" and assigned to the Little Ice Age (LIA) (Rull et al., 1987; Salgado-Labouriau, 1989). Moreover, relatively warm conditions occurring 9.4–6.3 and 3.6–2.5 ka BP (Miranda warm phases; Salgado- Labouriau et al., 1988; Schubert and Vivas, 1993).

2.2 Present-day climatic conditions

The climate of the northern tropics is mainly controlled by the Intertropical Convergence Zone (ITCZ). It is highly dependent on the seasonal cycle of solar declination. Average temperature in the MA varies little seasonally, but diurnal temperature fluctuations may be as much as 20°C (Schubert and Clapperton, 1990). These temperature variations are controlled by insolation and cloudiness factors (Monasterios and Reyes, 1980).

Moisture is predominantly derived from evaporation over the tropical Atlantic and evapotranspiration from the Orinoco River Basin (Pulwarty et al., 1998). Then, moisture is advected to the Andes by easterly trade winds. Also a modern climate data from the MA demonstrate the strong influence of equatorial Pacific Sea Surface Temperature

(SST, Polissar et al., 2013). Precipitation is highly seasonal, with a maximum during the boreal summer and minimum during winter. At high elevation, precipitation patterns are also affected by orographic controls and local mountain circulation systems (Pulwarty et al., 1998).

Climate in the MA is also influenced by surrounding Maracaibo, Los Llanos and Lara-Falcón basins (NE to the Maracaibo basin) (Monasterio y Reyes, 1980). The NE area is under the influence of the semi-arid Lara-Falcón basin. This area is characterized by a bimodal rainfall pattern and low rainfall values (e.g. Cende 653 mm). Los Llanos basin mainly influences the southern MA hillsides climate. This climate is characterized by an unimodal rainfall pattern and medium rainfall values (e.g. Mesitas 840 mm). Northernmost of the MA is characterized by a bimodal rainfall pattern originate from the Maracaibo Lake basin. Rainfall values could be higher than 1000 mm in this area (e.g. La Culata) (Monasterio y Reyes, 1980).

3. Materials and methods

3.1 ^{10}Be nuclide dating implications on deglaciation studies

Beryllium-10 (^{10}Be) is a cosmogenic nuclide isotope (Half-life 1.36+/- 0.07 Ma) produced by the interaction between cosmic rays and chemical targets of the Earth environment. The *in-situ* produced ^{10}Be is formed in the first meters of the lithosphere (Terrestrial Cosmogenic Nuclide TCN). And thus constitutes a suitable tool for dating exposure time of rock surfaces. Glaciers create landforms that, after deglaciation, are exposed to cosmic rays. TCN geochronology is thus suitable to date the onset of the exposure after complete ice melting. Because of the potential post-deglaciation processes that could erode the glacial surface, exposure ages are assumed as minimum ages (Nishiizumi et al., 1989; Briner and Swanson, 1998; Siame, 2000; Gosse and Phillips, 2001; Dunai, 2010; Balco, 2011).

Several methods have been used to date glacier dynamics, among them the radiocarbon determinations of organic materials. Two main limitations derive from this technique. A) Glaciers advances do not create organic material, meaning that radiocarbon dates provide glacial landforms bracketing ages only (Balco, 2011). B) Only a minority of

glaciers leave deposits that can be radiocarbon dated, due to the scarce vegetation in the glaciers environments (Balco, 2011).

In contrast to moraines, where eroded boulders may result in dispersed ages; bedrock surfaces are largely insensitive to postglacial disturbance. Therefore, these geomorphic markers provide a more accurate age control. However, insufficient erosion (less than 2-3 m) will not fully remove the inherited nuclide component in pre exposed bedrock. This implies overestimated exposure ages not related to the glacial retreat age (Gosse et al., 1995; Guido et al., 2007 and Balco, 2011).

In details, exposure dating of boulders located on the top crest of the terminal moraine represents the single exposure history of each individual boulder (Ivy-Ochs et al., 2007). The integrated population of ages, however, indicates the averaged age of final moraine stabilization, when all boulders became finally embedded in the moraine matrix (Putkonen and Swanson, 2003). We consider that boulders sampled in the crest of frontal moraines will indicate the beginning of the glacier front retreat. Meanwhile boulders sampled from the crest of lateral moraines will indicate the beginning of the glacier thinning.

In this paper, ages results are noted as exposure ages in ka, indicating deglaciation time or abandonment age. Also because origins of terminal moraines make possible to establish a relationship with maximum glacier advances (e.g. Winkler, 2005; Schaefer et al., 2009; Kaplan et al., 2010, Bickerton and Matthews, 1992, 1993; Matthews, 2005; Shakesby et al., 2006, Schaefer et al., 2009, Richards, 2000, Carcaillet et al., 2103., Wesnousky et al., 2011, Kirkbride and Winkler, 2012). In this paper, maximum glacier advances are related to the position of terminal or lateral-terminal moraines.

3.2 Samples collection

Samples were collected from the valley bottom and the valley side-wall (Fig. 2). All samples were collected in the Gavidia valley. Only the lower one (GA-1201) was sampled in the northernmost of the area (Fig. 2). Samples were collected on striated and/or polished rocks emerging from the surface, in order to minimize a potential late coverage by superficial deposits.

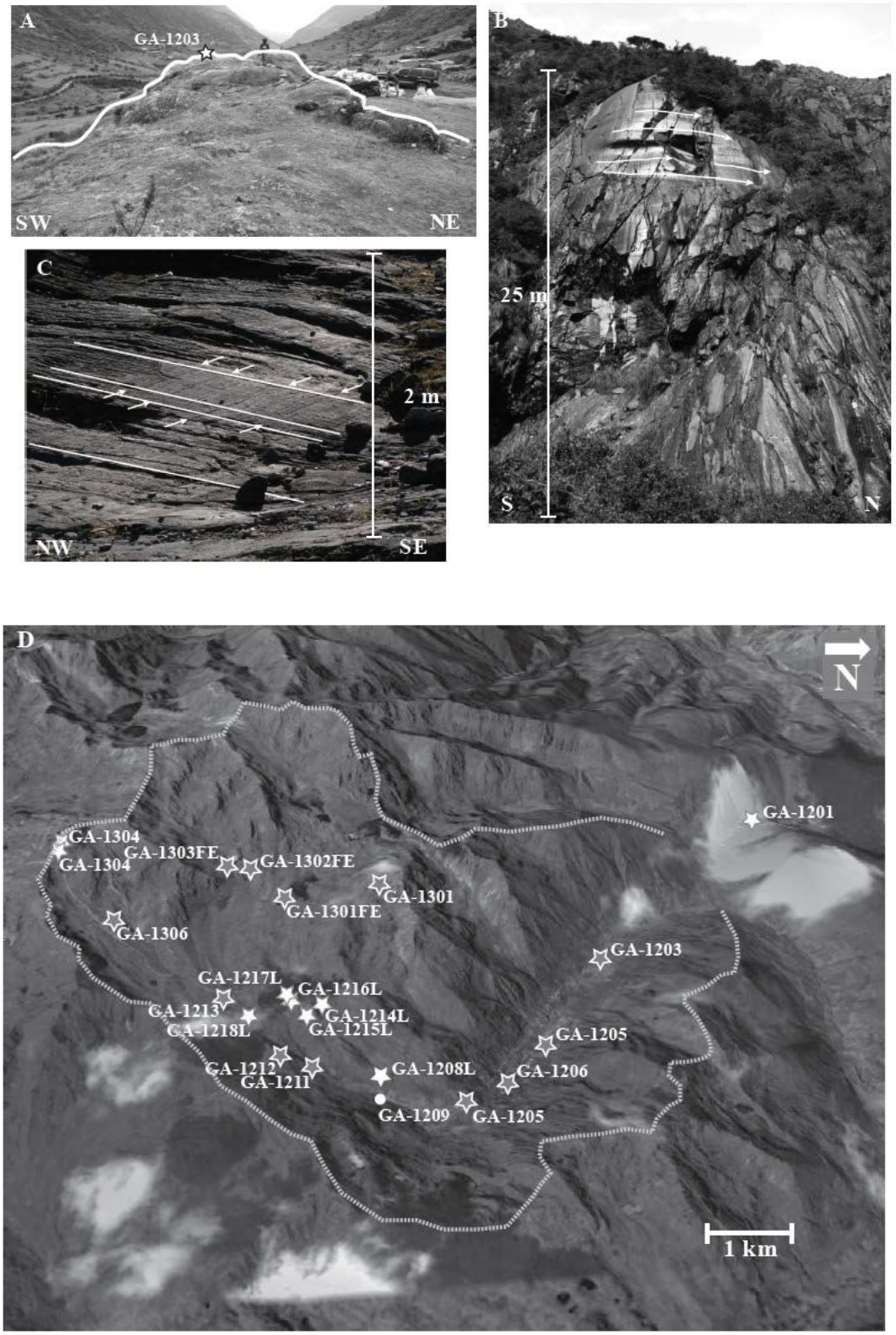

Figure 2. Examples of glacial landforms. A) Striated bedrock in the axis of the Gavidia Valley, (GA-1203 location). B) Sub-vertical polished surface in the northernmost of the Gavidia valley (close to GA-1201). Glacial striations directions are indicated by white

arrows C) Difference in orientation between glacier striation (white arrows) and foliation (white lines) on a sub horizontal glacial surface. D) Sample position in the Gavidia valley (Google earth, 2014b). White stars are polished surface, Grey stars are roches moutonnées, and white dots are moraine boulders.

TCN ^{10}Be chemical targets were prepared at the cosmogenic laboratory at ISTerre, France, following procedures adapted from Brown et al. (1991) and Merchel and Herpers (1999). Measurements were carried out at the French National AMS facility (Accelerator Mass Spectrometry) at ASTER in Aix-en-Provence. Ages were calculated using the online Cronus calculator (Balco et al., 2008). Recent reference ^{10}Be production rate (i.e., production rates by neutron spallation appropriate for sea-level, high-latitude sites SLHL) were determined in the tropical Andes; 3.78±0.09 at.g^{-1}.yr^{-1} when erosion is 0 cm/yr (Kelly et al., 2013). In this study we used Lago Argentino calibration in Cronus online calculator with a ^{10}Be production rate of 3.81±0.13 at.g^{-1}.yr^{-1} (Kaplan et al., 2011). This production rate was used because there are no significant differences with Kelly et al. (2013) value and calibration was available in Cronus online calculator. Ages were computed using the scaling scheme of time dependent model from Lal (1991) modified by Stone (2000). This scaling scheme was selected because it considers the geomagnetic field variation (Balco et al., 2008). This is important in the present study because the magnetic modulation has a particularly critical effect in the vicinity of the magnetic Equator where the samples were collected.

Long-term erosion rates of boulders in the tropical Andes have been reported between 0.3–0.5 m.Myr^{-1} (Smith et al., 2005) and 0.45 m.Myr^{-1} (Kelly et al., 2013). Comparison of extreme exposure ages with 0 and 4.5 m.Myr^{-1} give not significant differences at the "post-LGM scale". For this reason and because the clear observation of the striations and polished surfaces on sampled bedrock, erosion rate of 0 m.Myr^{-1} was considered for calculations. Based on valley side-wall samples GA-1208L and GA-1216L, glacier thickness could be more than 50-100 m. This glacier thickness should be enough to avoid TCN production during the last climatic cycle (i.e. during the presence of glacier tongue).

4. Results

Twenty-four rock samples were collected for TCN investigations in order to calculate exposure ages which represent time since the sampled landform was ice-free. ^{10}Be concentrations in the Gavidia valley range between 2.25 ± 0.08 (GA-1201) and 5.09 ± 0.16 (GA-1214) $.10^5$ atoms per gram of quartz ($at.g^{-1}$) (Table 1). Once computed as exposure ages, results range between 13.98 ± 1.19 and 27.22 ± 1.32 ka (Table 1). Table 1 summarizes exposure ages and input data used in the Cronus online calculator 2.2 (Balco et al., 2008). Analytical uncertainties are in general lower than 10% with only GA-1205 around 14% (Table 1).

Ages results could be divided in two groups, ages younger and older than ~20 ka (Fig. 3). Exposure ages of polished surfaces from the valley side-walls, are older than those from the valley bottom (Fig. 3). Two exceptions, GA-1214L (16.59±0.64 ka) and GA-1215L (16.06±0.63 ka) are significant different and younger. These landforms could be affected by post deglaciation processes (covered by sediments or focused limited erosion). For that, GA-1214L and GA-1215L were considered as outliers and will not be considered to in the following. GA-1218L (27.22±1.32 ka) is the oldest TCN age. However, it location at low elevation compared to GA-1216L and GA-1217L (Table 1) suggests a significant content of ^{10}Be inherited. This sample was thus considered as outlier and will not be considered to in the following.

5. Discussion

5.1 Deglaciation history in the Gavidia valley:

The valley bottom dating results indicate a correlation with elevation (Fig.2). However, higher altitude exposure ages (including the glacier cirque and surroundings) indicate no significant variations (Fig. 3). This suggests that all the target glaciers landforms were abandoned during the Late Mérida Glaciation.

Exposure ages issued from bedrock samples should give more accurate deglaciation ages compared to exposure ages issued from moraine boulders (Gosse et al., 1995; Guido et al., 2007 and Balco, 2011). However, it is difficult to consider these ages as representing the maximum glacier advance because of the absence of terminal or lateral terminal-moraines. Based on exposure ages from GA-1201, the maximum glacier advance period is bracketed between ~21 ka and ~16.5 ka. The homogeneous data set

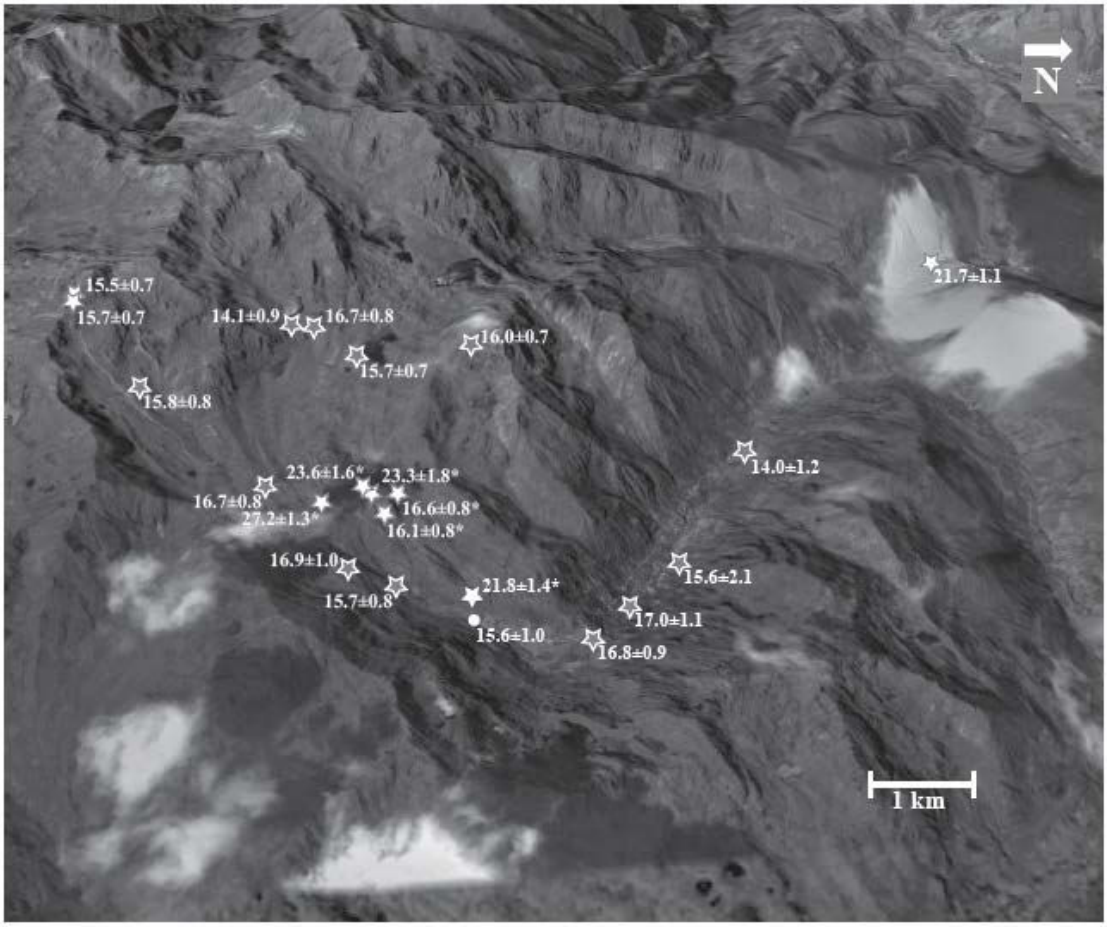

Figure 3. *In-situ* produced ^{10}Be dating of the Gavidia valley (Google earth, 2014b). * identifies to samples collected on the valley side-walls (see text for details).

obtained in the glacier cirque and surroundings suggests a complete deglaciation around ~16 ka (Fig. 3). Because of similar valley orientation, average altitudes and proximity of other higher glacier cirques presents in this area. Those related to the samples GA-1302 FE and GA-1303 FE, Fig. 3, Table 1), this area have possibly been ice free during the same period.

The valley bottom topography does not show significant slope variations. Considering the horizontal ice retreat, deglaciation happened in two phases. The first one happened from ~21 ka to ~16.5 ka; it yields an average glacier retreat rate of ~0.26 km/ka. While the second one happened after ~16.5 ka, it yields an average retreat rate of ~4.70 km/ka.

Side-wall valley samples (GA-1208L and GA-1216L) indicate a glacier maximum thickness ranging between 50 m and 100 m. Similar to thickness estimations in the

Table 1. TCN results of the Gavidia valley. (a) The topographic scaling factor has been calculated following the method of Dunne et al. (1999). (b) AMS analyses have been carried out at the French AMS facility ASTER. (c) Beryllium 10 concentrations were calibrated against NIST Standard Reference Material 4325 using its certified $^{10}Be/^{9}Be$ ratio of 2.79 10^{-11} and a ^{10}Be half life of 1.387 ± 0.012 10^{6} yr (Korschinek et al., 2009; Chmeleff et al., 2010). Results have been corrected from the chemical blank ($^{10}Be/\ ^{9}Be_{blank}$ = 2.625 ± 0.32 × 10^{-15}). Propagated uncertainties include counting statistics, a conservative estimate of 1% for instrumental variability, the uncertainty of the standard deviation and chemical blank. (d) Ages have been computed with the Cronus Calculator (Balco et al., 2008) using the time-dependent production rate of Lal (1991) modified by Stone (2000). (d) Internal uncertainties consider the analytical uncertainties, while the external uncertainties include 3.4% uncertainty in the production rate (Kaplan et al., 2011) and 8% uncertainty in the ^{10}Be decay constant. In the Results section, results are presented with the external uncertainties. No correction for snow or other coverage have been taken into account, the sample thickness correction has been calculated with a 2.7 density factor. *Moraine boulder GA-1209 with dimensions in meters of 1.5x1.8x1.2.

Samples	Latitude	Longitude	Elevation	Site information	Sample Thickness	Shielding factor[a]	Scaled production rates		$^{10}Be/^{9}Be$ blank corrected[b]	^{10} Be concentraction[c]		Ages[d, e]		
							Spallations	Muons		Value	Uncertainty	Value	External uncertainty	Internal uncertainty
	°N	°W	M		cm		atoms/g/yr		x 10^{-13}	10^{3} atoms/gQtz/yr		ka		
GA-1201	8.694	70.940	3198	Polished rock	3	0.488	8.88	0.480	2.04	225.00	8.31	21.679	1.085	0.899
GA-1203	8.674	70.919	3374	Roche moutonnée	1	0.942	19.10	0.510	1.90	294.39	22.92	13.977	1.188	1.178
GA-1205	8.667	70.912	3428	Roche moutonnée	1.5	0.927	19.24	0.515	2.48	334.48	43.33	15.640	2.096	2.207
GA-1206	8.663	70.909	3494	Roche moutonnée	2	0.920	19.66	0.523	4.22	375.30	19.66	17.025	1.062	0.983
GA-1207	8.662	70.906	3568	Roche moutonnée	2	0.989	21.93	0.533	4.17	410.76	18.19	16.752	0.933	0.817
GA-1208 L	8.654	70.909	3635	Polished rock (side-wall valley)	6	0.543	12.15	0.535	2.23	306.78	16.78	21.760	1.402	1.344
GA-1209	8.653	70.908	3592	Boulder in a lateral moraine	1.5	0.934	21.05	0.539	3.24	364.73	19.10	15.589	0.972	0.892
GA-1211	8.648	70.910	3654	Roche moutonnée	3	0.973	22.33	0.543	3.83	388.66	14.74	15.664	0.794	0.650
GA-1212	8.646	70.911	3737	Roche moutonnée	3.5	0.829	19.73	0.553	2.64	374.10	18.62	16.870	1.015	0.926
GA-1213	8.641	70.916	3810	Roche moutonnée	2	0.955	23.85	0.569	4.21	444.47	15.66	16.658	0.812	0.647
GA-1214 L	8.648	70.915	3884	Polished rock (side-wall valley)	5	0.999	25.21	0.571	4.80	467.38	16.45	16.587	0.808	0.644
GA-1215 L	8.648	70.916	3870	Polished rock (side-wall valley)	5	0.985	24.59	0.567	4.21	440.599	15.77	16.059	0.789	0.632
GA-1216 L	8.647	70.915	3840	Polished rock	2.3	0.523	13.22	0.572	1.88	363.55	24.36	23.337	1.757	1.790

				(side-wall valley)										
GA-1217 L	8.647	70.915	3820	Polished rock (side-wall valley)	3.5	0.520	12.89	0.565	2.70	359.80	21.77	23.633	1.643	1.640
GA-1218 L	8.644	70.914	3805	Polished rock (side-wall valley)	2.5	0.524	13.00	0.566	4.44	426.25	14.71	27.221	1.316	1.101
GA - 1301FE	8.646	70.926	3909	Roche moutonnée	2	0.958	25.08	0.583	4.48	438.48	13.71	15.740	0.723	0.540
GA - 1302FE	8.643	70.930	3964	Roche moutonnée	3	0.922	24.59	0.588	4.46	459.75	14.62	16.717	0.774	0.587
GA - 1303FE	8.641	70.930	3929	Roche moutonnée	4.5	0.922	23.88	0.579	3.75	37.93	20.96	14.122	0.928	0.865
GA - 1301	8.647	70.924	3930	Roche moutonnée	4	0.995	25.88	0.580	4.23	461.34	14.75	16.032	0.744	0.563
GA - 1302	8.649	70.923	3964	Roche moutonnée	1	0.973	26.38	0.597	2.23	469.50	16.66	16.029	0.784	0.625
GA - 1303	8.655	70.927	4150	Roche moutonnée	5	0.992	28.36	0.611	6.13	507.51	15.91	16.071	0.739	0.555
GA - 1304	8.626	70.933	4208	Striated rock	5	0.984	28.88	0.619	5.30	499.87	15.51	15.549	0.713	0.531
GA - 1305	8.625	70.933	4197	Striated rock	2	0.985	29.49	0.628	6.26	509.09	15.89	15.699	0.713	0.533
GA - 1306	8.631	70.924	3945	Roche moutonnée	2.5	0.982	26.06	0.587	4.72	454.03	17.19	15.811	0.795	0.652

Mucubají valley post Last Glacial Maximum (LGM) (Carcaillet et al., 2013). Considering samples GA-1208L, GA-1216L, GA-1209 and GA-1212 vertical ice thinning can be estimated. Thinning rates range between 7 m/ka to 18 m/ka (Fig. 2). However, these estimations need to be taken as first order. More data is required to establish a convincing vertical ice retreat behavior. Horizontal ice retreat is more significant than the vertical ice thinning.

5.2 Comparing with other deglaciation histories in the Venezuelan Andes deduced from ^{10}Be nuclide dating. Different glaciers dynamics and potential driving mechanisms.

Thirty-seven exposure ages are recently published from different valleys from the central MA (Table 2). We recalculate with the same ^{10}Be production rate of 3.81±0.13 at g^{-1} yr^{-1} (Kaplan et al., 2011) and scaling scheme (Lal, 1991; Stone, 2000). Original ^{10}Be ages in the Mucubají valley were calculated using production rate of 4.39±0.37 atoms g^{-1} yr^{-1} (Carcaillet et al., 2013). This value is ~15% higher than Kaplan et al. (2011) and Kelly et al. (2013) values. The new calculation for the Mucubají valley data yield an overall ageing of ~15% than original values (Table 2). For La Culata moraine, the ^{10}Be ages are < ~10% than the original dataset of Wesnousky et al. (2012).

Considering our updated calculation, exposure ages range in the MA between 10.95±0.97 ka to 23.63±1.64 ka (Fig.4, Fig.5, Table 1, and Table 2). All the data correspond to an abandonment of the different glacial landforms during the Late Pleistocene. All the landforms studied are consequently related to the Late Mérida Glaciation. The youngest and oldest ages are also obtained in glacial landforms from the Sierra Nevada de Mérida (10.52±0.48 ka and 23.63±1.64 ka). These ages comes from the Mucubají and the Gavidia valleys, respectively (modified exposure age from Carcaillet et al., 2013 and this study).

Because some time lag could happen between maximum glacier advance and deglaciation. We make the hypothesis that the age of the maximum glacier advance is older than the age of terminal or lateral-terminal moraine abandonment. However, considering the sensitive response of tropical glaciers to climate changes (Kaser and Osmaston, 2002), we would expect a minimum time lag between glacier advance and landform deglaciation or abandonment.

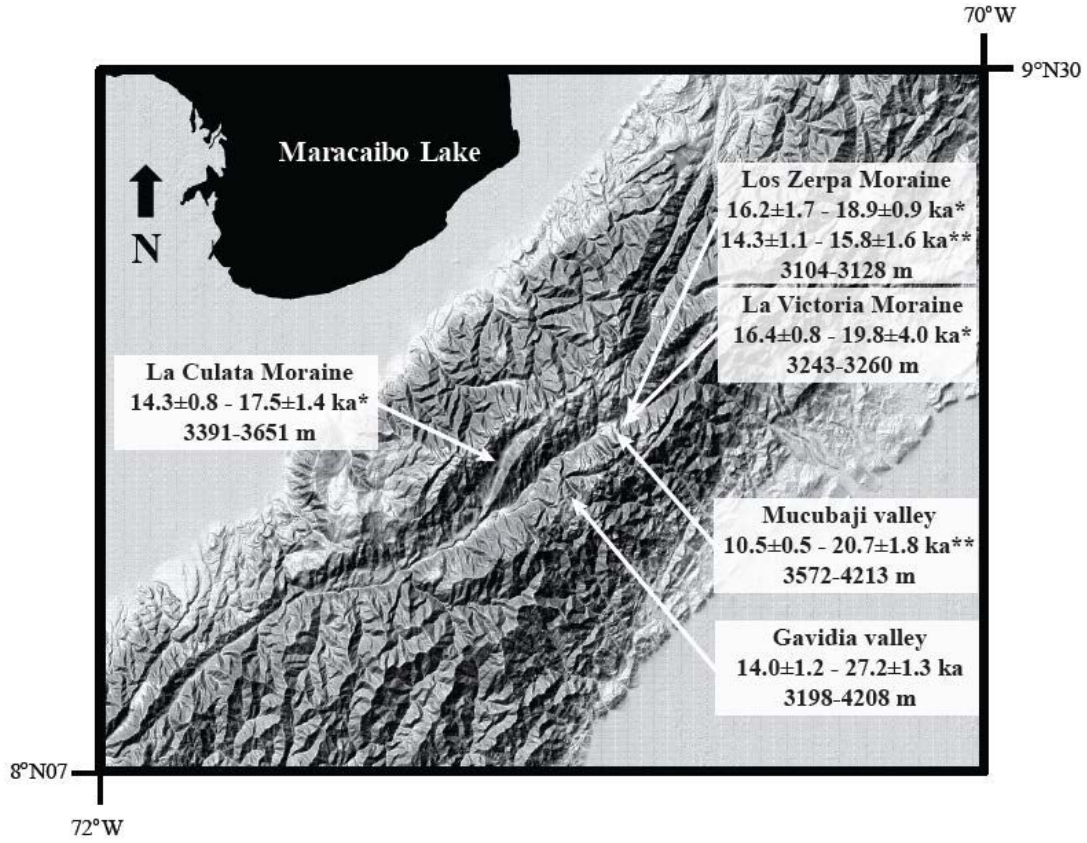

Figure 4. Published ^{10}Be ages distributions in the Venezuelan Andes. Ages were recalculated with Lago Argentino calibration (Kaplan et al., 2011) from previous works: ages with * correspond to Wesnousky et al. (2012) and ** correspond to, Carcaillet et al. (2013).

Concerning the Sierra Nevada, in the Gavidia valley, the maximum glacier advance happened between ~ 21 ka and ~ 16.5 ka. Meanwhile completely valley deglaciation occurred around 16 ka. In the NE part of the Gavidia valley, deglaciation began in the Mucubají valley at 20.66±1.79 ka. As suggested by a distal frontal ridge dated (located at ~3600 m a.s.l.; recalculated exposure age from Carcaillet et al., 2013). The former authors proposed the Mucubají glacier disappearance at ~11 ka. However, glacier activity has been estimated at ~6 ka based on peat bog radiocarbon ages (Stansell et al., 2005).

In the NE part of the Mucubají valley, updated exposure ages from La Victoria terminal moraine (located at ~ 3200 m a.s.l.) range from 16.37±0.76 to 19.75±4.00 ka (Table 2). These ages implying that the deglaciation starts at 17.16±0.71 ka (weighted average).

Table 2. ^{10}Be dating inventory of the Venezuelan Andes (Wesnousky et al., 2012; Carcaillet et al., 2013). (a) Modified ages correspond to recalculation using Lago Argentino production rate (Kaplan et al., 2011) and the scaling scheme model of Lal (1991) modified by Stone(2000).

Samples	Latitude	Longitude	Elevation	Sample information		Original ages (ka)	Modified ages (ka)[(a)]			Reference
							value	External uncertainty	Internal uncertainty	
	°N	°W	m	Sampled landforms	Location	ka	ka			
VEN1	8.7601	71.0516	3391	Boulder moraine	La Culata	15.9±0.8	17.06	1.00	0.90	Wesnousky et al., 2012
VEN3	8.7654	71.0477	3457	Boulder moraine	La Culata	15.4±0.7	16.61	0.89	0.76	Wesnousky et al., 2012
VEN4	8.7656	71.0476	3458	Boulder moraine	La Culata	14.2±0.4	15.38	0.65	0.43	Wesnousky et al., 2012
VEN5	8.7663	71.0471	3467	Boulder moraine	La Culata	14.4±0.6	15.63	0.82	0.76	Wesnousky et al., 2012
VEN6	8.7689	71.0457	3508	Boulder moraine	La Culata	16.2±0.6	17.39	0.88	0.73	Wesnousky et al., 2012
VEN7	8.7697	71.0467	3472	Boulder moraine	La Culata	14.3±0.7	15.52	0.91	0.81	Wesnousky et al., 2012
VEN8	8.7697	71.0466	3472	Boulder moraine	La Culata	13.1±0.6	14.27	0.82	0.72	Wesnousky et al., 2012
VEN9	8.7705	71.0466	3477	Boulder moraine	La Culata	13.2±0.5	14.38	0.75	0.62	Wesnousky et al., 2012
VEN11	8.7721	71.0464	3501	Boulder moraine	La Culata	15.4±0.7	16.61	0.93	0.82	Wesnousky et al., 2012
VEN12	8.7726	71.0463	3500	Boulder moraine	La Culata	14.7±0.7	15.96	0.94	0.85	Wesnousky et al., 2012
VEN13	8.7729	71.0393	3657	Boulder moraine	La Culata	14.2±0.5	15.38	0.76	0.61	Wesnousky et al., 2012
VEN14	8.7729	71.0395	3653	Boulder moraine	La Culata	16.3±1.2	17.52	1.42	1.43	Wesnousky et al., 2012
VEN15	8.7727	71.0400	3651	Boulder moraine	La Culata	14.7±0.7	15.89	0.96	0.87	Wesnousky et al., 2012
VEN19	8.8141	70.8006	3255	Boulder moraine	La Victoria	18.6±3.7	19.75	4.00	4.38	Wesnousky et al., 2012
VEN20	8.8142	70.8006	3258	Boulder moraine	La Victoria	16.9±1.0	18.07	1.17	1.10	Wesnousky et al., 2012
VEN21	8.8142	70.8010	3260	Boulder moraine	La Victoria	15.3±0.6	16.49	0.86	0.73	Wesnousky et al., 2012
VEN23	8.8139	70.7993	3243	Boulder moraine	La Victoria	15.1±0.5	16.37	0.76	0.58	Wesnousky et al., 2012
VEN25	8.8121	70.7881	3115	Boulder moraine	Los Zerpa	17.7±1.4	18.92	1.60	1.63	Wesnousky et al., 2012

VEN26	8.8120	70.7873	3104	Boulder moraine	Los Zerpa	15.0±1.6	16.20	1.74	1.80	Wesnousky et al., 2012
VEN27	8.8117	70.7875	3105	Boulder moraine	Los Zerpa	17.8±0.5	18.92	0.85	0.63	Wesnousky et al., 2012
VEN28	8.8118	70.7873	3106	Boulder moraine	Los Zerpa	16.9±0.9	18.20	1.10	1.01	Wesnousky et al., 2012
LZ09-01	8.81172	70.78837	3127	Boulder moraine	Los Zerpa	13.84±1.74	15.78	1.56	1.60	Carcaillet et al., 2013
LZ09-02	8.81168	70.78742	3113	Boulder moraine	Los Zerpa	12.48±1.39	14.33	1.14	1.17	Carcaillet et al., 2013
Mu09-01	8.80093	70.82794	3620	Boulder left side frontal moraine	Mucubaji	16.78±1.54	19.09	0.92	0.74	Carcaillet et al., 2013
Mu09-02	8.79535	70.8343	3589	Boulder frontal moraine crest	Mucubaji	18.14±2.11	20.66	1.79	1.85	Carcaillet et al., 2013
Mu09-03	8.79507	70.8267	3572	Boulder frontal moraine crest	Mucubaji	15.66±1.67	17.79	1.31	1.28	Carcaillet et al., 2013
Mu09-04	8.78741	70.82328	3607	Boulder frontal moraine crest	Mucubaji	13.27±1.20	15.19	0.69	0.51	Carcaillet et al., 2013
Mu09-05	8.78504	70.82292	3615	Boulder frontal moraine crest	Mucubaji	13.32±1.48	15.24	1.22	1.20	Carcaillet et al., 2013
Mu09-06	8.7852	70.82243	3620	Boulder frontal moraine crest	Mucubaji	15.96±1.80	18.14	1.49	1.50	Carcaillet et al., 2013
Mu09-07	8.77898	70.81973	3697	Striated bedrock	Mucubaji	13.84±1.32	15.78	0.88	0.76	Carcaillet et al., 2013
Mu09-08	8.7785	70.8189	3727	Striated bedrock	Mucubaji	14.20±1.34	16.17	0.86	0.73	Carcaillet et al., 2013
Mu09-10	8.76672	70.81287	4067	Striated bedrock	Mucubaji	9.08±0.82	10.52	0.48	0.36	Carcaillet et al., 2013
Mu09-11	8.76326	70.81187	4213	Moraine boulder	Mucubaji	10.63±0.96	12.30	0.56	0.41	Carcaillet et al., 2013
Mu09-12	8.76585	70.81214	4091	Striated bedrock	Mucubaji	9.48±1.11	10.95	0.97	0.97	Carcaillet et al., 2013
Mu09-13	8.76894	70.81635	3982	Moraine boulder	Mucubaji	9.73±0.88	11.23	0.52	0.40	Carcaillet et al., 2013
Mu09-14	8.77185	70.81516	3862	Moraine boulder	Mucubaji	9.93±1.16	11.46	1.01	1.01	Carcaillet et al., 2013
Mu09-15	8.77584	70.81613	3804	Striated bedrock	Mucubaji	12.86±1.57	14.75	1.38	1.40	Carcaillet et al., 2013

This is consistent with the exposure age of the neighbor Los Zerpa terminal moraine (located at ~3100 m) (17.57±0.52 ka weighted average, modified from Wesnousky et al., 2012; Carcaillet et al., 2013). La Victoria and Los Zerpas terminal moraines represent until present, the lowest post-LGM glacier advance in Sierra Nevada.

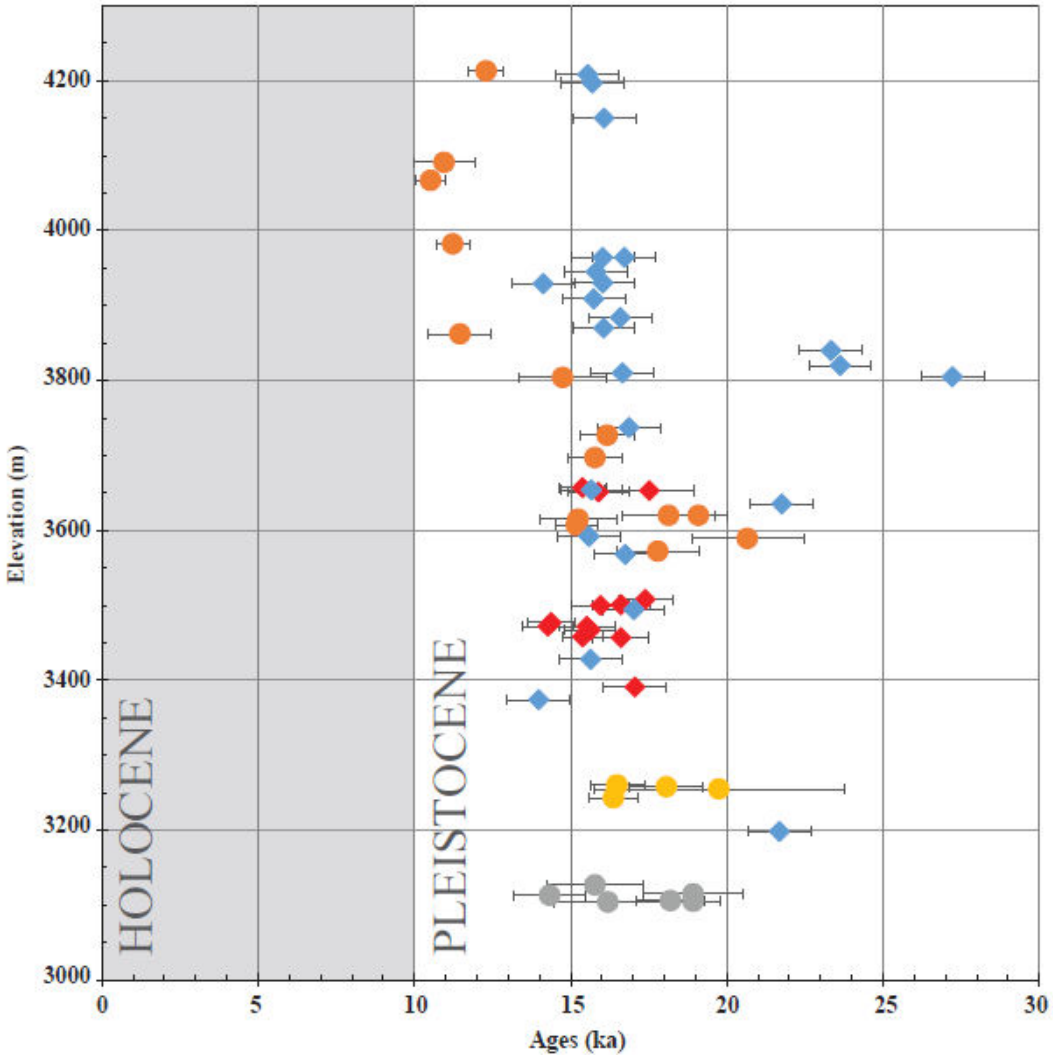

Figure 5. Altitudinal ages distribution of TCN dating in the Venezuelan Andes (This study, Wesnousky et al., 2013; Carcaillet et al., 2013). Blue and red diamonds are dating of the western side of the studied area (La Gavidia and La Culata valley respectively). Orange, yellow and grey dots are dating of the eastern part (Mucubají, La Victoria and Los Zerpa valley respectively).

In Sierra del Norte a deglaciation began at ~16 ka. Based on recalculated exposure ages from La Culata terminal moraine (located between ~ 3400-3500 m) (Wesnousky et al., 2012). This episode was related to La Victoria and Los Zerpa terminal moraines deglaciation.

Differences in local climate or topographic features of glacier catchments and former glacier features by itself (e.g. steepness, orientation, cloudiness, speed, insolation, hypsometry, precipitation, temperatures, etc.), could explain the observed different former glaciers behaviors (Paterson, 1994 in Bennett and Glasser, 2009; Barr and Lovell, 2014). Glacier spatial variability in the northern Sierra de Santo Domingo (includes Mucubají, Victoria and Zerpa glaciers) seems to be mainly driven by temperature differences (Stansell et al., 2007). This observation is based on LGM equilibrium line altitudes (ELA) and paleo-temperatures reconstructions. Paleoenvironmental records indicate regional drier conditions during the LGM (Bradbury et al., 1981; Bradley et al., 1985; Weingarten et al., 1991; Salgado-Labouriau et al., 1992). However, the gradient in ELA computations suggests also strong influence of local conditions, such as precipitation, cloud cover and valley aspect (Stansell et al., 2007).

Mucubají valley is formed by a lower flat sector (3550-3700 m a.s.l.) and an upper sector (3700-4600 m a.s.l.) with high slope (reaching ~20º). High steepness could contribute to a lower speed of glacier withdrawal than the one of the Gavidia valley (with slope values ranging between 3-7º). General valley topography may also influence the glacier dynamic. Gavidia is separated from the Chama valley by a narrow deep gorge whereas the Culata-Chama and Mucubají-Santo Domingo confluences are wider (Fig. 4). These topographical features may confer different atmospheric circulation which controls humidity, air temperature and rainfall. Insolation can be another strong playing factor. Faster extinction rates observed in the Gavidia valley could be explained by the different accumulation zone orientation (NE-SW orientation).

5.3 Correlation with global, regional and local paleoclimate data.

Gavidia valley exposure ages were compared with a global (i.e. $\delta^{18}O$ values in the GISP2; Stuiver et al., 1995), regional (i.e. Sea Surface Temperatures – SST - deduced

from Mg/Ca in sediment of the Cariaco Basin; Lea et al., 2003) and local paleoclimate proxies, extracted from proglacial sediments. Fluvioglacial terraces in the Paramo de La Culata, Mucubají or Miranda (Salgado-Laboriau and Schubert, 1976; Salgado-Laboriau, et al., 1977; Salgado-Laboriau, et al., 1988; Mahaney et al., 2008). Also glaciofluvial or glaciolacustrine sediments from Mesa del Caballo or El Pedregal fan complex (Schubert and Rinaldi, 1987, Rull, 1998, Rull, 2005, Dirszowsky et al., 2005, Mahaney et al., 2010). Paleosols (Mahaney et al., 2007) and lake sediments from the Sierra Nevada, Páramos Piedras Blancas and Agua Blanca (Rull et al., 2005, Stansell et al., 2005, Polissar et al., 2006, Rull et al., 2010, Stansell et al., 2014).

The maximum extension in the northernmost of the Gavidia glacier (~21 ka) correlates with negative values of $\delta^{18}O$ (Stuiver et al., 1995) and low SST (Fig.6). (Lea et al., 2003). At local scale, palynological analysis of Mesa del Caballo section confirms the cold conditions established during the LGM, between 19.96 ka and 22.75 ka (Schubert and Rinaldi, 1987).

The Oldest Dryas (OtD) was identified in the northern hemisphere as a cold period ranging between (~17.50 to ~14.60 cal ka BP) (Blunier et al., 1998). The OtD may have affected the northern South America between 17.50 to 17.00 cal ka BP, based on the SST record (Lea et al., 2003). In the MA a cold period was identified (called El Caballo Stadial) at 16.5±0.3 ka (Rull, 1998). With an estimated temperature 7°C lower than the present value (Fig.6). This cold episode was identified as the last cold event recorded in the Gavidia valley (Fig. 6). Here, the glacier drastically retreats even before the end of the OtD. This drastic retreat could be finally rather related to the end of the local El Caballo Stadial period.

For the Late Glacial, during the Younger Dryas (YD) is evidenced in GISP2 and SST records by significant drops of $\delta^{18}O$ and temperatures respectively (Fig.6). In the MA Salgado-Labouriau and Schubert (1977) defined a Mucubají phase with two stages ("Cold I" and "Warm"). Cold Mucubají phase I at 12.65 ka BP was defined based on paleoecological analysis of Mucubají valley terrace. This phase was related to YD (Rull et al., 2005; 2010). Based on magnetic susceptibility in sediment core from Mucubají Lake, Carrillo et al. (2008) also determined cold climate conditions during ~11.6- ~12.8 ka BP. Coherently with these observations, but based on geochemical and clastic

sediment analyses from Laguna Los Anteojos, Stansell et al. (2010) identified cold and drier conditions during the same period.

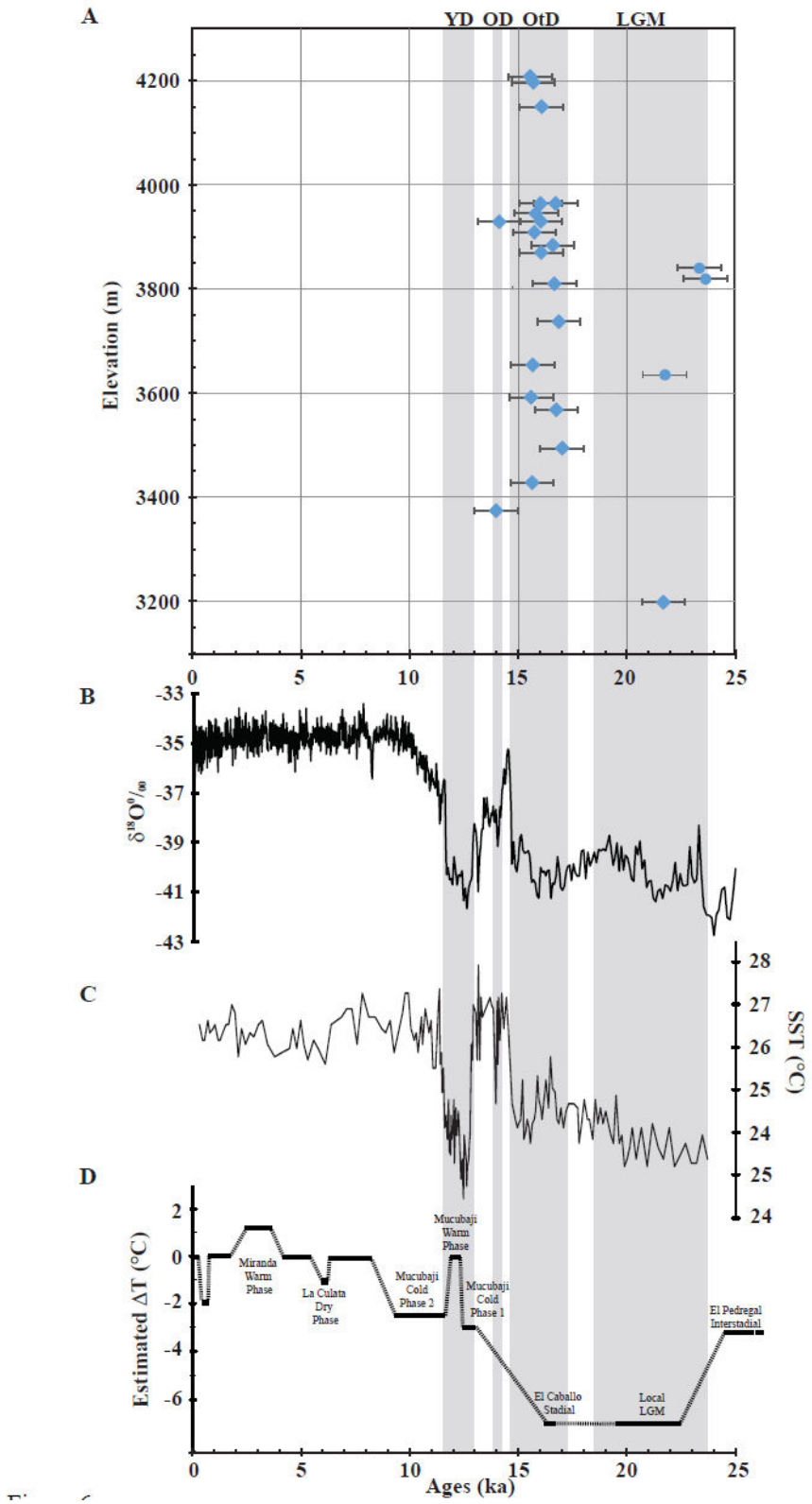

Figure 6. A) Altitudinal relation of the Gavidia glacier chronologies versus global (B), regional (C) and local (D) paleoclimatic proxy records. Dots are samples collected on

the valley bottom while diamonds are samples of the valley side-walls. B) GISP2 $\delta^{18}O$ values (‰) (Stuiver et al., 1995). C) Sea Surface Temperature (SST) deduced from Mg/Ca sediment record of the Cariaco Basin (Lea et al., 2003). D) Noticeable climatic episodes in the Mérida Andes deduced from palynological investigations (Based on Salgado-Laboriau and Schubert, 1976, Salgado-Laboriau et al., 1977, Schubert and Rinaldi, 1987, Salgado-Laboriau, et al., 1988, Rull, 1998, Dirszowsky et al., 2005). Cold periods based on GISP2 curves are in grey bands. YD: Younger Dryas, OD: Older Dryas and OtD: Oldest Dryas.

6. Conclusions

The first deglaciation chronology of the Gavidia valley is based on a coupled TCN dating and a detailed analysis of glacial landforms. Deglaciation happened in two separated and identified periods. The first one occurred between the LGM (21 ka) and the Oldest Dryas stadial (OtD at ~16.5 ka) or El Caballo Stadial. The second shorter period occurred after the El Caballo Stadial (at ~16.5 ka). Despite moderate topographic slopes (<7°) along the valley are evidenced, exposures ages point out two modalities of glacier retreat. During the LGM/OtD-El Caballo Stadial interval, relatively cold climate conditions were maintained, leading to low ice retreat (~0.26 km/ka). In contrast, the glacier extinction occurred by high ice retreat rates of about ~4.7 km/ka. This scheme disagrees with the Mucubají valley deglaciation history. In this valley, the glacier seems to last longer, reaching up to the end of the Younger Dryas. Mucubají former glacier experienced intercalation of cold short periods that permitted the development of small moraine ridges. Local paleoclimate contrasts and different valley orientations could explain geomorphic and deglaciation histories differences.

Acknowledgements

This research was founded by INSU-CNRS-IRD (France). FUNVISIS (Project Geodinámica Integral de los Andes de Mérida-GIAME-FONACIT 2012002202), CIGIR (Venezuela), FONACIT (Venezuela). ^{10}Be analyses were performed at the French Accelerator Mass Spectrometry Facility, ASTER (INSU-CNRS). We thank Maurice Arnold, Georges Aumaitre and Karim Keddadouche for assistance during AMS measurements. Eduardo Barreto for his valuable help in the fieldwork, Francis

Coeur for rock crushing. Alisse Geigher for paleoglaciological discussions. Finally, thanks to the staff of both Santo Domingo Hotel and Mucoposada Michicaba (Gavidia).

V-2.1.3 Mucuchache valley, El Caballo and Las Tapias moraines

V-2.1.3.1 Geomorphological descriptions and previous studies

Most of the Mucuchache valley is oriented NW-SE. Only at highest accumulation zone altitudes (> ~ 3700 m), it is NE-SW oriented. Catchments of lateral secondary valleys drain towards the Chama River. Below ~3500 m, glacial landforms are dominated by sedimentary features as lateral and frontal moraines, reaching up to 150 m high. Above around 3500 m, glacial landforms are dominated by erosional features as cirques and roches moutonnées (Figure V-4). The geomorphological description was proposed by González and Bezada (2006), but no deglaciation chronology was available. This valley was selected in order to complete the Sierra Nevada deglaciation history. The ^{10}Be deglaciation chronology attempted to answer the next scientific questions: What is the age of the glacier advance identified by the 150 m high lateral moraine? Is it a LGM glacier advance? How was the deglaciation history?

The NW-SE trending El Caballo moraine complex, next to of the Mucuchache valley to the NE, extends 1.6 km long and 85 m high oriented NW-SE. This catchment is smaller than the Mucuchache valley (Caballo area 2.1 km^2 and the Mucuchache 17.2 km^2) and also drains toward the Chama River (Figure V-5). Las Tapias moraine complex is located 10 km to the NE of the Mucuchache valley (Figure V-6) in the Sierra de Santo Domingo. Las Tapias moraines are separated from the Mucuchache ones by the moraine complexes of El Caballo, Mucubají, La Victoria and Los Zerpa, from SW to NE; all resting on the northwestern slope of the Sierra Santo Domingo. Las Tapias moraine is 0.9 km long NW-SE oriented (Figure V-6). As was mentioned in Los Zerpas, origin of the moraines in Sierra de Santo Domingo higher than 3000 m was assigned older than 10-13 ka BP (Schubert, 1970, 1972) but no absolute ages were proposed. ^{10}Be deglaciation chronologies attempted to contribute answering the next scientific questions: Are these maximum glaciers advances synchronous? How were the glaciers advances between the dry Chama river comparde to the wet Santo Domingo river catchments?

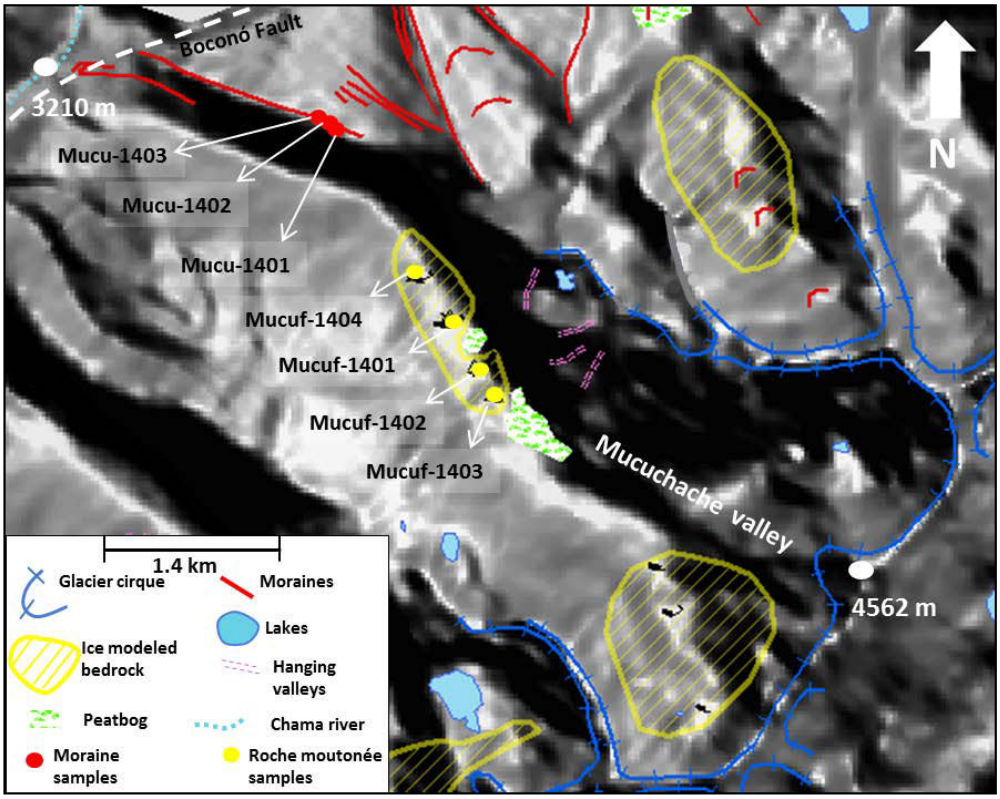

Figure V-4. A) Glacial geomorphology of the Mucuchache valley in the Mérida Andes. Location of collected samples reported on a digital elevation model (DEM). B) Characteristic U-shaped valley of La Mucuchache, look at boulders atop right side moraine crestline (person stands for relative scale). B) Example of a moraine boulder in La Mucuchache (white arrow indicates sample location).

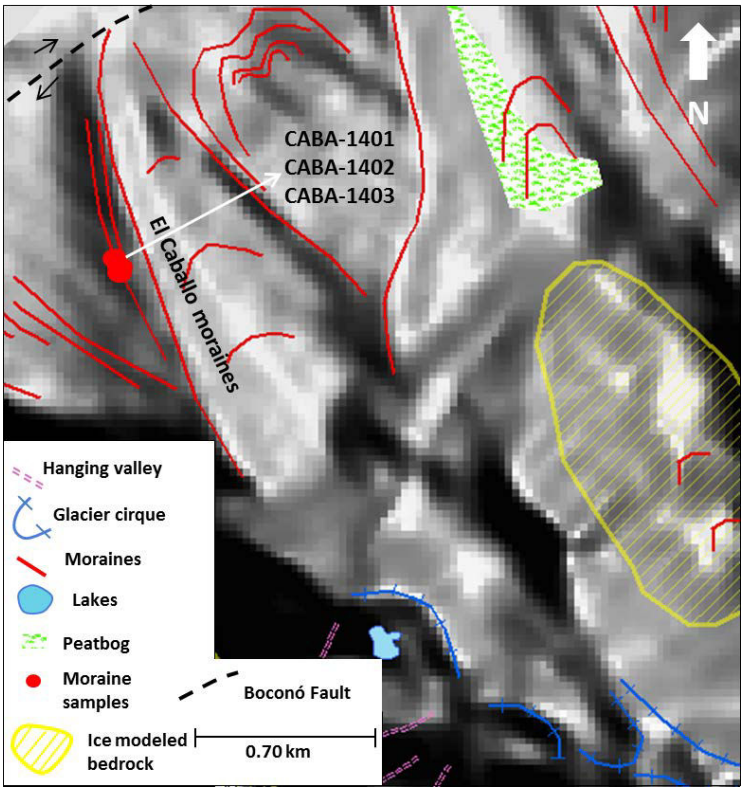

Figure V-5. El Caballo moraines in the Mérida Andes. Samples location are the red dots.

V-2.1.3.2 Exposure ages and outliers

The Mucuchache valley exposure ages range from 5.78±0.71 ka and 36.95±1.58 ka (Table V-3). Most of analytical uncertainties are lower than 5% which is lower than the usual published uncertainties range (Balco et al., 2008; Dunai, 2010). MUCUF-1402 is the only one sample with an uncertainty higher than 5%. This sample was collected in a roche moutonnée at 3683 m and it is 5.78±0.71 ka. MUCUF-1402 is located between MUCUF-1401 18.09 ± 0.86 ka at 3603 m and MUCUF-1403 18.75 ± 0.75 ka at 3704 m (Figure V-4). In comparison with these surroundings samples MUCUF-1402 exposure age is inconsistent. It can reflect a post deglaciation event. This roche moutonnée was not as high as other sampled ones above ground surface. In fact, it is only around 30 cm high. Although sample was carefully collected, bedrock may have been covered by debris after deglaciation, which limited the direct impact of the cosmic rays. So, a minimal ^{10}Be production may have occurred. This sample was considered as an outlier and was not considered for discussions.

Exposure ages from the Mucuchache valley rage between 18.09±0.86 ka (MUCUF-1401, roche moutonnée) and 36.95±1.58 ka (MUCU-1403, boulder moraine; Table V-3). Exposure ages are in accordance with location of sampled landforms; i.e. exposure ages decrease up-valley.

Geomorphological investigations indicate the presence of more than one lateral moraine in the Mucuchache valley (Figure V-4). These moraines are difficult to relate to their respective frontal moraines. The frontal moraines absence could be simply explained by the Chama river erosion. However, the Quaternary Boconó fault movement created the Mucuchache frontal moraines displacement and alteration. New weakness planes created in the frontal moraines probably strengthen the Chama river erosion and the frontal moraines denudation. In the innermost lateral moraine three samples were collected (Figure V-4): MUCU-1401 25.66±1.39 ka, MUCU-1402 35.48±1.60 ka and MUCU-1403 36.95±1.58 ka. Considering the last two samples are not significant different. These two ages are used to stablish the exposure age of this lateral moraine. Since MUCU-1401 was collected at around 1 m high, exposure age of this boulder can reflect a post deglaciation process, presumably due to enhanced erosion (spalling). This process remove bedrock surface and a significant quantity of ^{10}Be is lost. Apparent exposure age is younger than the real one. Weighted average exposure age of the innermost lateral moraine sampled is 36.20±1.13 ka (Figure V-4).

As in the Mucuchache valley, in El Caballo moraines complex, some frontal moraines are absent. These frontal moraines denudation could be explained by the Chama river erosion and the Quaternary Boconó fault action as was explained to the Mucuchache moraines. Three samples were collected. Exposure ages are: CABA-1401-30.53±1.42 ka, CABA-1402-33.16±1.51 ka and CABA-1403-27.44±1.14 ka. The last sample CABA-1403 is significantly different and was rejected in the following. It can reflect enhanced erosion (spalling) as in the Mucuchache boulder MUCU-1401. A weighted average exposure age of the outermost lateral moraine is 31.76±1.03 ka (n=2) (Figure V-5).

Las Tapias moraines are located on the NE flank of the Sierra de Santo Domingo and appears to be the last most conspicuous moraine to the NE on this side of the Sierra. Three samples were collected, which are not significantly different (Table V-3). A

weighted average exposure age from the outermost lateral Las Tapias moraine is 19.028±0.574 ka (n=3).

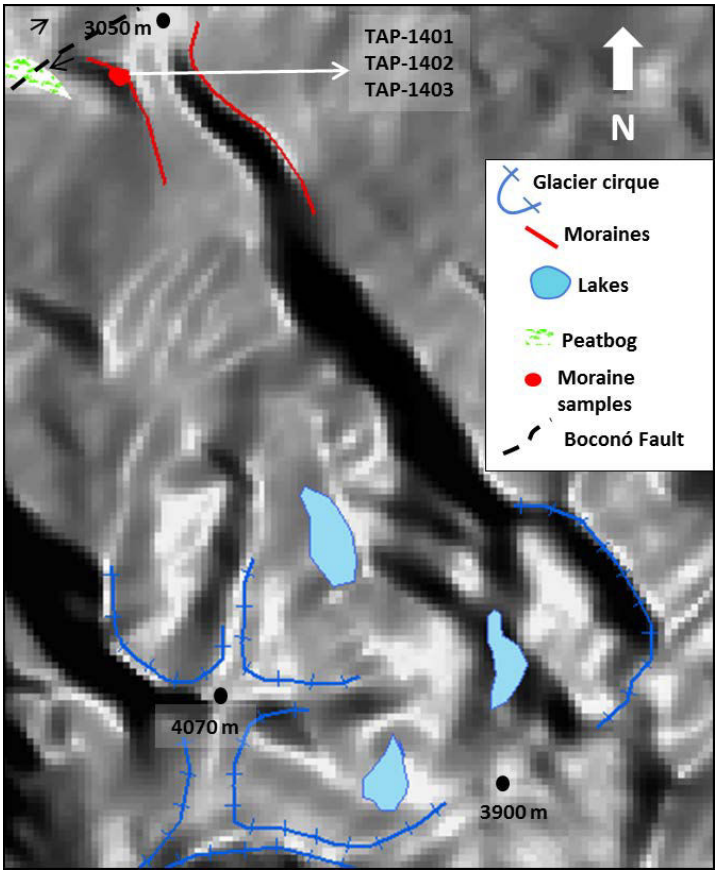

Figure V-6. A) Las Tapias moraines in the Mérida Andes. Samples locations are identified by red dots.

V-2.2 Sierra del Norte:

V-2.2.1 La Culata moraines/Mucujún valley

V-2.2.1.1 Geomorphological descriptions and previous studies

In the Mucujún valley, mainly erosional glacial landforms, as glacial cirques at elevations between 4000 m and 4500 m are present. At elevations lower than 4000 m, glacier activity is evidenced by moraines presence (lateral, frontal and terminal) (Figure V-7). A conspicuous lateral-terminal moraine is located between around 3160 m and 4000 m (moraine **1**). This lateral moraine is oriented NE-SW with a length of ~4 km and ~150 m height (Figure V-7, **1**). A geomorphological description of this area was presented by Schubert and Valastro (1974). They described an altered till outwash covered by vegetation at 1600 m which was related to the Early Mérida Glaciation.

Authors presented radiocarbon ages from fluvioglacial terraces, dry lakes and a bottom moraine from the Mucujún valley. Radiocarbon ages from a soil sample collected in the terrace upper layer are 3.82 ± 0.09 ^{14}C ka BP and 4.79 ± 0.07 ^{14}C ka BP. Medium terrace layer ages are 2.41 ± 0.08 ^{14}C ka BP, 5.06 ± 0.09 ^{14}C ka BP and 5.63 ± 0.07 ^{14}C ka BP. The base of the terrace was dated at 3.97 ± 0.06 ^{14}C ka BP. Authors indicate ages are inconsistent because of the young age of the base compare to the others. Authors do not discuss a possible cause of the ages inconsistency. A moraine located 1 km southwest of El Saladito was dated at 2.49 ± 0.05 ^{14}C ka BP (green circle, letter A, Figure V-7), a sample from the top of dry lake sediments located in a glacier cirque at 4000 m is 5.06 ± 0.09 ^{14}C ka BP. The moraine age indicates a glacier advance younger than 2.5 ka while the lakes age indicates glacier cirque was ice free at least since ~5 ka. Authors do not explain inconsistency of ages. Based on stratigraphic correlation and moraines complex alteration features, Schubert and Valastro (1974) correlate La Culata moraines complexes to the Santo Domingo moraines located between 3000-3500 m. They related these landforms to the Late Mérida Glaciation with ages younger than 13 ka. However, a question still existed: how old is La Culata conspicuous moraine? To answer this question and contribute to better constrain glacier advances in the Sierra del Norte, La Culata moraines complexes was selected to date. Seven samples were collected along the lateral-terminal moraine (Figure V-7; Table V-3). Five other samples were collected in smaller secondary lateral-terminal moraines with a NW-SE orientation (Figure V-7, **2, 3;** Table V-3).

V-2.2.1.2 Exposure ages and outliers

Exposure ages for the samples collected at La Culata range from 16.01±0.65 and 22.36±2.64 ka (Table V-3). Exposure ages uncertainties are in general lower or close to 10%. Only sample CU-1310 (22.36±2.54 ka) was significantly different and older compare to its neighbor sample CU-1311 (17.78±0.78 ka). According to the location of the sampled moraine **2**, it would be at least of the same age or younger than moraine **1** (Figure V-7, Table V-3). Weighted average exposure age of moraine **1** is 17.02 ± 0.35 ka (n=7). This weighted average age considered CU-1301, CU-1302, CU-1303, CU-1304, CU-1305, CU-1306 and CU-1309 ages which are not significantly different (Figure V-7, Table V-3). Therefore, CU-1310 suggests a significant ^{10}Be inheritance due to complex exposure history of the boulder before its abandonment (i.e. during the glacier transport and /or stay in up-valley landforms). CU-1310 was considered as an

outlier and it was not considered in the following. Exposure age of moraine **2** is 17.78±0.78 ka (n=1). Weighted average exposure age of moraine **3** is 17.94 ± 0.47 (n=3, CU-1312, CU-1313 and CU-1315; ages not significantly different). Moraines **2** and **3** are related to secondary glacier valleys oriented NW-SE. TCN ages data set suggest a major episode of ice withdrawal during the same period leaving behind the entire set of glacial landforms studied (1 through 3 in Figure V-7). The geomorphological study of this area reveals the presence of several other moraines, which suggest a deglaciation interrupted by different glaciers stops and advances, within the overall trend of ice withdrawal.

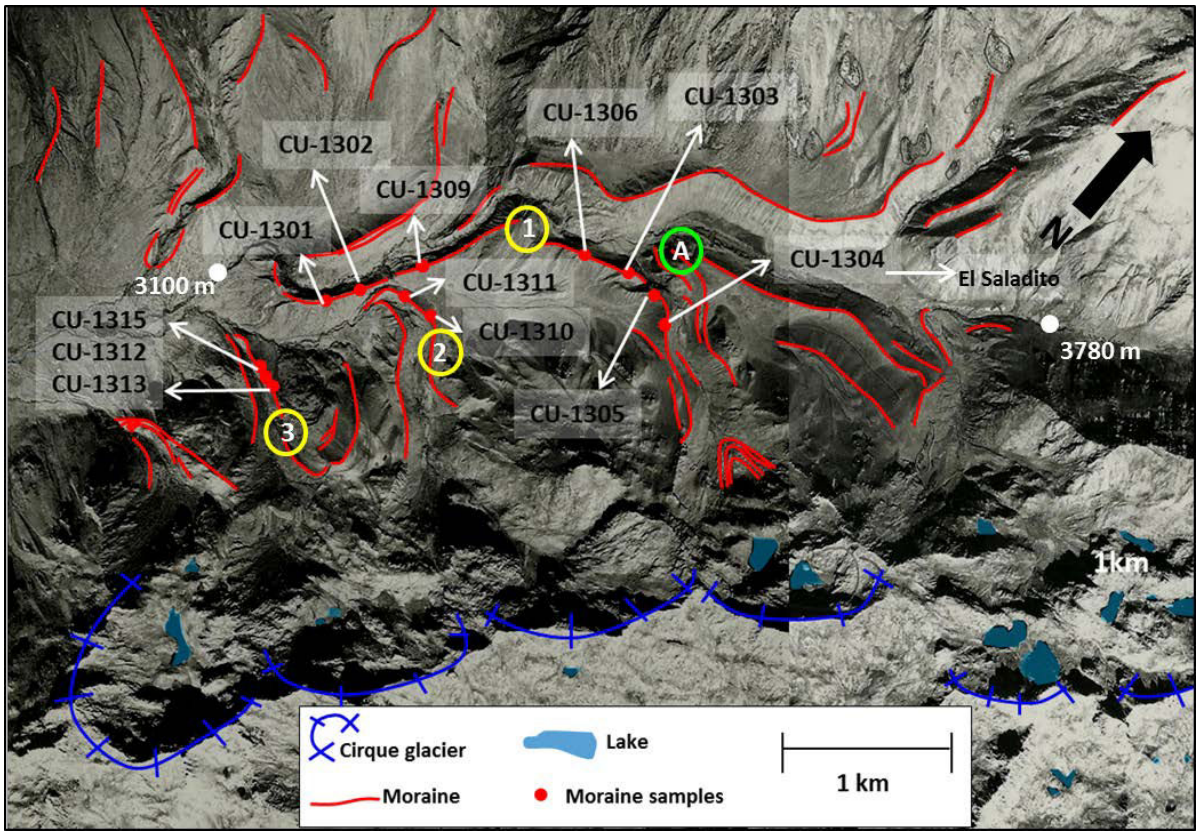

Figure V-7. La Culata moraines complexes in the Mucujún valley *(Sierra del Norte). In yellow circles moraines 1, 2 and 3 and samples collected for this dissertation. In green circle, letter A, chronological data in a moraine at 3600 m elevation from Schubert and Valastro (1974).*

V-2.2.2 Mifafí valley and El Desecho moraine

V-2.2.2.1 Geomorphological descriptions

In the Sierra del Norte, developments of depositional glacial landforms are not as well developed as those of the Mucujún valley where are located La Culata moraines

complexes (Figures V-1 and Figure V-7). Glacial landforms are mainly dominated by erosional features as glacial cirques at elevations higher than 4000 m (Figure V-8).

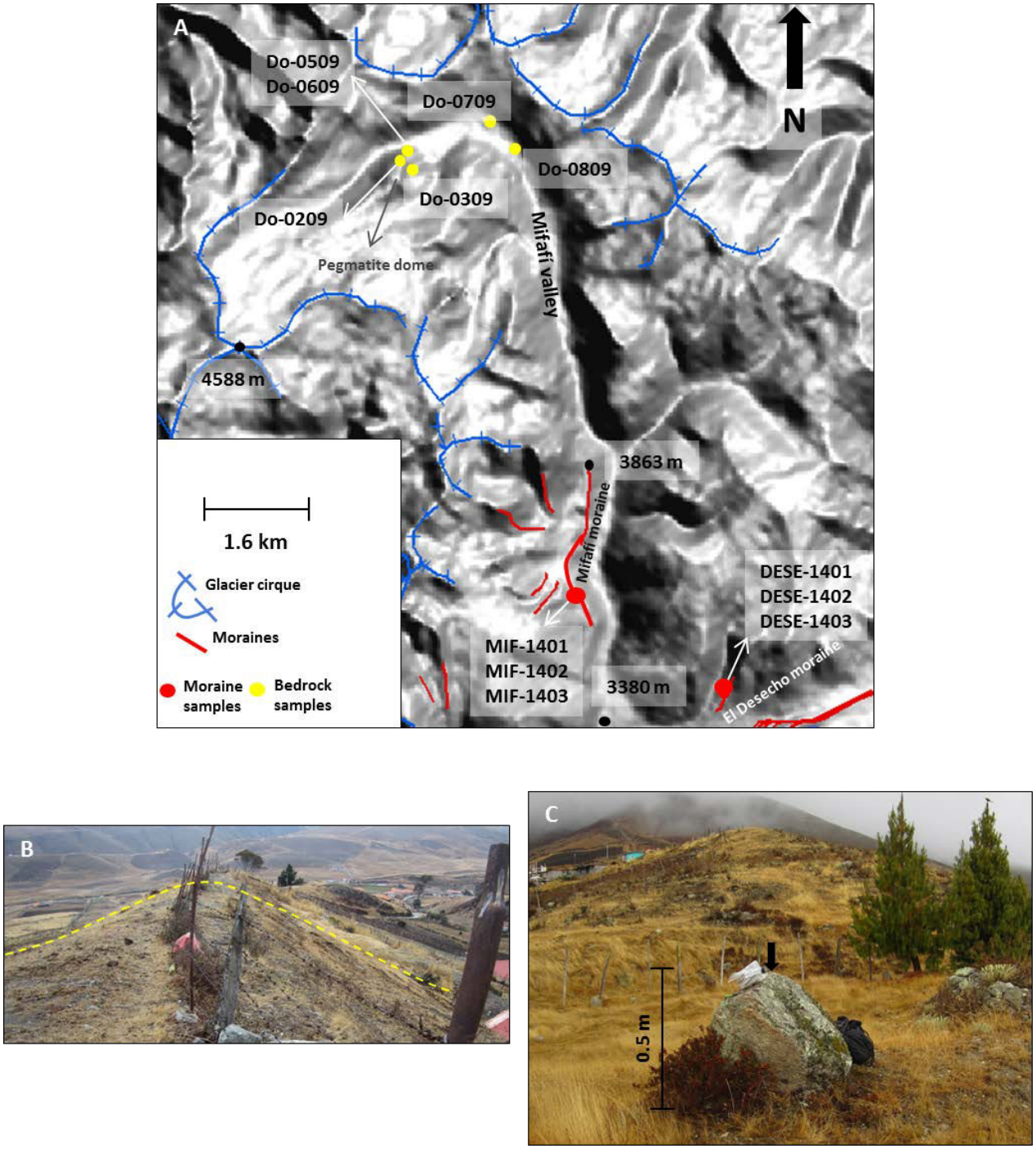

Figure V-8. A) Mifafí valley and El Desecho moraines in Sierra del Norte. Samples locations are the red and yellow dots (moraines and bedrock samples respectively). B) View of the El Desecho moraine ridge. C) Moraine boulder sampled in El Desecho moraine (DESE-1401).

Six samples were collected along the Mifafí valley (Figure V-8; Table V-3). At around 4080 m is located an around 300 m high pegmatite dome. This pegmatite dome allows studying a vertical deglaciation profile. This valley presents two main orientations with N-S orientation for the lower section (< 4000 m) and NE-SW orientation for the higher section (> 4000 m, peak at 4588 m). Slopes are lower than 7%. In the low section, a lateral moraine is located below 3863 m (2.8 km long and N-S orientation) (Figure V-8A- Table V-3). Three boulder samples were collected along its crestline. No previous deglaciation chronology was available for the Mifafí valley. This valley was selected to study a deglaciation history in the Sierra del Norte and compare to others from the Sierra Nevada. How was the glacier dynamic in this valley? Is there any difference in comparison with the Gavidia valley which has a similar accumulation zone in the Sierra Nevada? These were the scientific questions made and answered based on the deglaciation chronology obtained.

El Desecho lateral moraine is located south of the Mifafí valley, it is ~ 1 km long and NE-SW oriented (Figure V-8B, C; Table V-3). This moraine was studied to date glacier advances in Sierra del Norte and contribute to answer: How compares glaciers advances of Sierra del Norte with Sierra Nevada? Were advances synchronous or asynchronous?

V-2.2.2.2 Exposure ages and outliers

The Mifafí valley age results at the pegmatite dome range from 16.52±1.45 to 19.19±2.05 ka (Table V-3; Figure V-8A). Exposure ages from the Mifafí lateral moraine are between 17.32±1.01 and 19.70±1.52 ka (Table V-3; MIF samples in Figure V-8). The El Desecho lateral moraine results range between 17.70±0.98 and 21.78±3.09 ka. Exposure ages are not significantly different. El Desecho weighted average exposure age is 17.97±0.58 ka (n=3) (Table V-3; DESE samples in Figure V-8). Analytical uncertainties including AMS measurement and Cronus computation are low (lower than ~10%). There is no significant difference between the moraine MIF exposure ages (located below 3863 m) and inside the Mifafí valley close to the pegmatite dome (Do-07-09) (Figure V-8).

V-2.3 Cordillera de Trujillo (Pueblo Llano valley/La Canoa)

V-2.3.1 Previous studies

These glacial landforms are located in the northernmost east (NE) of the study area (Cordillera de Trujillo) at lowest elevations (2500-2900 m) (Figures V-1 and V-9). Glacial chronologies from the RF3 section (based on OSL ages) in La Canoa moraine established a MIS 5 (early Mérida Glaciation) and a LGM (late Mérida Glaciation) glacier advance (Mahaney et al., 2000; Figure V-9). Ages assigned were 81±15 ka and younger than 26±2 ka, respectively. In the Pueblo Llano valley a north-south oriented lateral outwash fan was proposed (Vivas, 1979; Bezada, 1989; Figure III-5). However, Guzmán, (2013) proposed these landforms as frontal moraines based on a geomorphological and sedimentological description. These moraines are located at 2467 m and date 17.32±1.72 ka (based on ^{10}Be dating; Guzmán, 2013). Schubert (1974) localized the late Mérida Glaciation landforms (13-25 ka) at elevations between 2900-3500 m. Recent moraine dating (Guzmán, 2013) emphasize the requirement of new research to precise the Mérida Glaciation chronology in the Cordillera de Trujillo.

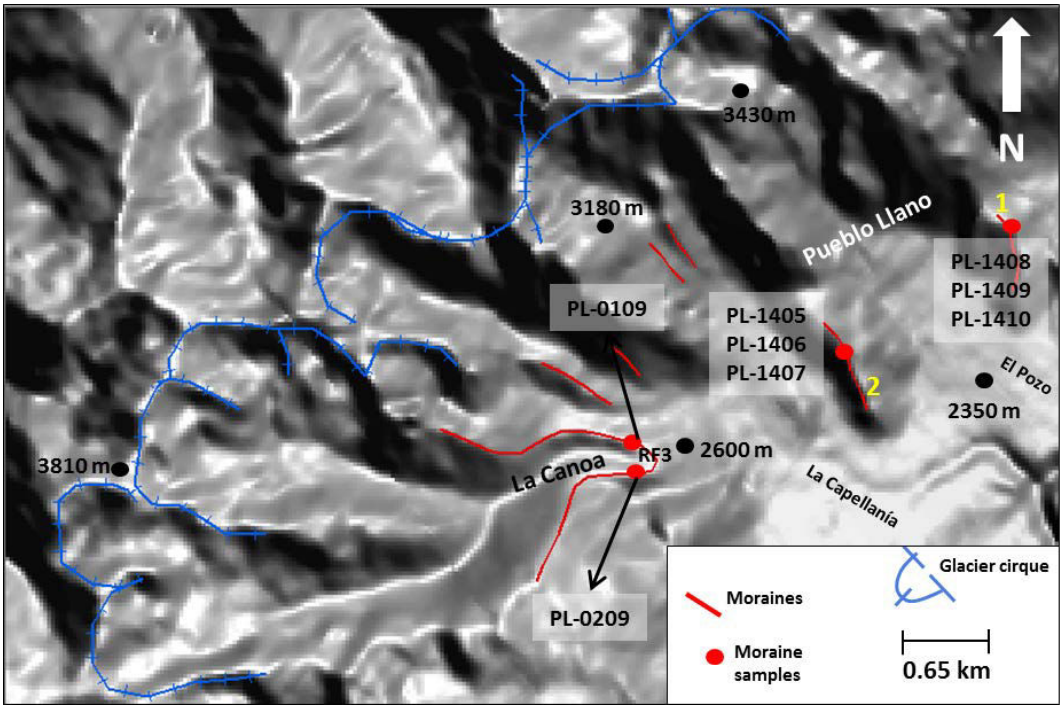

Figure V-9. La Canoa and Pueblo Llano moraines. Studied Pueblo Llano moraines are the yellow numbers. Samples locations are in red dots.

The scientific questions made for this valley were: Is La Canoa moraine younger than 26 ka *sensus stricto* related to the LGM as suggested Mahaney et al., 2000? Is there any previous MIS 2 glacier advance different from the RF3 section detected in the Pueblo Llano valley? The study of this area was significantly contributed to elucidate if MIS 2 or late Mérida Glaciation glacier advances arrived at elevations lower than currently recognized. Also, the study of the Pueblo Llano valley is important because evidences of previous MIS 2 glacier advances could be found.

V-2.3.2 Glacial geomorphological features

Glacial cirques are located between 3400-3800 m, whereas depositional glacial landforms (moraines) are between 2300-3200 m (Figure V-9). La Canoa lateral-terminal moraines are E-W in orientation and ~1.4 km long and ~40 m high (Figure V-9).

A detailed geomorphological description of the Pueblo Llano valley was published by Bezada (1989; Figure III-5). Outwash fans were interpreted close to la Capellanía and El Pozo (green rectangle in Figure V-10 C). Two ridges constituted by a diamicton material are developed between the outwash fans (Figure V-10 A, B, D). These ridges which are easily observed both on field and on aerial photography are more altered and discontinuous than those of La Canoa. In the present study, these ridges are proposed as the Pueblo Llano moraines (Figure V-10). Moreover, it is important to note that the Pueblo Llano area is strongly influenced by anthropic activity (Figure V-10 E).

Moraines **1** (samples PL-1408, PL-1409, PL-1410) and **2** (PL- 1405, PL-1406, PL-1407) are N-S oriented. These moraines are 0.9 km 1.4 km long respectively. Moraine 1 is deformed toward La Capellanía town and seems to indicate a stress which changed the original ridge orientation. This stress seems to be orientated almost E-W along the Pueblo Llano valley. Guzmán (2013) proposed the presence of frontal moraines through the Pueblo Llano valley axis close to La Capellanía. This suggests a glacier activity in the Pueblo Llano valley with an E-W orientation during the Late Pleistocene. Thus, moraine **1** deformation could be related to a glacier deformation during younger glacier advance.

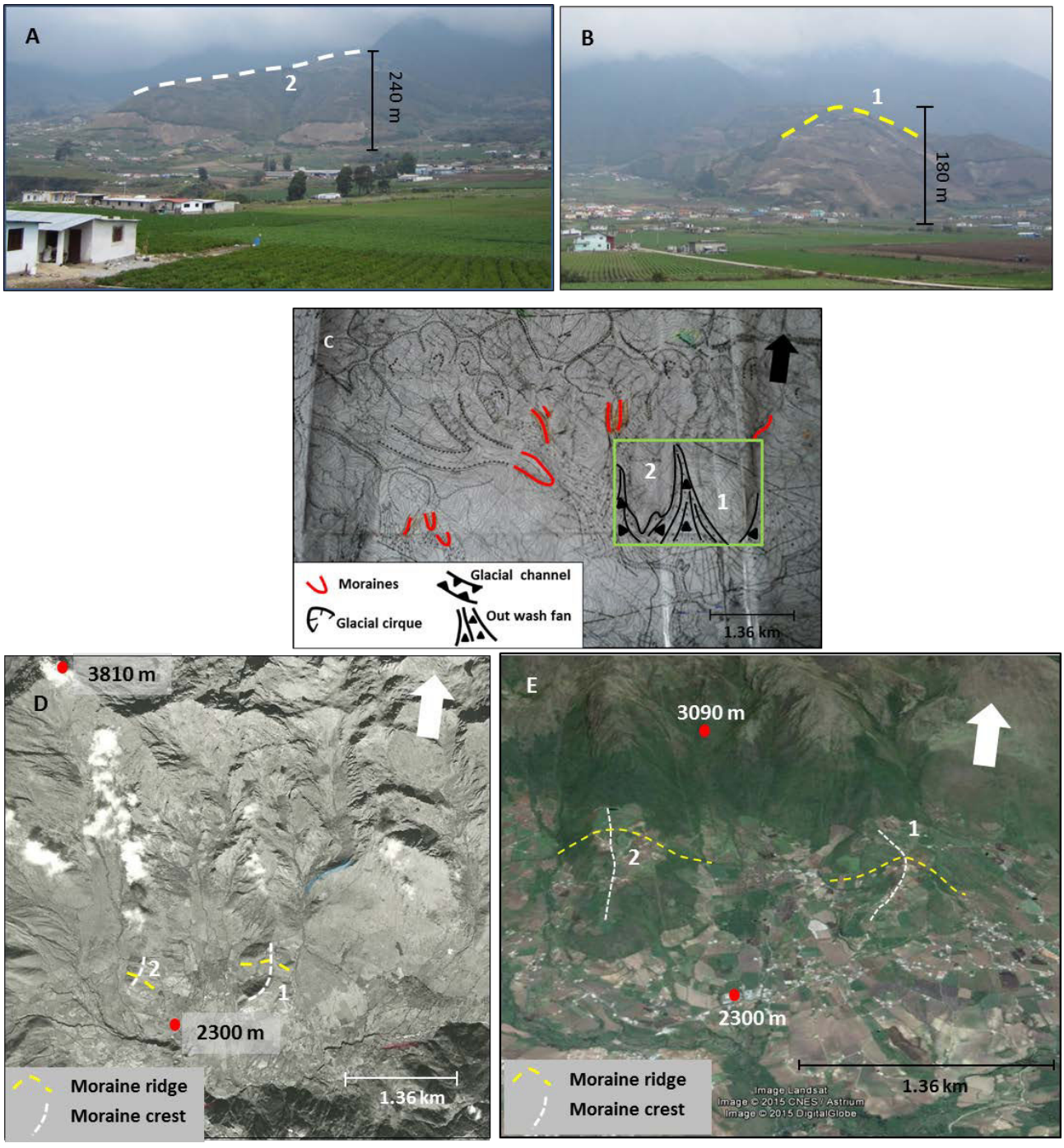

Figure V-10. Pueblo Llano moraines with A) Moraine 2 and B) Moraine 1. C) geomorphological map (Bezada, 1989). The green rectangle localizes the outwash fans described by Bezada (1989). D) View of moraines in aerial picture mission A-34. E) Anthropogenic impact in the Pueblo Llano moraines (Google Earth image).

V-2.3.2 Exposure ages and outliers

La Canoa exposure ages vary from 17.57±1.55 to 18.21±1.55 ka (n=2) and Pueblo Llano moraines from 45.73±1.80 to 86.66±3.37 ka (n=6; Table V-3).

Weighted average exposure age of La Canoa moraine is 17.89 ± 1.09 ka (n=2). Exposure ages for moraines **1** and **2** in the Pueblo Llano valley are more scattered and significantly different and older (Table V-3). It is important to consider the strong anthropogenic impact (agriculture activity) on these moraines. Moreover, moraines boulders are not as big as those observed in other moraines (Table V-3). Exposure ages from the moraine **2** (weighted average 71.96 ± 1.74 ka) and moraine **1** (weighted average 50.33 ± 1.15 ka) suggest that both ridges seem to be related to different glacier advances. These glacier advances seem implied a former glacier E-W oriented along the Pueblo Llano valley, apparently retreating eastward.

V.3.0 Paleo ELA values

V- 3.1 Previous studies

Schubert (1974) and Schubert and Valastro (1974) suggest, based on a constant elevation of the lowest cirque floor, a late Pleistocene snowline of 3500 m for most of the Venezuelan Andes. This value was not assigned to a specific time. Lachniet-Selem (2005) determined ELA_{LGM} using the toe-to-headwall–altitude ratio (THAR) method, accumulation area ratio (AAR) and accumulation area balance ratio (AABR). The AAR and AABR methods are explained in **Section IV-7.0**. THAR method is based on the empirical observation that the firn (material between fresh snow and glacier ice) limit on temperate glaciers at the end of the ablation season is often located at a halfway altitudes between the head of a glacier and its terminus (Porter, 2001). THAR method considers that not all glaciers have the same behavior and the paleo ELA is located at an elevation lower than the median altitude between the head of a glacier and its terminus. Lachniet-Selem (2005) drew former glaciers surface using frontal and lateral moraines from the Mucubají valley and La Victoria and La Canoa terminal moraines. Lachniet-Selem (2005) assigned the Mucubají frontal moraine to a LGM glacier advance based on Schubert and Rinaldi (1987) (details in section V-2.1.1). La Canoa moraine was related to the LGM based on Mahaney et al. (2000) chronology (details in section V-2.3). Mahaney et al. (2000) suggested ages younger than 26 ka. Lachniet-Selem (2005) related La Victoria former glacier to a LGM glacier advance presumably based on a correlation to the beside Mucubají valley. ELA_{LGM} (BR=1.8) are thus calculated for Mucubají (3836 m), La Victoria (3719 m) and La Canoa (3439 m). Whereas for a BR of 4.0, ELA_{LGM} are 3760, 3604, and 3364 m respectively, with an average ELA_{LGM} of 3576 ± 163 m.

Stansell et al. (2007) determined ELA_{LGM} for former glaciers from Sierra del Norte, Northern and Southern Sierra de Santo Domingo. Authors used AAR (ratios from 0.66 to 0.86) and AABR (ratios from 5 to 15) methods. Chronology data to support all the glacier landforms related to the LGM was not presented. ELA_{LGM} in Sierra del Norte were estimated from 3880 to 4030 m. In the northern Santo Domingo ELA_{LGM} were estimated from 3590 to 3725 m. In the Southern Santo Domingo values were from 3210 to 3505 m.

All the previous studies mainly determined paleo ELA for the LGM. But are all the glacier landforms used precisely related to the LGM? What is the paleo ELA at times different from the LGM? Glacial landforms related to the LGM are not extensively based on a robust chronological data. The lack of robust chronological data produces wrong paleo ELA interpretations. Moreover, in a frame of methodological development, it can be interesting to evaluate if glacier thickness calculations (Ben and Hulton, 2010) provide more accurate paleo ELA values. To answer these questions, paleo ELA determinations were made at different ages in the central MA, based on the chronology obtained in this dissertation.

V- 3.2 Results

Since AAR and BR ratios for tropical glaciers are not well constrained (e.g. Smith, 2005 and Rea et al., 2009), calculations were performed for various ratios range. Published ratios for tropical glaciers from Kaser and Osmaston (2002) and Stansell et al. (2007) were used (AABR: 5, 10; AAR: 0.73, 0.82) (Tables V-4 and V-5).

Table V-4. Paleo ELA values (m a.s.l) computed for the Mucuchache valley former glaciers and for different basal shear stresses (Table 5).

		Paleo ELA (m)			
Basal shear Stress (kPa)	Deglaciation age (ka)	AABR		AAR	
		5	10	0.73	0.82
50	36	3730	3630	3730	3630
100		3780	3730	3830	3730
150		3831	3781	3931	3831
50	20	3857	3807	3857	3807
100		3907	3857	3957	3857
150		3957	3907	4007	3907
50	18	3930	3880	3930	3880
100		3980	3930	4030	3980
150		4030	3980	4080	4030

Table V-5. Paleo ELA values (m a.s.l) calculated based on AABR and AAR methods (Porter, 2001 and Benn et al., 2005) using GIS tools from Pellitero et al. (2015). Since no significant differences were observed between both methods, weighted average paleo ELA are presented.

Valley or moraine	Latitude	Longitude	AABR		AAR		Weighted Average Paleo ELA (m)
			5	10	0.73	0.82	
Mucuchache 36 ka	8.78º	- 70.86 º	3780 ± 51	3714 ± 77	3830 ± 101	3730 ± 101	3765±37
Mucuchache 20 ka			3907 ± 50	3857 ± 50	3940 ± 76	3857 ± 50	3882±27
Mucuchache 18 ka			3980 ± 50	3930 ± 50	4013 ± 76	3963 ± 76	3965±30
Caballo 30 ka	8.80 º	- 70.82 º	3847 ± 50	3797 ± 50	3897 ± 50	3830 ± 29	3839±20
Mucubají 22 ka	8.79 º	- 70.84 º	3812 ± 77	3762 ± 77	3862 ± 77	3795 ± 77	3808±39
Mucubají 18 ka			3887 ± 50	3820 ± 29	3887 ± 50	3837 ± 50	3845±20
Mucubají 16 ka			3907 ± 29	3857 ± 29	3907 ± 29	3857 ± 29	3882±15
Victoria 18 ka	8.81 º	- 70.80 º	3677 ± 30	3610 ± 59	3760 ± 78	3627 ± 78	3669±24
Zerpa 17 ka	8.81 º	- 70.79 º	3686 ± 51	3586 ± 51	3803 ± 30	3586 ± 51	3665±89
Mifafi 18 ka	8.88 º	- 70.87 º	4405 ± 76	4372 ± 50	4439 ± 76	4405 ± 76	4397 ± 33
La Canoa 17 ka	8. 93 º	- 70.69 º	3475 ± 76	3392 ± 50	3592 ± 50	3442 ± 50	3475 ± 27

Paleo ELA calculations involve the reconstruction of former glacier surfaces and thicknesses (see **Section IV-6.0**). However, former glaciers thicknesses could involve significant uncertainties. In main cases, field landforms allowing the estimation of glacier thickness are scarce or eroded (moraines and outwash, trimline, etc.). Moreover, sampling along vertical profiles is rarely performed.

Glaciers thicknesses are related to the basal shear stress and current glaciers flows with a basal shear stress between 50-150 kPa (Paterson, 1981). Thus, glaciers thicknesses were calculated considering this shear stress range using the excel spreadsheet from Benn and Hulton, (2010) (see Methodology section IV). Three paleo ELA values were obtained considering the specific ratio (50, 100 and 150 kPa) (Table V-4). An average paleo-ELA with one standard deviation (σ) was calculated for each former glacier at a specific age and ratio (e.g. for Mucuchache valley at 36 ka and AABR of 5, average ELA was obtained considering paleo ELA to 50, 100 and 150 kPa: 3730 m, 3780 m and 3831 m, respectively) (Table V-4, Table V-5). Former glaciers were drawn based on chronological data and geomorphology.

Paleo ELA values obtained using different AAR (0.73/0.82) or AABR (5/10) ratios are not significant different when comparison to a specific valley and age is made (Table V-5). For example, for the Mucuchache valley at 36 ka, paleo ELA are 3780 ± 51 and 3730 ± 77 m at AABR of 5 and 10, respectively, whereas at AAR of 0.73 and 0.82 are

3830 ± 101 and 3730 ± 101 m, respectively. Paleo ELA from the Mucuchache valley at 36 ka are not significantly different. Therefore, weighted averages paleo ELA values are presented (Table V-5). These values range between 3475±27 from La Canoa moraines at ~ 17 ka m until 4397±33 m from the Mifafí valley at ~ 18 ka (Figure V-11).

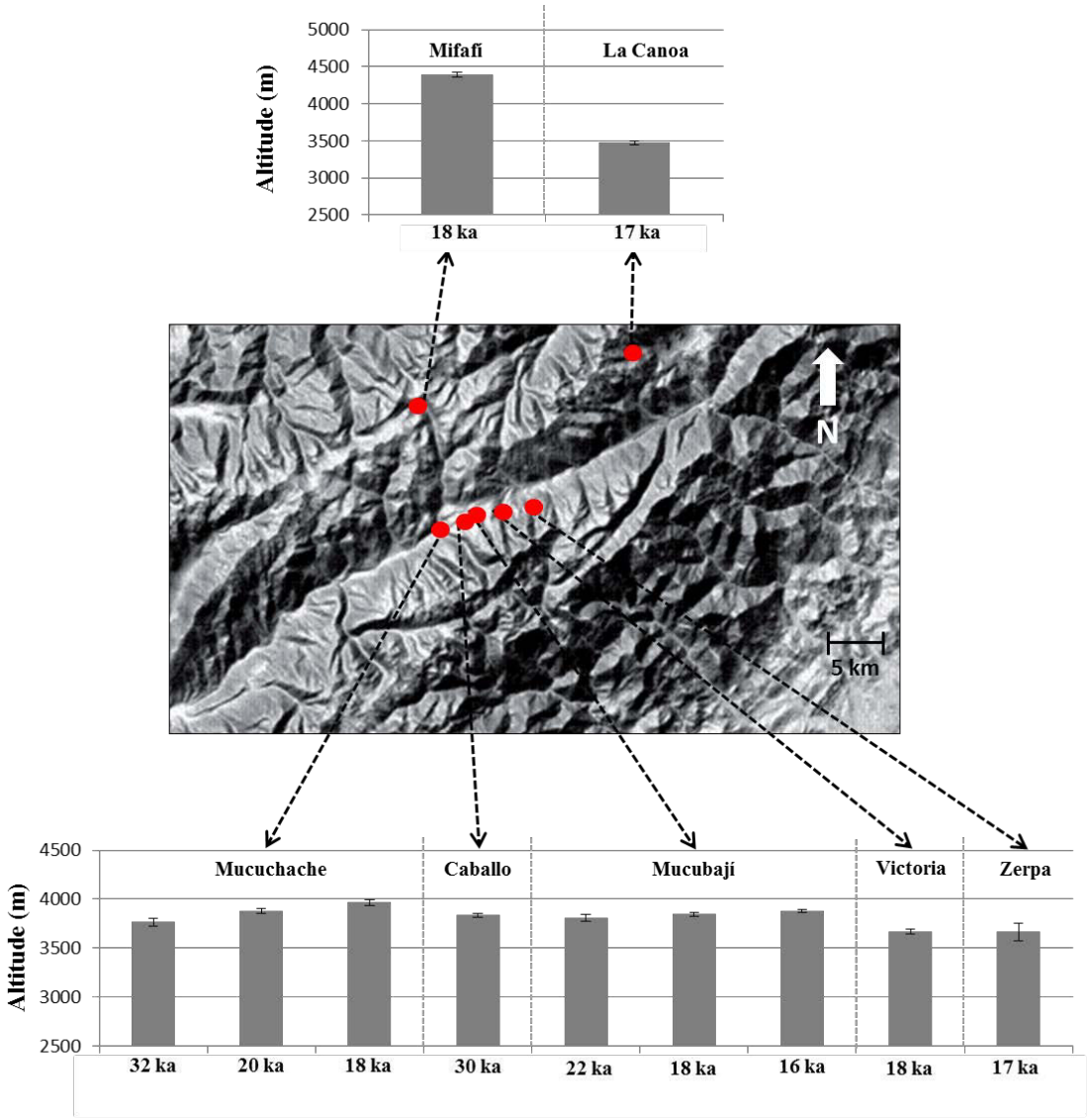

Figure V-11. Paleo ELA variations in different valleys and moraines studied in the central Mérida Andes last 36 ka.

In the Sierra Nevada, paleo ELAs are more consistent for periods older than 30 ka (Mucuchache 3765±37 m and El Caballo 3839±20 m) (Table V-5), as well as for 20-22 ka (Mucuchache 3882±27 m and Mucubají 3808±39 m). However, strong paleo ELA differences exist between Sierra Nevada and Sierra de Santo Domingo (e.g. at 18 ka Mucuchache ELA=3965±30 m and La Victoria ELA=3669±24 m).

A difference between the glacial landforms formation age (moraine construction, bedrock surface erosion by glacier abrasion) and the glacial landform deglaciation age assessed by TCN exposure dating exists. Exposure ages, deglaciation ages or abandonment ages represent time since the sampled landforms were ice-free. Exposure ages represent valuable markers for the interpretation and reconstruction of glaciation periods and paleoclimate. Despite the observation of low erosion in the field (glacial striation and polished surfaces are present), potential post-deglaciation processes could slightly erode the original surface. Thus, exposure ages are assumed as minimum ages (Nishiizumi et al., 1989; Briner and Swanson, 1998; Siame et al., 2000; Gosse and Phillips, 2001; Dunai, 2010; Balco, 2011).

When climate conditions provide positive mass balances, glaciers advance and build ice-marginal moraines (Hughes et al, 2005; Bennet and Glasser, 2009; Kirkbride and Winkler, 2012). Moraines deglaciation occurs during a period with negative mass balances. A time lag could happen between glacier advance and deglaciation. This time lag is assumed as a minimum, considering the sensitive response of the tropical glaciers to climate changes (Kaser and Osmaston, 2002). This minimum time lag is difficult to quantify. The accelerated retreat of the current tropical Andean glaciers occurred at the same time as a major increase in the global temperature curve after 1976 (Rabatel et al., 2013). It seems to indicate tropical glacier response to climate changes occurs in some years, in a decade.

This discussions section is subdivided in three main parts: **VI-1) Deglaciation histories and parameters that control different former glaciers dynamics, with a focus on geomorphic and topographic features.** To discuss in this subsection, the more complete deglaciation histories were selected (from the Mucubají, Mucuchache, Gavidia and Mifafí valley). **VI-2 Implications of the deglaciation chronologies in the glaciations reconstructions.** This subsection presents an analysis of glaciers advances (geographical distribution, timing and integration with data from other studies). **VI-3 Our paleoglaciology contributions to the paleoclimate record and comparisons with the local, regional and global paleoclimate proxy records.** Paleoclimate inferences and its influence on the former glaciers dynamics are discuss. This analysis

was realized based on the paleo ELA interpretations, in comparison with GISP 2 and Cariaco basin paleoclimate proxy records.

VI-1 Deglaciation histories in the central Mérida Andes and principal geomorphic parameters driving the former glaciers dynamics

Deglaciation chronologies along the Gavidia, Mifafí, Mucuchache and Mucubají valleys are detailed and discussed. The TCN ages and previous published data allow proposing new complete deglaciation records in several valleys of the central part of the Merida Andes (MIS 1-MIS 3).

VI-1.1 Deglaciation histories in the central Mérida Andes

VI-1.1.1 Mucubají valley (Sierra Nevada)

Updated exposure ages with SLHL production rate recently published (Kelly et al., 2013) are significantly different from the original values previously published (Carcaillet et al., 2013). The exposure ages indicate a negative relation with elevation (see details in Carcaillet et al., 2013, section *V-2.1.1*, this issue, Figure 3A). Deglaciation began before 21.5±1.3 ka, considering three moraines lower than around 3600 m were observed in a recent geomorphological interpretation (Figure VI-1). Glacier extinction occurred at ages younger than 11.0±0.4 ka (modified ages from Carcaillet et al., 2013). Mucubají valley is characterized by noticeable moraine developments in the flatter lower valley (Level 1 to Level 5, Carcaillet et al., 2013, section *V-2.1.1* Figure 2B). At elevations higher than ~3700 m moraines are not as evident as those of the lower area (Level 6, Carcaillet et al., 2013, section *V-2.1.1* Figure 2B). The construction of massive moraines could have been more difficult because of preexistent high valley bottom steepness (~20º). At higher valley bottom steepness, till stabilization in the glacier margins was not as effective as in the flatter areas. Till deposition and moraine stabilization could be limited by the gravity force influence which leads till sediments fall down. Smaller moraines at higher elevations could be also related to smaller glacier areas at younger times, which controls till sediments supply. The erosion of a smaller glacier produces smaller quantities of till sediment, thus smaller moraines could be related. Finally, smaller moraines developments at higher elevations could be related to short periods of glacier stabilization with climate. Rapid changes between cold and warm climate conditions make difficult and even prevent the ice-marginal moraines stabilization and large

developments. It is important to note that small moraines at elevations higher than 3700 m form around 12.50 ka. These moraines could be related to the Younger Dryas (YD), the short and cold period between 12.85 to 11.65 Cal kyr BP (Blunier et al., 1998). However, it is difficult to relate to it all the moraines with elevation differences between them of as much as 400 m. The YD is close to the Late Pleistocene-Holocene transition, a period of climate change. It is possible that this period in the Mucubají valley was characterized by fast climate changes to induce multiple glacier advances in this short period. It is necessary to perform more paleoclimate studies in the central MA focusing in the YD. Based on the Mucubají valley geomorphological features, glacier dynamics between the LGM and Late Pleistocene/Early Holocene (~11 ka) were characterized by successive stages of glacier stop-advance; all being part of an overall glacier withdrawal.

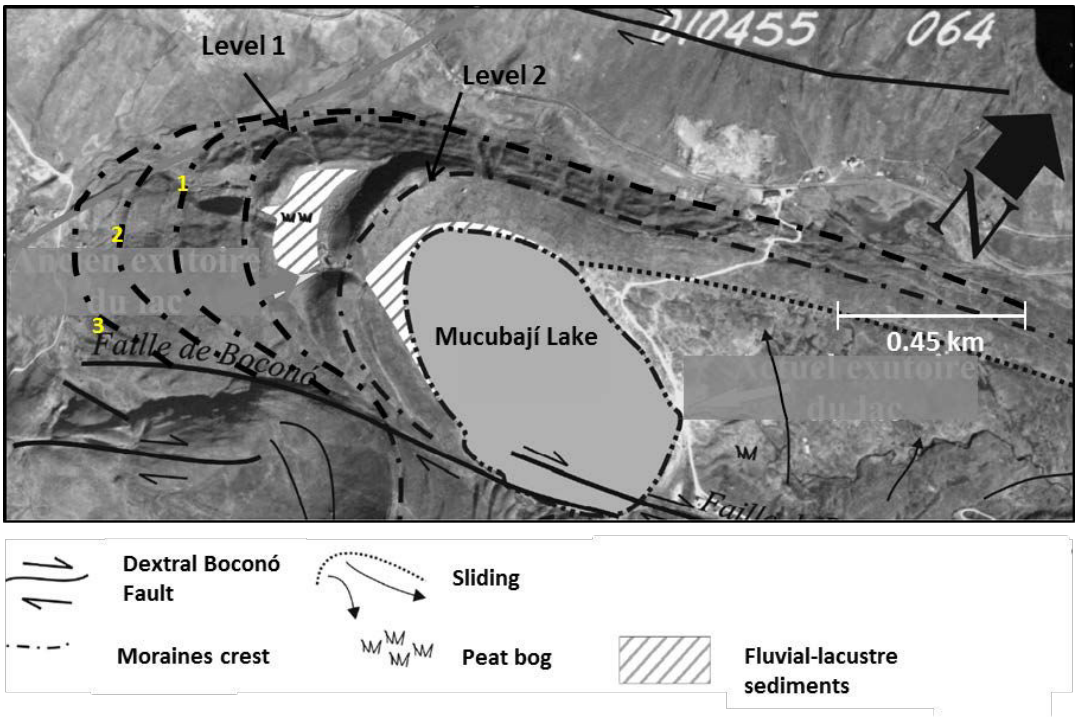

Figure VI-1. Glaciers advances in the Mucubají valley. Maximum glacier advance is related to a frontal moraine below moraine Level 1, originally assigned by Carcaillet et al. (2013). Moraines were signaled based on ridges morphology along moraines level 1 and level 2. Also interpretations are made based on field observations. Moraines 1-3 numbers do not have an age connotation (Modified from Carrillo, 2006).

In the Mucubají valley the maximum glacier advance is related to a damaged frontal moraine at elevations lower than 3589 m (lower elevations than Level 1, moraine

number 3, Figure VI-1). A new geomorphological interpretation of aerial photographs realized in this dissertation shows three additional frontal moraines (lower elevations than Level 1, moraines labelled 1, 2 and 3, Figure VI-1). These moraines are located below the most external frontal moraine dated by Carcaillet et al. (2013) (moraine level 1, Figure VI-1). It suggests the maximum glacier advance happened at ages older than 22 ka. Considering that no significant exposure ages differences between moraines level 1 and level 2 are observed (Figure VI-1, Table V-3), the maximum glacier advance seems not to be much older than 22 ka. It occurred maybe during the same local LGM (defined between 22.75 and 19.96 Cal ka BP, Schubert and Rinaldi, 1987). Exposure ages from moraines level 1 and 2 correlates with previous radiocarbon dated outwash fan located at 3400 m. This outwash fan is located moraine level 1 down valley and has a basal age of 19.08±0.82 ^{14}C kyr BP (Schubert and Rinaldi, 1987). To form the outwash fan, it was necessary to have the moraine developed at an elevation higher than 3400 m. Moraine level 1 needed to be older than 19 ka (it is 21.5±1.3 ka). TCN exposure ages data presented a deglaciation history until the Pleistocene/Holocene transition. The Holocene activity of the Mucubají glacier seems to have occurred at least until 6.25 cal. kyr BP (5.46±0.40 ^{14}C kyr BP ka from aquatic moss, Stansell et al., 2005). This glacier activity was deduced from the Laguna de Mucubají sediment descriptions, characterized by low clastic content and low magnetic susceptibility (Stansell et al., 2005; Carrillo, 2006; Carrillo et al., 2008). A more recent glacier activity seems occurred between (0.64±0.05 ^{14}C kyr BP) 0.61 Cal. kyr BP and 0.13 Cal. kyr BP (Stansell et al., 2005).

The correlation between exposure ages and elevations allows estimating glacier front retreat rates (Mucubají article, Figure 3B). Glacier retreated in two distinct periods (Carcaillet et al., 2013). The oldest one occurred between the LGM and the Late Glacial (~15 ka). Ice retreat rate was estimated at ~25 m/ka (Carcaillet et al., 2013). The second one occurred between 15 ka and the Early Holocene (~11 ka). Ice retreat rate was ~310 m/ka. In addition, Late Pleistocene/Early Holocene climate change seems to prevent glacier development and produced a faster glacier retreat (Carcaillet et al., 2013).

VI-1.1.2 Mucuchahe valley (Sierra Nevada)

Mucuchache valley deglaciation ages range between 18.09±0.86 ka (MUCUF-1401) and 36.95±1.58 ka (MUCU-1403) (Table V-3). Results show a normal trend, with exposure ages decreasing up-valley. Geomorphological interpretation shows more than

one lateral moraine ridges, whose relation to their corresponding frontal moraine is unavailable (Figure V-4). Frontal moraines are absent. The Quaternary Boconó fault and Chama River activities could have erased the frontal moraines (see details in results **section V-2.1.2)**. A weighted average exposure age from the innermost lateral moraine indicate deglaciation and maximum glacier advance happening at ages older than 36.20±1.10 ka (n=2) (Figure V-4). Exposure age from the bottom valley indicate that glacier extinction happened at ages younger than ~18 ka.

A gradual glacier retreat could be deduced from the deglaciation chronologies. Between late MIS 3 and MIS 2 the glacier retreated at ~0.25 km/ka in the Mucuchache valley. The available data set does not allow proposing a more detailed ice retreat rate.

VI-1.1.3 Gavidia valley (Sierra Nevada)

Discussions on the deglaciation chronologies in the Gavidia valley, read the Gavidia article in **section V-2.1.2**. Gavidia article **5. Discussion-** *5.1 Deglaciation history in the Gavidia valley.*

VI-1.1.4 Mifafí valley (Sierra del Norte)

Exposure ages of lateral moraines indicate the beginning of the ice retreat at around 17-18 ka (Figure V-8, Table V-3). The Mifafí valley presents a regular slope along the valley bottom (~ 7º). Glacier retreated quickly at ~7 km/ka. This quickly ice retreat rate could be related to the very flat topography of the valley bottom. Vertical ELA variations in flatter valleys imply a significant accumulation zone areas variation (Kerr, 1993; Pedersen and Egholm, 2013). Accumulation zone areas are obtained from the hypsometric curves of former glaciers. A former glacier hypsometric curve is a graphic representation of the elevations distribution of the former glacier surface. This curve is obtained using the Cumulative area in the "x" axis and the Elevation in the "y" axis. Cumulative areas are summed until 100%. The area at elevations higher than the ELA indicates the accumulation zone proportion. In the Mifafí valley, the accumulation area of the former glacier at around 17 ka was 20% (Figure VI-2).

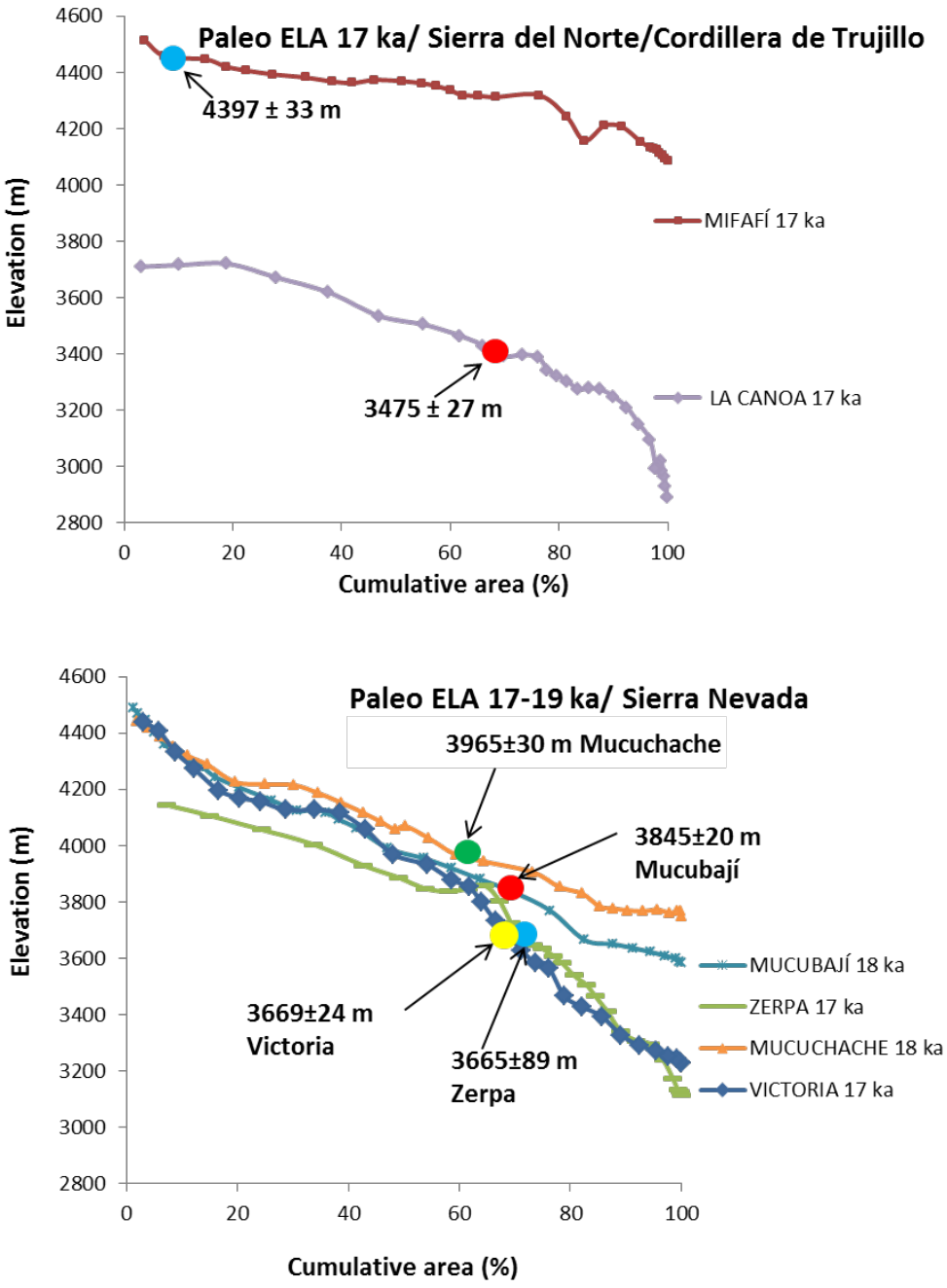

Figure VI-2. Hypsometric curves of former glaciers. Accumulation zone proportions are in general between 55-70%. The lowest value is related to the Mifafí former glacier at 17 ka.

The paleo ELA in the Mifafí valley is the highest at 4397±33 m (Figure VI-2). Paleo ELA differences could indicate different paleo precipitations, which could have been the lowest in the Mifafí valley. The Mifafí valley has a particular accumulation zone aspect (NE-SW) which receives more insolation. Accumulation zone receives the sun radiation longer time, which induces faster ablation rates. This lowest accumulation

zone area proportion, flat slopes, low paleo precipitations and accumulation zone aspect with more insolation produced the fastest ice retreat rate. Considering the ice retreat rate and horizontal distance between headwall and samples collected in the pegmatite dome (3.4 km, Figure V-8), complete deglaciation (i.e. glacier extinction) occurred at ~17 ka. Indeed, the glacier thinning occurred quickly as could be suggested by the insignificant difference between the highest sample collected in the pegmatite dome (Do-0309, 18.2±1.1 ka, 4172 m) and the valley axis (Do-0709, 17.8±1.6 ka, 4081 m). The glacier thinning (~100 m) occurred in few decades to hundreds of years.

VI-1.2 Non climatic parameters driving different dynamics of the former glaciers

The geomorphological description of the different valleys indicates the presence of glaciers cirques, striated bedrocks, polished surfaces and "roches moutonnées" (see geomorphological descriptions, in results section). These geomorphological features suggest that all studied former glaciers had warm-based thermal regime (Bennet and Glasser, 2009). Temperatures in the base of the glaciers define the thermal regime. Thermal regimes could be warm and cold. In warm-based glaciers melt water is released at the base of the glacier and the glacier abrasion is significant (Bennet and Glasser, 2009).

The noticeable moraines developments and preservation (between 50-150 m of apparent height) in the area formed by the Mucubají, Mucuchache and El Caballo can be related to the wide plain where moraines were deposited. This wide plain has low bottom valley slopes (~ 5º) and is observed from the Mucubají until the Mucuchache valley (Figure VI-3 B). Toward the Santo Domingo river catchment (between Victoria and Las Tapias catchment), slopes are also low around 5-7º (Figure VI-3 D). In contrast and despite the low bottom valley slopes, the Mifafí and the Gavidia valleys do not drain towards a large plain as the one described in the Mucubají or Mucuchache valleys (Figure VI-3 A, C).

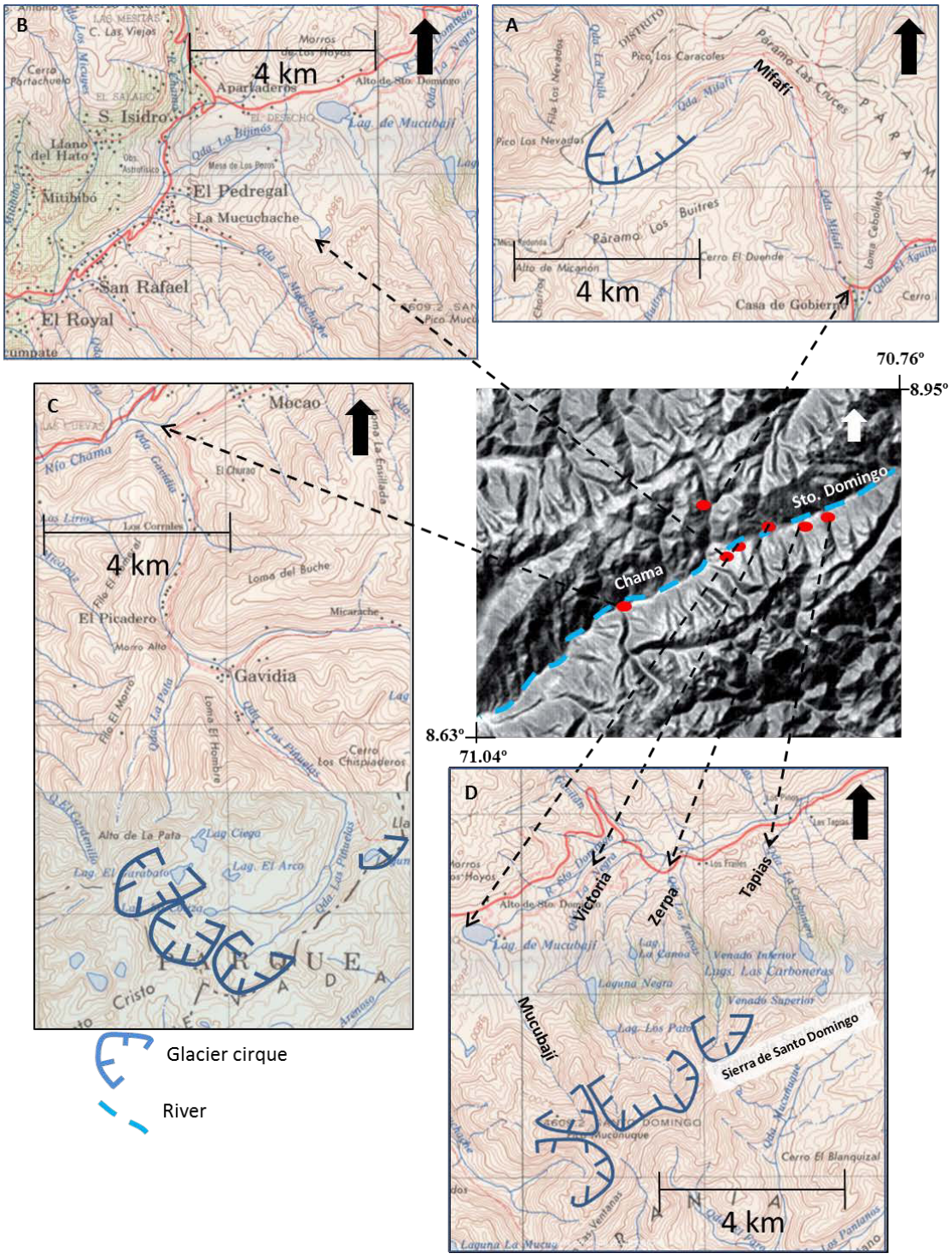

Figure VI-3. Field slopes inferences in areas from the Sierra Nevada and Sierra del Norte based on contours density. Very close contours involve field slopes higher than fields with more open contours. A) Mifafí valley. B) Plain close to the Mucubají valley. C) Gavidia valley. D) Sierra de Santo Domingo (La Victoria, Los Zerpa and Las Tapias moraines).

Glaciers in the central Mérida Andes had different glacier dynamics since MIS 3. Abrupt or gradual glaciers extinctions occurred in the same mountain range. In the Mucubají and the Mucuchache valleys, glaciers retreated gradually. In the Mucubají valley glacier existed between the LGM until the Holocene at least at around 6 ka. In the Mucuchache valley glaciers lived from MIS 3 at least to the LGM-OtD. In the Gavidia valley glacier retreated at slow ice retreat rates between 21 to 16.5 ka. In the Mucuchache valley upper area, in the vicinity of glacier cirques, the deglaciation chronology is unavailable. The history before 18 ka is not documented to describe the modality of post-LGM glacier retreat. In contrast, glacier evolutions after 16.5 ka in the Gavidia and at 17-18 ka in Mifafí indicate the fastest ice retreat rates (between ~ 4-7 km/ky). Former glacier extinctions occurred during a period as long as 0.5-1 ky. Gavidia and Mifafí valleys have similar geomorphic features such analogous cirques topography, NE-SW orientation of the accumulation zone. The configuration is thus more suitable to receive more solar radiation in comparison to the NW-SE accumulation zone orientation and cirques shapes of the Mucubají and Mucuchache. At least, insolation radiation differs at regional scale with lower radiation in northern Sierra Nevada hillside (Mucubají and Mucuchache valleys).

Another important factor which could control glacier dynamic is related to the accumulation zones areas. A comparison of these areas is made using the hypsometric curves of the former glaciers at 17-18 ka. Mucubají, Mucuchache and Mifafí curves were compared (Figure VI-2). Accumulation zone proportions in valleys from Sierra Nevada were between 60-70% whereas in Mifafí was lower than 20%. Low accumulation zones areas also controlled the rapid glacier extinction in the Mifafí valley.

Morphometric features as glaciers bottom valleys slopes, accumulation zones topography (glaciers cirques with steep walls), proportions and aspect (orientation), are parameters which control glaciers dynamics. Climate conditions which control glaciers dynamics are discussed in section VI-3.

VI-2 Deglaciation chronologies and glaciation reconstructions implications in the central MA

Possible evidences of the previous MIS 5 glaciers advances have been observed in the Sierra del Norte-Sierra Nevada (Chama, Mucujún valleys at 2600 m), close to Cordillera de Trujillo (Aracay valley) and Sierra Nevada-Sierra de Santo Domingo (Santo Domingo valley). These previous MIS 5 glaciers advances are suggested from diamicton outcrops (Schubert, 1984). In Mesa del Caballo (~3500 m, Figure VI-4), Mahaney et al. (2010a) evidenced two previous MIS 5 glaciers advances, based on analysis of mineral composition and weathered state of light and heavy minerals between till layers. The sharp contact between two glaciers advances (named LAG 4 and 5) indicated, a hiatus of unknown length of time. Authors indicate the studied LAG sections are below PED 5 section which was dated until around 60 ka (Mahaney et al., 2001). However, a stratigraphic correlation to corroborate LAG sections stratigraphic positions and ages is not present. LAG sediments relation to a previous MIS 5 glacier advance must be clarified.

The oldest evidence of the Early Mérida Glaciation (MIS 5) is identified in La Canoa moraine (RF3 section, ~2800 m) from analysis of glaciotectonized diamict dated at 81 ka (Mahaney et al., 2000). The PED 5 till material underlying peat (~60 ka) is related to the MIS 4 glacier advance in the Mesa del Caballo at ~ 3500 m (Mahaney et al., 2010b). In this work, MIS 4 glacier advance has been identified from the frontal moraine in the Pueblo Llano valley (moraine **1**, ~2500 m) at 71.96±1.74 ka (Table VI-1).

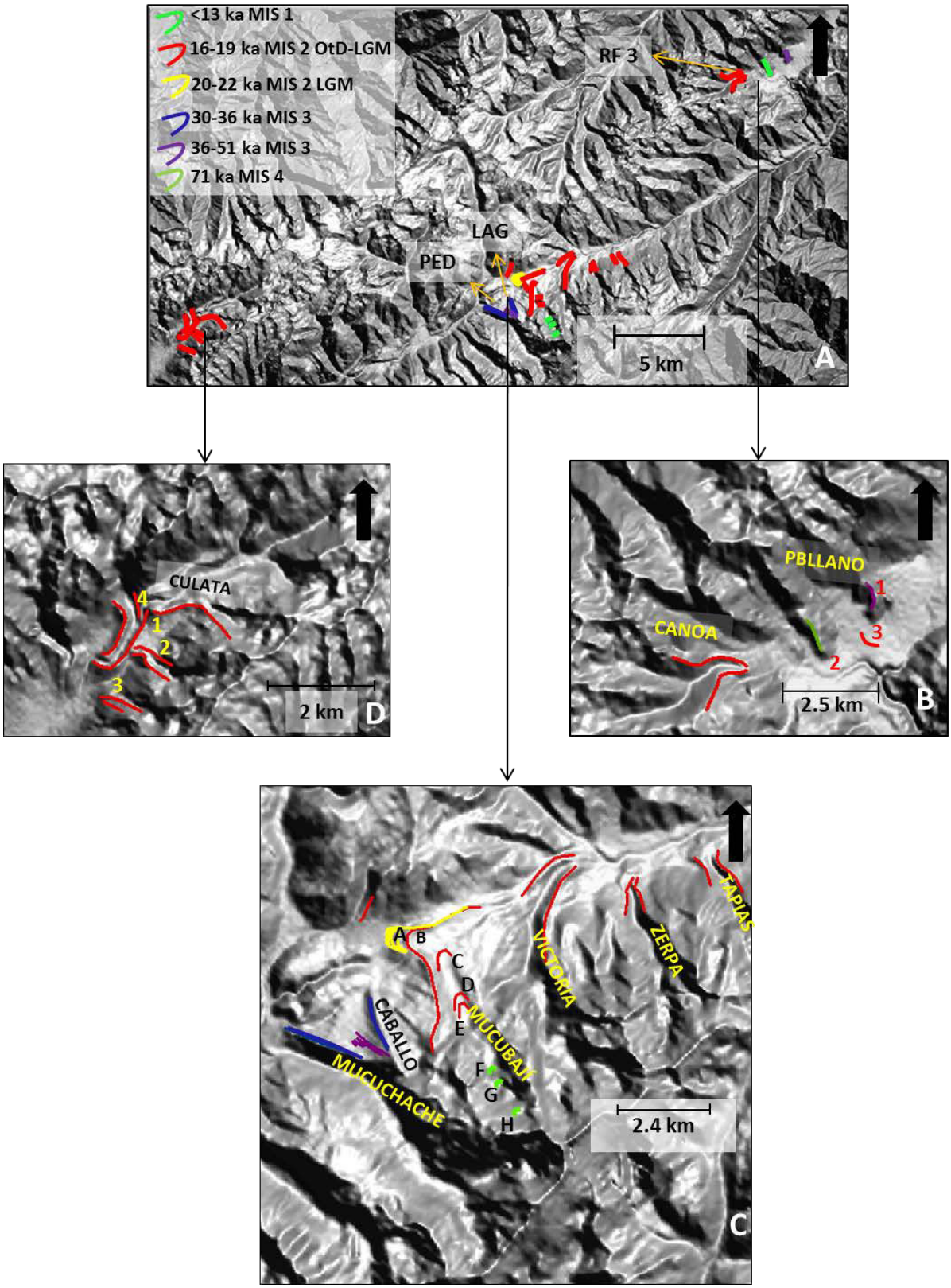

Figure VI-4. A) Glaciers advances in the central Mérida Andes. RF3 is La Canoa section where Mahaney et al. (2000) defined a MIS 5 glacier advance. PED section in Mesa del Caballo defined MIS 4 and MIS 2 glacier advances (Mahaney et al., 2010a). LAG section in Mesa del Caballo defined glaciers advances previous to MIS 5

(Mahaney et al., 2010b). B) Glacier advances in the Cordillera de Trujillo. C) Glacier advances in Sierra Nevada-Sierra de Santo Domingo. D) Glacier advances in La Culata, Mucujún catchment. Exposure ages of different moraines are in Table VI-1.

*Table VI-1. Glaciers advances deduced from frontal/lateral moraines weighted average exposure ages. Glaciers advances are inferred older than exposure ages presented but inside MIS 3. *, **, *** Weighted average exposure ages using updated values determined with ^{10}Be production rate (Kelly et al., 2013). Original values from: * Carcaillet et al. (2013), ** Wesnousky et al. (2012) and *** Guzmán (2013).*

Location	Moraine	Age	Elevation (m)	Stage
SIERRA NEVADA	ZERPA*	18.3±0.5	3100	MIS 2
	VICTORIA**	17.5±0.5	3140	
	TAPIAS	19.0±0.6	3100	
	MUCUBAJÍ A	21.5±1.8	3589	
	MUCUBAJÍ B	19.9±0.8	3620	
	MUCUBAJÍ C	18.5±1.3	3572	
	MUCUBAJÍ D	15.8±0.6	3615	
	MUCUBAJÍ E	17.1±0.9	3620	
	MUCUBAJÍ F	12.0±1.0	3862	MIS 1
	MUCUBAJÍ G	11.8±0.5	3982	
	MUCUBAJÍ H	12.5±0.9	4212	
	CABALLO	31.8±1.0	3600	MIS 3
	MUCUCHACHE	36.2±1.1	3400	
SIERRA DEL NORTE	CULATA 1*	16.9±0.2	3160	MIS 2
	CULATA 2	17.8±0.8	3500	
	CULATA 3	17.9±0.5	3300	
	CULATA 4 **	15.8±0.4	3400	
	DESECHO	18.0±0.6	3550	
CORDILLERA DE TRUJILLO	CANOA	17.9±1.1	2850	MIS 2
	PBLLANO3***	17.3±1.7	2467	
	PBLLANO1	50.3±1.2	2500	MIS 3
	PBLLANO2	72.0±1.7	2500	MIS 4

MIS 3 glacier advances were recorded at different locations of the Sierra Nevada and Cordillera de Trujillo (Figure VI-4, Table VI-1). 1) At ~50 ka in the Pueblo Llano

valley at ~2500 m, 2) between 30-36 ka in Sierra Nevada in the Mucuchache valley and El Caballo (~3400 m and ~3600 m respectively). Because of lateral moraines are not related to frontal moraines, accurate glacier advance ages are difficult to achieve. An age difference between lateral and frontal moraines in the Tatra Mountain was 3 ky (Makos et al., 2014). The Caballo and Mucuchache glacier advances are older than the TCN ages determined from the lateral moraines sampled. However, considering results from Makos et al. (2014) glacier advances occurred during the same MIS 3. Undated lateral moraines parallel to the dated Mucuchache valley moraine, have been related to glaciers advances older than around 36 ka (moraines interpreted in the geomorphological descriptions, Results section V-2.1.3) (Figure V-4 and Figure VI-4). These moraines could be related to MIS 3 glaciers advances based on its ridges appearance (shape and alteration). The ridges morphology and denudation are more alike to the Mucuchache moraine than for example to the Mucubají or Sierra de Santo Domingo moraines.

MIS 2 glacier advances are extensively evidenced in the Sierra Nevada (including Sierra de Santo Domingo), Sierra del Norte and Cordillera de Trujillo (Figure VI-4, Table VI-1). Only *sensu-stricto* LGM glacier advances are evidenced in the Mucubají valley (~3600 m, 21.5±1.3 ka and 19.9±0.8 ka) and at Las Tapias ~3100 m, 19.03±0.57 ka (Table VI-1, Figure VI-5). The more frequent glacier advances in the central MA occurred between 17-19 ka and correspond to the end of the LGM and beginning of the OtD (LGM-OtD) (Figure VI-5). In the Mucubají valley, this is located between 3572 m and 3620 m (Figure VI-4 and Table VI-1). In Sierra de Santo Domingo, the (LGM-OtD) glaciers advances were identified in La Victoria (~3140 m, 17.45±0.47 ka) and in Los Zerpa (~3100 m, 18.30±0.46 ka). In Sierra del Norte the LGM-OtD glaciers advances are related to La Culata moraines complex between 3160 m and 3500 m (moraines 1, 2, 3, 16.88±0.22 ka, 17.78 ±0.78 ka and 17.94±0.47 ka, respectively) (Table VI-1). At El Desecho moraine (~3500 m), the LGM-OtD was dated at 17.97±0.58 ka. In Cordillera de Trujillo, La Canoa moraine corresponds to the LGM-OtD (~2800 m, 17.89±1.09 ka). Finally, a moraine located between La Capellanía and El Pozo in the Pueblo Llano valley (~2467 m , 17.32 ± 1.72 ka) can be also related (Guzmán, 2013).

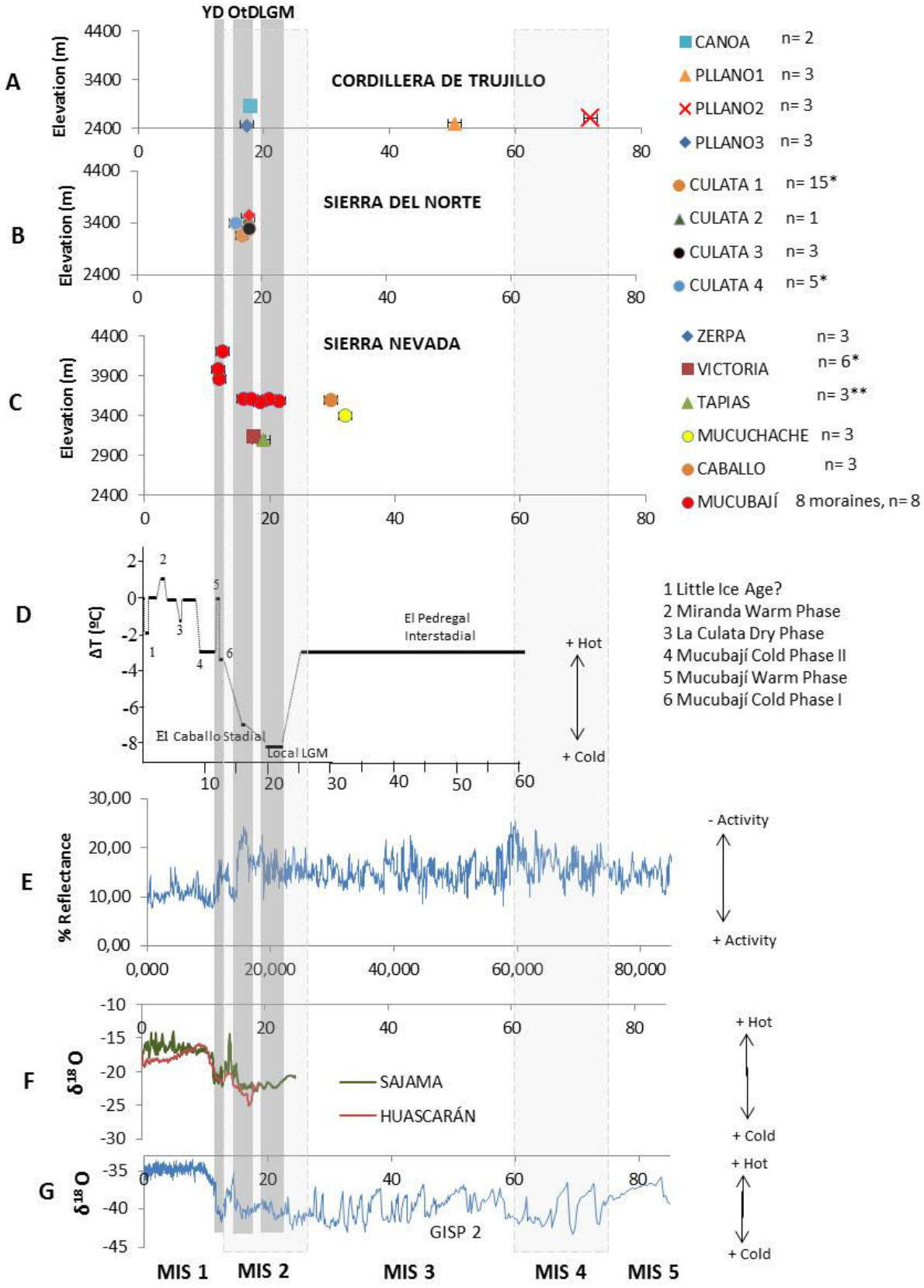

Figure VI-5. *Climate forcing driving central Mérida Andes glacier advances. Glacier advances in A) Cordillera de Trujillo, B) Sierra del Norte and C) Sierra Nevada-Sierra de Santo Domingo. D) Temperatures variations in the central Mérida Andes deduced*

from palynological and paleo ELA analysis (Stansell et al., 2007). E) Intertropical Convergence Zone (ITCZ) variability from the Cariaco Basin (Peterson et al., 2000). F) $\delta^{18}O$ variations from tropical ice cores: Sajama (Thompson et al., 1998) and Huascarán (Thompson, 2001). G) $\delta^{18}O$ variations from the ice core GISP 2 (Greenland) (Stuiver et al., 1995).

Late Pleistocene MIS 1 glaciers advances in the central MA are not extensively evidenced (Table VI-1, Figure VI-4 and Figure VI-5). The Younger Dryas (YD) glacier advance was recorded close to Lago Verde (~4000 m) in the Humboldt Massif (Sierra Nevada) at 10.52±2.00 ^{14}C BP (12.40 ka cal BP, Figure III-6 number 13), (Mahaney et al., 2008). Moreover, in the Humboldt Massif the YD glacier advance was suggested from geochemical and sedimentological analyses of Laguna Los Anteojos at 4045 m but no geomorphological evidences that attest this glacier advance is presented (Stansell et al., 2010). In the Mucubají valley, YD has been documented from dating (13.29±0.22, 13.64±0.15 and 13.66±0.44 cal ka BP) of peat samples covered by glaciofluvial materials (site MUM7B, ~3800 m, Mahaney et al., 2008). Authors "approximately" associated a down valley small push moraine to a YD glacier advance (at ~3700-3800 m). However, this push moraine down valley is older than ~ 13.4 ka; it is not in agreement with a YD glacier advance. New TCN exposure ages support this assumption. The push moraine is surrounded by data MU15-09, 15.4±1.4 ka, and MU08-09, 16.8±0.8 ka (level 6-level 7, Carcaillet at al., 2013 Figure 2B). The YD glacier advance in the Mucubají valley could rather be related to a moraine located at 3862 m (12.0±1.0 ka). In the Mucubají valley the YD was evidenced based on the magnetic susceptibility variations of the lake sediments (Carrillo, 2006; Carrillo et al., 2006).

Until present, YD glaciers advances have been recognized in the Sierra Nevada at elevations higher than 3860 m (3862 m in the Mucubají valley and 4000 m in the Humboldt Massif). The OtD-LGM advances are now evidenced in the Mucubají valley between 3570 m and 3620 m, and in Sierra de Santo Domingo at 3100 m. The OtD-LGM advances are now also evidenced in Sierra del Norte at 3100 and 3500 m and, in the Cordillera de Trujillo between 2400-2800 m. MIS 3 glacier advances are evidenced in Sierra Nevada in the Mucuchache and El Caballo at around 3400-3600 m and in Cordillera de Trujillo at 2500 m. MIS 4 glaciers advances are evidenced in the Mesa del

Caballo at 3500 m as well as in the Pueblo Llano valley at 2500 m. MIS 5 glacier advance are evidenced in La Canoa moraine in Cordillera de Trujillo at 2800 m. Glaciations older than the MIS 5 are not sufficiently documented. The only evidences correspond to the LAG section from Mesa del Caballo (3500 m).

At regional scale, the relation of glacier advances and elevations is not obvious (Table VI-1). MIS 4, MIS 3 and MIS 2 glacier advances produced glacial landforms at similar elevations. The Mérida Glaciation was described based on two moraine complexes observed between 2600-3500 m (Schubert, 1974). Mérida Glaciation was divided (Early and Late Mérida) based on chronological data (radiocarbon ages) from the moraines between 3000-3500 m (older than 13 cal kyr BP). Mérida Glaciation was also divided based on correlations between the Venezuelan and the Colombian Andes moraines complexes. Moraines located between 2600 m and 2800 m are related to the Early Mérida. Moraines between 2900 and 3500 m are related to the Late Mérida. This definition was a good first approximation to understand the Venezuelan Andes Glaciation. However, exposures ages determinations from Guzmán (2013) or from this dissertation provide new results to complement and precise the original knowledge of the Mérida Glaciation. Exposure ages of the Pueblo Llano valley (Guzmán, 2013, this dissertation) seems indicate glaciers arrived at elevation lower (2300 m, 2500 m respectively) than the previous established by Schubert (1974) (2600 m). The Mucuchache, El Caballo and Pueblo Llano MIS 3 glaciers advances also provide new information to the Mérida Glaciation. Considering the original Mérida Glaciation definitions, Mucuchache (3400 m) and El Caballo (3600 m) would be related to the late Mérida and the Pueblo Llano (2500 m) would be related to the early Mérida. However, exposure ages indicate that these moraines are related to El Pedregal Interstadial identified in the central MA between 25-60 ka (Figure VI-5) (Dirszowsky et al., 2005; Rull, 2005).

Maximum glaciers advances occurred at ages younger than the LGM *sensu stricto* during the MIS 2, between the LGM and OtD (17-19 ka). Also as in the Mucuchache and El Caballo, maximum glaciers advances were reached during the MIS 3. In an overall view, all the studied valleys, maximum glacier advances are not related to the global LGM *sensu stricto*. The central MA glaciation dynamic has a behavior similar to those of the other glacial areas of the tropical Andes. In the Ecuadorian, Peruvian and Bolivian Andes, maximum glacier advances mainly occurred during the MIS 3 (see

detail in Tropical Andes Glaciation, **section I-3.0**). Another similarity with the tropical Andes glaciations is the poor evidence of the YD glacier advances (see detail in Tropical Andes Glaciation, **section I-3.0**). It could suggest that the YD was not enough to produce significant ice volumes to produce glaciers advances. However, it is necessary to continue research on the topic of the YD impact in the tropical Andes.

VI-3.0 Paleoglaciology contributions to the paleoclimate record in the central MA

Local and global paleoclimate conditions, as temperature and precipitation, are determined from former glacier ELAs (e.g. Lachniet Vazquez-Selem, 2005; Stansell et al., 2007; Smith et al., 2011). However, considering that the absence of well constrained modern balance ratios are in the tropics (e.g. Rea et al., 2009), it is important keep in mind paleo ELA interpretations in this area yield significant uncertainty. In the following, paleo ELA results are used to infer local paleoclimate conditions trends.

Paleo ELA in the Mucubají valley during the LGM has been determined by Stansell et al. (2007). Values ranged between 3640-3710 m considering BR ratios between 5, 10 and AAR between 0.63-0.78. Lachniet and Vazquez-Selem, (2005) also determined paleo ELA in the Mucubají valley during the LGM. Paleo ELA ranged between 3626-4012 m using THAR ratios from 0.2 to 0.5, AAR ratios between 0.65 and 0.8 and, AABR with BR ratios of 5 and 25. In the frame of our project, Mucubají paleo ELA (LGM) was determined between 3769 m and 3847 m, which is slightly above Stansell et al., 2007 values and in the range proposed by Lachniet and Vazquez-Selem, (2005).

For La Victoria former glacier (LGM-OtD at 17.5 ka), paleo ELA was 3385-3813 m (Lachniet and Vásquez-Selem, 2005) or 3560-3725 m (Stansell et al., 2007). In this dissertation, paleo ELA is between 3645-3708 m; in agreement with previous researches. Finally, for La Canoa former glacier (LGM-OtD at 18 ka) Lachniet and Vazquez-Selem, (2005) determined values between 3040 and 3475 m, while calculations developed in this project yield an elevation between 3448 and 3502 m. New paleo ELA altitudes computed in the frame of this project are in the same order of previous studies in the central MA (Table VI-2, Table V-5).

Changes in temperature, precipitation, solar radiation or a combination of these factors are mainly responsible for glacier variability in the tropics (Kaser and Osmaston, 2002).

Lowest paleo ELA in the Mucuchache valley during MIS 3 (3765±37 m) (Figure V-11) should reflect more humid climate conditions in comparison with LGM or post LGM. This could be in agreement with a palynological analysis in the Sierra Nevada, which established a temperature rise of ~5º C during MIS 3 compared to the LGM (Dirszowsky et al., 2005; Rull, 2005). This temperature rise could provide more moisture during the MIS 3. Therefore, Mucuchache and El Caballo glaciers advances during the MIS 3 seem have been more driven by higher paleo precipitation.

In the Mérida Andes the LGM was dated between 22.75 and 19.96 cal ka BP (Schubert and Rinaldi, 1987). Paleo ELA was 3882±27 m in the Mucuchache valley and 3808±39 m in the Mucubají valley. LGM ELA gradient is relatively similar but increase during post LGM period (Mucuchache at 3965±30 m and Mucubají at 3845±20 m, at ~ 18 ka) (Figure V-11, Table V-5). This reflects that climate conditions in the vicinity of the Mucubají and Mucuchache valleys are more similar during the LGM. However, in this area, these climate conditions became more different post LGM.

More significant paleo ELA differences are observed at ages younger than 18 ka (Table V-5, Figure V-11). In Sierra Nevada values are 3965±30 m (La Mucuchache, 18 ka), 3845±20 m (Mucubají, 18 ka) and 3882±15 m (Mucubají, 16 ka); in Sierra de Santo Domingo, 3669±24 m (La Victoria) and 3669±89 m (Los Zerpa); in Sierra del Norte, 4397±33 m (Mifafí valley) and in Cordillera de Trujillo 3475±27 m. Variations observed between Sierra Nevada and Sierra de Santo Domingo former glaciers were originally attributed to differences in precipitation regimes (Lachniet and Vazquez-Selem, 2005). Stansell et al. (2007) suggested these paleo ELA variations were mainly due to different paleo temperatures. However, chronological control of the Sierra de Santo Domingo terminal moraines was not as documented as at present. Ages considered for Mucubají and La Victoria former glaciers by Lachniet and Vazquez-Selem, (2005) and, Stansell et al. (2007) were not strictly the same. In the Mucubají and La Victoria area, age of moraines were 21.5±1.8 ka (modified age from Carcaillet et al., 2013) and 17.45±0.47 ka (modified age from Wesnousky et al., 2012), respectively. To strictly compare paleo ELA based on glacial landforms with similar ages, it would be necessary to compare La Victoria with Mucubají at 16-18 ka. These moraines involve different former glaciers polygon with a different paleo ELA (3845±20 m, for Mucubají at 18 ka and 3882±15 m, for Mucubají at 16 ka). These paleo ELA could involve

different paleo temperatures presented by Stansell et al. (2007). La Victoria glacier advance could also be related to the Oldest Dryas (OtD) or El Caballo cold event. Seltzer (1992) concluded that in humid regions, temperature plays a larger role than precipitation in driving ELA variability. However, Pierrehumbert (1995) indicates that tropical temperatures variations were low at similar elevations during the late glacial. This was attributed to the weak Coriolis Effect and lack of north–south movement of air mass in the tropics.

Paleo ELA computed in Sierra del Norte presented the more significant difference in comparison with those of Sierra Nevada and Cordillera de Trujillo. These variations around 900 m indicate a different precipitation pattern during the 16-19 ka periods. The Mifafí valley in Sierra del Norte was the driest area. The wettest areas are the Sierra de Santo Domingo and Cordillera de Trujillo. This precipitation pattern is similar to the present day climate conditions in the central MA.

VI-3.1 Regional and Global climate forcing driving central Mérida Andes glacier variabilities

The most significant maximum glaciers advances occur at different periods at the scale of the central MA. Maximum glaciers advances have happened mainly during MIS 3 and particularly during MIS 2 at ages around 17-19 ka (Figure VI-5). The MIS 4 glacier advance seems to leave a strong imprint in the Pueblo Llano area; however the scatter data limit its interpretation.

The tropical climate is mainly controlled by insolation, which modulates the changes in the ITCZ position (Wang et al., 2001). During the last ~90 ka, influence of ITCZ in the Northern part of South America has been deduced from sediments studies from the Cariaco Basin (Peterson et al., 2000). During periods of continental high precipitations, high amount of terrigenous sediments reach into the basin. These sediments richer in iron and titanium (i.e. proxies of terrigenous sediments) show low reflectance values in comparison to carbonated sediments. High ITCZ activity implies high atmospheric moisture available to create precipitation. Low ITCZ activity is related to low moisture periods and consequent low runoff. In an overall trend, the highest ITCZ activity in the north of South America occurred during the MIS 3 between around 27-40 ka and during the MIS 5 between 75-85 ka (Figure VI-5).

MIS 4 Pueblo Llano glacier advance is related to intermediate precipitation values in the north of South America based on the Cariaco Basin sediments reflectance (Figure VI-5 A, E, F). Intermediate temperatures prevailed in the Northern Hemisphere based on the $\delta^{18}O$ values in GISP 2 (Figure VI-5 A, E, F). MIS 3 glaciers advances in the study area were related to ITCZ variations, which produced high runoff in the northern part of South America (Figure VI-5 E). During the same period, temperatures in the North Hemisphere were higher than during the MIS 2 as suggested by more positive $\delta^{18}O$ values in GISP 2 (Figure VI-5 F). In the MA, MIS 3 climatic conditions were warmer than the LGM and locally named El Pedregal Interstadial (Dirszowsky et al., 2005; Rull, 2005). Between MIS 3 and MIS 2 temperature dropped ~5 ºC as suggested by palynological analysis of continental sediment (Figure VI-5 D). These high temperatures during MIS 3 could imply high atmospheric moisture. High atmospheric moisture increases the precipitation rates and induces high accumulation gradients. High accumulation gradients imply more positive mass balances which produced the Mucuchache, El Caballo and Pueblo Llano former glaciers advances.

MIS 2 glacier advances corresponding to the LGM *sensu stricto* (in the Mucubají valley and Las Tapias) are related to the lowest temperatures in the North Hemisphere. It is deduced from the more negative values of the $\delta^{18}O$ values in GISP 2 (Figure VI-5 F). Paleoenvironmental proxies recorded in the MA indicate drier climate conditions during the LGM (Bradbury et al., 1981; Bradley et al., 1985; Weingarten et al., 1991; Salgado-Labouriau et al., 1992). Temperatures were ~8 ºC cooler than the current temperature (Stansell et al., 2007) (Figure VI-5 D). However, in the north of South America high runoff is still inferred from the sediments reflectance in the Cariaco basin (Figure VI-5 C, E). The LGM glacier advance in the Mucubají was driven by the temperature decrease (Stansell et al., 2007). During the final LGM-OtD (17-19 ka) the runoff was lower than the one recorded during LGM ITCZ. The glaciers advances correlate with the coldest temperatures recorded in the tropical ice core from Huascarán and Sajama in the Bolivian Andes (Thompson et al., 1998; 2001). The glaciers advances correlate also with the coldest temperatures recorded in the North Hemisphere (Stuiver et al., 1995) (Figure VI-5 F). In the central MA, cold climatic conditions were determined at 16.5±0.3 ka BP during El Caballo Stadial (Rull, 1998; Figure VI-5 D). El Caballo Stadial was identified based on pollen content of fluvioglacial sediments from Mesa del Caballo section (PED 5). Temperatures were around 7°C lower than today.

Warm and wet climate conditions during MIS 3 and MIS 4 could generate glacier advances mainly driven by precipitation. In an overall trend, deglaciation processes in the central part of the MA began in the Sierra Nevada valleys towards the Chama river catchment (Mucuchache, El Caballo and Mucubají). Elevations of the former glacier snout (or front) were the lowest in the Mucuchache valley. Deglaciation progressed through the wettest areas, towards the Santo Domingo river catchment (Victoria, Los Zerpa, Las Tapias). Most of these glacier valleys (except Gavidia) have similar accumulation zone morphology (NW-SE oriented, headwall around 4300-4500 m) (Figure VI-3 and Figure VI-4). The glaciers preservation seems to have mainly occurred in the Sierra de Santo Domingo area and Sierra del Norte. Deglaciation pattern seems to indicate differences in the local climatic conditions between Sierra Nevada and Sierra de Santo Domingo as was inferred from the paleo ELA analysis.

This dissertation represents a contribution to the knowledge of the glaciations in the Northern Andes. Late Pleistocene deglaciation histories in the central Mérida Andes (MA) were determined using the TCN dating (^{10}Be cosmonuclide). Knowledge about Late Pleistocene glacier dynamics variabilities was obtained from the deglaciation record deduced from TCN dating (100 samples) and compilation of published data. Our new contributions to reconstruct the Last Glaciation in the MA are provided by dating the different glaciers landforms, glaciers advances and retreats. Results represent also a new paleoglaciology contribution to the paleoclimate record in the central Mérida Andes.

Deglaciation histories and origin of variabilities

Different Late Pleistocene glacier's dynamics occurred in the central MA. In the Mucubají and the Mucuchache valleys, successive stages of glacier stop-advance were identified during an overall glacier withdrawal. In the Mucubají valley the glacier withdrawal occurred in two main periods. The oldest one between the LGM and the Late Glacial (~15 ka), when ice retreat rate was ~25 m/ka. The second one, between 15 ka and the Early Holocene (~11 ka), when ice retreat rate increased to ~310 m/ka. In the Mucuchache valley, maximum advance was earlier than ~36 ka (corresponding to the MIS 3) and glacier withdrawal occurred from late MIS 3 (~36 ka) until MIS 2 (~18 ka) with an ice retreat rate of ~0.25 km/ka. However, additional data is required to precise the glacial chronologies until the glacier extinction.

In the Gavidia and the Mifafí valleys, the moraine complexes absence (excepted limited lateral moraines) indicates that glacier dynamic was not intercalated by stages of glacier stop-advance during the overall glacier withdrawal. In the Gavidia valley, deglaciation happened in two separate periods. The first one occurred between the LGM (21 ka) and the Oldest Dryas stadial (OtD at ~16.5 ka or El Caballo Stadial). The second shorter period occurred at ages similar to the El Caballo Stadial (at ~16.5 ka). During the LGM/OtD-El Caballo Stadial interval, relatively cold climate conditions were maintained, leading to low glacier retreat (~0.26 km/ka). In contrast, the glacier extinction during the period younger than ~16.5 ka, occurred at high rates of ~4.7

km/ka. In the Mifafí valley in the Sierra del Norte, glacier withdrawal was the fastest with glacier retreat rate of ~7 km/ka.

The Gavidia and the Mifafí valleys experienced the fastest glaciers withdrawal at similar periods (OtD-El Caballo Stadial), despite the prevailing cold temperatures. This particular glacier dynamics could be explained by the NE-SW orientation of the accumulation zone compared to the NW-SE orientation in the Mucubají and Mucuchache valleys. The NW-SE orientation allows higher solar radiation in the glacier cirques. This condition contributes to a strong glacier reaction to climate change in comparison to less exposed cirques. In addition, different valley bottom slopes could explain different glacier dynamics. In the Mifafí and Gavidia valleys, the slopes are the lowest (5-7º). This topographical feature involves strong glacier surface reactivity to temperature raise. Climate changes also controlled glacier dynamics in the central MA. The transition from cold toward warm climate conditions during the Late Pleistocene-Early Holocene increased glacier withdrawal in the Mucubají valley. Whereas the lowest glacier withdrawal rates occurred during the transition LGM-OtD, when cold climate conditions still prevailed.

Last Glaciation (Mérida Glaciation) reconstruction

Glaciers advances from the MIS 4 to MIS 1 were recognized at elevations between 2500-4200 m. A MIS 4 glacier advance occurred in the Pueblo Llano valley, in Cordillera de Trujillo at around 2500 m. MIS 3 glaciers advances are located in the Sierra Nevada at around 3400-3600 m (Mucuchache and El Caballo lateral moraines, respectively). MIS 2 Glaciers advances are the most evidenced and located at elevations between around 2460-3620 m. The impact of the LGM *sensu stricto* in the central Mérida Andes was not extensively evidenced. Glacier advances related to the LGM occurred in the Mucubají valley (frontal moraine at around 3600 m) and Las Tapias (lateral-terminal moraine around 3100 m). Other significant group of glacier advances mainly occurred related to the OtD-El Caballo Stadial at around 17 ka (La Culata between 3100-3400 m; Sierra de Santo Domingo at ~ 3100 m and La Canoa at 2800 m). MIS 1 glacier evidences are poorly documented. MIS 1 glacier advances have been only identified in the Sierra Nevada (Mucubají valley at ~3800 m) during the YD. Maximum glacier advances in the central MA occurred mainly during MIS 2 between around 17-

19 ka or during MIS 3 at ages older than 30 ka. There is not a correlation between glaciers advances and elevations.

The knowledge about the Last Glaciation in the Mérida Andes, traditionally called Mérida Glaciation, is not completely understood. Schubert glaciological works (e.g. 1972; 1974) significantly contributed to this topic but classification currently needs to be improved. MIS 3 glaciers advances are firstly recognized in the Mérida Andes and are not considered in the Mérida Glaciation classification.

Paleoglaciology contribution to the Venezuelan Andes paleoclimate

Similar climate conditions seems to occur in the Sierra Nevada vicinity of the Mucubají and Mucuchache valleys during the LGM. It is based on more uniform paleo ELA in these valleys (3882±27 m and 3808±39 m, respectively). These climatic conditions become more different in post-LGM times. The precipitation pattern at around 16-19 ka (LGM-OtD-El Caballo Stadial) seems to be similar to the current one, based on the paleo ELA distribution. The driest area at this time could be related to the Mifafí valley in Sierra del Norte whereas wettest areas were related to Sierra de Santo Domingo and Cordillera de Trujillo.

MIS 3 and MIS 4 glacier advances are related to the highest ITCZ activity and global warming (locally identified as El Pedregal Interstadial). MIS 2 maximum glacier advances are related to the cold temperatures in the North Hemisphere and the coldest temperatures in the tropical Andes. Majority of these glacier advances seems to be more related to the coldest temperatures in the tropical Andes (LGM-OtD).

Perspectives

Many new scientific questions are raised. Numerous glacial landforms are still not described and not dated. This opens the opportunity to undertake new dating campaigns and thus improve the glacier chronologies in the MA. Special attention must be paid to the dating of glacier behavior during the pre-LGM period. Two suitable areas have been identified: the Sierra Nevada (NW of the Mucuchache valley) and the Pueblo Llano valleys in Cordillera de Trujillo. In fact, we sampled from the glacier´s cirque down to low lands during our 2014 field trip. Studying the Sierra del Norte and the Sierra Nevada towards the Bolivar and Humboldt Peaks, will allow improving the knowledge

of the MIS 2 and MIS 1 glacier advances. In this last site, one peak still is covered by a glacier.

In terms of tropical paleoclimate, this dissertation results could contribute to quantify the paleoclimate conditions using paleo ELA values and glacier modelling (e.g. Plummer and Phillips, 2003). Paleo ELA evolutions for many valleys are now available and could be used as input for the glacier models. During this dissertation, isotope stables results were obtained for sediments in the Mucubají Lake, which was possible thanks to the CSIC Institute collaboration (Spain). The original idea was to integrate paleoclimate inferences obtained using both paleoglaciology and isotopes. However, it was not possible to validate the isotopes results. In the future, it should be very helpful to integrate these results and new ones from other sediment lakes to improve the MA paleoclimate knowledge.

Chronological data obtained also open the opportunity to study Neotectonics in the central Mérida Andes. Glacier landforms from the Sierra de Santo Domingo or Sierra del Norte as El Desecho moraine are affected by the Boconó Fault. Geochronological dating of the glacial landforms allows calculating the moraines Quaternary offsets and will provide a contribution to quantify the Boconó Fault displacement rate since MIS 2.

Finally, another line of research could be the analysis of water volumes release during glacier recession and the contribution in terms of hydrological balance and sediments transport.

A

Alley, R.B., Marotzke, J., Nordhaus, W.D., Overpeck, J.T., Peteet, D.M., Pielke, R.A., Pierrehumbert, R.T., 2003. Abrupt climate change. Science 299 (5615), 2005-2010. http://dx.doi.org/10.1126/science.1081056.

Andrews, J.T., 1972. Glacier power, mass balance, velocities and erosion potential. Z. Geomorphol. 13, 1-17.

Angel, I., Carrillo, E., Carcaillet, J., Audemard, F.A., Beck C., 2013. Geocronología con el isótopo cosmogénicos ^{10}Be, aplicación para el estudio de la dinámica glaciar cuaternaria en la región central de los Andes de Mérida. GEOS. 44, 73-82.

Armstrong, R. A. 2004. Lichens, lichenometry and global warming. Microbiologist 4, 32-35.
Audemard, F.A., 1999. Morpho-structural expression of active thrust fault systems in humid tropical foothills of Colombia and Venezuela. Zeitschrift fur Geomorphologie 118, 1–18.

Audemard, F. E., 1991. Tectonics of Western of Venezuela. Ph.D. Thesis, Rice University, Texas, 245 pp + appendices.

Audemard, F.A., 2003. Geomorphic and geologic evidence of ongoing uplift and deformation in the Mérida Andes, Venezuela. Quat. Int. 101-102, 43-65.

Audemard, F.E., Audemard, F.A., 2002. Structure of the Mérida Andes, Venezuela: relations with the South America-Caribbean geodynamic interaction. Tectonophysics 345, 299–327.

Audemard, F.A., Ollarves R., Bechtold M., Díaz G., Beck C., Carrillo E., Pantosti D., Diederix H., 2008. Trench investigation on the main strand of the Boconó fault in its central section, at Mesa del Caballo, Mérida Andes, Venezuela. Tectonophysics 459, 38–53.

Azócar, A. and Monasterio, M., 1980. Caracterización ecológica del clima en el Páramo de Mucubají. In: Monasterio, M. (Ed). Estudios Ecológicos en los Páramos Andinos. Editorial de la Universidad de Los Andes, Mérida, 207-223.

B

Balco, G., 2011. Contributions and unrealized potential contributions of cosmogenicnuclide exposure dating to glacier chronology, 1990-2010. Quat. Sci. Rev. 30, 3-27.

Balco, G., Stone, J.O., Lifton, N.A., Dunai, T.J., 2008. A complete and easily accessible means of calculation surface exposure ages or erosion rates from ^{10}Be and ^{26}Al measurements. Quaternary Geochronology 3, 174-195.

Barr, I. D. and Lovell, H., 2014. A review of topographic controls on moraine distribution. Geomorphology 226, 44–64.

Benn, D.I., 1992. The genesis and significance of 'hummocky moraine': evidence from the Isle of Skye, Scotland. Quat. Sci. Rev. 11 (7–8), 781–799.

Benn D.I., Evans D.J.A., 2010. *Glaciers and Glaciation*. Second edition, Hodder Education, Abingdon, United Kingdom.

Benn, D., Hulton, N. R. J., 2010. An ExcelTM spreadsheet program for reconstructing the surface profile of former mountain glaciers and ice caps. Computers & Geosciences 36, 605–610

Benn, D.I., Owen, L. A., Osmaston, H.A., Seltzer, G. O., Porter, S. C., Mark, B., 2005. Reconstruction of equilibrium-line altitudes for tropical and sub-tropical glaciers. Quaternary International 138-139, 8-21.

Bennett, M. and Glasser, N., 2009. Glacial Geology Ice Sheets and Landforms. 2nd edition. Wiley-Blackwell, 385 pp.

Bermúdez, M., 2009. Cenozoic Exhumation Patterns across the Venezuelan Andes: Insights from Fission-track Thermochronology. Ph.D. thesis. Joseph Fourier University, France, p. 305.

Bermúdez, M.A., Kohn, B., van der Beek, P., Bernet, M., O'Sullivan, P., Shagam, R., 2010. Spatial and temporal patterns of exhumation across the Venezuelan Andes: Implications for Cenozoic Caribbean geodynamics. Tectonics 29, doi:10.1029/2009TC002635.

Bezada, M., 1989. Geología Glacial del Cuaternario de la región de Santo Domingo -Pueblo Llano - Las Mesitas (Estados Mérida y Trujillo). PhD. Sc Tesis. Instituto Venezolano de Investigaciones Científicas, Caracas, Venezuela.

Bickerton, R.W., Matthews, J.A., 1992. On the accuracy of lichenometric dates: an assessment based on the 'Little Ice Age' moraine sequence of Nigardsbreen, southern Norway. The Holocene 2, 227-237.

Bickerton, R.W., Matthews, J.A., 1993. "Little Ice Age" variations of outlet glaciers from the Jostedalsbreen ice-cap, southern Norway. A regional lichenometric dating study of ice-marginal moraine sequences and their climatic significance. Journal of Quaternary Science 8, 45-66.

Bierman P. R., 1994. Using in situ produced cosmogenic isotopes to estimate rates of landscape evolution: A review from the geomorphic perspective. J. Geophys. Res., 99 (B7), 13885-13896.

Blard, P.H., Braucher, R., Lavé, J., Bourlès, D., 2013. Cosmogenic Be-10 production rate calibrated against He-3 in the high Tropical Andes (3800–4900 m, 20–22° S). Earth and Planetary Science Letters, 382, 140-149.

Blunier, T., Chappellaz, J., Schwander, J., Dallenbach, A., Stauffer, B., Stocker, T.F., Raynaud, D., Jouzel, J., Clausen, H.B., Hammer, C.U., Johnsen, S.J., 1998. Asynchrony of Antarctic and Greenland climate change during the last glacial period. Nature 394, 739-743.

Bond, G., Showers,W., Elliot, M., Evans, M., Lotti, R., Hajdas, I., Bonani, G., et al., 1999. The North Atlantic's 1-2 kyr climate rhythm: relation to Heinrich Events, Dansgaard/Oeschger cycles and the Little Ice Age. In: Clark, P.U., Webb, R.S., Keigwin, L.D. (Eds.), Mechanisms of Global Clime Change at Millennial Time Scales, Geophysical Monography. Washington, pp. 35-58.

Boyle, E.A., 2000. Is ocean thermohaline circulation linked to abrupt stadial/interstadial transitions? Quat. Sci. Rev. 19 (1-5), 255e272 http://dx.doi.org/10.1016/ S0277-3791(99)00065-7.

Bradbury, J.P., Leyden, B., Salgado-Labouriau, M., Lewis Jr., W.M., Schubert, C., Binford, M.W., Frey, D.G., Whitehead, D.R., Weibezahn, F.H., 1981. Late quaternary environmental history of Lake Valencia, Venezuela. Science 214, 1299–1305.

Bradley, R.S., Yuretich, R., Salgado-Labouriau, M.L., Weingarten, B., 1985. Late Quaternary paleoenvironmental reconstruction using lake sediments from the Venezuelan Andes: preliminary results. Zeitschrift für Gletscherkunde und Glazialgeologie 21, 97–106.

Braithwaite, R. J., 1985. Calculation of degree-days for glacier-climate research. Zeitschrift für Gletscherkunde und Glazialgeologie 20, 1-8.

Braithwaite, R. J., 2008. Temperature and precipitation climate at the equilibrium-line altitude of glaciers expressed by the degree-day factor for melting snow. Journal of Glaciology 54 (186), 437-444.
Braucher, R., Brown, E. T., Bourlès, D. L. Colin, F., 2003. In situ produced 10Be measurements at great depths: implications for production rates by fast muons. Earth Planet. Sci. Lett., 211, 251-258.

Braun, C., Bezada, M., 2013. The history and disappearance of glacier in Venezuela. Journal of Latin American Geography. 12, 85-124.

Briner, J. P., 2011. Dating glacial landforms. In: Singh, V.P., Singh, P., Haritashya, U.K. (Eds.), Encyclopedia of snow, ice and glaciers. Springer, Dordrecht, 175-186.

Briner, J.P., Swanson, T., 1998. Using inherited cosmogenic ^{36}Cl to constrain glacial erosion rates of the Cordilleran ice sheet. Geology, 26, 3-6.

Brown, E.T., Edmond, J.M., Raisbeck, G.M., Yiou, F., Kurz, M.D., Brook, E.J., 1991. Examination of surface exposure ages of Antartic moraines using in situ produced ^{10}Be and ^{26}Al. Geochimica Cosmochimica Acta 55, 2269–2283.

C

Carcaillet, 2003. Modulation de la production atmosphérique du cosmonucléide béryllium-10 lors des excursions et inversions géomagnétiques depuis 1,3 Ma. Ph.D. Thesis. Université Aix-Marseille III. 215 p.

Carcaillet, J., Angel, I., Carrillo, E., Audemard, F.A., Beck, C., 2013. Timing of the last deglaciation in the Sierra Nevada of the Mérida Andes, Venezuela. Quat. Res. 80 (3), 482-494.

Carr, S.J., Coleman, C.G., 2007. An improved technique for the reconstruction of former glacier mass-balance and dynamics. Geomorphology 92, 76-90.

Carr, S.J., Lukas, S., Mills, S.C., 2010. Glacier reconstruction and mass-balance modelling as a geomorphic and palaeoclimatic tool. Earth Surface Processes and Landforms 35, 1103-1115

Carrillo, E., 2006. L'Enregistrement sédimentaire de la sismicité récente le long de la frontière sudoccidentale de la plaque caraïbe 'Faille de Boconó) : Modalités et chronologie. Contribution à l'estimation de l'aléa sismique régional. Ph.D. Thesis, Université de Savoie, France, 335 pp.

Carrillo, E., Yépez, S., 2008. Evolución de glaciares en Venezuela: glaciares de los Picos Humboldt y Bonpland. Boletín Geológico 42, 97-108.

Carrillo, E., Beck, C., Audemard, F.A., Moreno, M., Ollarves, R., 2008. Disentangling Late Quaternary climatic and seismo-tectonic controls on Lake Mucubají sedimentation (Mérida Andes, Venezuela). Palaeogeography, Palaeoclimatology, Palaeoecology 259, 284–300.

Cediel, F., Shaw, R. P., Cáceres, C., 2003. Tectonic assembly of the Northern Andean Block. In: Bartolini, C., Buffler, R.T., Blickwede, J. (Eds), The Circum-Gulf of Mexico and the Caribbean: Hydrocarbon habitats, basin formation, and plate tectonics. AAPG Memoir 79, 815-848.

Clapperton CM, McEwan C. 1985. Late Quaternary moraines in the Chimborazo area, Ecuador. Arctic and Alpine Research 17: 135–142.

Clapperton CM, Hall M, Mothes P, Hole MJ, Still JW, Helmens KF, Kuhry P, Gennell A. M. D., 1997. A YD icecap in the equatorial Andes. Quaternary Research 47: 13–28.

CLIMAP Project Members, 1976. The surface of the ice-age earth. Science 191 (4232), 1131-1137.

CLIMAP Project Members, 1981. Seasonal Reconstruction of the Earth's Surface at the Last Glacial Maximum.

Colletta, B., Roure, F., De Toni, B., Loureiro, D., Passalacqua, H., Gou, Y., 1997. Tectonic inheritance, crustal architecture, and contrasting structural styles in the Venezuelan Andes. Tectonics 16 (5), 777–794.

Coronato, A. and Rabassa, J. 2007. Late Quaternary in South America. Encyclopedia of Quaternary Science, 1101-1108.

Chmeleff, J., von Blanckenburg, F., Kossert, K., Jakob, J., 2010. Determination of the ^{10}Be half-life by multicollector ICP-MS and liquid scintillation counting. Nuclear Instruments and Methods in Physics Research B 268 (2), 192–199.

Chiang, J. C. H., 2009. The Tropics in Paleoclimate. Annu. Rev. Earth Planet. Sci. 37, 263–297.

D

Dansgaard, W., Johnsen, S.J., Clausen, H.B., Dahl-Jensen, D., Gundestrup, N.S., Hammer, C.U., Hvidberg, C.S., 1993. Evidence for general instability of past climate from a 250-kyr ice-core record. Nature 364 (6434), 218-220. http:// dx.doi.org/10.1038/364218a0.

De Toni, B., Kellogg, J., 1993. Seismic evidence for blind thrusting of the Northwestern flank of the Venezuelan Andes. Tectonics 12, 1393-1409.

Dirszowsky, R.W., Mahaney, W.C., Hodder, K.R., Milner, M.W., Kalm, V, Bezada, M., Beukens, R.P., 2005. Lithostratigraphy of the Mérida (Wisconsinan) glaciation and Pedregal interstade, Mérida Andes, northwestern Venezuela. Journal of South American Earth Sciences 19, 525–536.

Dunai, T., 2010. Cosmogenic Nuclides : Principles, Concepts and Applications in the Earth Surface Sciences. Cambridge University Press. 180 pages.

Dunne, J., Elmore, D., Muzikar, P., 1999. Scaling factors for the rates of production of cosmogenic nuclides for geometric shielding and attenuation at depth on sloped surfaces. Geomorphology 27 (1–2), 3–11.

E

Eyles, N., 1983.Modern Icelandic glaciers as depositional models for 'hummocky moraine' in the Scottish Highlands. In: Evenson, E.B., Schlüchter, C., Rabassa, J. (Eds.), Tills and Related Deposits. Balkema, Rotterdam, pp. 47–60.

F

Fairbanks, R.G., 1989. A 17,000-year glacio-eustatic sea level record: influence of glacial melting rates on the Younger Dryas event and deep-ocean circulation. Nature 342, 637–642.

FAQ, 2004. Shuttle Radar Topography Mission (SRTM). http://seamless.usgs.gov/website/seamless/faq/srtm_faq.asp (accessed 8 April 2007).

Farber DL, Hancock GS, Finkel RC, Rodbell D. 2005. The age and extent of tropical alpine glaciation in the Cordillera Blanca, Peru. Journal of Quaternary Science 20, 759–776.

Fox, A.N., 1993. Snowline altitude and climate at present and during the Last Pleistocene Glacial Maximum in the Central Andes (5°–28°S). Ph.D. Thesis. Cornell University.

Francou, B. and Pouyaud, B., 2007 In: ¿EL FIN DE LAS CUMBRES NEVADAS? Glaciares y Cambio Climático en la Comunidad Andina. IRD PNUMA, Lima, Peru. 103 pages.

Francou, B., Ribstein, P., Saravia, R., Tiriau, E., 1995. Monthly balance and water discharge of an inter-tropical glacier: Zongo glacier Cordillera Real, Bolivia, 16°S. J. Glaciol. 41 (137), 61–67.

G

Goering, 1962, Venezuela, el más bello país tropical.: Mérida, Ediciones de la Universidad de los Andes, 172 páginas.

Golledge, N.R., 2007. An ice cap landsystem for palaeoglaciological reconstructions: characterizing the Younger Dryas in western Scotland. Quat. Sci. Rev. 26 (1), 213–229.

Gosse, J.C., Phillips, F.M., 2001. Terrestrial in situ cosmogenic nuclides: theory and application. Quaternary Science Reviews, 20, 1475-1560.

Gosse, J.C., Klein, J., Evenson, E.B., Lawn, B., Middleton, R.1995. ^{10}Be Dating of the Duration and Retreat of the Last Pinedale Glacial Sequence. Science, 268, 1329-1333.

Gonzalez, E., van der Hammen, T., Flint, R.F., 1965. Late Quaternary glacial and vegetation sequence in Valle de Lagunillas, Sierra Nevada del Cocuy, Colombia. Leidse Geologische Medelingen 32, 157–182.

González, O., Bezada, M., 2006. GEOLOGÍA GLACIAL Y POSTGLACIAL DEL VALLE DE LA QUEBRADA SAISAY, ANDES CENTRALES VENEZOLANOS (ESTADO MÉRIDA). Acta Científica Venezolana, 57 (4): 159-166.

Guido, Z.S., Ward, D.J., Aderson, R.S., 2007. Pacing the post-Last Glacial Maximum demise of the Animas Valley glacier and the San Juan Mountain ice cap, Colorado. Geology, 35,739-742.

Guzmán, O., Vassallo, R., Audemard, F., Mugnier,J-L., Oropeza, J, Yepez, S., Carcaillet, J., Alvarado, M, Carrillo, E., 2013. ^{10}Be dating of river terraces of Santo Domingo river, on Southeastern flank of the Mérida Andes, Venezuela: Tectonic and climatic implications. Journal of South American Earth Sciences 48, 85-96.

Guzmán, O. 2013. Timing and dynamics of river terraces formation in moderate uplifted ranges: the example of Venezuela and Albania. Ph.D. Thesis, Université de Grenoble, France, 269 pp.

H

Hackley, P.C., Urbani, F., Karlsen, A.W., Garrity, C.P., 2005. Geologic shaded relief map of Venezuela. Open-File Report - U. S. Geological Survey. 2005. U. S. Geological Survey. Reston, VA, United States. Pages: 2 sheets. 2005.

Hanebuth, T., Stattegger, K., and Grootes, P. M., 2000. Rapid flooding of the Sunda Shelf: A late-glacial sea-level record. Science 288, 1033–1035.

Hansen BCS, Rodbell DT, Seltzer GO, León B, Young KR, Abbott M. 2003. Late glacial and Holocene vegetational history from two sites in the western Cordillera of southwestern Ecuador. Palaeogeography, Palaeoclimatology, Palaeoecology 194, 79–108.

Hastenrath, S., 1985. A review of Pleistocene to Holocene glacier variations in the tropics. Zeitschrift fu¨ r Gletscherkunde und Glazialgeologie 21, 183–194.

Haug, G. H., et al., 2005. North Pacific seasonality and the glaciation of North America 2.7 million years ago, Nature, 433, 821-825.

Heine K., 1995. Late Quaternary glacier advances in the Ecuadorian Andes: a preliminary report. Quaternary of South America and Antarctic Peninsula 9, 1–22.

Heine K, Heine J., 1996. Late glacial climatic fluctuations in Ecuador: glacial retreat during YD time. Arctic and Alpine Research 28, 496–501.

Heinrich, H., 1988. Origin and consequences of cyclic ice rafting in the Northeast Atlantic Ocean during the past 130,000 years. Quat. Res. 29 (2), 142-152. http://dx.doi.org/10.1016/0033-5894.

Helmens, K.F., 1988. Late Pleistocene glacial sequence in the area of the high plain of Bogotá (eastern cordillera, Colombia). Palaeogeography, Palaeoclimatology, and Palaeoecology 67, 263–283.

Henderson-Sellers, A., Robinson, P.J., 1986. Contemporary Climatology. Longman, Essex (UK) (439 pages).

Hemming, S.R., 2004. Heinrich events: massive late Pleistocene detritus layers of the north Atlantic and their global climate imprint. Reviews of Geophysics 42. doi:10.1029/2003RG000128 RG1005

Heyman, J., 2014. Paleoglaciation of the Tibetan Plateau and surrounding mountains based on exposure ages and ELA depression estimates. Quaternary Science Reviews 91, 30-41.

Hoffman, J.A., 1975. Climate Atlas of South America: Ginebra, Hungary, World Meteorological Organization.

Hospers, J., Van Wijnen, J., 1959. The gravity field of the Venezuelan Andes and adjacents basins. Verslag van de Gewone Vergadering van de Afdeling Natuurkunde, Koninklijke Nederlandse Akademie van Wetenschappen 23 (1), 1-95.

Huber, C., Leuenberger, M., Spahni, R., Flückiger, J., Schwander, J., Stocker, T.F., Johnsen, S., 2006. Isotope calibrated Greenland temperature record over Marine Isotope Stage 3 and its relation to CH4. Earth and Planetary Science Letters 243 (3-4), 504-519. http://dx.doi.org/10.1016/j.epsl.2006.01.002.

Hughes P.D., Gibbard P.L., Woodward J.C., 2005. Quaternary glacial records in mountain regions: a formal stratigraphical approach. *Episodes* 28, 85–92.

Hughes P.D., Gibbard P.L., 2014. A stratigraphical basis for the Last Glacial Maximum (LGM). Quaternary International xxx, 1-12

I

Iversen, J., 1954. The Late-glacial Flora of Denmark and its Relation to Climate and Soil. In: Danmarks Geologiske Undersøgelser, Række II, 80.

Ives, J.D.,Andrews, J.T.,Barry, R.G., 1975. Growth and decay of the Laurentide ice sheet and comparisons with Fenno-Scandinavia. Die Naturwiss. 62, 118–125.

Ivy-Ochs, S., Kerschner, H., Schlüchter, C., 2007. Cosmogenic nuclides and the dating of Late Glacial and Early Holocene glacier variations: the Alpine perspective. Quaternary International 164–165, 53–63.

Ivy-Ochs, S., Kerschner, H., Reuther, A., Maisch, M., Sailer, R., Schaefer, J., Kubik, P.W., Synal, H.A., Schlüchter, Ch., 2006. The timing of glacier advances in the northern European Alps based on surface exposure dating with cosmogenic ^{10}Be, ^{26}Al, ^{36}Cl, and ^{21}Ne. In: Siame, L.L., Bourlès, D.L., Brown, E.T. (Eds.), In Situ– Produced Cosmogenic Nuclides and Quantification of Geological Processes: Geological Society of America Special Paper, vol. 415, pp. 43–60. doi:10.1130/2006.2415(04).

J

Jácome, M., Audemard, F. E., Graterol, V., 1995. A Seismic, Gravimetric and Geologic Interpretation of a Transandean Profile Across the Venezuelan Andes. I Latinoamerican Geophys. Congress, Rio de Janeiro, Brasil, 15-18.

Jahn, A., 1912. La cordillera venezolana de los Andes.: Revista Técnica del Ministerio de Obras Públicas 2, No. 21, 451-488.

Jahn, A., 1925. Observaciones glaciológicas en los Andes Venezolanos: Cultura Venezolana 64, 265-280.

Jahn, A., 1931. Los páramos venezolanos: Boletín de la Sociedad Venezolana de Ciencias Naturales 1, No. 3, 93-132.

Jomelli, V., Favier, V., Rabatel, A., Brunstein, D., Hoffmann, G., and Francou, B., 2009. Fluctuations of glaciers in the tropical Andes over the last millennium and palaeoclimatic implications: A review, Palaeogeogr. Palaeocl., 281, 269–282, doi:10.1016/j.palaeo.2008.10.033.

K

Kalm, V., Mahaney, W. C., 2011. Late Quaternary Glaciation in the Venezuelan (Mérida) Andes. Developments in Quart. Sci. 15. 835-841.

Kaplan, M.R.,Hein, A.S.,Hubbard, A.,Lax, S.M., 2009. Can glacial erosion limit the extent of glaciation? Geomorphology 103 (2), 172–179.

Kaplan, M.R., Schaefer, J., Denton, G.H., Barrell, D.J.A., Chinn, T.J.H., Putnam, A.E., Anderson, B.G., Finkel, R.C., Schwartz, R., Doughty, A.M., 2010. Glacier retreat in New Zealand during the Younger Dryas Stadial. Nature 467, 194e197.

Kaplan, M.R., Strelin, J.A., Schaefer, J.M., Denton, G.H., Finkel R.C., Schwartz, R., Putnam, A.E., Vandergoes, M.J., Goehring B.M., Travis, S.G., 2011. In-situ cosmogenic ^{10}Be production rate at Lago Argentino, Patagonia: Implications for late-glacial climate chronology. Earth and Planetary Science Letters 309, 21–32.

Kaser, G., 1995. How do tropical glaciers behave? Some comparisons between tropical and mid-latitude glaciers. In: Ribstein, P., Francou, B. (Eds.), Aguas Glaciares y Cambios Climaticos en los Andes Tropicales. Conferencias y Posters del Seminario Internacional, La Paz, 13–16 Junio 1995, pp. 207–218.

Kaser, G., 2001. Glacier–climate interaction at low-latitudes. J. Glaciol. 47 (157), 195–204.

Kaser, G., Georges, Ch., 1997. Changes of the equilibrium line altitude in the tropical Cordillera Blanca (Perú) between 1930 and 1950 and their spatial variations. *Ann. Glac*., **24**. Papers from the International Symposium on Changing Glaciers held in Fjærland, Norway, 24.-26. June 1996, 344-349.

Kaser, G., Osmaston, H., 2002. Tropical Glaciers. Cambridge University Press, Cambridge 207 pp.

Kellogg, J., Bonini, W., 1982. Subduction of the Caribbean Plate and basement uplifts in the overriding South- American Plate. Tectonics 1(3), 251-276.

Kelly, M.A., Lowell T.V., Applegate, P.J., Phillips, F. M., Schaefer, J. M., Smith, C. A., Kim, H., Leonard, K.C., 2013. A locally calibrated, late glacial ^{10}Be production rate from low-latitude, high-altitude site in the Peruvian Andes. Quaternary Geochronology, *In Press*, Corrected Proof, 1-16.

Kerr, A., 1993. Topography, climate and ice masses: a review. Terra Nova 5 (4), 332–342.

Kessler, M.A.,Anderson, R.S.,Stock, G.M., 2006. Modeling topographic and climatic control of east–west asymmetry in Sierra Nevada glacier length during the Last Glacial
Maximum. J. Geophys. Res. 111 (F2) (F02002).

Kirkbride M.P., Brazier V., 1998. A critical evaluation of the use of glacial chronologies in climatic reconstruction, with reference to New Zealand. *Quaternary Proceedings* 6, 55-64.

Kirkbride, M.P.,Winkler, S., 2012. Correlation of Late Quaternary moraines: impact of climate variability, glacier response, and chronological resolution. Quat. Sci. Rev. 46, 1–29.

Korschinek, G., Bergmaier, A., Faestermann, T., Gerstmann, U.C., Knie, K., Rugel, G., Wallner, A., Dillmann, I., Dollinger, G., von Gostomski Lierse, Ch., Kossert, K., Maitia, M., Poutivtsev, M., Remmert, A., 2009. A new value for the half-life of 10Be by heavy-ion elastic recoil detection and liquid scintillation counting. Nuclear Instruments and Methods in Physics Research B 268 (2), 187–191.

Kotlyakov, V.M., Krenke, A.N., 1982. Investigation of the hydrological conditions of alpine regions by glaciological methods. In: Glen, J.W. (Ed.) Hydrological Aspects of Alpine and High Mountain Areas, IAHS Publication, vol. 138, pp. 31–42.

Kuhn, M., 1979. Climate and Glaciers. Sea Level, Ice, and Climatic Change (Proceedings of the Canberra Symposium, December 1979). IAHS Publ., p. 131.

L

Lachniet, L. Vazquez-Selem., 2005. Quaternary International (138– 139), 129–144.

Lal. D., 1991. Cosmic ray labeling of erosion surfaces: in situ nuclide production rates and erosion models. Earth and Planetary Science Letters 104, 429-439.

Lea, D. W., Pak, D. K., Peterson, L. C., Hughen, K. A., 2003. Synchroneity of tropical and high-latitude Atlantic temperatures over the last glacial termination. Sci. 301, 1361 64.

Le Roy, M. 2012. Reconstitutions des fluctuations glaciares holocènes dans les Alpes occidentales. Apports de la dendrochronologie et des datations par isotopes cosmogéniques produits *in situ.* Ph.D. Thesis, Université de Grenoble, France, 363 pp.

Li, W., Fu, R., Dickinson, R.E., 2006. Rainfall and its seasonality over the Amazon in the 21st century as assessed by the coupled models for the IPCC AR4. J. Geophys. Res. 111, D02111 doi: 02110.01029/02005JD006355.

Libby, W F., 1955. Radiocarbon dating. University of Chicago press, 2nd edition, Chicago, 175 pp.

Lisiecki, L.E., Raymo, M.E., 2005. A Pliocene-Pleistocene stack of 57 globally distributed benthic $\delta^{18}O$ records. Paleoceanography 20 (1), PA1003. doi:10.1029/2004PA001071.

Loewe, F., 1971. Considerations of the origin of the Quaternary ice-sheet in North America. Arctic and Alpine Research, 3, 331–344.

Lukas S., Graf A., Coray S., Schlüchter C., 2012. Genesis, stability and preservation potential of large lateral moraines of Alpine valley glaciers – towards a unifying theory based on Findelengletscher, Switzerland. *Quaternary Science Reviews* 38, 27-48.

M

Manley, G., 1955. On the occurrence of ice domes and permanently snow-covered summits. J. Glaciol. 1 (17), 453–456.

Mahaney, W.C., Milner, M.W., Kalm, V. Dirszowsky, R.W., Hancock, R.G.V., Beukens, R.P., 2008. Evidence for a Younger Dryas glacial advance in the Andes of northwestern Venezuela. Geomorphology 96, 199-211.

Mahaney, W. C., Volli, K., Menzies, J., Milner, M. W., 2010a. Reconstruction of the Early Mérida, pre-LGM glaciation with comparison to Late Glacial Maximum till, northwestern Venezuelan Andes. Sedimentary Geology 226, 29–41.
Mahaney, W. C., Kalm, V., Menzies, J., Hancock, R.V.V., Milner, M. W., 2010b. Reconstruction of the pre-Merida glaciation, northwestern Venezuelan Andes. Sedimentary Geology 230, 10–20.

Mahaney, W.C., Russell S.E., Milner, M.W., Kalm V., Bezada M., Hancock, R.G.V., Beukens R.P., 2001. Paleopedology of Middle Wisconsin/Weichselian paleosols in the Mérida Andes, Venezuela. Geoderma 104, 215–237.

Mahaney, W.C., Dirszowsky, R. W., Milner , M. W., Harmsen, R., Finkelstein, S. A., Kalm, V., Bezada, M., Hancock, R.G.V. 2007. Soil stratigraphy and plant–soil interactions on a Late Glacial–Holocene fluvial terrace sequence, Sierra Nevada National Park, northern Venezuelan Andes. Journal of South American Earth Sciences 23, 46-60.

Mahaney, W.C., Milner, M.W., Voros, J. Kalm, V. Hütt, G., Bezada, M., Hancock, R.G.V., Autreiter, S., 2000. Stratotype for the Mérida Glaciation at Pueblo Llano in the Northern Venezuela Andes. Journal of South American Earth Sciences 13, 761-774.

Makos, M., Dzierżek, J., Nitychoruk, J., Zreda, M., 2014. Timing of glacier advances and climate in the High Tatra Mountains (Western Carpathians) during the Last Glacial Maximum. Quaternary Research 82, 1–13.

MARGO Project Members, 2009. Constraints on the magnitude and patterns of ocean cooling at the Last Glacial Maximum. Nature Geoscience 2, 127-132.

Martin, L.C.P. ., Blard, P.H., Lavé, J., Braucher, R. Lupker, M., Condom, T., Charreau, J., Mariotti, V., ASTER Team, Davy, E. 2015. In situ cosmogenic 10Be production rate in the High Tropical Andes. Quaternary Geochronology, Volume 30, Part A, Pages 54-68

Matthews, J.A., 2005. "Little Ice Age" glacier variations in Jotunheimen, southern Norway: a study in regionally-controlled lichenometric dating of recessional moraines with implications for climate and lichen growth rates. The Holocene 15, 1-19.

Mercer, J.H., Palacios, M.O., 1977. Radiocarbon dating of the last glaciation in Peru. Geology 5, 600–604.

Merchel, S., Herpers, U., 1999. An update on radiochemical separation techniques for the determination of long-lived radionuclides via Accelerator Mass Spectrometry Radiochimica Acta 84, 215–219.

Mix, A.C., Bard, E., Schneider, R., 2001. Environmental processes of the ice age: land, oceans, glaciers (EPILOG). Quaternary Science Reviews 20, 627-657.

Monasterio, M. and Reyes, S. 1980. Diversidad ambiental y variación de la vegetación en los páramos de los Andes Venezolanos. En: M. Monasterio (Ed): Estudios Ecológicos en los Páramos Andinos, Editorial de la Universidad de Los Andes, Mérida, pp. 47-91.

Monod, B., Dhont, D., Hervouët, Y., 2010. Orogenic float of the Venezuelan Andes. Tectonophysics 490, 123–135.

Morales, J., Sarmiento, L., 2002. Dinámica de los macroinvertebrados edáficos y su relación con la vegetación en una sucesión secundaria en el páramo venezolano. ECOTROPICOS 15(1), 99-110.

N

Naafs, B.D.A., Hefter, J. and Stein, R., 2013. Millennial-scale ice rafting events and Hudson Strait Heinrich(-like) Events during the late Pliocene and Pleistocene: a review. Quaternary Science Reviews 80, 1-28.

Nesje, A. and Olaf Dehl, S., 2000. Glaciers and environmental change. Oxford University Press Inc. (203 pages).

NGRIP members, 2004. High-resolution record of Northern Hemisphere climate extending into the last interglacial period. Nature 431 (7005), 147-151. http:// dx.doi.org/10.1038/nature02805.

Nishiizumi, K., Imamura, M., Caffee, M.W., Southon, J.R., Finkel, R.C., McAninch, J., 2007. Absolute calibration of ^{10}Be AMS standards. Nuclear Instruments and Methods B259, 403–413.

Nishiizumi, K., Winterer, E.L., Kohl, J.R., Klein, J., Middleton, R., Lal, D., Arnold, J.R., 1989. Cosmic ray production rates of ^{10}Be and ^{26}Al in quartz from glacially polished rocks. Journal of Geophysical Research 94, 17907-17915.

Nobre, P., Shukla, J., 1996. Variations of sea surface temperature, wind stress, and rainfall over the tropical Atlantic and South America. J. Clim. 9, 2464-2479.

O

Oerlemans J., 2001. Glaciers and climate change. A. A. Balkema Publishers, Rotterdam, 244 pages.

Ohmura, A., Kasser, P., Funk, M., 1992. Climate at the equilibrium line of glaciers. Journal of Glaciology, 38 (130), 397-411.

Osmaston, H., 2006. Should quaternary sea-level changes be used to correct glacier ELAs, vegetation belt altitudes and sea level temperatures for inferring climate changes. Quaternary Research 65, 244–251.

P

Paillard, D., 2015. Quaternary glaciations: from observations to theories. Quaternary Science Reviews 107, 11-24.

Paterson,W.S.B., 1981. The Physics of Glaciers. Pergamon Press Inc., New York.

Paterson, W.S.B., 1994. The Physics of Glaciers, third ed. Pergamon, Oxford (480 pages).

Pedersen, V.K., Egholm, D.L., 2013. Glaciations in response to climate variations preconditioned by evolving topography. Nature 493 (7431), 206–210.

Pellitero, R., Rea, B.R., Spagnolo, M., Bakke, J., Ivy-Ochs, S., Hughes, P., Lukas, S., Ribolini, A. A GIS tool for automatic calculation of glacier equilibrium-line altitudes. Computer & Geosciences 82, 55-62.

Peterson, L. C., Haug, G. H., Hughen,K. A., Rohl, U. Rapid Changes in the Hydrologic Cycle of the Tropical Atlantic During the Last Glacial. SCIENCE 290, 1947-1951.

Philip D. Hughes, P.D and Gibbard, P. L., 2014. A stratigraphical basis for the Last Glacial Maximum (LGM). Quaternary International, *In Press, Corrected Proof*, 1-12.

Pierrehumbert R. and Roca R., 1998. Evidence for control of Atlantic Subtropical humidity by large scale advection, Geophysical Research Letters, 25, 4537-4540.

Plummer, M.A., Phillips, F.M., 2003. A 2-D numerical model of snow/ice energy balance and ice flow for paleoclimatic interpretation of glacial geomorphic features. Quaternary Science Reviews 22, 1389-1406.

Polissar, P.J., Abbott, M.B., Wolfe, A.P., Bezada, M., Rull, V., Bradley, R.S., 2006. Solar modulation of Little Ice Age climate in the tropical Andes. Proceedings of the National Academy of Science 103, 8937-8942.

Polissar, P.J., Abbott, M.B., Wolfe, A. P., Vuille, M., Bezada, M., 2013. Synchronous interhemispheric Holocene climate trends in the tropical Andes. Proceedings of the National Academy of Science 110, 14551–14556.

Porter, S.C., 1975. Equilibrium-line altitudes of late quaternary glaciers in the Southern Alps, New-Zealand. Quaternary Research 5, 27-47.

Porter, S.C., 2001. Snowline depression in the tropics during the last glaciation. Quaternary Science Reviews 20, 1067–1091.

Poveda, G., Waylen, P. R., Pulwarty, R. S., 2006. Annual and inter-annual variability of the present climate in northern South America and southern Mesoamerica. Palaeogeography, Palaeoclimatology, Palaeoecology 234, 3 – 27.

Pulwarty, R.S., Barry, R.G., Hurst, C.M., Sellinger, K. and Mogollon, L.E., 1998. Precipitation in the Venezuelan Andes in the Context of Regional Climate. Meteorology and Atmospheric Physics 67, 217-237.

Putkonen, J., Swanson, T., 2003. Accuracy of cosmogenic ages for moraines. Quaternary Research 59, 255-261.

R

Rabatel, A., Francou, B., Soruco, A., Gomez, J., Cáceres, B., Ceballos, J. L., Basantes, R., Vuille, M., Sicart, J.-E., Huggel, C., Scheel, M., Lejeune, Y., Arnaud, Y., Collet, M. Condom, T. Consoli, G. Favier, V. Jomelli, V. Galarraga, R., Ginot, P., Maisincho, L., Mendoza, J. Ménégoz, M., Ramirez, E., P. Ribstein, W. Suarez, Villacis, M., Wagnon, P., 2013. Current state of glaciers in the tropical Andes: a multi-century perspective on glacier evolution and climate change. The Cryosphere 7, 81–102.

Rabatel, A., V. Jomelli, P. Naveau, B. Francou, D. Grancher. 2005. Dating fluctuations of glaciers during the Little Ice Age in the tropical Andes: Charquini glaciers (Bolivia, 16°S). Comptes-Rendus Géoscience, 337 (15), 1311-1322. doi: 10.1016/j.crte.2005.07.009.

Rabatel, A., Francou, B., Jomelli, V., Naveau, P., Grancjer, D., 2006. A chronology of the Little Ice Age in the tropical Andes of Bolivia (16°S) and its implications for climate reconstruction. Quaternary Research 70 (2), 198-212.

Railsback, L., Gibbard, P. H., Head, M. J., Voarintsoa, N. R. G and Toucanne, S., 2015. An optimized scheme of lettered marine isotope substages for the last 1.0 million years, and the climatostratigraphic nature of isotope stages and substages. Quaternary Science Reviews 111, 94-106.

Ramirez, E., Homann, G., Taupin, J.D., Francou, B., Ribstein, P., Caillon, N., Ferron, F. A., Landais, A., Petit, J.R., Pouyaud, B., Schotterer, U., Simoes, J.C., Stievenard, M.. 2003. A new Andean deep ice core from Nevado Illimani (6350 m), Bolivia. Earth and Planetary Science Letters 212,337-350.

Rea, B.R., 2009. Defining modern day Area-Altitude Balance Ratios (AABRs) and their use in glacier-climate reconstructions. Quaternary Science Reviews 28 237–248.

Ribstein, P., Tiriau, E., Francou, B., Saravia, R., 1995. Tropical climate and glacier hydrology; a case study in Bolivia. J. Hydrobiol. 165 (n°1–4), 221–234.

Richards, B.W.M., 2000. Luminescence dating of Quaternary sediments in the Himalaya and High Asia: a practical guide to its use and limitations for constraining the timing of glaciation. Quaternary International 65-66, 49-61.

Rod, E., 1956. Strike-slip faults of northern Venezuela. Bulletin of the American Association of Petroleum Geologists 40, 457-476.

Rodbell, D. T., Smith, J. A., Mark, B. G., 2009. Glaciation in the Andes during the Lateglacial and Holocene. Quaternary Science Reviews 28, 2165–2212.

Rosi M. 1989. Mapa geológico del Volcán Guagua Pichincha. Elaborado por Geotermica Italian Srl. Instituto Geográfico Militar: Quito, Ecuador.

Royo y Gómez, J., 1959. El Glaciarismo Pleistoceno en Venezuela. Boletín Informativo Asociación Venezolana de Geología Minería y Petróleo 2, 333-357.

Rull, V., 1998. Palaeoecology of pleniglacial sediments from the Venezuelan Andes. Palynological record of El Caballo stadial, sedimentation rates and glacier retreat. Review of Palaeobotany and Palynology 99, 95-114.

Rull, V., 1999. Palaeoclimatology and sea-level history in Venezuela. New data, land sea correlations, and proposals for future studies in the framework of the IGBP-PAGES project. Interciencia 24 (2), 92–101.

Rull, V., 2005. A Middle Wisconsin interstadial in the northern Andes. Journal of South American Earth Sciences 19, 173-179.

Rull, V., Salgado-Labouriau, M.L., Schubert, C., Valastro, S., 1987. Late Holocene temperature depression in the Venezuelan Andes. Palynological evidence. Palaeogeogr. Palaeoclimatol. Palaeoecol. 60, 109–121.

Rull, V., Stansell, N.D., Montoya, E., Bezada, M., Abbott, M. B., 2010. Palynological signal of the Younger Dryas in the tropical Venezuelan Andes. Quaternary Science Reviews 29, 3045-3056.

Rull, V., Abbott, M.B., Polissar, P.J., Wolfe, A.P., Bezada, M., Bradley, R.S., 2005. 15,000-yr pollen record of vegetation change in the high altitude tropical Andes at Laguna Verde Alta, Venezuela. Quaternary Research 64, 308-317.

Rutherford S. and D'Hondt S., 2000. Early onset and tropical forcing of 100,000-year Pleistocene glacial cycles, Nature, 408, 72-75.

S

Salgado-Labouriau, M.L., Schubert, C., 1976. Palynology of Holocene peat bogs from central Venezuelan Andes. Palaeogeography, Plaeoclimatology, Palaeoecology 19, 147-156.

Salgado-Labouriau, M.L., Schubert, C., 1977. Pollen analysis of a peat bog from Laguna Victoria (Venezuelan Andes). Acta Cientifica Venezolana 28, 428-432.

Salgado-Labouriau, M.L., Schubert, M.L., Valastro, S.J., 1977. Paleoecologic analysis of a Late Quaternary terrace from Mucubají, Venezuelan Andes. Journal of Biogeography 4, 313–325.

Salgado-Laboriau, M.L., Rull, V., Schubert, C., Valastro JR., S., 1988. The establishment of vegetation after Late Pleistocene deglaciation in the Páramo Miranda, Venezuelan Andes. Review of Palaeobotany and Palynology, 55, 5-17.

Salgado-Labouriau, M.L., 1989. Late Quaternary climatic oscillations in the Venezuelan Andes. Biology International 18, 12–14.

Salgado-Labouriau, M.L., Bradley, R.S., Yuretich, R., Weingarten, B., 1992. Paleoecological analysis of the sediments of lake Mucubají, Venezuelan Andes. J. Biogeogr. 19, 317–327.

Schaefer, J.M., Denton, G.H., Kaplan, M., Putnam, A., Finkel, R.C., Barrell, D.J.A., Andersen, B.G., Schwartz, R., Mackintosh, A., Chinn, T., Schlüchter, C., 2009. High-frequency Holocene glacier fluctuations in New Zealand differ from the northern signature. Science 324, 622–625.

Schomacker, A., 2011. Moraine. In: Singh, V.P., Singh, P., Haritashya, U.K. (Eds.), Encyclopedia of snow, ice and glaciers. Springer, Dordrecht, 175-186.

Schubert, C., 1970. Glaciation of the Sierra de Santo Domingo, Venezuelan Andes. Quaternaria 13, 225-246.

Schubert, C., 1972. Geomorphology and glacier retreat in the Pico Bolívar area, Sierra Nevada de Mérida, Venezuela: Zeitschrift für Gletscherkunde und Glazialgeologie 8, No. 1-2, 189-202.

Schubert, C., 1974. Late Pleistocene Merida Glaciation, Venezuelan Andes. Boreas 3, 147-151.

Schubert, C., 1980. Contribución al inventario mundial de glaciares. Boletín de la Sociedad Venezolana de Ciencias Naturales 34 (137), 267-279.

Schubert, C., 1980. Morfología neotectónica de una falla rumbo deslizante e informe preliminar sobre la falla de Boconó, Andes merideños. Acta Científica Venezolana 31, 98–111.

Schubert, C., 1982. Neotectonics of Boconó Fault, western Venezuela. Tectonophysics 85, 205–220.

Schubert, C. 1984. The Pleistocene and recent extent of the glaciers of the Sierra Nevada de Mérida, Venezuela. Erdwissenshaftliche Forshung 18, 269- 278

Schubert, C., 1992. The glaciers of the Sierra Nevada de Mérida (Venezuela): A photographic comparison of recent deglaciation. Erkunde 46, 58-64.

Schubert, C., 1998. Glaciers of Venezuela. In: Satellite Image Atlas of Glaciers of the World, eds. R.S. Williams and J.G. Ferrigno. U.S. Geological Survey Professional Paper 1386-I, Washington D.C.

Schubert and Valastro Versión castellana de un artículo a publicarse en Geologische Rundschau" Band 63 (1974).

Schubert, C., Clapperton, C.M., 1990. Quaternary Glaciations in the northern Andes (Venezuela, Colombia and Ecuador). Quaternary Science Reviews 9, Issues 2-3, 123-135.

Schubert, C. and Rinaldi, M., 1987. Nuevos datos sobre la cronología del estadio tardio de la Glaciacion Mérida, Andes Venezolanos. Acta Cientifica Venezolana 38, 135-136.

Schubert, C., Valastro, S., 1980. Quaternary Esnujaque Formation, Venezuelan Andes: preliminary alluvial chronology in a tropical mountain range. Z. Dtsch. Geol. Ges. 131, 927–947.

Schubert, C., Vaz, J.E., 1987. Edad termoluminiscente del complejo aluvial cuaternario de Timotes Andes Venezolanos. Acta Científica Venezolana 38, 285-286.

Schubert, C., Vivas, L., 1993. El Cuaternario de la Cordillera de Mérida, Andes Venezolanos. Universidad de Los Andes / Fundación POLAR, Mérida, Venezuela, 345 pp.

Seltzer, G.O., 1992. Late Quaternary glaciation of the Cordillera Real, Bolivia. Journal of Quaternary Science 7, 87–98.

Shackleton, N.J., Lamb, H.H., Worssam, J.M., Hodgson, J.M., Lord, A.R., Shotton, F.W., Schove, D.J., Cooper, L.H.N., 1977. The oxygen isotope stratigraphic record of the Late Pleistocene (and discussion). Philosophical Transactions of the Royal Society of London B 280, 169-182.

Shagam, R., 1972. Andean research project, Venezuela: principal dat and tectonic implications. Geological Soc. of America. Memoir 132, 449-463.

Shakesby, R.A., Matthews, J.A., Owen, G., 2006. The Schmidt hammer as a relative age dating tool and its potential for calibrated-age dating in Holocene glaciated environments. Quaternary Science Reviews 25, 2846-2867.

Shakun, J.D., Carlson, A.E., 2010. A global perspective on Last Glacial Maximum to Holocene climate change. Quaternary Science Reviews 29, 1801-1816.

Siame, L., Braucher, R. y Bourlès D., 2000. Les nucléides cosmogéniques in situ : de nouveaux outils en géomorphologie quantitative. Bull. Soc. Geól. France. 171(4), 383-396.

Sievers, W., 1885. Über Schneeverhältnisse in der Cordillere Venezuelas. Jahresbericht der Geographischen Gesellschaft in München 10, 54-57.

Silva L. G. A., 2001. Los picos más altos del estado Mérida-Venezuela The highest peaks in Merida State Venezuela. Rev. Geog. Venez. Vol 42(1), 73-97.

Smith, J.A., Finkel, R. C., Farber, D. L., Rodbell, D. T. and Seltzer, G. O., 2005 b. Moraine preservation and boulder erosion in the tropical Andes: interpreting old surface exposure ages in glaciated valleys. Journal of Quaternary Science 20(7-8), 735-758.

Smith, J.A., Seltzera, G.O., Rodbellb, D.T., Kleinc, A.G., 2005a. Regional synthesis of last glacial maximum snowlines in the tropical Andes, South America. Quaternary International 138–139, 145–167.

Smith, J.A., Seltzer G. O., Farber D. L., Rodbell D. T., Finkel R. C., 2005a. Early local last glacial maximum in the tropical Andes. Science 308, 678– 681.

Smith, J.A, Mark, B. G. and Rodbell, D. T., 2008. The timing and magnitude of ç mountain glaciation in the tropical Andes. Journal of Quaternary Science 23(6-7) 609- 634.

Stansell, N.D., 2009. Rapid climate change in the Tropical Américas during the Late-Glacial interval and the Holocene. Pittsburgh University, 93 pp.

Stansell,N.D., Polissar, P.J.,Abbott,M.B., 2007. Last glacialmaximum equilibrium-line altitude and paleo-temperature reconstructions for the Cordillera deMérida, Venezuelan Andes. Quatern. Res. 67, 115–127.

Stansell, N.D., Abbott, M.B., Polissar, P.J., Wolfe, A.P., Bezada, M., Rull, V., 2005. Late Quaternary deglacial history of the Mérida Andes, Venezuela. Journal of Quaternary Science 20(7-8), 801-812.

Stansell, N. D., Abbott, M. B., Rull, V., Rodbell, D. T., Bezada, M., and Montoya, E., 2010. Abrupt Younger Dryas cooling in the northern tropics recorded in lake sediments from the Venezuelan Andes. Earth and Planetary Science Letters 293, 154-163.

Stansell, N. D., Polissar, P.J., Abbott, M.B., Bezada, M., Steinman, B.A., Braun, C., 2014. Proglacial lake sediment records reveal Holocene climate changes in the Venezuelan Andes. Quaternary Science Reviews 89, 44-55.

Stéphan, J-F., 1982. Evolution geodynamique du domaine caraibe Andes et chaines caraibe sur la transversele de Barquisimeto, Venézuéla. Ph.D. Thesis, Universitè Pierre et Marie Curie, Paris 1 and 2, 512 pp.

Stone, J.O., 2000. Air pressure and cosmogenic isotope production. Journal of Geophysical Research 105, 23753–23759.

Stuiver, M., Grootes, P.M., 2000. GISP2 Oxygen isotope ratios. Quaternary Research 53 (3), 277-284. http://dx.doi.org/10.1006/qres.2000.2127.

Stuiver, M., Grootes, P. M., Braziunas, T.F. 1995. The GISP2 $\delta^{18}O$ climate record of the Past 16,500 years and the role of the sun, ocean, and volcanoes. Quaternary Research 44(3), 341-354.

Soulas, J.-P., 1985. Neotectónica del flanco occidental de los Andes de Venezuela entre 70º30´ y 71º00´W (Fallas de Boconó, Valera, Piñango y del Piedemonte). VI Congreso Geológico Venezolano, Vol. 4, Caracas, pp. 2690-2711.

Soulas, J.-P., Rojas, C., Schubert, C., 1986. Neotectónica de las fallas de Boconó, Valera, Tuñame y Mene Grande. Excursión No. 4. VI Congreso Geológico Venezolano, Vol. 10, Caracas, pp. 6961–6999.

Sugden, D.E., John, B.S., 1976. Glaciers and Landscape: A Geomorphological Approach. Edward Arnold, London. 376 pages.

T

Taboada, A., Rivera, L.A., Fuenzalida, A., Cisternas, A., Philip, H., Bijwaard, H., Olaya, J., Rivera, C., 2000. Geodynamic of the northern Andes: Subductions and intracontinental deformation (Colombia). Tectonics 19 (5), 787–813.

Taylor, J.A., Lloyd, J.L., 1992. Sources and sinks of atmospheric CO2. Aust. J. Bot. 40, 407–418.

Thompson, L.G., Mosley-Thompson, E., Davis, M. E., Lin, K.A., Henderson, J., Cole-Dai, J. F., Bolzan, Liu, K. B. 1995. Late Glacial Stage and Holocene tropical ice core records from Huascarán, Peru. Science 269, 46-50.

Thompson, L.G., Davis, M. E., Thompson, E. M., Sowers, T. A., Henderson, K. A., Zagorodnov, V. S., Lin, P. N., Mikhalenko, V. N., Campen, R. K., Bolzan, F. F., Cole-Dai, J., Francou, B. 1998. A 25,000 year tropical climate history from Bolivian ice cores. Science, 282 (5295), 1858-1864.

Thompson, W.G., Goldstein, S.L., 2006. A radiometric calibration of the SPECMAP timescale. Quaternary Science Reviews 25, 3207-3215.

Troll, C., 1941. Studien zur vergleichenden Geographie der Hochgebirge der Erde, Bonner Mitteilungen, Bonn, Germany.

U

Uriarte, A., 2003. Historia del clima. Gobierno Vasco. 305 pages.

V

Vergara,W., Deeb, A. M., Valencia, A. M., Bradley, R. S., Francou, B., Zarzar, A., Grünwaldt, A., and Haeussling, S. M., 2007. Economic impacts of rapid glacier retreat in the Andes, Eos, 88, 261–264.

Vivas, L., 1979. Aracay y Pueblo Llano. Comparacion de las condiciones geomorfologicas de las cuencas de los rios Aracay y Pueblo Llano. Trabajo de ascenso inédito. Facultad de Ciencias Forestales. Universidad de Los Andes, 123 pp

W

Wesnousky, S.G., Aranguren, R., Rengifo, M., Owen, L.A., Caffee, M. W., Krishna Murari, M., Pérez, O. J. 2012. Toward quantifying geomorphic rates of crustal displacement, landscape development, and the age of glaciation in the Venezuelan Andes Geomorphology 141-142, 99-113.

Wang, Y.J., Cheng, H., Edwards, R.L., An, Z.S., Wu, J.Y., Shen, C.C., Dorale, J.A., 2001. A highresolution absolute-dated late Pleistocene monsoon record from Hulu cave, China. Science 294, 2345–2348.

Weingarten, B., Salgado-Labouriau, M.L., Yuretich, R., Bradley, R., 1991. Late quaternary environmental history of the Venezuelan Andes. In: Yuretich, R. (Ed.), Late Quaternary Climatic Fluctuations of the Venezuelan Andes. University of Massachusetts, Amherst, MA, pp. 63–94.

Winkler, S., 2005. The 'Schmidt hammer' as a relative-age dating technique: potential and limitations of its application on Holocene moraines in Mt Cook National Park, Southern Alps, New Zealand. New Zealand Journal of Geology and Geophysics 48, 105-116.

Winkler S., Matthews J.A., 2010. Observations on terminal moraine-ridge formation during recent advances of southern Norwegian glaciers. Geomorphology 116, 87-106.

Winsor, K., Carlson, A.E., Rood D.H., 2014. ^{10}Be dating of the Narsarsuaq moraine in southernmost Greenland: evidence for a late-Holocene ice advance exceeding the Little Ice Age maximum. Quaternary Science Reviews, Volume 98, 135-143.

Y

Yin, L., Fu, R., Zhang, Y.-F., Arias, P.A., Fernando, D.N., Li, W., Fernandes, K., Bowerman, A.R., 2014. What controls the interannual variation of the wet season onsets over the Amazon. J. Geophys. Res. Atmos. 119, 2314-2328.

Yoris, F., Ostos, M., 1997. Well Evaluation Conference. Schlumberger Oilfield Services, Caracas, Venezuela, 1- 40.

Yokoyama, Y., Lambeck, K., DeDeckker, P., Johnston, P., Fifield, K., 2000. Timing of the Last Glacial Maximum from observed sea-level minima. Nature 406, 713-716.

Z

Zebre, M. and Stepisnik, U. 2014. Reconstruction of Late Pleistocene glaciers on Mount Lovcen, Montenegro. Quaternary International 353, 225-235

GEOCRONOLOGÍA CON EL ISÓTOPO COSMOGÉNICO ^{10}Be, APLICACIÓN PARA EL ESTUDIO DE LA DINÁMICA GLACIAR CUATERNARIA EN LA REGIÓN CENTRAL DE LOS ANDES DE MÉRIDA

Isandra ANGEL[1], Eduardo CARRILLO[1], Julien CARCAILLET[2], Franck AUDEMARD[3] & Christian BECK[4]

[1]Centro de Geología, Instituto de Ciencias de la Tierra, Facultad de Ciencias, Universidad Central de Venezuela. Caracas 1040.Correo-e.: iangel_ceballos@yahoo.com. [2]ISTerre Université de Grenoble 1, UMR CNRS 5275, F-38041. Francia. [3]Fundación Venezolana de Investigaciones Sismológicas, FUNVISIS, El Llanito, Caracas 1070, Venezuela. [4]ISTerre Université de Savoie. UMR CNRS 5275 Le Bourget du Lac. Francia

RESUMEN

El estudio de los glaciares tropicales es una temática de gran importancia para las áreas de paleo-clima, gestión de riesgos naturales, manejo del recurso agua, generación de energía, etc. El presente trabajo muestra algunos adelantos en el estudio de la dinámica glaciar cuaternaria en Los Andes Centrales de Mérida. La reconstrucción de los glaciares deducida de la geocronología con el ^{10}Be *in-situ*, contribuyen con el conocimiento climático regional y global desde el Último Máximo Glaciar. En el valle de Mucubají, el avance máximo del glaciar ocurrió hace más de18000 años y el retiro definitivo hace menos de 9000 años. El proceso transcurrió en dos grandes etapas. El glaciar retrocedió durante el Pleistoceno de ~3500 m a ~3850 m. La parte superior del glaciar estuvo confinado y desapareció rápidamente durante el Holoceno. En Los Zerpa el avance máximo ocurrió hace aproximadamente 13000 años.

Palabras claves: Glaciología Forense, Nucleídos cosmogénicos, Andes de Mérida

ABSTRACT

Tropical glaciers studies are extremely important for knowledge of paleoclimatology, natural hazards, water resources management, power generation, etc. This article reports the recent progress in the understanding of quaternary glacier dynamics in the Mérida Central Andes. Glacier reconstruction deduced from *in-situ* produced ^{10}Be dating, contributes with the regional and global climatic knowledge since the Last Glacial Maximum. The maximum glacier advance in Mucubají valley occurred over 18,000 years ago and glaciers disappeared less than 9,000 years ago. The retreat process happened in two main stages. Glacier has moved back during the Pleistocene from ~3500 m to ~3850 m. The upper ice tongue was confined and rapidly disappeared during the Holocene. In Los Zerpa the maximum advance took place 13,000 years ago.

Keywords: Forensic Glaciology, Cosmogenic nuclides, Andes de Mérida.

INTRODUCCIÓN

Los elementos producidos por acción de los rayos cósmicos son llamados nucleídos cosmogénicos (o cosmonucleídos). Los rayos cósmicos son partículas cargadas con energía suficiente para producir reacciones nucleares en los primeros metros de la atmósfera y litósfera (DUNAI 2010).

El ^{10}Be es un cosmonucleído con un tiempo de vida media de: 1,36+/- 0,07 Ma (NISHIIZUMI E *et al.* 2007). Tiene dos orígenes, ambos debido a la acción de los rayos cósmicos sobre la materia terrestre. Una parte del ^{10}Be es producida en la atmósfera por reacciones nucleares sobre átomos de nitrógeno y oxígeno; la otra, es la generada en la litósfera, producida principalmente por reacciones nucleares en los átomos de O y, en menor proporción, en los de Mg, Al, Si y Ca presentes en los minerales (KOBER *et al.* 2005). Este tipo de ^{10}Be es conocido como isótopo cosmogénico producido *in-situ*.

Los factores que controlan la producción de los isótopos cosmogénicos (^{10}Be) son: la variabilidad del campo magnético terrestre (latitud), la altitud, la profundidad y la topografía (LAL 1991, GOSSE & PHILLIPS 2001, DUNAI 2010).

En las geociencias, la geocronología mediante el estudio del ^{10}Be ha permitido resolver interrogantes que no habían sido resueltas con otros métodos. Puede ser empleado con el ^{26}Al para estudiar procesos que resultan de una historia compleja de exposición. Debido al tiempo de vida medio del isótopo ^{10}Be, es posible estudiar procesos ocurridos durante el Cuaternario y el Plioceno Tardío (DUNAI 2010).

Con el desarrollo del presente trabajo se pretende aportar información que permita la reconstrucción de la dinámica glaciar cuaternaria en los Andes centrales de Mérida y, considerando a escala global, el uso de los glaciares tropicales como indicadores de los cambios climáticos.

MÉTODOS

El área de trabajo se encuentra remarcada en la figura 1. Corresponde precisamente a la morrena terminal de Los Zerpa, morrenas de Mucubají y su valle glaciar.

Para el desarrollo de este trabajo fueron recolectadas 16 muestras, distribuidas como se muestra en la figura 2.

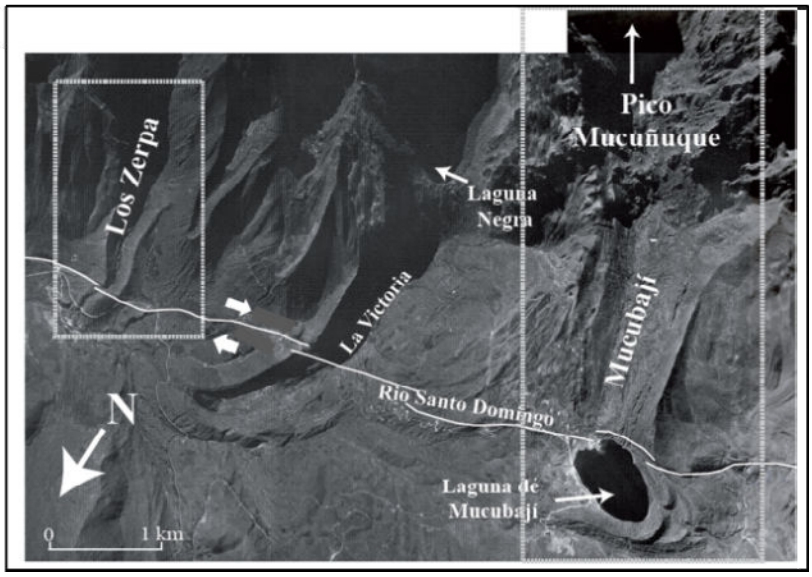

Fig. 1. Área de estudio, sector de la Sierra de Santo Domingo comprendido por los complejos morrénicos y valles glaciares de Mucubají y Los Zerpa.

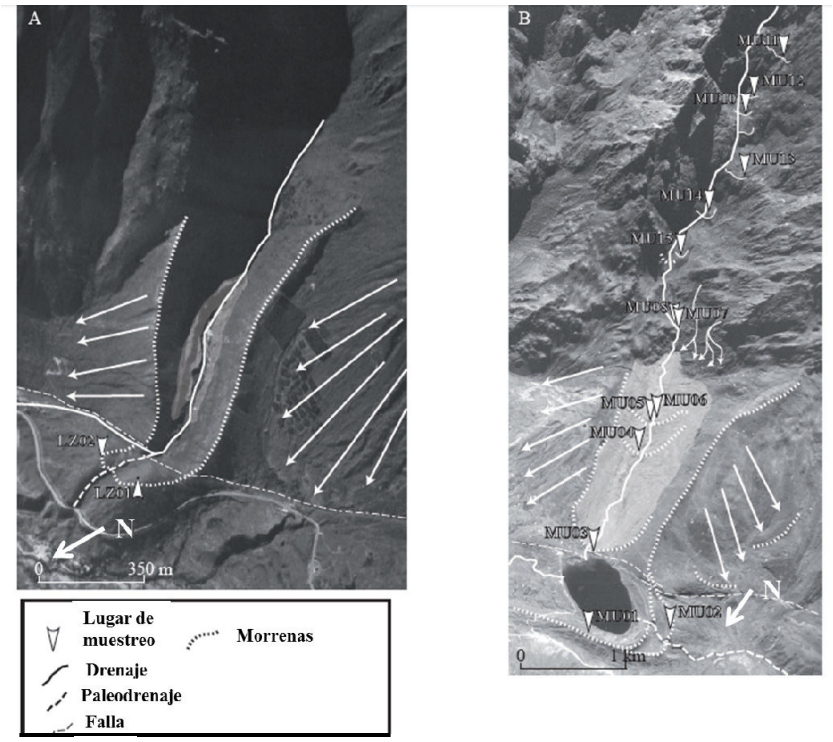

Figura 2. Sitios de recolección de las muestras del presente trabajo, a) Morrenas de Los Zerpa y b) Valle de Mucubají.

La recolección se realizó en dos tipos de sitios distintos: 1) bloques de roca de gran tamaño (> 1 m) abandonados dentro de las morrenas (Figs. 3a, 3b), para evitar efectos por removilización post-depósitos y 2) dentro del macizo rocoso, en los valles glaciares en zonas con rocas con estrías o rocas aborregadas (Fig.3c).

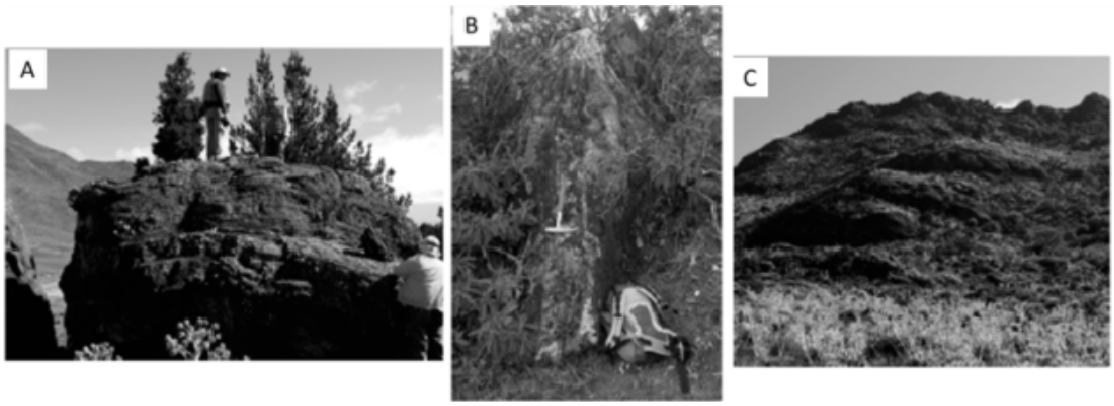

Fig.3. Ejemplos de los bloques, rocas aborregadas y estriadas en donde fueron recolectadas las muestras, a) y b) bloques abandonados dentro de la morrena, c) rocas aborregadas y estriadas.

Para calcular la tasa de producción del ^{10}Be, se tomó nota de los valores de coordenadas geográficas (latitud, longitud), altitud y topografía de los alrededores en el campo. Los espesores de las muestras (desde la superficie hacia el interior de la roca) se encontraban entre 2-4 cm.

La extracción del ^{10}Be comienza con un procesamiento físico: la muestra de roca es pulverizada, tamizada y los minerales pesados son separados magnéticamente. Sigue con el tratamiento químico, el cual consiste en digestiones con ácidos fuertes: ácido fluorhídrico (HF), ácido clorhídrico (HCl), ácido nítrico (HNO_3) y ácido perclórico ($HClO_4$). Sigue una etapa de separaciones a través de resinas de intercambio iónico. Posteriormente se lleva a cabo la purificación a través de la precipitación con amoníaco (NH_3) y finalmente la calcinación. El procesamiento químico de las muestras fue llevado a cabo en el laboratorio del ISTerre, Francia según el procedimiento químico adaptado de BROWN *et al*. (1991) y MERCHEL & HERPERS (1999). Las mediciones de las muestras fueron llevadas a cabo en las instalaciones del Laboratorio Nacional Francés ASTER mediante espectrometría de masas con acelerador AMS.

Las edades fueron determinadas a través de la calculadora online Cronus (BALCO *et al*. 2008), usando la tasa de producción dependiente del tiempo de LAL (1991) modificado por STONE (2000), la cual toma en cuenta el efecto de los cambios del campo magnético.

RESULTADOS Y DISCUSIONES

En los estudios con los isótopos cosmogénicos existen múltiples fuentes de error, las cuales pueden alterar los valores de concentraciones y por ende de la edad. Los errores de la etapa analítica y metodológica pueden contribuir con 5-15% y los errores debidos a los factores geológicos, meteorológicos y otros entre 0-50%. Las incertidumbres externas comúnmente sobrepasan el 10% (BALCO *et al*. 2008) y las internas se encuentran entre el 1-5% (DUNAI 2010).

Una fuente de error importante que hay que considerar es el efecto de la erosión. Este error intenta minimizarse durante la etapa de recolección de las muestras, seleccionando bloques de gran tamaño que no puedan ser fácilmente transportados y que se encuentren en la parte superior de una morrena. Por otra parte, en muestras de basamento rocoso debe identificarse la presencia de estrías glaciares y las rocas aborregadas que aseguren la permanencia *in-situ* de los cuerpos glaciares (véase Fig. 2c).

Las incertidumbres obtenidas en los resultados se encuentran generalmente alrededor del 10 %, mientras que la mayoría de los errores internos son menores a los errores externos, lo que garantiza la confiabilidad de las edades determinadas. Las concentraciones de ^{10}Be se encuentran entre $270{,}19*10^3$ atoms/gqtz/año y $522{,}40*10^3$ atoms/gqtz/año; las edades entre 9,08 ± 0.82 y 18,14 ± 2.11 ka (tabla 1).

Tabla 1: Resultados obtenidos en concentración de ^{10} Be en x10^{3}átomos/gqtz/año y las edades en kiloaños (ka).

Muestra	Latitud	Longitud	Elevación	Información del sitio	Información de las muestras	Espesor	Concentración ^{10}Be		Edades		
							Valor	Error	Valor	Error externo	Error interno
	°N	°O	m.s.n.m		Tamaño aparente (largo*ancho*alto)	cm	x10^3 átomos/gQtz/año		ka		
LZ09-01	8,8117	70,7884	3127	Morrena frontal, en la cresta	Bloque(4.2*2.7*1)	3	301,42	27,95	13,837	1,74	1,352
LZ09-02	8,8117	70,7874	3113	Morrena frontal en la cresta	Bloque(3.7*2*2.3)	3	270,19	19,41	12,481	1,386	0,944
Mu09-01	8,8009	70,8279	3620	Lado izquierdo de la morrena frontal, en la cresta	Bloque (7*4.5*4)	4	477,12	16,54	16,784	1,536	0,625
Mu09-02	8,7954	70,8343	3589	Morrena frontal en la cresta	Bloque(1.6*1.2*0.9)	3	522,40	41,55	18,144	2,112	1,563
Mu09-03	8,7951	70,8267	3572	Morrena frontal en la cresta	Bloque (1.7*1.5*0.7)	3	440,60	28,60	15,661	1,673	10,84
Mu09-04	8,7874	70,8233	3607	Morrena frontal en la cresta	Bloque (1.3*1*0.8)	4	372,93	11,46	13,273	1,195	0,431
Mu09-05	8,7850	70,8229	3615	Morrena frontal en la cresta	Bloque (3.5*1.5*1.2)	4	375,45	27,10	13,321	1,483	1,016
Mu09-06	8,7852	70,8224	3620	Morrena frontal en la cresta	Bloque (1.4*1.3*0.8)	2	463,22	34,48	15,957	1,801	1,269
Mu09-07	8,7790	70,8197	3697	Basamento con estría en eje del valle		3	374,12	16,53	13,841	1,322	0,647
Mu09-08	8,7785	70,8189	3727	Basamento con estría en eje del valle	~2 m alto	3	408,50	16,71	14,201	1,335	0,615
Mu09-10	8,7667	70,8129	4067	Basamento con estría en eje del valle	~2 m alto	4	306,04	9,55	9,078	0,818	0,304
Mu09-11	8,7633	70,8119	4213	Morrena lateral	Bloque (2*1.5*1)	3	334,55	10,27	10,629	0,956	0,348
Mu09-12	8,7659	70,8121	4091	Basamento con estría en eje del valle		3	324,42	26,38	9,483	1,113	0,825
Mu09-13	8,7689	70,8164	3982	Morrena en el eje del valle	Bloque (3*2*1.5)	3	301,52	9,74	9,732	0,881	0,336
Mu09-14	8,7719	70,8152	3862	Morrena en el eje del valle	Bloque (1.5*1.5*1.5)	3	305,27	24,76	9,925	1,164	0,858
Mu09-15	8,7758	70,8161	3804	Basamento con estría en eje del valle		3	390,44	34,08	12,864	1,566	1,188

La última época glaciar (Würm/Wisconsin) está representada por la glaciación Mérida (SCHUBERT 1974) y caracterizada por dos etapas principales: Mérida Temprana hace unos 30000 años (Wisconsin Intermedia) y Mérida Tardía (Wisconsin Tardía), la cual incluye el último máximo glaciar (LGM, según sus siglas en inglés) entre 13000 y 25000 años (SCHUBERT & CLAPPERTON 1990).

El estudio cuantitativo de la geomorfología glaciar en Los Andes venezolanos es un tema novedoso y actualmente en auge. En la bibliografía puede encontrarse el trabajo de WESNOUSKY *et al*. (2012), quién estudió las morrenas de la Victoria y Los Zerpa mediante la geocronología con el isótopo cosmogénico ^{10}Be.

Sus valores arrojaron edades entre 15000 años y alrededor de 18000 años. Al comparar con los resultados de este trabajo, los valores deberían ser más cercanos a los obtenidos para la morrena de Los Zerpa,

sin embargo, se observan discrepancias (véase Fig. 4, tablas 1 y 2).

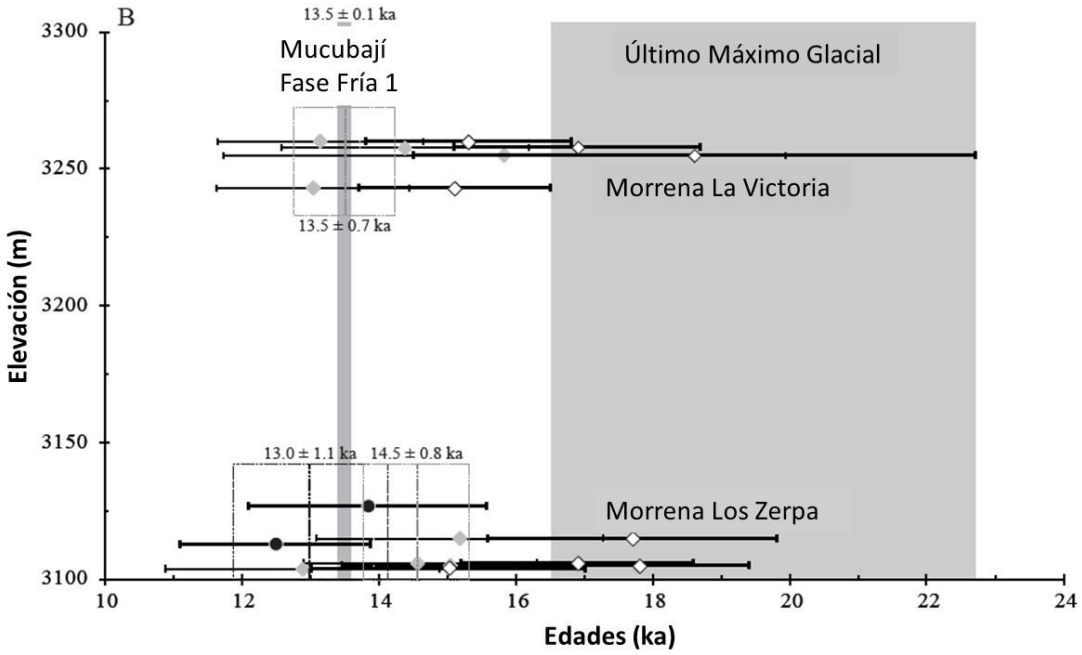

Fig. 4. Gráfico de Edades (ka) vs. Altura (m). A) Morrena de Los Zerpa y morrena de la Victoria. B) Puntos negros pertenecen a este trabajo, rombos blancos son datos publicados (revisar tablas 1 y 2 para detalles), rombos grises son los datos de Wesnousky et al. 2012 recalculados con el modelo de tasa de producción del cosmogénico dependiente del tiempo.

Al considerar las incertidumbres de los valores, los datos del trabajo de WESNOUSKY *et al*. (2012) podrían entrar dentro del rango de edades que han sido determinadas en este trabajo. Dichas discrepancias podrían ser causadas por el tratamiento matemático utilizado, ya que la metodología de recolección y el tratamiento químico fueron los mismos. Los cálculos en este trabajo han sido realizados considerando la variación de la tasa de producción del cosmogénico dependiente del tiempo, de LAL (1991) modificado por STONE (2000), mientras que WESNOUSKY *et al*. (2012) escogieron una tasa de producción invariante en el tiempo, la cual no considera cambios en el campo magnético terrestre.

Considerando la información de SCHUBERT & CLAPPERTON (1990), los resultados obtenidos en este trabajo coinciden con la Glaciación Mérida, específicamente la etapa de Mérida Tardía, la que incluye el último máximo glaciar e incluso edades más jóvenes.

Los resultados en el valle glaciar de Mucubají muestran una correlación inversa entre la altitud y la edad, característica de un proceso en el que el glaciar va desapareciendo, dejando primero al descubierto la morfología más baja hasta que desaparece completamente a mayores altitudes (véase Fig.5).

En función del resultado de la muestra Mu09-02, perteneciente a la morrena frontal más externa, podemos establecer que el avance máximo del glaciar en el Valle de Mucubají ocurrió hace más de 18000 años. En función de la muestra Mu09-11, ubicada en el circo glaciar más alto, podemos establecer que la completa desaparición, al menos temporalmente, del glaciar en el Valle de Mucubají, ocurrió hace menos de 9000 años aproximadamente.

Velocidades que pueden ser indicativas del proceso de desaparición del glaciar en el valle de Mucubají pueden ser inferidas al graficar edad vs. altura. Logran observarse dos grandes tendencias. Las muestras del Pleistoceno presentan una menor velocidad de retroceso del glaciar comparadas con el grupo de muestras del Holoceno (Fig. 5). Las diferentes etapas de desaparición del glaciar podrían estar asociadas con diferentes eventos climáticos globales.

Comparando los valores de Los Zerpa y Mucubají, en la primera las muestras se encuentran cerca de 3100 m con una edad alrededor de 13000 años, mientras que en Mucubají, las muestras con edades cercanas a los 13000

años corresponden a altitudes superiores a 3600 m (Figs. 4 y 5).

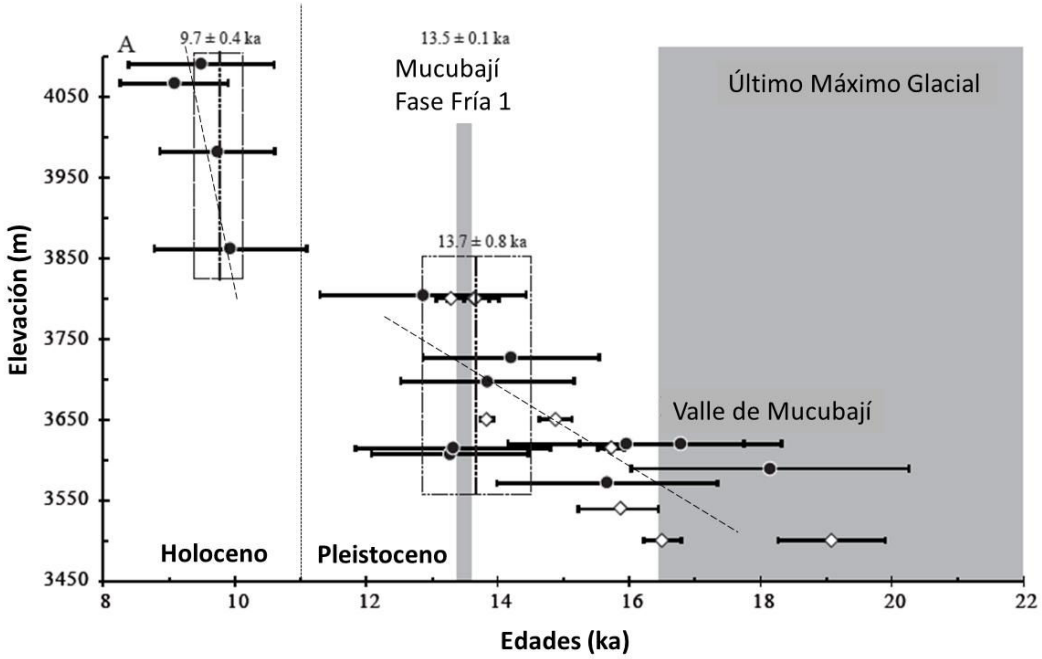

Fig. 5. Resultados de las Edades (ka) vs. Altura (m) para las muestras del valle glaciar de Mucubají. Puntos negros son resultados del presente estudio, rombos blancos son datos publicados. Rectas punteadas inclinadas representan las diferentes tendencias en velocidades del retroceso del glaciar durante el Pleistoceno y Holoceno.

Además de la diferencia en altitud entre las morrenas de Los Zerpa y el Valle de Mucubají, se encuentra también la orientación de los valles, aunado a la afectación estructural diferente en ambas zonas. Posiblemente las diferencias en las orientaciones de los valles generen condiciones meteorológicas variantes, por ejemplo la pluviometría, que influyan en la desaparición de los glaciares.

CONCLUSIONES

Todas las muestras presentadas en este trabajo arrojaron ^{10}Be edades que corresponden a la Etapa Tardía de la Glaciación Mérida e incluso edades más jóvenes. En el valle glaciar de Mucubají, parte de la dinámica del glaciar puede plantearse de la siguiente manera: el avance máximo hace más de 18000 años y la completa desaparición hace menos de 9000 años. A grosso modo este proceso transcurrió en dos grandes etapas, durante el Pleistoceno con una menor velocidad de desaparición del glaciar y durante el Holoceno a una mayor velocidad.

BIBLIOGRAFÍA

BALCO G., J.O. STONE, N.A. LIFTON & T.J. DUNAI. 2008. A complete and easily accessible means of calculation surface exposure ages or erosion rates from ^{10}Be and ^{26}Al measurements. *Quaternary Geochronology* 3:174-195.

BROWN E.T., J.M. EDMOND, G.M. RAISBECK, F. YIOU, M.D. KURZ & E.J. BROOK. 1991. Examination of surface exposure ages of Antarctic moraines using in situ produced ^{10}Be and ^{26}Al. *Geochim. Cosmochim. Acta* 55:2269–2283.

DIRSZOWSKY R. W., W.C. MAHANEY, K.R. ODRE, M.W. MILNER, V. KALM, M. BEZADA & R.P BEUKENS. 2005. Lithostratigraphy of the Mérida (Wisconsinan) glaciation and Pedregal interstade, Mérida Andes, northwestern Venezuela. *Journal of South American Earth Sciences* 19:525-536.

DUNAI T. 2010. Cosmogenic Nuclides: Principles, Concepts and Applications in the Earth Surface Sciences. Cambridge University Press. 180 p.

GOSSE J.C. & F.M. PHILLIPS. 2001. Terrestrial in situ cosmogenic nuclides: theory and application. *Quaternary Science Reviews* 20:1475-1560.

KOBER F., S. IVY-OCHS, I. LEYA, H. BAUR, T. MAGNA, R. WIELER & P.W. KUBIK. 2005. In situ cosmogenic ^{10}Be and ^{21}Ne in sanidine and in situ cosmogenic ^{3}He in Fe–Ti-oxide minerals. *Earth and Planetary Science Letters* 236(1–2):404-418.

LAL D. 1991. Cosmic ray labeling of erosion surfaces: in situ nuclide production rates and erosion models. *Earth and Planetary Sciences Letters* 104:429-43.

MAHANEY W. C., S.E. RUSSELL, M.W. MILNER, V. KALM, M. BEZADA, R.G.V HANCOCK & R.P. BEUKENS. 2001. Paleopedology of Middle Wisconsin/Weichselian paleosols in the Mérida Andes, Venezuela. *Geoderma* 104:215–237.

MAHANEY W.C., M.W. MILNER, V. KALM, R.W. DIRSZOWSKY, R.G.V HANCOCK & R.P. BEUKENS. 2008. Evidence for a Younger Dryas glacial advance in the Andes of northwestern Venezuela. *Geomorphology* 96:199-211.

MERCHEL S. & U. HERPERS. 1999. An Update on Radiochemical Separation techniques for the determination of Long-Lived Radionuclides via Accelerator Mass Spectrometry. *Radiochim. Acta* 84:215-229.

NISHIIZUMI K., M. IMAMURA, M.W. CAFFEE, J.R. SOUTHON, R.C. FINKEL & J. MCANINCH. 2007. Absolute calibration of ^{10}Be AMS standards. *Nucl. Instr. Meth. Phys. Res. B* 258:403-413.

SALGADO-LABOURIAU M.L., M.L. SCHUBERT & S.J. VALASTRO. 1977. Paleoecologic analysis of a Late Quaternary terrace from Mucubají, Venezuelan Andes. *Journal of Biogeograph* 4:313–325.

SCHUBERT C. 1974. Late Pleistocene Merida Glaciation, Venezuelan Andes. *Boreas* 3:147-151.

SCHUBERT C. & C.M. CLAPPERTON. 1990. Quaternary Glaciations in the northern Andes (Venezuela, Colombia and Ecuador). *Quaternary Science Reviews* 9:123-135.

SCHUBERT C. & M. RINALDI. 1987. Nuevos datos sobre la cronología del estadío tardío de la Glaciación Mérida, Andes Venezolanos. *Acta Científica Venezolana* 38:135-136.

STANSELL N.D., M.B. ABBOTT, P.J. POLISSAR, A.P. WOLFE, M. BEZADA & V. RULL. 2005. Late Quaternary deglacial history of the Mérida Andes, Venezuela. *Journal of Quaternary Science* 20(7-8):801-812.

STONE J.O. 2000. Air pressure and cosmogenic isotope production. *J. Geophys. Res.* 105:23753–23759.

WESNOUSKY S.G., R. ARANGUREN, M. RENGIFO, L.A. OWEN, M.W. CAFFEE, M. KRISHNA MURARI & O.J. PÉREZ. 2012. Toward quantifying geomorphic rates of crystal displacement, landscape development, and the age of glaciation in the Venezuelan Andes. *Geomorphology* 141-142:99-113.

Tabla 2: Información cronológica de rasgos geomorfológicos del área de estudio publicada: Mesa del Caballo, Valle de Mucubají y morrenas de Los Zerpa y La Victoria.

Muestra	Latitud	Longitud	Elevación (m)	Información de las muestras	Edades				Referencia
					Método	Valor	Error -	Error +	
	°N	°W	m.s.n.m.		ka				
Ped 5-3 VI	8.78	70.84	3500	Capa de turba - Mesa del Caballo	^{14}C unCal. BP	60,24	2,84	2,84	Mahaney et al., 2001
Ped 5-3 VII Top	8.78	70.84	3500	Capa de turba - Mesa del Caballo	^{14}C unCal. BP	58,35	2,79	2,79	Mahaney et al., 2001
Ped 5-3 VII Middle	8.78	70.84	3500	Capa de turba - Mesa del Caballo	^{14}C unCal. BP	>64.64	0	0	Mahaney et al., 2001
Ped 5-3 VII Bottom	8.78	70.84	3500	Capa de turba - Mesa del Caballo	^{14}C unCal. BP	>63.48	0	0	Mahaney et al., 2001
Ped 5-3 VII Top	8.78	70.84	3500	Capa de turba - Mesa del Caballo	^{14}C unCal. BP	56,94	2,26	2,26	Mahaney et al., 2001
PED 5	8.78	70.84	3500	Capa de turba - Mesa del Caballo	^{14}C cal. BP	22.75 - 19.96	1.04 - 0.27	1.14 - 0.28	Schubert and Rinaldi, 1987

Tabla 2: Información cronológica de rasgos geomorfológicos del área de estudio publicada: Mesa del Caballo, Valle de Mucubají y morrenas de Los Zerpa y La Victoria. (Continuación)

Muestra	Latitud	Longitud	Elevación (m)	Información de las muestras	Edades				Referencia	Edades modificadas	
					Método	Valor	Error -	Error +		Valor	Error
	°N	°W	m.s.n.m.			ka				ka	
CAMS-104915	8,784	70,82	3615	Macrofósiles acuáticos	^{14}C cal. BP	15,73	0,207	0,195	Stansell et al., 2005		
0	8.78	70.82	3650	Sedimentos de terraza de Mucubají	^{14}C cal. BP	14,88	0,25	0,25	Salgado-Labouriau et al., 1977		
0	8.78	70.82	3650	Sedimentos de terraza de Mucubají	^{14}C cal. BP	13,83	0,1	0,1	Salgado-Labouriau et al., 1977		
MUM 7B	8.77	70.81	3800	Aluvión orgánico	^{14}C cal. BP	13,29	0,22	0,19	Mahaney et al., 2008		
MUM 7B	8.77	70.81	3800	Turba	^{14}C cal. BP	13,64	0,15	0,22	Mahaney et al., 2008		
MUM 7B	8.77	70.81	3800	Turba	^{14}C cal. BP	13,66	0,44	0,36	Mahaney et al., 2008		
CAMS-104914	8,784	70,82	3615	Turba	^{14}C cal. BP	6,28	0,063	0,021	Stansell et al., 2005		
VEN 19	8,8141	70,8006	3255	Bloque de Gneiss de Morrena La Victoria	^{10}Be	18,6	4,1	4,1	Wesnousky et al., 2012	15,8	3,4

Tabla 2: Información cronológica publicada de rasgos geomorfológicos del área de estudio: Mesa del Caballo, Valle de Mucubají y morrenas de Los Zerpa y La Victoria.(Continuación)

Muestra	Latitud	Longitud	Elevación (m)	Información de las muestras	Edades				Referencia	Edades modificadas	
					Método	Valor	Error -	Error +		Valor	Error
	°N	°W	m.s.n.m.			ka				ka	
VEN 23	8,8139	70,7993	3243	Bloque de Metagranito de Morrena La Victoria	^{10}Be	15,1	1,4	1,4	Wesnousky et al., 2012	13,0	1,2
VEN 25	8,8121	70,7881	3115	Bloque de Gneiss de Los Zerpa	^{10}Be	17,7	2,1	2,1	Wesnousky et al., 2012	15,2	1,7
VEN 26	8,812	70,7873	3104	Bloque de Gneiss de Los Zerpa	^{10}Be	15	2	2	Wesnousky et al., 2012	12,9	1,7
VEN 27	8,8117	70,7875	3105	Bloque de Gneiss de Los Zerpa	^{10}Be	17,8	1,6	1,6	Wesnousky et al., 2012	15,1	1,4
VEN 28	8,8118	70,7873	3106	Bloque de Gneiss de Los Zerpa	^{10}Be	16,9	1,7	1,7	Wesnousky et al., 2012	14,6	1,4